An approach towards identification of anti-tubercular lead molecules by targeting *Mycobacterium tuberculosis* Glutamine Synthetase

Thesis submitted to University of Pune
For the degree of

DOCTOR OF PHILOSOPHY
IN
BIOTECHNOLOGY
By

UPASANA SINGH

Research Supervisor

Dr. Dhiman Sarkar

Combichem Bioresource Center
Organic Chemistry Division
National Chemical Laboratory
Pune – 411008
India

October 2010

Dedications

I dedicate this work to my Grandmother Mrs. Shanti Devi, My father Mr. Krishna Singh, My mother Mrs. Sandhya Singh and My Husband Mr. Dibyendu Dhar who have cooperated with me and tolerated my long hours of work patiently. They have endured my preoccupation with my work, at times neglecting them. Without their understanding and encouragement it would have been impossible to finish this work. My sincere dedication also goes to my brother Mr. Nitesh Singh and My sister Miss Aradhana Singh who have continuously put up with me all along during my work. I would be failing in my duty if I do not express my deep sense of gratitude to my father in law Dr. Nanda Dulal Dhar and My mother in law Mrs. Aruna Dhar.

TABLE OF COTENTS

Chapter – 2

Chapter -5

ACKNOWLEDGEMENT

Acquiring a PhD is a team effort. Though this work is my own, it would never have been possible without the help of numerous people who have provided me enormous support in various ways during my long and demanding years of study.

I take this opportunity to express my deep sense of gratitude to my research supervisor, mentor and guide Dr. Dhiman Sarkar (Scientist, National Chemical Laboratory, Pune) for his expert and inspirational guidance, keen interest in and dedication to my work and constant helpful hints. His wide knowledge and his logical way of thinking have been of great value to me. His understanding and motivating nature have provided a good foundation for my work. Indeed, he is an embodiment of the ideal relationship that exists between a teacher and a student.

He has endowed me with several gifts, the greatest being a completely different outlook from the one I had when I commenced my doctoral studies. It was his passion for 'An approach towards identification of anti-tubercular lead molecules by targeting Mycobacterium tuberculosis Glutamine Synthetase' which encouraged me to join his laboratory. He helped me imbibe critical thinking and a problem solving approach with the help of experiments. I thank him for allowing me freedom and resources to conduct my research.

I am deeply indebted to Dr. K. N. Ganesh, Dr. M. I. Khan, Dr. Vidya Gupta and Dr. J. K. Pal for supporting and encouraging me and engaging me in fruitful discussions during this work. They have consistently supported me and pushed me on towards success.

I owe a deep debt of gratitude to Dr. S. Sivaram, Director NCL and Dr. G. Pandey, our HOD, for exceptional leadership and a motivating working atmosphere they have provided in this institution. I am equally thankful to Dr. Sourav Pal, Chairman, SAC for his unconditional support during my research work at NCL. I am fortunate to be a part of the scientific community of NCL where high levels of excellence and commitment to research have been established and maintained.

I am equally thankful to Dr. Absar Ahmed, Dr. S.N. Mukherjee, Dr. S.P. Joshi, Dr. Ashok P. Giri, Dr. Pankaj Poddar, Dr. Mahesh Kulkarni, Dr. Alok Sen and Dr. Narendra Kadoo for their precious support.

I extent my sincere thank to Dr. D. Eisengberg, University of California, Los Angeles, for providing the E. coli clone YMC21E of M. tuberculosis GS as a gift. I am very much thankful to Dr. Jayachandran, Scientist, BARC for the synthesis of S^{35} labelled L-MSO, which helped me to derive an important conclusion. I express my deep thanks to Mr. Kishore Kulkarni of SRL for providing necessary chemicals on time.

During my P.hD, I have worked in partnership with many colleagues for whom I have great regard and I wish to extend my special thanks to Shamim, Abhiskek, Ketki, Jawid, Sampa and Arshad for their extraordinary support during my trying times and being there with and for me. I am grateful to all of them for cheering me up from time to time in this difficult task.

I would like to show sincere gratitude to few of my amazing friends Bhuban, Ashutosh, Sashidhar, Manashwini, Roopa, Mahesh, Swaroop, Satish, Arvind, Himangi, Sumita, Firoz, Fazal, Pooja, Jyoti, Sangeeta, Gitali and Ashwani for their support, encouragement, patience and advice during this challenging period in my life. I owe you all dearly and wish success in your future endeavors. I also owe a big thanks to my aunty Miss Bina Kushwaha who was not here in Pune but always with me silently.

Finally none of this would have been possible were it not for the lifelong love and encouragement of my parents and husband. What I am today I owe to them.

Upasana Singh

CERTIFICATE

This is to certify that the work incorporated in the thesis entitled "**An approach towards identification of anti-tubercular lead molecules by targeting *Mycobacterium tuberculosis* Glutamine Synthetase"** submitted by **Upasana Singh** was carried out under my supervision at Combichem Bioresource Center, Organic Chemistry Division, National Chemical Laboratory, Pune – 411008, Maharashtra, India. Materials obtained from other sources have been duly acknowledged in the thesis.

Dr. Dhiman Sarkar

(Research Guide)

DECLARATION BY RESEARCH SCHOLAR

I hereby declare that the thesis entitled "**An approach towards identification of anti-tubercular lead molecules by targeting *Mycobacterium tuberculosis* Glutamine Synthetase"**, submitted for the Degree of ***Doctor of Philosophy*** to the University of Pune, has been carried out by me at Combichem Bioresource Center, Organic Chemistry Division, National Chemical Laboratory, Pune - 411 008, Maharashtra, India, under the supervision of Dr. Dhiman Sarkar (Research supervisor). The work is original and has not been submitted in part or full by me for any other degree or diploma to any other University.

Upasana Singh

(Research Scholar)

ABSTRACT OF THESIS

*Mycobacterium tuberculosis (*Mtb*)* remained a leading cause of morbidity and mortality worldwide, and is the leading cause of death in AIDS patients. This thesis describes four approaches using Glutamine Synthetase (GS) as target for the discovery of novel therapeutic agents against the disease. The first approach was biochemical characterization of *Mycobacterium tuberculosis Glutamine synthetase* (*MtbGS*) using biosynthetic and transfer activity to develop simple screening assay protocols which could be used to pick up novel inhibitors of tuberculosis in greater numbers. The second approach was a detail characterization of the interaction between potent inhibitor named L-Methionine Sulfoximine (L-MSO) with the enzyme, elucidation of which might be helpful to develop better analogues as potent anti-tubercular agents in future. The third approach was activity guided isolation and structure determination of the active molecules identified from the screening of in-house natural product library on HTS protocol developed using *MtbGS*. The fourth approach of the thesis was focused on utilization of nitrogen sources as essential nutrient for its survival during aerobic and anaerobic stage of *Mycobacterium tuberculosis*. This study could lead to a better understanding on how to use nitrogen metabolism for the development of inhibitors against of *Mycobacterium tuberculosis.*

Earlier studies on *MtbGS* had already indicated it as a possible target for the development of drug against the disease. GS is an essential enzyme for the survival of *Mycobacterium tuberculosis.* This enzyme is secreted by all pathogenic mycobacteria.

It was suggested that this extracellular enzyme functions in the regulation of ammonia in the phagosomal compartment to inhibit phagosome–lysosome fusion and phagosome acidification, as well as synthesis of cell wall component poly (L-glutamic - acid glutamine) complex that is found only in pathogenic mycobacterial cell wall. The extracellular localization of *MtbGS* was associated with its involvement in the synthesis of a cell wall component poly (L-glutamic acid- glutamine complex). Its extracellular function had made it an attractive target for drug development against *Mycobacterium tuberculosis*. Inhibition of extracellular enzyme activity in *M. tuberculosis* culture, in infected THP-1 cell as well as in, *in vivo* condition of guinea pig model by the substrate analogues, showed the potential of GS as a drug target against TB. The extracellular location means that drugs aimed at GS need not penetrate the mycobacterial cell wall. The crystal structure of the enzyme had also been elucidated along with the proposed transition state analogue of L-MSO. The enzyme activity was monitored by Transfer reaction as well as Biosynthetic reaction.

The screening of a compound library using a robust high-throughput screening (HTS) assay was thought to be the most efficient way of getting lead molecules as potent inhibitors of this enzyme. By using both the reactions catalyzed by *MtbGS*, two HTS protocol has been developed. The in-house compound library consisting of sep box fractions and synthetic molecules was used for validation of the assays. The developed assay was robust and met all the stringent HTS criteria. The screening of the in house samples was done on HTS platform.

Extract of *Byttneria Spp*. was discovered from one such screens having significant anti-tubercular activity against the active stage of the bacilli with promising intracellular

efficacy. One compound from this extract was discovered with significant target based anti-tubercular activity as well as against the growth of *M. tuberculosis* along with their intracellular efficacy.

Considering the importance of glutamine biosynthesis pathway and its inhibition by L-MSO, it became interesting to study the kinetics of L-MSO inhibition in greater detail. Crystallographic studies using L-MSO phosphate a proposed transition state analogue clearly indicated a non-covalent interaction with the enzyme which leads to the conclusion of a tight binding mechanism. In fact, there was no other experimental proof available in favor of this conclusion. In absence of any biochemical or kinetic data, it could not gain the interest to the drug developers from pharmaceutical industry. In order to gain further insight into the mechanism of inhibition by L-MSO, we first determined the irreversibility of the enzyme activity by 1) time dependent measurement of enzyme activity and then 2) regain it by micro-dilution of the assay mix. Our experimental data indicated that dilution of reaction mix to reduce the effective concentration of the inhibitor failed to regain the enzyme activity. Then, we measured the kinetic parameters for this inactivation. This indicated an irreversible nature of enzyme inhibition by L-MSO. In order to further validate the observation, radio-labeled S35 L-MSO was used to investigate the nature of bonding developed between the inhibitor and the enzyme. It was also observed that the binding of the inhibitor with the enzyme was directly proportional to the inhibitor concentration. It was also found that the stoichiometry of inhibitor binding to the enzyme was 1:1. Further studies related to identification of the covalently bound amino acid at the site of the enzyme could be determined by proteomic analysis.

In the context of nitrogen metabolism and use of GS during pathogenesis within the host milieu, a detail investigation was made in this thesis to understand the amino acid utilization as sole nitrogen source of *Mycobacterium tuberculosis* growth. Major obstacle in carrying out this study was the lack of suitable platform to monitor the transport and utilization of different nitrogen sources in anaerobic stage of the bacilli. For this reason, a whole cell based assay in micro-plate format was developed in which the nitrogen source could be changed in the medium. A comparative study of amino acid utilization on three strains of mycobacteria could help in developing better understanding of nitrogen metabolism as well as its use in drug discovery.

ABBREVIATIONS

ATP:	Adenosine triphosphate
ADP:	Adenosine diphosphate
AMP:	Adenosine monophosphate
BCG:	Bacillus Calmette Guerin
CDC:	Centers for Disease Control and Prevention
CFU:	Colony Forming Unit
DMSO:	Dimethyl sulfoxide
DOTS:	Directly observed therapy short course
E. coli:	*Escherichia coli*
EMB:	Ethambutol
FHA:	Fork-Head Associated
GOGAT:	Glutamate Synthase
GDH:	Glutamate Dehydrogenase
Glu~P:	γ - glutamyl phosphate
GS:	Glutamine Synthetase
HCL:	Hydrochloric Acid
HBC:	High-burden countries
HIV:	Human Immunodeficiency Virus
HL-60:	Human promyelocytic leukemia cells
HPLC:	*High Performance Liquid Chromatography*
HXRMA:	Hypoxia induced XTT reduction microplate assay
HSR:	Head Space Ratio
HTS:	High throughput screening
IFN-γ:	Interferon-γ
INH:	Isoniazid
IUATLD:	International Union Against Tuberculosis and Lung Disease
LTBI:	Latent TB Inhibitor
L-MSO:	L-Methionine Sulfoximine
MSO-P:	L-methionine-*S*-sulfoximine phosphate
MBEI:	Mechanism-Based Enzyme Inhibitors
MtbGS:	*Mycobacterium tuberculosis Glutamine Synthetase*
M. bovis:	*Mycobacterium bovis*
MDR:	Multidrug resistance
MIC:	Minimum Inhibitory Concentration
M. smegmatis:	*Mycobacterium smegmatis*
M. tuberculosis:	*Mycobacterium tuberculosis*
MW:	Molecular Weight
NAD:	Nicotinamide adenine dinucleotide
NADH:	Nicotinamide adenine dinucleotide reduced
NADP:	Nicotinamide adenine dinucleotide phosphate
NADPH:	Nicotinamide adenine dinucleotide phosphate reduced
NCE:	New Chemical Entities
NH4:	Ammonia

Nir:	Nitrite Reductase
NO3:	Nitrate
NO2:	Nitrite
NR:	Nitrate Reductase
NO:	Nitric Oxide
OSDD:	Open Source Drug Discovery
PAS:	para-amino salicylic acid
PTB:	Pulmonary tuberculosis
PCR:	Polymerase Chain Reaction
PK/PD:	Pharmacokinetics Pharmacodynamics
PPD:	Purified Protein Derivative
PZA:	Pyrazinamide
RP:	Reverse Phase
RIF:	Rifampicin
SAR:	Structure Activity Relationship
SDS - PAGE:	Sodium Dodecyl Sulphate- Polyacrylamide Gel Electropho
STM:	Streptomycin
StGS:	*Salmonella typhimurium Glutamine Synthetasee*
S/N :	*Signal:Noise*
TCA	*Trichloro Acetic Acid*
TLC:	*Thin Layer Chromatography*
TB:	Tuberculosis
TEM:	Transmission Electron Microscopy
THP-1:	Human acute monocytic leukemia cell line
WHO:	World Health Organization
XRMA:	XTT Reduction Menadione Assay
XDR:	Extremely Drug resistant
XTT:	Reduction of 2, 3-bis [2-methyloxy-4-nitro-5-sulfophenyl]-2H- tetrazolium-5-carboxanilide
ZN:	Ziehl-Neelsen

Publications from thesis

1. Singh U, Panchnadhikar V, Sarkar D. Development of a Simple Assay Protocol for High-Throughput Screening of *Mycobacterium tuberculosis* Glutamine Synthetase for the Identification of Novel Inhibitors. Journal of Biomolecular Screening 2005; 10: 725-729.

2. Singh U, Sarkar D. Development of a simple HTS protocol based on biosynthetic activity of Mycobacterium tuberculosis Glutamine synthetase for the identification of novel inhibitors. Journal of Biomolecular Screening July 2006. 11: 1035-1042

3. Singh U, Joshi S.P,Surpali K, Kulkarni R, Sarkar D. Inhibitory activity of *Byttneria species.* Communicated

4. Singh U, Sarkar D. Biochemical inhibition profile of L-Methionine Sulfoximine – A Selective inhibitor of *Mycobacterium Tuberculosis* Glutamine Synthetase. Comminicated

5. Singh U, Sarkar D. A novel screening method based on menadione mediated rapid reduction of XTT for testing of antimycobacterial agents Communication in second revision with Journal of Microbiological methods

Chapter -1

General points on *Mycobacterium tuberculosis*: Complete story from history of Tuberculosis to modern epidemic

1.1. Classification and Cellular characteristics of *Mycobacterium tuberculosis*

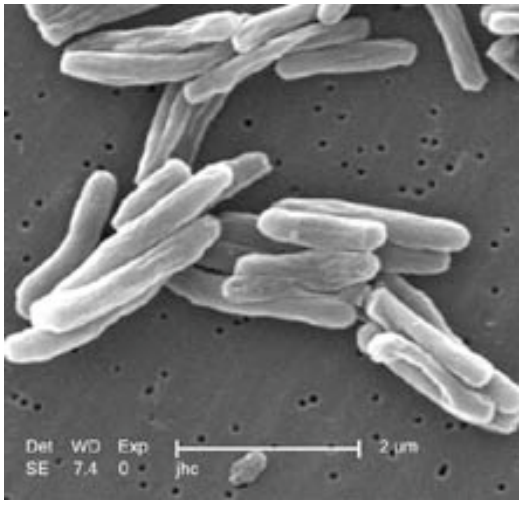

Figure – 1. Scanning Electron Micrograph of Mycobacterium tuberculosis extracted from http://en.wikipedia.org/wiki/Tuberculosis

Domain: Bacteria
Phylum: Actinobacteria
Class: Actinobacteridae
Order: Actinomycetales
Suborder: Corynebacterineae
Family: Mycobacteriaceae
Genus: *Mycobacterium*
Species: *Mycobacterium tuberculosis*

Mycobacterium tuberculosis is a bacterium belonging to the Mycobacterium genus, which is the only genus in the Mycobacteriaceae family, Actinomycetales order and Actinomycetes class (1).

The Mycobacterium genus, one of the most extensively studied bacterial texa, was described by Leham and Neuman in 1896. Its identification is based on the following characteristics a) Shape of the colonies, b) growth rate and c) biochemical reactivity. To date, 71 species have been described within this genus, and they are subdivided in two main groups based on their growth rates (Fast Vs Slow) (2). The majority of the slow growing mycobacterium species are pathogenic for humans and animals

(*Mycobacterium tuberculosis, Mycobacterium absecessus, Mycobacterium fortuitum, Mycobacterium porcinum*). The species responsible for TB in human and for which no animal reservoir are found are *Mycobacterium tuberculosis, Mycobacterium africanum* and *Mycobacterium canactii*. *Mycobacterium tuberculosis* are the main species of human TB, the other species are less frequent in humans (e.g. *M.africanum* is characterized mainly in Africa and *M.canactii* was isolated in a few cases of human TB in East Africa). Furthermore an attenuated strain of *M.bovis BCG* (Calmatte and Guerin 1921) is used as a vaccine for preventing human TB (6). The other species are also isolated specifically in animal, such as *M.microti* which is the agent of rodent TB, *M.caprae*, which predominantly affects cattle, and *M.pinnipeddi*, which has pinnipeds as natural host (3, 4 and 5). These later species can affect other animal and human to a very limited extent. All mycobacterial species are rod shaped (0.2-0.6 μM wide and 1-10 μM) and, non motile, non-encapsulated gram positive aerobes (Growing most successfully in tissues with high oxygen contents such as lungs) or facultative anaerobe (1). They are facultative intracellular pathogen usually infecting mononuclear phagocyte (e.g. Macrophage). As concluded from its genome, *M. tuberculosis* has the potential to manufacture all of the machinery necessary to synthesize its essential vitamins, amino acids and enzyme cofactors (1). *M. tuberculosis* has an unusual cell wall, with an additional layer beyond the peptidoglycan layer, which is rich in unusual lipids, glycolipids and polysaccharides (1). These bacteria can be detected by optical microscopy after Ziehl-Neelsen (ZN) acid fast stain of sputum from a person with active TB. Bacilli appear as thin red rods in the microscopic field, where all other materials in the sputum pick up the blue counter-stain (1).

1.2 Current TB epidemic

Over the centuries, tuberculosis has accounted for more human misery, suffering, loss of earnings, and failure of socio-economic development than any other disease. TB is one of the most common infectious diseases known to man. About 32% of the world's

population (6) or 1.86 billion people are infected with *M. tuberculosis*. Every year, approximately 8 million of these infected people develop active TB, and almost 2 million of these will die from the disease (6). TB is the world's longest running catastrophe, killing more than 200 people every hour and more than 5000 every day. In India alone, one person dies of TB every minute. Each of the 3.5 million new infectioon that occur each year might transmit TB to more than 20 other people (6).

TABLE 1.2
Estimated epidemiological burden of TB, 2007

		INCIDENCE[a]				PREVALENCE[a]		MORTALITY				
		ALL FORMS		SMEAR-POSITIVE		ALL FORMS		HIV-NEGATIVE		HIV-POSITIVE		HIV PREV. IN INCIDENT TB CASES[b]
	POPULATION 1000s	NUMBER 1000s	PER 100 000 POP PER YEAR	NUMBER 1000s	PER 100 000 POP PER YEAR	NUMBER 1000s	PER 100 000 POP PER YEAR	NUMBER 1000s	PER 100 000 POP PER YEAR	NUMBER 1000s	PER 100 000 POP PER YEAR	%
1 India	1 169 016	1 962	168	873	75	3 305	283	302	26	30	2.5	5.3
2 China	1 328 630	1 306	98	585	44	2 582	194	194	15	6.8	0.5	1.9
3 Indonesia	231 627	528	228	236	102	566	244	86	37	5.4	2.4	3.0
4 Nigeria	148 093	460	311	195	131	772	521	79	53	59	40	27
5 South Africa	48 577	461	948	174	358	336	692	18	38	94	193	73
6 Bangladesh	158 665	353	223	159	100	614	387	70	44	0.4	0.3	0.3
7 Ethiopia	83 099	314	378	135	163	481	579	53	64	23	28	19
8 Pakistan	163 902	297	181	133	81	365	223	46	28	1.4	0.9	2.1
9 Philippines	87 960	255	290	115	130	440	500	36	41	0.3	0.3	0.3
10 DR Congo	62 636	245	392	109	174	417	666	45	72	6.0	10	5.9
11 Russian Federation	142 499	157	110	68	48	164	115	20	14	5.1	3.6	16
12 Viet Nam	87 375	150	171	66	76	192	220	18	20	3.1	3.5	8.1
13 Kenya	37 538	132	353	53	142	120	319	10	26	15	39	48
14 Brazil	191 791	92	48	49	26	114	60	5.9	3.1	2.5	1.3	14
15 UR Tanzania	40 454	120	297	49	120	136	337	12	29	20	49	47
16 Uganda	30 884	102	330	42	136	132	426	13	41	16	52	39
17 Zimbabwe	13 349	104	782	40	298	95	714	6.9	52	28	213	69
18 Thailand	63 884	91	142	39	62	123	192	10	15	3.9	6.0	17
19 Mozambique	21 397	92	431	37	174	108	504	10	45	17	82	47
20 Myanmar	48 798	83	171	37	75	79	162	5.4	11	0.9	1.9	11
21 Cambodia	14 444	72	495	32	219	96	664	11	77	1.8	13	7.8
22 Afghanistan	27 145	46	168	21	76	65	238	8.2	30	0.0	0	0
High-burden countries	**4 201 761**	**7 423**	**177**	**3 245**	**77**	**11 301**	**269**	**1 058**	**25**	**339**	**8.1**	**14**
AFR	792 378	2 879	363	1 188	150	3 766	475	357	45	378	48	38
AMR	909 820	295	32	157	17	348	38	33	3.6	7.9	0.9	11
EMR	555 064	583	105	259	47	772	139	97	17	7.7	1.4	3.5
EUR	889 278	432	49	190	21	456	51	56	6.3	8.1	0.9	9.8
SEAR	1 745 394	3 165	181	1 410	81	4 881	280	497	28	40	2.3	4.6
WPR	1 776 440	1 919	108	859	48	3 500	197	276	16	15	0.8	2.7
Global	**6 668 374**	**9 273**	**139**	**4 062**	**61**	**13 723**	**206**	**1 316**	**20**	**456**	**6.8**	**15**

[a] Incidence and prevalence estimates include TB in people with HIV.
[b] Prevalence of HIV in incident TB cases of all ages.

Table 1 Summary of estimated epidemiological burden of TB, 2006. Extracted from Global tuberculosis control 2009 Epidemiology, strategy and finance.

TB case notifications are soaring in the newly independent states of the former Soviet Union (6). HIV is fueling the TB epidemic in many countries in sub-Saharan Africa (6). Five-fold increases in TB incidence have been seen in Kenya in spite of a well-functioning control program and good cure rates. In Zambia and Zimbabwe, more than

70% of TB patients are also infected with HIV, and case notifications are rising. HIV and TB together account for nearly half of the adult mortality in the worst affected countries. With the global spread of HIV, especially in Asia, similar increases in TB incidence rates and mortality are to be feared in countries like India, which is home to 4 million people with TB and now also to 3.5 million HIV infected individuals, the largest number of any single country. Moreover, there has been a recent and disturbing increase in the number of TB cases that are caused by organisms that are resistant to the two most important drugs, Isoniazid and Rifampin. A 1994-97 survey found that rates of Multi Drug Resistant -TB (MDR –TB) were alarmingly high in several areas of the world (6). A more recent survey in 72 countries suggested that the MDR-TB problem is more widespread than previously thought and likely is worsening (6). For example, 5.8% of TB cases in Iran are MDR, as are 10.8% in China and 14.1% in Estonia. MDR-TB appears to be especially serious in the Russian Federation, where it has spread in prisons and throughout the general population (6). Although the estimated rate of MDR-TB in newly diagnosed patients worldwide has been estimated to be less than 2%, new data suggest that the rate is increasing (6). If not prevented and controlled, MDR-TB is likely to become more widespread in other areas of the world, including developed countries in Western Europe and in the United States, Canada, and Australia. Widespread use of bacille Calmette-Guerin vaccine, which is the only available TB vaccine, has limited impact on the global burden of TB. Although BCG vaccination does prevent the development of severe and fatal forms of TB in young children, it has not been effective in reducing the greater numbers of infectious pulmonary cases in adults (7). Recently there has been increased attention given to the development of a new effective TB vaccine, which is thought to be essential to the eventual elimination of TB (8). However, this effort might take 25 years or more, and in that time interval 50 million lives will be lost due to TB (9).

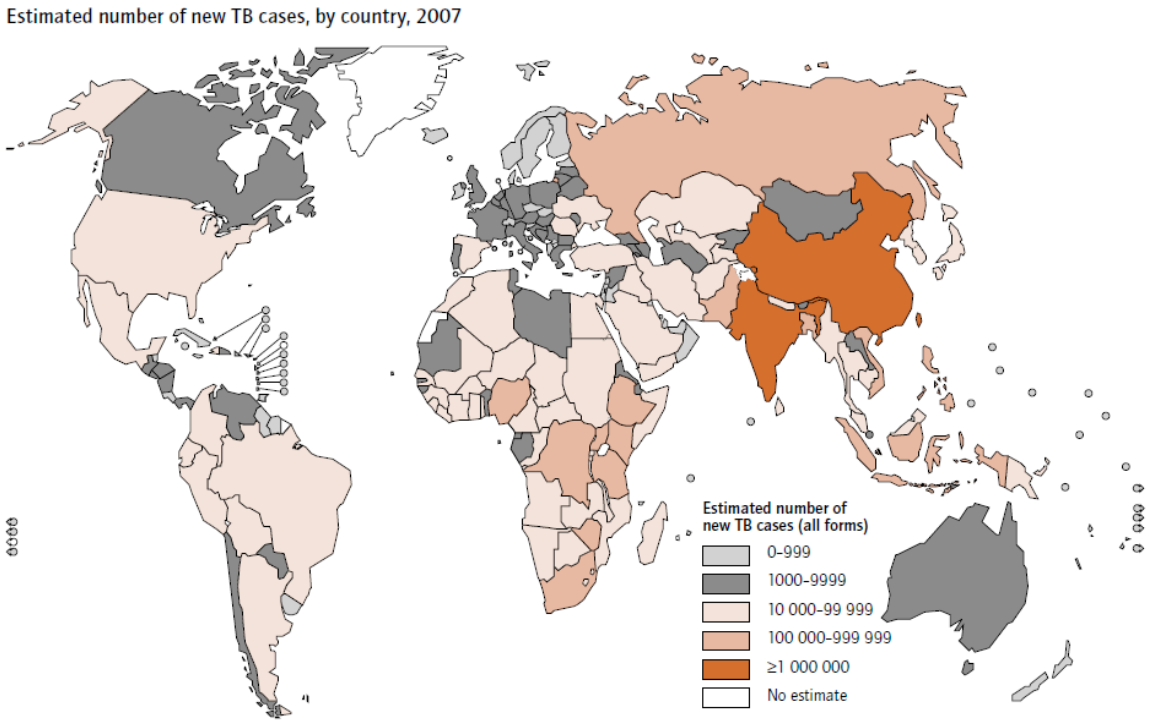

Figure – 2 Estimated number of new TB cases, by country, 2007

Map showing the 22 high-burden countries (HBC) that according to WHO account for 80% of all new TB cases arising each year. The Global Plan is especially aimed at these countries. Extracted from Global tuberculosis control 2009 Epidemiology, strategy and finance**.**

1.3 History of Tuberculosis

1.3.1 Early History of Tuberculosis

Tuberculosis probably occurred as an endemic disease among animals long before it affected humans (Steele and Ranney, 1958). *Mycobacterium bovis* was the most likely infecting organism, and the first human infections may have been with *M.bovis*. Since *M.tuberculosis* infects all primate species, it is also possible that this species existed in subhuman primates before it became established in humans (10).

As centuries and millennia passed, human beings began to live in larger and larger communities, and with this shift came environmental changes that were associated with a change in the delicate balance between humans and the tubercle bacillus. Tuberculosis probably occurred as a sporadic and unimportant disease of human in their early history. Epidemic spread began slowly with increasing population density. This spread and the selective pressure it has exerted, have occurred at different times around the globe. The epidemic slowly spread worldwide as a result of infected Europeans travelling to and colonizing distant sites (10). In the 1700s and early 1800s, tuberculosis prevalence peaked in Western Europe and the United States and was undoubtedly the largest cause of death (1), and 100 to 200 years later, it had spread in full force to Eastern Europe, Asia, Africa and South America. Within a particular population in a defined geographic area, the tuberculosis epidemic reached its peak within 50 to 75 years after its beginning and then slowly declined, possibly as the more resistant host survivors reproduced (10).

1.4 Tuberculosis and the drawing of medical science

From the time of Hippocrates, tuberculosis was known as “phthisis” a term derived from the Greek for “wasting away”. The swollen glands of the neck were known as “scrofula,” and because crowned kings of England and France were believed to have special healing powers, the most desired treatment of this “King’s Evil”. Tuberculosis of the skin was termed lupus vulgaris, and that of the spine was termed Pott’s disease. The vertebral fusion and deformity of the spine that characterize Pott’s disease have enabled historians to establish the existence of tuberculosis in mummies dating from 2000 to 4000 B.C (10).

As Europe emerged from the Dark Ages, there was a renaissance not only of the arts but also of medical science. Observant scientist described their world and explored its nature and mechanism. This European intellectual renaissance began in an era of extraordinarily high tuberculosis prevalence fueled by the industrial revolution and the grinding poverty it engendered in its huddled masses. Hence, it is not surprising that

many fundamental concepts of biology emerged in the context of inquiry about the nature of tuberculosis (10).

1.5 Transmission and Multiplication of *M. tuberculosis*

TB is considered a disease with an *inter-human transmission.* Tuberculous bacilli are spread out by infected patients coughing, sneezing, or speaking, and can be inhaled by another individual in close contact. The inhalation of these sprays, called Flugge's droplets – small aerodynamics particles – presents a risk of tuberculosis infection. These particles can also remain in the air and play the role of reservoir. These particles are small enough to be able to reach the lower respiratory tract. Indeed, among the infectious particles inhaled, only those with two or three bacilli can reach the bronchic cells, the largest ones are stopped upstream and eliminated (11). The success of such infection and the development of the pulmonary form if TB depends on four successive stages: bacilli phagocytosis, intracellular multiplication, the stationary stage, and the pulmonary form of TB. These different stages can evolve into different outcomes: spontaneous healing, acute tuberculosis, latent infection and reactivation or re-infection (11).

(i) Bacilli phagocytosis :

The bacilli that reach the pulmonary alveolus are phagocyted by the mature macrophages. This step which takes place in the first week following particle inhalation is the first stage of infection, and it depends on two main factors: the bacillus virulence and the bactericide activity of the macrophage. In general, the bacteria are destroyed by the alveolar macrophages and the infection is stopped at this stage, otherwise they begin an intracellular cycle of multiplication (11).

(ii) Intracellular multiplication :

This second stage occurs between the 7th and the 21st day. It corresponds to intracellular bacilli multiplication in the macrophage alveoli and is also called the

symbiotic stage. Indeed, the bacteria that are not destroyed by the alveolar macrophages will multiply. They are released after cellular lysis, and can thus infected other circulating macrophages and continue their multiplication. At the end of this stage, due to a symbiosis event, a huge number of macrophages and bacilli are concentrated at the level of early pulmonary lesions (11).

(iii) Stationary stage :

Following the induction of the immune response of the host, practically cell-mediated immunity, bacterial growth becomes stationary. This is the third stage of the infection called *primary infection (11).* Because of delayed-type hypersensitivity, the macrophages in which bacilli multiply are destroyed. Bacterial toxins and cellular products are released, and this leads to the formation of solid caseous necrosis (11), where pseudo-equilibrium settles between inactivated and mature macrophages. At this stage, either the number of infected cells in the caseous center decreases, if the released bacilli are phagocyted by the mature macrophages or it increases if the bacilli multiply in the inactivated macrophages. Thus, the progression of the disease depends on which macrophage type prevails (12, 13). At this stage, bacilli may become dormant and never induce TB at all, which is referred to as a latent infection that is detected only by a positive tuberculin skin test, or the latent organism can eventually begin to grow, with resultant clinical disease, known as TB reactivation.

(iv) Pulmonary form of TB (PTB):

When the equilibrium between the inactivated and mature macrophages is broken, the infection reaches the last stages and the disease called PTB. This step is characterized by the liquefaction of the caseous center, leading to the formation of a cavity detected by pulmonary radiography. The liquefied material present in this cavity constitutes an excellent growth media for the bacteria, and macrophages do not survive in this environment. At this stage of the disease, the person becomes

contagious by releasing the bacilli into the air. Furthermore, without treatment, this individual can develop a chronic TB, presumably leading to death (11).

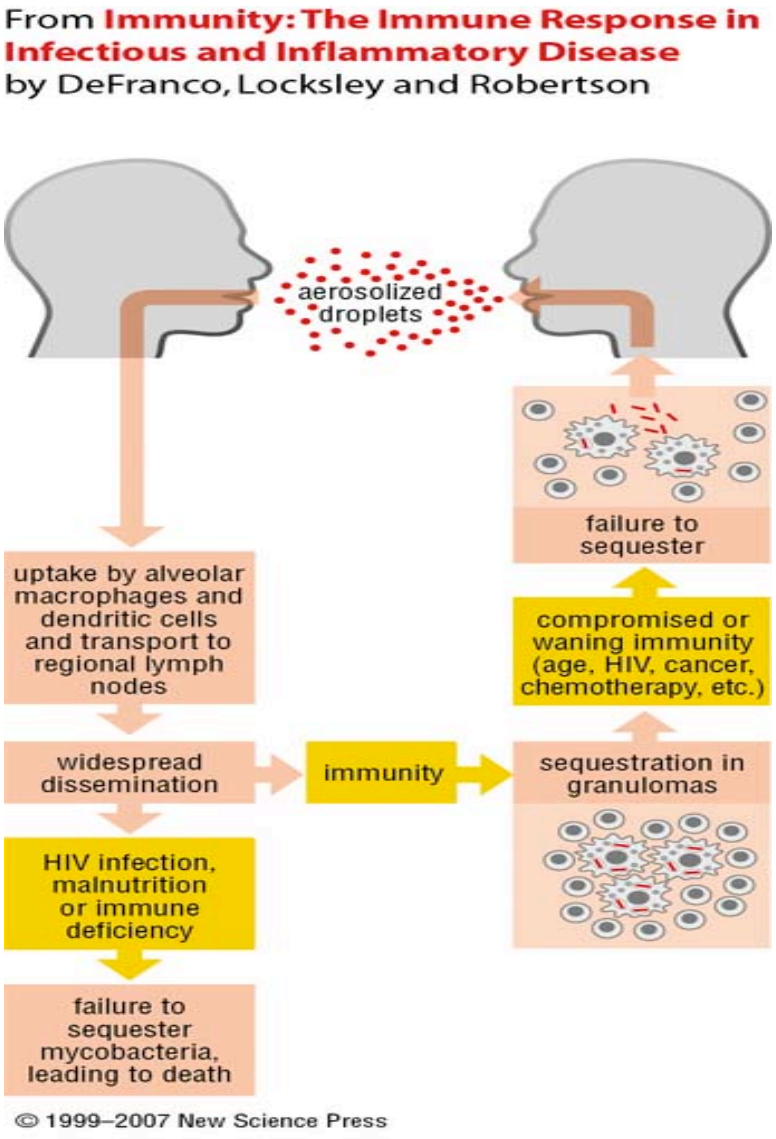

Figure – 3 Tuberculosis begins when droplet nuclei reach the alveoli.

When a person inhales air that contains droplets most of the larger droplets become lodged in the upper respiratory tract (the nose and throat), where infection is unlikely to develop. However, the smaller droplet nuclei may reach the small air sacs of the lung (the alveoli), where infection begins

1.6 Clinical and Subclinical TB

The term "TB infection" refers to a positive TB skin test with no evidence of active disease: this state is also called latent infection. "TB disease" refers to cases that have a positive acid-fast smear or culture for *M.tuberculosis* or radiographic and clinical presentation of TB (11).

The most common clinical manifestation of TB is pulmonary disease; nevertheless, extrapulmonary TB can also occurs, but is little or not contagious. Without minimizing the importance of extra pulmonary TB, which currently accounts for 20 % of reported cases of TB, we will focus here only on the cases of pulmonary infection. Furthermore, as described above, although some people develop active TB disease after infection, almost all TB infection is asymptomatic and remains latent (14).

A) Active disease

A patient with PTB presents with the symptoms of chronic or persistent cough and sputum production. If the disease is at an advance stage, the sputum will contain blood, and the patient will be diagnosed with lack of appetite, weight loss, fever, night sweats and thoracic pains. Patients with PTB are classified in different categories because a specific treatment is needed for each category (11). The main categories are as follows:

- **New case**: TB in a patient who either has never received anti-tuberculosis treatment or started a treatment for less than 1 month.
- **Relapse:** TB already treated and declared cured after sufficient treatment time, which has become active again.
- **Chronic TB:** A case of relapse from which the microscopic exam of expectation remains positive after a second complete treatment.

- **Primary resistance case**: This characterizes the bacilli that are resistant to treatment, although patients have never been treated by anti-tuberculous drugs.
- **Multidrug resistance case**: *M.tuberculosis* resistant at least to both major anti-tubercular drugs (Isoniazid and rifampicin).
- **Extremely Drug resistance cases:** XDR TB is characterized by resistance developed by two most important anti - TB drugs (isoniazid and rifampin) plus additional resistance to at least one fluoroquinolone and one injectable antibiotic.

B) Latent diseases

About 90% of people who get infected with TB develop a latent TB infection, which means the infecting bacteria are alive in the body, but inactive. People who have latent infections do not have TB symptoms and cannot spread the infection to others, but they are at risk of developing an active infection that is both symptomatic and contagious. About 3% to 5% of latent TB becomes active TB in the first year and about 5 - 15% after that (11).

1.7 Diagnosis of *M. tuberculosis* species

Tuberculosis is diagnosed by finding *Mycobacterium tuberculosis* bacteria in a clinical specimen taken from the patient. A complete medical evaluation for tuberculosis (TB) must include a medical history, a physical examination, a chest X-ray and microbiological examination (of sputum or some other appropriate sample) (15). It may also include a tuberculin skin test, other scans and X-rays, surgical biopsy. The medical history includes obtaining the symptoms of pulmonary TB: productive, prolonged cough of three or more weeks, chest pain, and hemoptysis. Systemic symptoms include low grade remittent fever, chills, night sweats, appetite loss, weight loss, easy fatigability, and production of sputum that starts out mucoid but changes to purulent. Other parts of the medical history include prior TB exposure, infection or disease; past TB treatment; demographic risk factors for TB; and medical conditions that increase

risk for TB disease such as HIV infection. Tuberculosis should be suspected when a persistent respiratory illness in an otherwise healthy individual does not respond to regular antibiotics (15). A physical examination is done to assess the patient's general health and find other factors which may affect the TB treatment plan. It cannot be used to confirm or rule out TB. A definitive diagnosis of tuberculosis can only be made by culturing *Mycobacterium tuberculosis* organisms from a specimen taken from the patient (most often sputum, but may also include pus, CSF, biopsied tissue, etc). A diagnosis made other than by culture may only be classified as "probable" or "presumed" (16).

Sputum, smears and cultures should be done for acid-fast bacilli testing if the patient is producing sputum (16). The preferred method for this is fluorescence microscopy (auramine-rhodamine staining), which is more sensitive than conventional Ziehl-Neelsen staining (17). If no sputum is being produced, specimens can be obtained by inducing sputum, gastric washings, a laryngeal swab, bronchoscopy with bronchoalveolar lavage, or fine needle aspiration of a collection. A comparative study found that inducing three sputum samples is more sensitive than three gastric washings (18).

In some cases, a specimen cannot be supplied by sputum culture or bronchoscopy. In these cases, a biopsy of tissue from the suspected system can be obtained by mediastinoscopy. Other mycobacteria are also acid-fast. If the smear is positive, PCR or gene probe tests can distinguish *M. tuberculosis* from other mycobacteria. Even if sputum smear is negative, tuberculosis must be considered and is only excluded after negative cultures.

Many types of culture media are available (19). Traditionally, media used for mycobacterial growth are Löwenstein-Jensen (LJ), Kirchner, or Middlebrook media (7H9, 7H10, and 7H11). From the pattern of growth, the AFB can be distinguished from other various forms of mycobacteria, although results from this may take four to eight weeks for a conclusive answer. Nowadays, new automated systems are available

for monitoring growth of AFB that are faster which includes MB/BacT, BACTEC 9000, and the Mycobacterial Growth Indicator Tube (MGIT). The Microscopic Observation Drug Susceptibility assay culture may also be a faster and more accurate method (20).

1.7.1 Chest X-ray

Tuberculosis creates cavities visible in x-rays in the patient's right upper lobe (figure – 4). In active pulmonary TB, infiltrates or consolidations and/or cavities are often seen in the upper lungs with or without mediastinal or hilar lymphadenopathy or pleural effusions (tuberculous pleurisy). However, lesions may appear anywhere in the lungs. In disseminated TB a pattern of many tiny nodules throughout the lung fields is common. In HIV and other immunosuppressed persons, any abnormality may indicate TB or the chest X-ray may even appear entirely normal (16).

Figure – 4 The Chest X-ray of a patient suffering with far-advanced tuberculosis. The picture is extracted from http://en.wikipedia.org/wiki/File:Tuberculosis-x-ray-1.jpg

A variant of the chest X-Ray, abreugraphy (from the name of its inventor, Dr. Manuel Dias de Abreu) was a small radiographic image, also called miniature mass radiography (MMR) or miniature chest radiograph. Though its resolution is limited (it doesn't allow the diagnosis of lung cancer, for example) it is sufficiently accurate for diagnosis of tuberculosis.

1.7.2 Mantoux test

The Mantoux test (also known as the Mantoux screening test, Tuberculin Sensitivity Test, Pirquet test, or PPD test for Purified Protein Derivative) is a diagnostic tool for tuberculosis (Figure - 5). It is one of the two major tuberculin skin tests used in the world, largely replacing multiple-puncture tests such as the Tine test. Until 2005, the Heaf test was used in the United Kingdom, but the Mantoux test is now used. The Mantoux test is also used in Australia, Canada, Hungary, Poland, Russia, The Netherlands, Spain, Portugal, South Africa and the United States and is endorsed by the American Thoracic Society and Centers for Disease Control and Prevention (CDC). It was also used in the USSR and is now prevalent in most of the former Soviet states (21,22).

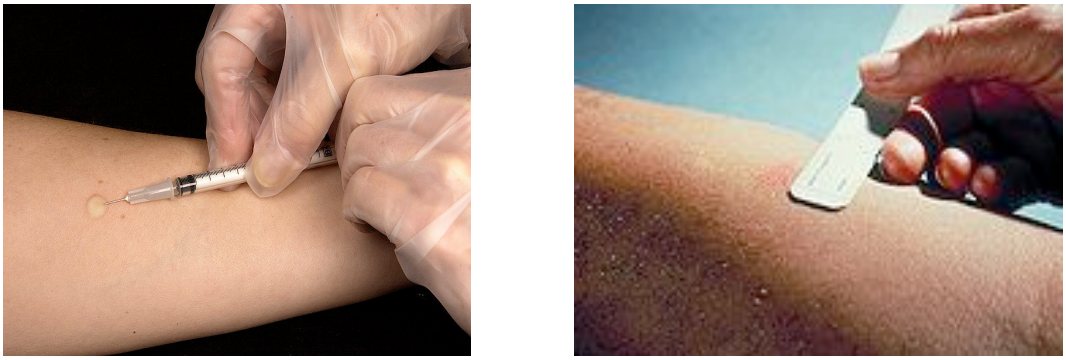

Figure – 5 Skin Testing is performed as the tuberculin or Mantoux test.

PPD (purified protein derivative) is employed as the test antigen in the **Mantoux test**. PPD is generated by boiling a culture of M. tuberculosis. The size of indurations is

measured 48–72 hours later. The lesion is characterized by erythema (redness) and swelling and induration (raised and hard). Erythema (redness) should not be measured.

1.7.3 BCG vaccine and tuberculin skin test

There is disagreement on the use of the Mantoux test on people who have been immunized with BCG. The US recommendation is that in administering and interpreting the Mantoux test, previous BCG vaccination should be ignored. The UK recommendation is that interferon-γ tests should be used to help interpret positive tuberculin tests, also, the UK do not recommend serial tuberculin skin testing in people who have had BCG (a key part of the US strategy). In general the US approach is likely to result in more false positives and more unnecessary treatment with potentially toxic drugs; the UK approach is as sensitive in theory and should also be more specific, because of the use of interferon-γ tests (23).

Under the US recommendations, latent TB infection (LTBI) diagnosis and treatment for LTBI is considered for any BCG-vaccinated person whose skin test is 10 mm or greater, if any of these circumstances are present:

- Was in contact with another person with infectious TB
- Was born or has resided in a high TB prevalence country
- Is continually exposed to populations where TB prevalence is high.

1.8 Immunology of Tuberculosis

This organism is spread easily, and pulmonary infection usually results from inhalation of small droplets of respiratory secretions containing a few bacilli. The inhaled bacilli are ingested by alveolar macrophages and are able to survive and multiply intracellularly by inhibiting formation of phagolysosomes (24). When the infected macrophages lyse, as they eventually do, large numbers of bacilli are released. A cell-

mediated response involving CD4+ T cells, which is required for immunity to tuberculosis, may be responsible for much of the tissue damage in the disease. CD4+ T-cell activity is the basis for the tuberculin skin test to the purified protein derivative (PPD) from *M. tuberculosis.* Upon infection with *M. tuberculosis,* the most common clinical pattern, termed pulmonary tuberculosis, appears in about 90% of those infected. In this pattern, CD4+ T cells are activated within 2–6 weeks after infection, inducing the infiltration of large numbers of activated macrophages (24). These cells wall off the organism inside a granulomatous lesion called a tubercle. A tubercle consists of a few small lymphocytes and a compact collection of activated macrophages, which sometimes differentiate into epithelioid cells or multinucleated giant cells. The massive activation of macrophages that occurs within tubercles often results in the concentrated release of lytic enzymes. These enzymes destroy nearby healthy cells, resulting in circular regions of necrotic tissue, which eventually form a lesion with a caseous (cheese like) consistency (Figure – 6).

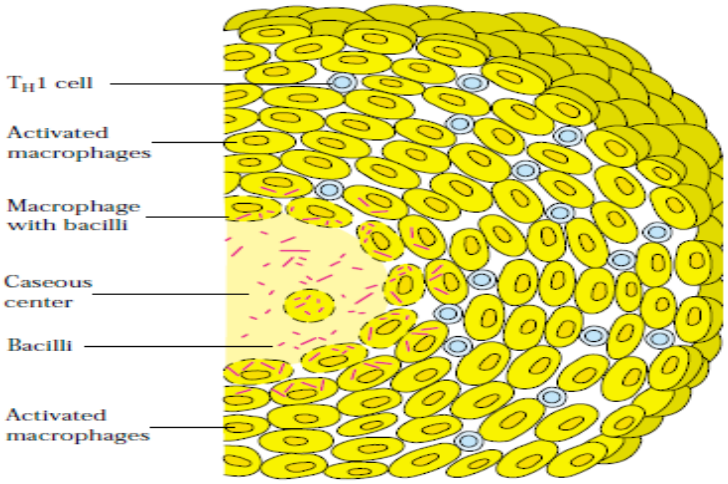

Figure – 6 When these caseous lesions heal, they become calcified and are readily visible on x-rays, where they are called Ghon complexes. Extracted from http://en.wikipedia.org/wiki/Tuberculosis

As these caseous lesions heal, they become calcified and are readily visible on x-rays, where they are called Ghon complexes. As the activated macrophages suppress proliferation of the phagocytosed bacilli, infection is contained. Cytokines produced by CD4+ T cells (Th1 subset) play an important role in the response by activating macrophages, so that they are able to kill the bacilli or inhibit their growth. The role of IFN-γ in the immune response to mycobacteria has been demonstrated with knockout mice lacking IFN-γ. These mice died when they were infected with an attenuated strain of mycobacteria (BCG), whereas IFN-γ normal mice survive (23). Recent studies have revealed high levels of IL-12 in the pleural effusions of tuberculosis patients. The high levels of IL-12, produced by activated macrophages, are not surprising; given the decisive role of IL-12 in stimulating TH1 mediated responses (Figure 7). In mouse models of tuberculosis, IL-12 has been shown to increase resistance to the disease. Not only does IL-12 stimulate development of TH1 cells, but it also may contribute to resistance by inducing the production of chemokines that attract macrophages to the site of infection (24). When IL-12 is neutralized by antibody to IL-12, granuloma formation in tuberculous mice is blocked. The CD4+ T-cell–mediated immune response mounted by the majority of people exposed to *M. tuberculosis* thus controls the infection and later protects against re-infection. However, about 10 % of individuals infected with *M. tuberculosis* follow a different clinical pattern: the disease progresses to chronic pulmonary tuberculosis or extra-pulmonary tuberculosis. This progression may occur years after the primary infection. In this clinical pattern, accumulation of large concentrations of mycobacterial antigens within tubercles leads to extensive and continual chronic CD4+ T-cell activation and ensuing macrophage activation. The resulting high concentrations of lytic enzymes cause the necrotic caseous lesions to liquefy, creating a rich medium that allows the tubercle bacilli to proliferate extracellularly. Eventually the lesions rupture, and the bacilli disseminate in the lung and/or are spread through the blood and lymphatic vessels to the pleural cavity, bone, urogenital system, meninges, peritoneum, or skin. Tuberculosis is treated with several drugs used in combination, including isoniazid, rifampin, streptomycin, pyrazinamide, and ethambutol. The combination therapy of isoniazid and rifampin has been particularly effective (24). The intracellular growth of *M. tuberculosis* makes it difficult

for drugs to reach the bacilli. For this reason, drug therapy must be continued for at least 9 months to eradicate the bacteria. Some patients with tuberculosis do not exhibit any clinical symptoms, and some patients with symptoms begin to feel better within 2–4 weeks after treatment begins. To avoid the side effects associated with the usual antibiotic therapy, many patients, once they feel better, stop taking the medications long before the recommended treatment period is completed. Due to incomplete treatment organisms may not eradicate and that are somewhat resistant to the antibiotics or a multidrug-resistant strain can emerge. Noncompliance with required treatment regimes, one of the most troubling aspects of the large number of current tuberculosis cases, clearly compromises efforts to contain the spread of the disease (24).

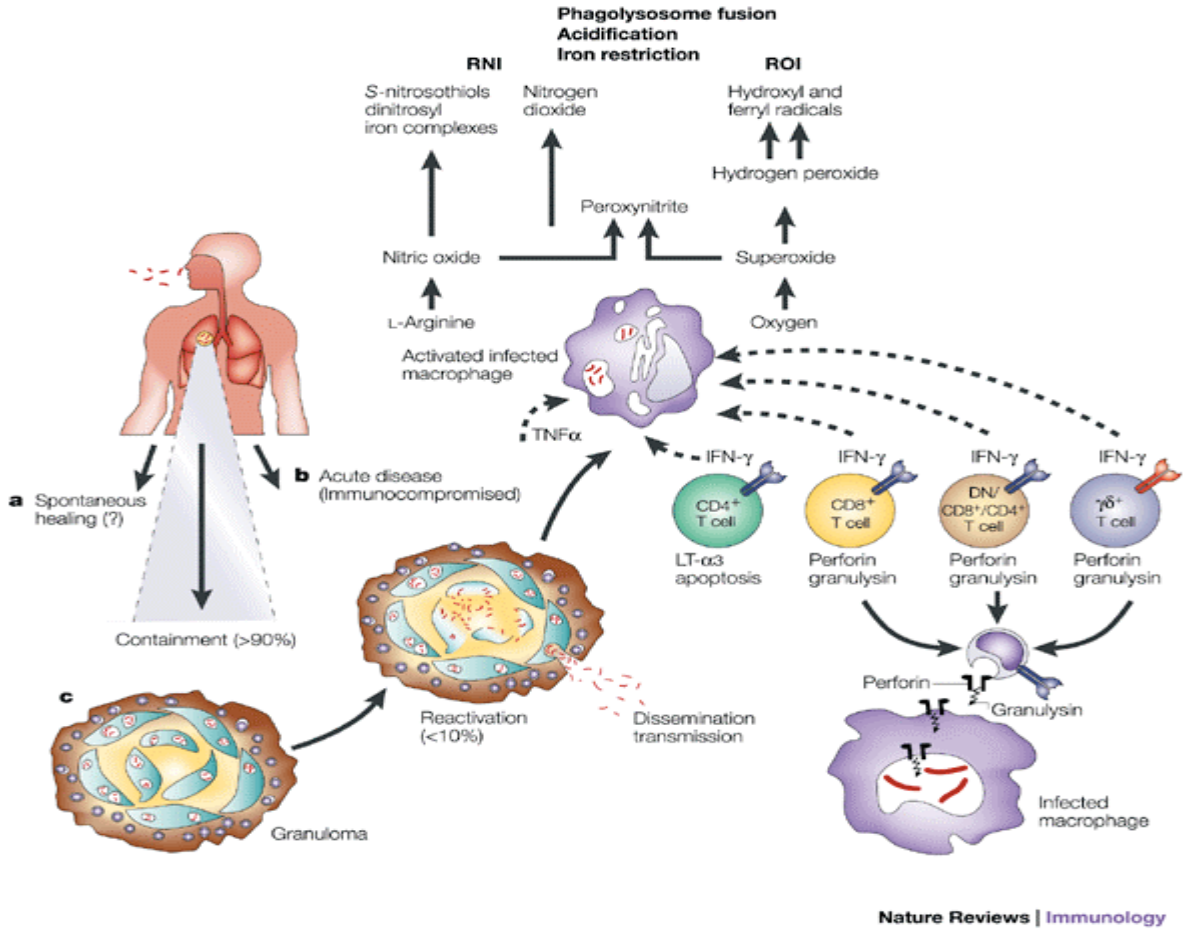

Figure – 7 There are three potential outcomes of infection of the human host in *Mycobacterium tuberculosis*. a) The frequency of abortive infection resulting in spontaneous healing is unknown, but is assumed to be minute. **b**) In the immuno-compromised host, disease can develop directly after infection. **c**) In most cases, mycobacteria are initially contained and disease develops later as a result of reactivation. The granuloma is the site of infection, persistence, pathology and protection. Effecter T cells (including conventional CD4+ and CD8+ T cells, and unconventional T cells, such as γ - T cells, and double-negative or CD4/CD8 single-positive T cells that recognize antigen in the context of CD1) and macrophages participate in the control of tuberculosis. Interferon-γ (IFN-γ) and tumor-necrosis factor-α (TNF-α), produced by T cells, are important macrophage activators. Macrophage activation permits phagosomal maturation and the production of antimicrobial molecules such as reactive nitrogen

intermediates (RNI) and reactive oxygen intermediates (ROI). Extracted from Nature reviews immunology Volume 1 October 2001

1.9 Treatment of tuberculosis

Administration of a single drug often leads to the development of a bacterial population resistant to that drug; effective regimens for the treatment of TB must contain multiple drugs to which the organisms are susceptible. When two or more drugs are used simultaneously, each helps prevent the emergence of tubercle bacilli resistant to the others. However, when the *in vitro* susceptibility of a patient's isolate is not known, which is generally the case at the beginning of therapy, selecting two agents to which the patient's isolate is likely to be susceptible can be difficult, and improper selection of drugs may subsequently result in the development of additional drug-resistant organisms. Hence, tuberculosis is usually treated with four different antimicrobial agents. The course of drug therapy usually lasts from 6 - 9 months. The most commonly used drugs are rifampin (RIF) isoniazid (INH), pyrazinamide (PZA) and ethambutol (EMB) or streptomycin (SM). When adherence with the regimen is assured, this four-drug regimen is highly effective. Based on the prevalence and characteristics of drug - resistant organisms, at least 95% of patients will receive an adequate regimen (at least two drugs to which their organisms are susceptible) if this four-drug regimen is used at the beginning of therapy (25). Furthermore, a patient who is treated with the four-drug regimen, but who defaults therapy, is more likely to be cured and not relapse when compared with a patient treated for the same length of time with a three-drug regimen. Widespread use of bacille Calmette-Guerin vaccine, which is the only available TB vaccine, has had limited impact on the global burden of TB. Although BCG vaccination does prevent the development of severe and fatal forms of TB in young children, it has not been effective in reducing the greater numbers of infectious pulmonary cases in adults (25). Recently there has been increased attention given to the development of a new effective TB vaccine, which is thought to be essential to the eventual elimination of TB (26). However, this effort might take 25 years or more, and in the interval 50 million lives will be lost to TB.

1.10 Current status of TB control: DOTS

In response to the global TB epidemic, the WHO has developed an effective control strategy largely based on the pioneering work of the BMRC and the IUATLD. This strategy is known as DOTS (directly observed treatment, short course). The essential elements of DOTS are as follows:

1) Strong government commitment to TB control
2) Diagnosis by smear microscopy (or by culture where resources permit)
3) Standardized short course chemotherapy with directly observed treatment for at least the first 2 months
4) Secure supply of safe, high-quality drugs
5) Individual reporting of treatment outcome and monitoring of programme performance.

WHO's strategy has been adopted by high-burden countries at a remarkable rate. Although it was used by only 10 countries in 1990, DOTS had been adopted by 119 countries by end 1998, (27) including all 22 of the high-burden countries that account for 80% of the world's TB burden. Some 21% of all TB cases are now treated under DOTS program. Although DOTS is highly effective 82% of patients managed under DOTS in 1997 in the 22 countries with the highest TB burden were successfully treated (28) its implementation has been slow and overall coverage is low, estimated at only 28% worldwide in 1998. Moreover, DOTS is cumbersome and labor intensive, particularly because currently available anti-TB drugs require minimum treatment duration of 6 months. Even if WHO achieves its treatment targets under DOTS by the year 2010, it will have prevented only 23% (48 million) of the TB cases predicted between 1998 and 2020.

1.11 Initial development of TB drugs

Following the discovery of Streptomycin (STR) in 1944, researchers demonstrated its efficacy against TB in mice and guinea pigs. The first report of STR's clinical efficacy came in 1945 from a small, uncontrolled series of patients with progressive TB at the Mayo Clinic in the United States (29). In 1947, the BMRC and the USPHS began the first randomized, controlled trials of STR, with the BMRC reporting its results 1 year later (30). These studies demonstrated STR's remarkable ability to reduce mortality and improve clinical status. However, monotherapy with STR led to drug-resistant TB in a high proportion of patients, whose ultimate fate was little better than that of patients who did not receive STR (31). The ability of a second drug, para-amino salicylic acid (PAS), to prevent the development of resistance to STR was demonstrated in several studies by the BMRC beginning in 1948. The main aim of subsequent work was to develop regimens that prevented the development of drug-resistant TB. The next major advance in TB treatment occurred in 1952 with the initial report of a BMRC study of Isoniazid (INH) (32). During the next several years, a number of studies were undertaken to evaluate combinations of the three available drugs. An IUATLD study showed that a regimen starting with a three-drug combination of STR, INH, and PAS followed by INH plus PAS was highly effective in centers with a high standard of patient care (33). This regimen was adopted as standard treatment in many technologically advanced countries but was too expensive for developing countries. With the scientific basis for TB chemotherapy firmly established, attention turned to the next drugs available for clinical study: Pyrazinamide (PZA), ethionamide (ETH), and cycloserine. Initial evaluation of PZA suggested that the drug was too toxic for use as a first-line agent. This was also the case with the other two agents. However, the basis was established for treating patients with drug-resistant TB using these second-line drugs. While continuing to conduct treatment efficacy studies, the USPHS also embarked on pioneering studies using INH to prevent tuberculosis in persons with latent TB infection. Between 1955 and 1959, the USPHS studied nearly 65,000 persons, including children with primary TB, persons in contact with infectious TB patients, TB patients in mental institutions, and Alaskan villagers. These placebo-

controlled trials demonstrated the efficacy of INH for treatment of LTBI (34). Beginning in 1958 and continuing into the 1960s, the BMRC conducted a series of studies in Africa suggesting that PAS could be replaced with thiacetazone. Considering its low cost, thiacetazone became an established TB drug for use in low-income countries throughout the world. In industrialized countries, PAS was replaced by EMB, which was introduced in 1962 and subsequently studied by USPHS. Ethambutol also replaced thiacetazone in many low-income countries during the AIDS epidemic, when HIV-infected patients were found to experience a high rate of serious and sometimes fatal skin reactions to thiacetazone (35).

1.12 Modes of action and activities of the anti-TB drugs

Current chemotherapy for TB relies largely on mycobacteria specific drugs that inhibit bacterial metabolism with a heavy emphasis on inhibitors of the cell wall super polymer. The four first-line agents are INH, RMP, PZA and EMB (Figure -8). Streptomycin is widely used as second-line therapy. Isoniazid is a prodrug that requires oxidative activation by the mycobacterial catalase-peroxidase *katG*. The poorly understood active form of INH subsequently interacts with the enzymatic machinery that synthesizes mycolic acids, essential components of the cell wall. *katG* mutations affecting this activation process are found in the vast majority of INH-resistant patient isolates (36). Rifampicin interferes directly with the bacterial machinery for transcribing ribonucleic acid (RNA) from DNA. Patient isolates that are resistant to RMP almost invariably have mutations within the beta-subunit of the RNA polymerase gene (*rpoB*) (37).

Pyrazinamide is also a pro-drug that requires activation by a hydrolytic pyrazinamidase that converts it to pyrazinoic acid. Pyrazinoic acid has been proposed to have both specific and nonspecific effects due to an intracellular accumulation of the liberated acid. Patient isolates that are resistant to PZA typically show mutation within the gene encoding the pyrazinamidase *pncA* (38). Ethambutol interferes with the construction of the arabinogalactan layer of the mycobacterial cell wall. Although definitive proof is

lacking, it appears that EMB directly inhibits an enzyme that introduces arabinose into one of the branching structures of arabinogalactan (39). Streptomycin is one of the families of aminoglycoside antibiotics that act by inhibiting protein synthesis. Mutations in patient isolates associated with STR resistance include alterations in the gene encoding the 16S rRNA and in the ribosomal protein S12 (40).

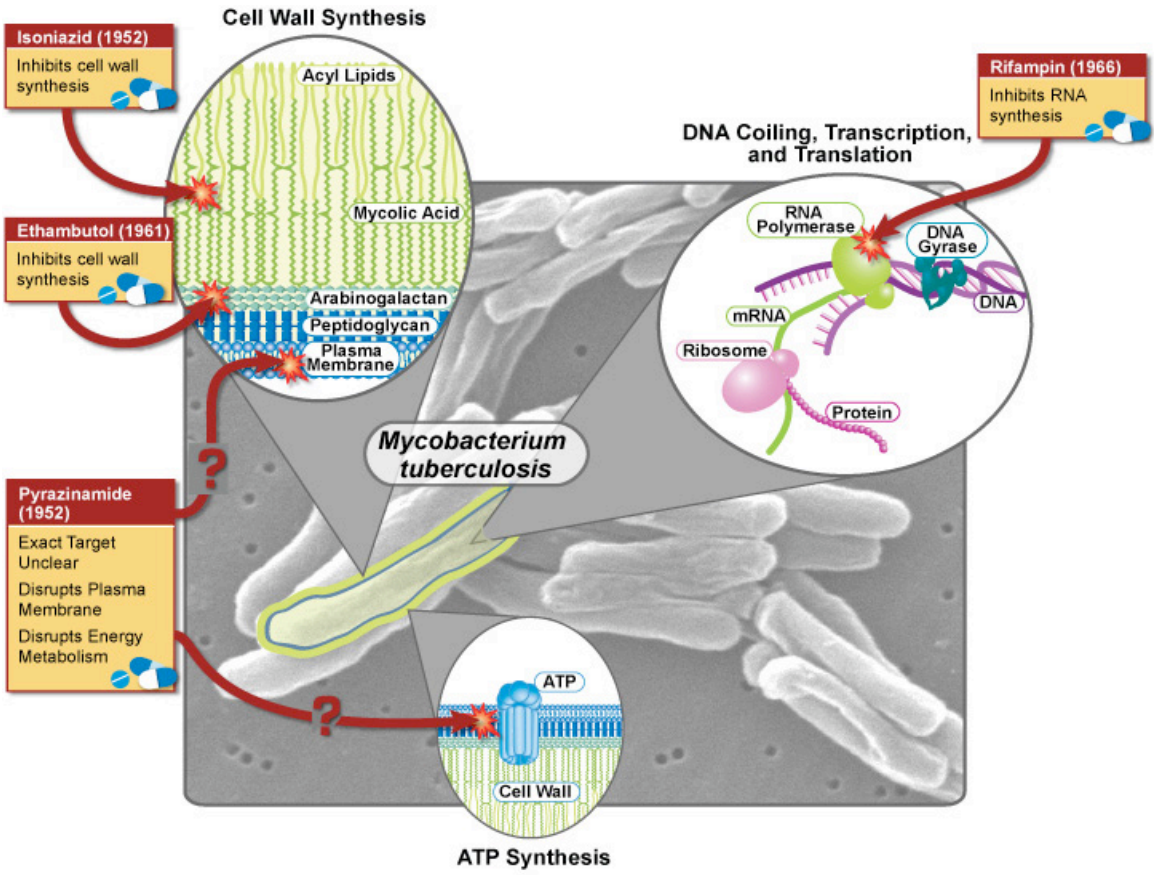

Figure -8 Mode of action for first line drugs of Tuberculosis

Tuberculosis, which results from an infection with *Mycobacterium tuberculosis*, can usually be cured with a combination of first-line drugs taken for several months. Shown here are the four drugs in the standard regimen of first-line drugs and their modes of action. Also shown are the dates these four drugs were discovered—all more than 40 years ago. Extracted from www. niaid. nih.gov// firstlineillustration.aspx

1.13 Animal Models of Tuberculosis

M. tuberculosis infection of humans results in a variety of outcomes, in terms of both disease and pathology. Organized immune structures called granulomas are produced that evolve morphologically during the course of infection with the formation of areas of necrosis called caseum and the deposition of fibrin and calcium. Various animal models are used to study at least some of these aspects of *M. tuberculosis* pathogenesis in humans. Mice are most commonly used for reasons of cost, convenience, their amenability to genetic manipulation, and the availability of inbred strains and immunological reagents (43). However, tuberculosis in the mouse model differs from human disease in several important aspects. In susceptible strains, bacterial burden can be very high, reaching 106 per lung, and are never cleared. Moreover, mouse granulomas do not caseate or calcify. Guinea pig exhibits many pathological features similar to those seen in humans, but unlike humans they are exquisitely sensitive to a progressive pulmonary infection (43). Rabbits display pathology more characteristics of human diseases, ranging from spontaneous healing to caseous and cavitary pulmonary lesions. However, most rabbits are resistant to *M. tuberculosis* (mild illness, eventually cleared) and *M. bovis* (Severe, lethal diseases) (43). Lurie bred rabbits that were highly susceptible to *M. tuberculosis* (43), but unfortunately this strain was lost. The rabbit model is being revived and susceptible strain may be redeveloped (Y.C. Manabe, A.M. Dannenberg Jr. & W.R. Bishai, personal communication). Nonhuman primates are also used to model *M. tuberculosis* infection (43), and intra-tracheal inoculation of C*ynomolgus macaques* leads to a spectrum of outcomes similar to that seen in humans (J. Flynn, personal communication).

1.14 Animal Models for latency

In an effort to provide structure to this field, different animal models of tuberculosis latency (44, 45) were recently categorized as either “Cornell/drug-induced” or “low-dose/chronic” (46). In the Cornell model (47), mice are infected with *M. tuberculosis*

and then drug treated (traditionally with isoniazid and pyrazinamide) for an extended period. Although no viable mycobacteria are detected immediately following treatment, disease reactivates in a fraction of the animals within several months (46, 47). This system models the state in humans in that the load of bacilli in infected organs is often undetectable. However, unlike in humans, drug intervention is needed to induce the latent state. Also, Cornell model experiments require several critical choices: route and dose of infection, type and timing of drug treatment, timing of recovery phase, and type of immunosuppressive drug used for recovery. Currently, no standard protocol exists and results depend materially on the parameters used to establish the latent infection (44). The low-dose (or chronic) model of latent tuberculosis grew from observations of mice inoculated with small numbers of *M. tuberculosis* (48). After an initial growth phase the bacillary burden in the lungs remains steady and the mice appear healthy until the disease reactivates as much as 18 months later. In comparison with the Cornell model, the immune-suppression (49, 50) or innate immunodeficiency model (51, 52, 53) leads to faster and more comprehensive reactivation. This chronic model resembles latency in humans where it depends solely on the host immune response to contain the infection. However, unlike latent tuberculosis in humans this model results in a high bacillary burden. In addition, histological examination of chronically infected mice showed that lung damage accumulates steadily throughout the chronic period (50, 54, 55), and thus the disease is not really latent. Recent research offers hope that animal models can be improved. First, nonhuman primates currently being used to study other aspects of human tuberculosis (51, 52, 53) may also provide a faithful model of latent tuberculosis in humans. Second, the C57BL/6 mouse that is commonly used in latency studies may be a poor choice, in part because the bacterial burden in the chronic state is too high. Recent studies with C57BL/6xDBA/2 F1 hybrid (50, 54, 55) suggest that low-dose inoculation of these mice results in a lower bacterial burden coincident with a subclinical infection that activates to fulminant disease upon immune-suppression. It will be important to determine the proportion of the mice that eventually succumb to infection and to document whether lung pathology accumulates during the apparently latent phase, as was shown for the low-dose infected C57BL/6 mouse (56).

1.15 In Vitro Models of latency

On the basis of the pervasive but unproven idea that bacteria during clinical latency are in a non-replicating, metabolically inactive state, several researchers have attempted to produce growth-arrested bacilli using culture systems that manipulate temperature (57), pH (58), or nutrient starvation (59). Other factors potentially associated with the establishment and maintenance of latent tuberculosis include host-generated nitric oxide (NO) (60) and hypoxia (61). Of these, the role of reduced oxygen tension has received the most attention to date because tuberculosis infections are preferentially associated with the most-oxygen-rich sites within the body (62) and lesions in communication with open airways generally have a larger number of bacilli (61). Reactivation disease occurs most frequently in the upper lobes of the lung, thought to be the single most oxygenated regions of the body (62, 63). Although replication of *M. tuberculosis* requires oxygen, the bacteria can survive for years without oxygen *in vitro* (60). These findings have been interpreted to suggest that latent *M. tuberculosis* may exist in an oxygen-limited environment *in vivo*. However, it is important to note that direct measurements of granuloma oxygen tension have not been made. On the basis of these observations, Wayne and others have explored the use of hypoxic culture conditions (referred to as the Wayne model) to generate non-replicating persistent bacilli in vitro and to identify *M. tuberculosis* genes/proteins potentially important for development or maintenance of the latent state (60). As expected in the Wayne model, nonreplicating bacteria were found to down-regulate many metabolic enzymes, but the activities of isocitrate lyase and glycine dehydrogenase were induced, which suggests an induction of the glyoxylate shunt pathway (64). Three subsequent studies have some bearing on the Wayne model. First, a mutation in the isocitrate lyase gene *icl* renders the bacteria attenuated in a mouse model but only at later (>2 weeks) times, which suggests that the glyoxylate shunt may indeed be activated at this stage (65, 66). However, the mutant was not attenuated under hypoxic conditions in vitro. Another study showed that the *M. marinum* gene *ald*, which encodes glycine/alanine dehydrogenase, was induced in granulomas (65) but was not induced by short-term hypoxia (67). A recent approach combined hypoxic culture conditions with microarray

readout to define the *M. tuberculosis* genes that respond rapidly to decreased oxygen tension (68, 69, 70). An Expression of more than 100 genes was altered significantly, although none of these corresponded to those identified in the Wayne model. Predicted functions for many of the 60 repressed genes indicate that low oxygen tension is associated with broad adaptation to reduced metabolic activity. In comparison, about two thirds of the 47 induced genes are of unknown function, which suggests that the adaptation to hypoxia is not yet well characterized. Several induced genes have postulated functions that could help promote survival in vivo. Among the hypoxia-induced loci is the predicted two-component response regulator Rv3133c, also called *devR* and *dosR* (dormancy survival regulator) (71). Computer analysis identified a consensus DosR-binding motif, a variant of which is located upstream of nearly all *M. tuberculosis* genes rapidly induced by hypoxia, and DosR binding to the *acr* promoter has been demonstrated (70, 71). Furthermore, *dosR* mutant bacteria fail to induce the hypoxic response genes (68) and are significantly attenuated for survival in the Wayne model of hypoxic dormancy (72). Thus DosR appears to play a critical role in mediating expression of a series of hypoxia-induced genes, which have been termed the DosR regulon.

It is now clear that significant overlap exists between the *M. tuberculosis* responses to hypoxia and NO. Nitric oxide is one of few host products known to be directly toxic to mycobacteria at clinically relevant concentrations (73, 74) but at sub-lethal concentrations NO reversibly inhibits aerobic respiration and has a distinct role as a signaling molecule (75). Recent work shows that, similar to hypoxia, low levels of NO reversibly inhibit growth of *M. tuberculosis in vitro* and that NO and hypoxia are additive in their inhibitory effects (M. Voskuil, D. Sherman & G. Schoolnik, unpublished data). Further, concentrations of NO that impede *M. tuberculosis* growth were shown to induce the DosR regulon in a DosR dependent fashion. Similarly, a study of *S. typhi* genes induced by growth in cultured macrophages found that 70% were also induced by hypoxia, again suggesting a strong overlap between hypoxia- and NO-induced genes (75). In summary, although hypoxia has long been assumed to affect mycobacteria in vivo, it is entirely possible that NO, alone or in conjunction with

hypoxia, is responsible for induction of the so-called hypoxia response genes. Indeed, whether bacterial respiration is inhibited by NO, by a lack of oxygen, or by a combination may be indistinguishable by the organism. Several observations suggest that the DosR response has a role in vivo. The NOS2 locus encoding inducible NO synthase is expressed in *M. tuberculosis*– infected mouse (76, 77) and human lungs (78), and interfering with host NO production either by specific inhibitors (79,80) or by gene disruption (76) greatly exacerbates tuberculosis infection. Genes of the DosR regulon are powerfully expressed when *M. tuberculosis* infects mice (81) or humans (82, 83). It will be interesting to test *dosR*-deleted *M. tuberculosis* strains in animal infection models. Because these instances of NO production and *M. tuberculosis* gene expression occurred in the context of active tuberculosis disease, the relevance of these data to latent tuberculosis is not clear. Like the other hypotheses based on in vitro model, the link between hypoxia, NO, DosR, and latency must be substantiated by an animal model that recapitulates human infection.

1.16 New targets

The major potential TB drug development components were DNA gyrase, RNA polymerase, cell wall synthesis components, ribosome (50 S), protease, energy metabolism and unknown targets (84). A DNA gyrase inhibitor Moxifloxacin are currently being enrolled in a Phase III trial aimed at shortening TB treatment to four months. Quinolone TBK-613 was a preclinical candidate which was recently selected and is progressing toward clinical trials. A-824 was a multiple target compound which has completed, phase II-a clinical trial. Nitroimidazoles were new generation molecules, with improved efficacy and metabolic stability, were identified and were approaching the selection of preclinical candidates. Pleuromutilins was identified as lead compound for *in vivo* testing. Malate Synthase Inhibitors were identified as promising hits .The nitroimidazole-oxazolidinone class, which is comprised of multifunctional compounds, were selected for further optimization. Riminophenazines were novel analogs with improved activity and pharmacokinetics have been identified as energy metabolism inhibitor. TB trail takes long time and after the patients are

recruited, the treatment continues for 6 months (or more for drug-resistant TB), and then results are only clear after one or more additional years of follow-up. Non profit making organizations like Global TB alliance (Bill Gates and Milinda Gates foundation) , Stop Tb (WHO Partnership) and OSDD (CSIR India) has come with strong commitment to make a dramatic difference in eradication of tuberculosis. The Stop TB Strategy is WHO's recommended approach to reducing the burden of TB in line with global targets. The six major components of the strategy are: pursue high-quality DOTS expansion and enhancement; address TB/HIV, MDR-TB, and the needs of poor and vulnerable populations, contribute to health system strengthening based on primary health care, engage all care providers, empower people with TB, and communities through partnership, and enable and promote research.

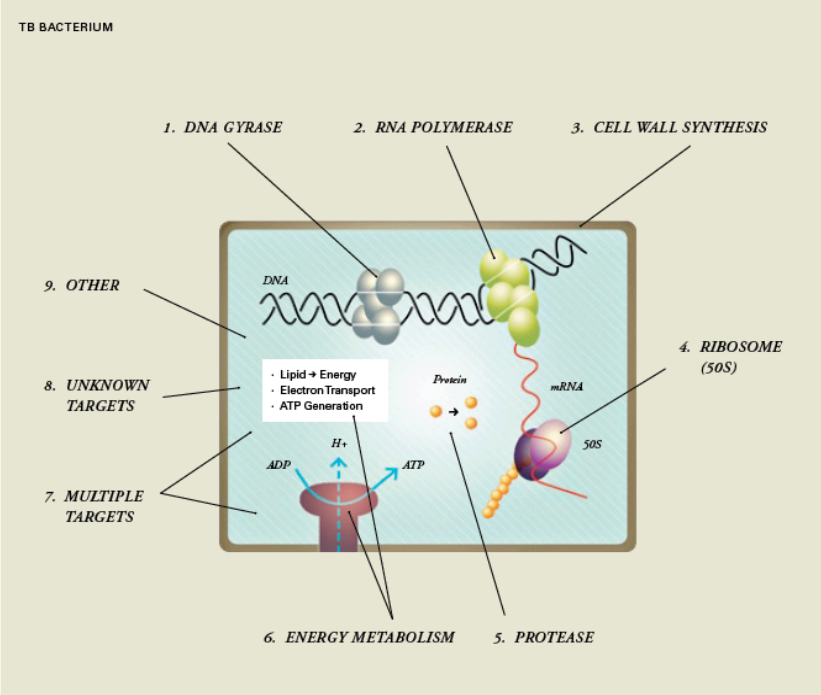

Figure – 9 New and known targets for tuberculosis, which are taken up for development of antitubercular drugs. Several new types of TB drugs currently under development are shown here with their mechanisms of action. The picture is extracted from http :// www.tballiance .org /downloads /publications /TBA _Annual _2008_web.pdf

1.17 Glutamine synthetase as a potentially important target

Some of the targets have been suggested in the current literature, inhibitors of which might lead to development of novel inhibitors against the pathogen (85-89). The enzyme *Mycobacterium tuberculosis* Glutamine synthetase has been identified among them, as a target for the disease (89-96). Glutamine synthetase is an essential enzyme for the survival of *Mycobacterium tuberculosis* (92 - 95). This enzyme is secreted by all pathogenic mycobacteria (92). It is suggested that this extracellular enzyme functions in the regulation of ammonia in the phagosomal compartment to inhibit phagosome–lysosome fusion and phagosome acidification, as well as synthesis of cell wall component poly (L-glutamic acid glutamine complex) that is found only in pathogenic mycobacteria component (93). The extracellular localization of *M. tuberculosis* GlnA1 (*Mt*GS) is associated with its involvement in the synthesis of a cell wall component poly (L-glutamic acid glutamine). Its extracellular function has made it an attractive target for drug development against *Mycobacterium tuberculosis* (94). Inhibition of extracellular enzyme activity in *M. tuberculosis* culture, in infected THP-1 cell as well as in, *in vivo* condition of guinea pig model by the substrate analogues, showed the potential of GS as a drug target against TB (95). The extracellular location means that drugs aimed at GS need not to penetrate the mycobacterial cell wall. The crystal structure of the enzyme has also been elucidated and specific inhibitors are available (96). The enzyme activity was monitored by 1) Transfer reaction as well as 2) Biosynthetic reaction. In most cases, lead compounds are identified through successfully implemented high-throughput assays and surveys of chemical diversity for compounds that inhibit the target selected (99, 100). The process of lead compound identification has been greatly enhanced by the advent of combinatorial chemical approaches to generating compound diversity. We have already developed HTS assay protocols using both the reactions to screen extracts and fractions obtained from medicinal plants of Indian origin (101-103). In general, the isolation and structure elucidation of natural products are done aiming at identifying new active compounds or new lead-structures as starting points for the search of new drugs.

Glutamine synthetase also plays a central role in nitrogen metabolism by converting glutamate and ammonia to glutamine (97-98). Nitrogen metabolism in *Mycobacterium tuberculosis* is probably the most important aspect which needs to be looked at more critically. Bacteria can utilize a wide range of nitrogen compounds as sole source of cellular nitrogen. These nitrogen compounds range from simple inorganic compound such as di-nitrogen and nitrate to complex compound like amino acid. In bacteria externally available amino acids can be used directly for protein synthesis and on the other hand can be catabolized, serving as nitrogen source. In aerobic stage, the growth promoting effect and utilization of L- alanine, L- aspartic acid and L – glutamate were studied in comparison with L – aspargine. A considerable difference was observed in the response of actively growing cells of *Mycobacterium smegmatis* and Mycobacterium *tuberculosis* (H37Ra). In mycobacteria nitrogen metabolism and transport of amino acid may well differ between aerobic and anaerobic growth stage.

1.18 Objective of the thesis

The extracellular location means that drugs aimed at GS need not penetrate the formidable mycobacterial cell wall. The closest human analogue has very low similarity (23% amino acid sequence identity). The combined observation suggested that *MtbGS* was a potential target for drug design. The detail biochemical characterizations of *MtbGS* remained unexplored due to limitation in phosphate estimation procedure if we consider the biochemical reaction only to occur under physiological environment. Probably this was the major reason for the absence of any simple assay protocol developed using this enzyme with high throughput efficiency. Our initial objective became the development of a HTS assay protocol based on biosynthetic activity as well as transfer activity of the enzyme to identify novel chemical structure against *Mycobacterium tuberculosis*. So, even though L-MSO and DL–Phosphothriacin inhibited both the activities of the enzyme, finding quality inhibitors for *MtbGS* could give a new direction to the tuberculosis treatment.

The second objective was to screen the in-house compound library containing 2000 samples consisting of synthetic molecules, natural product extracts and fractions to validate the assay protocol as well as find novel inhibitors against the enzyme. As a result of screening this library, 12 samples were initially found as actives against the enzyme and one sample was confirmed as active against *M. bovis* BCG. The sample was originally identified as sep box fraction isolated from methanol extracts of aerial part of *Byttneria spp.* and needed purification of the active ingredient from the extract using standard techniques.

Another objective of the thesis was to characterize the nature of interaction between the target protein (*MtbGS*) and inhibitor L-MSO under *in vitro* condition. L-MSO followed a time dependent loss of enzyme activity. Then, the kinetic parameters of its inactivation were estimated to understand the nature of binding of the inhibitor with the enzyme. Apart from the kinetic studies, binding of radio-labeled inhibitor followed by SDS/heat treatment was carried out to monitor the nature of bonding with the inhibitor. Although the results indicated a covalent linkage being formed with the inhibitor, a validation of this observation could be carried out by identifying the modified amino acid using proteomic techniques. On the basis of our current understanding, it will be now easier to design better analogues by *in-silico* as well as medicinal chemistry approaches.

The other objective was to study the metabolite controls of *MtbGS* to understand the mechanism of regulation of the enzyme. As GS is an important enzyme for nitrogen metabolism and being regulated by allosteric modulators, feedback inhibitors as well as through covalent modification, it became necessary to understand the role of this enzyme particularly at different stages of developing infection within the host system. Similar studies from our group and others earlier on nitrate reductase clearly established the role of metabolites in this pathway on the survival of bacilli during transition to anaerobic stage. GS converts glutamate and ammonia to glutamine. Bacteria can utilize a wide range of nitrogenous compounds as sole source of cellular nitrogen. In bacteria, externally available amino acids can be used directly for protein synthesis and catabolized as well, serving as nitrogen source. Hence, all 20 amino acids were applied on the biosynthetic activity of the enzyme and on *in vitro* growth of the

bacilli. The utilization of nitrogen sources like nitrate, nitrite, ammonia and amino acids during growth of mycobacteria was checked in presence of L-MSO. But the major challenge was to identify the nitrogen sources utilized by mycobacteria during its survival under anaerobic environment. The growth of mycobacterium in different nitrogen sources and their utilization was monitored using *M.pheli* medium. In *M.pheli* medium was a minimal medium in which the different nitrogen sources can be used.

1.18 References

1) Encyclopedia of infectious diseases: Modern Methodologies by Micheal Tibayrenc (2007)

2) Levy-Frebault VV, Portaels F., Proposed minimal standards for the genus Mycobacterium and for description of mew slowly growing Mycobacterium species. Int.J.Syst.Bacteriology 1992;42(2):315-23

3) Ayele Wy, Neill SD, Zinsstag J, Weiss MG, Pavlik I. , Bovine tyberculosis : an old disease but a new threat to Africa . Int. Tuberc. Lung. Dis. 2004: 8(8) :924-37

4) Aranaz A., Cousins D., Mateos A., Dominguez L. Elevation of Mycobacterium tuberculosis subsp. Caprae to species rank as Mycobacterium caprae comb. Nov., sp. Nov. Int. J. Syst. Evol. Microbial. 2003 ; 53(Pt 6) : 1785 -9.

5) Cousins DV., Bastida R., Cataldi A, Tuberculosis in seals caused by a novel member of the Mycobacterium tuberculosis complex: Mycobacterium pinnipedii sp. Nov. Int J. Syst Evol. Microbiol 2003 ; 53 (Pt 5) : 1305 -14

6) WHO report 2009 Global Tuberculosis control epidemiology, strategy and financing.

7) Centers for Disease Control and Prevention. Primary multidrugresistant tuberculosis Ivanovo Oblast, Russia, 1999. MMWR
Morb Mortal Wkly Rep 1999; 48: 661}664.

8) Styblo K, Meijer J. Impact of BCG vaccination programs in children and young adults on the tuberculosis problem. Tubercule 1976; 57: 17} 43.

9) Scientific Blueprint for Tuberculosis Drug Development (http://www.tballiance.org)

10) Tuberculosis pathogenesis, protection and control (Book) Bary R.Bloom

11) Dannenberg AM, Immune mechanisms in the pathogenesis of pulmonary tuberculosis. Rev. Infect. Dis. 1989; 11 (suppl 2) S369 -78.

12) Dannenberg AM Delayed – type hypersensitivity and cell-mediated immunity in the pathogenesis of tuberculosis. Immunol Today 1991; 12 (7):228-33

13) Dannenberg AM Immune mechanism in the pathogenesis of pulmonary tuberculosis Rev. Infec. Dis. 1989; (suppl 2); S369-78

14) Brodie D., Schluger NW. The diagnosis of tuberculosis. Clin. Chest. Med. 2005; 26 (2) : 247 – 71,

15) Diagnostic Standards and Classification of Tuberculosis in Adults and Children. American Thoracic Society. THIS OFFICIAL STATEMENT OF THE AMERICAN THORACIC SOCIETY AND THE CENTERS FOR DISEASE CONTROL AND PREVENTION WAS ADOPTED BY THE ATS BOARD OF DIRECTORS, JULY 1999. THIS STATEMENT WAS ENDORSED BY THE COUNCIL OF THE INFECTIOUS DISEASE SOCIETY OF AMERICA, SEPTEMBER 1999

16) Kumar, Vinay; Abbas, Abul K.; Fausto, Nelson; & Mitchell, Richard N. (2007). Robbins Basic Pathology (8th ed.). Saunders Elsevier. Pp. 516-522

17) Steingart K, Henry M, Ng V, et al. (2006). "Fluorescence versus conventional sputum smears microscopy for tuberculosis: a systematic review". Lancet Infect. Dis. 6 (9): 570–81

18) Brown M, Varia H, Bassett P, Davidson RN, Wall R, Pasvol G (2007). "Prospective study of sputum induction, gastric washing and bronchoalveolar lavage for the diagnosis of pulmonary tuberculosis in patients who are unable to expectorate". Clin Infect Dis 44 (11): 1415–20

19) Drobniewski F, Caws M, Gibson A, Young D (2003). "Modern laboratory diagnosis of tuberculosis". Lancet Infect Dis 3 (3): 141–7.

20) Moore D, Evans C, Gilman R, Caviedes L, Coronel J, Vivar A, Sanchez E, Piñedo Y, Saravia J, Salazar C, Oberhelman R, Hollm-Delgado M, lachira D, Escombe A, Friedland J (2006). "Microscopic-observation drug-susceptibility assay for the diagnosis of TB". N Engl J Med 355 (15): 1539–50.

21) DTBE - Mantoux TB Skin Test Faciliator Guide - Part 1: Administering

22) http:// www.immunisation.nhs.uk/files/mantouxtest.

23) http://en.wikipedia.org/wiki/Mantoux_ test

24) Stefan H.E. Kaufmann HOW CAN IMMUNOLOGY CONTRIBUTE TO THE CONTROL OF TUBERCULOSIS? Nature reviews immunology Volume 1 Octuber2001

25) http://www.tballiance. Org

26) Centers for Disease Control and Prevention. Development of new vaccines for tuberculosis. Recommendations of the Advisory Council for the Elimination of Tuberculosis (ACET). MMWR Morb Mortal Wkly Rep 1998; 47(RR-13): 1}6.

27) WHO Global Tuberculosis Programme. Framework for Effective Tuberculosis Control (publication no. WHOB/94.179). Geneva: World Health Organization, 1994.

28) Netto EM, Dye C, raviglionemc. Progress in global tuberculosis control 1995}1996, with emphasis on 22 high-incidence countries. Global Monitoring and Surveillance Project. Int J Tuberc Lung Dis 1999; 3: 310}320

29) Hinshaw H C, Feldman W H. Streptomycin in the treatment of clinical tuberculosis: a preliminary report. Proc Mayo Clin 1945; 20: 313}318.

30) British Medical Research Council. Streptomycin treatment of pulmonary tuberculosis. A Medical Research Council investigation. Br Med J 1948; 2: 769}782.

31) Fox W, Sutherland I. A 9ve-year assessment of patients in a controlled trial of streptomycin with different doses of paraaminosalicylic acid in pulmonary tuberculosis. Q J Med 1959; 28: 77}95.

32) Medical Research Council. The treatment of pulmonary tuberculosis with isoniazid. Br Med J 1952; 2: 735}746.

33) Bignall J R, Rist N. An international investigation of the ef9cacy of chemotherapy in previously untreated patients with pulmonary tuberculosis: a trial by the committee on treatment and the committee on bacteriology of the International Union against Tuberculosis. Bull Int Union Tuberc 1964; 34: 80}91.

34) Ferebee S H. Controlled chemoprophylaxis trials in tuberculosis. A general review. Bibl Tuberc 1970; 26: 28}106.

35) Nunn P P, Kibuga D, Gathua S, et al. Cutaneous hypersensitivity reactions due to thiacetazone in HIV-1 seropositive patients treated for tuberculosis. Lancet 1991; 337: 627}630.

36) Slayden R A, Barry C E 3rd. The genetics and biochemistry of isoniazid resistance in mycobacterium tuberculosis. Microbes Infect 2000; 2: 659}669.

37) Cole S T. Rifamycin resistance in mycobacteria. Res Microbiol 1996; 147: 48}52.

38) Scorpio A, Zhang Y. Mutations in pnca, a gene encoding pyrazinamidase/nicotinamidase, cause resistance to the antituberculous drug pyrazinamide in tubercle bacillus. Nat Med 1996; 2: 662}667.

39) Belanger A E, Besra G S, Ford M E, et al. The embab genes of Mycobacterium avium encode an arabinosyl transferase involved in cell wall arabinan biosynthesis that is the target for the antimycobacterial drug ethambutol. Proc Natl Acad Sci USA 1996; 93: 11919}11924.

40) Lee R E, Mikusova K, Brennan P J, Besra G S. Synthesis of the mycobacterial arabinose donor b-D-arabinofuranosyl-lmonophosphoryl- decaprenol, development of a basic arabinosyl-transferase assay, and identi9cation of ethambutol as an arabinosyl transferase inhibitor. J Am Chem Soc 1995; 117: 11829}11832.

41) Heym B, Philipp W, Cole S T. Mechanisms of drug resistance in Mycobacterium tuberculosis. Curr Top Microbiol Immunol 1996; 215: 49}69.

42) Ramaswamy S, Musser J M. Molecular genetic basis of antimicrobial agent resistance in Mycobacterium tuberculosis: 1998 update. Tuber Lung Dis 1998; 79: 3}29.

43) Ashwin S. Dharmadhikari, Edward A. Nardell,. What Animal Models Teach Humans about Tuberculosis,. Translational Reviews Am J Respir Cell Mol Biol Vol 39. Pp 503–508, 2008

44) Orme IM. 1988. A mouse model of the recrudescence of latent tuberculosis in the elderly. Am. Rev. Respir. Dis. 137:716–18

45) Rees RJM, Hart PD. 1961. Analysis of the host-parasite equilibrium in chronic murine tuberculosis by total and viable bacillary counts. Br. J. Exp. Pathol. 42:83–88

46) Scanga CA, Mohan VP, Joseph H, Yu K, Chan J, Flynn JL. 1999. Reactivation of latent tuberculosis: variations on the Cornell murine model. Infect. Immun. 67:4531–38

47) mccune RM, Feldmann FM, Lambert HP, mcdermottw. 1966. Microbial persistence. I. The capacity of tubercle bacilli to survive sterilization in mouse tissues. J. Exp. Med. 123:445–68

48) Flynn JL, Scanga CA, Tanaka KE, Chan J. 1998. Effects of aminoguanidine on latent murine tuberculosis. J. Immunol. 160:1796–803

49) Saunders BM, Frank AA, Orme IM. 1999. Granuloma formation is required to contain bacillus growth and delay mortality in mice chronically infected with Mycobacterium tuberculosis. Immunology 98:324–28

50) Rhoades ER, Frank AA, Orme IM. 1997. Progression of chronic pulmonary tuberculosis in mice aerogenically infected with virulent Mycobacterium tuberculosis. Tuber. Lung Dis. 78:57–66

51) Croix DA, Capuano S 3rd, Simpson L, Fallert BA, Fuller CL, et al. 2000. Effect of mycobacterial infection on virus loads and disease progression in simian immunodeficiency virus-infected rhesus monkeys. AIDS Res. Hum. Retrovir. 16:1895–908

52) mcmurray DN. 2000. A nonhuman primate model for preclinical testing of new tuberculosis vaccines. Clin. Infect. Dis. 30(Suppl. 3):S210–12

53) Walsh GP, Tan EV, dela Cruz EC, Abalos RM, Villahermosa LG, et al. 1996. The Philippine cynomolgus monkey (Macaca fasicularis) provides a new nonhuman primate model of tuberculosis that resembles human disease. Nat. Med. 2:430–36

54) Arriaga AK, Orozco EH, Aguilar LD, Rook GA, Hernandez Pando R. 2002. Immunological and pathological comparative analysis between experimental latent tuberculous infection and progressive pulmonary tuberculosis. Clin. Exp. Immunol. 128:229–37

55) Phyu S, Mustafa T, Hofstad T, Nilsen R, Fosse R, Bjune G. 1998. A mouse model for latent tuberculosis. Scand. J. Infect. Dis. 30:59–68

56) Rhoades ER, Frank AA, Orme IM. 1997. Progression of chronic pulmonary tuberculosis in mice aerogenically infected with virulent Mycobacterium tuberculosis. Tuber. Lung Dis. 78:57–66

57) Dickinson JM, Mitchison DA. 1981. Experimental models to explain the high sterilizing activity of rifampin in the chemotherapy of tuberculosis. Am. Rev. Respir. Dis. 123:367–71

58) Betts JC, Lukey PT, Robb LC, mcadam RA, Duncan K. 2002. Evaluation of a nutrient starvation model of Mycobacterium tuberculosis persistence by gene and protein expression profiling. Mol. Microbiol. 43:717–31

59) Nathan C, Shiloh MU. 2000. Reactive oxygen and nitrogen intermediates in the relationship between mammalian hosts and microbial pathogens. Proc. Natl. Acad. Sci. USA 97:8841–48

60) Wayne LG, Sohaskey CD. 2001. Nonreplicating persistence of Mycobacterium tuberculosis. Annu. Rev. Microbiol. 55:139–63

61) Adler JJ, Rose DN. 1996. Transmission and pathogenesis of tuberculosis. In Tuberculosis, ed. SM Garay, pp. 129–40. Boston: Little, Brown & Co.

62) Canetti G. 1955. Growth of the tubercle bacillus in the tuberculosis lesion. In The Tubercle Bacillus in the Pulmonary Lesion of Man, pp. 111–26. New York: Springer 38.

63) Corper HJ, cohnml.1933. The viability and virulence of old cultures of tubercle bacilli. Ann. Rev. Tuberc. 28:856–74

64) mckinney JD, Honer zu Bentrup K, Munoz-Elias EJ, Miczak A, Chen B, et al. 2000. Persistence of Mycobacterium tuberculosis in macrophages and mice requires the glyoxylate shunt enzyme isocitrate lyase. Nature 406:735– 38

65) Chan K, Knaak T, Satkamp L, Humbert O, Falkow S, Ramakrishnan L. 2002. Complex pattern of Mycobacterium marinum gene expression during long-term granulomatous infection. Proc. Natl. Acad. Sci. USA 99:3920–25

66). Davis JM, Clay H, Lewis JL, Ghori N, Herbomel P, Ramakrishnan L. 2002. Real-time visualization of Mycobacterium-macrophage interactions leading to initiation of granuloma formation in zebrafish embryos. Immunity 17:693–702

67) Sherman DR, Voskuil M, Schnappinger D, Liao R, Harrell MI, Schoolnik GK. 2001. Regulation of the Mycobacterium tuberculosis hypoxic response gene encoding alpha-crystallin. Proc. Natl. Acad. Sci. USA 98:7534–39

68) Boon C, Dick T. 2002. Mycobacterium bovis response regulator essential for hypoxic dormancy. J. Bacteriol. 184:6760– 67

69) Dasgupta N, Kapur V, Singh KK, Das TK, Sachdeva S, et al. 2000. Characterization of a two-component system, devr-devs, of Mycobacterium tuberculosis. Tuber. Lung Dis. 80:141–59

70) Sherman DR, Voskuil M, Schnappinger D, Liao R, Harrell MI, Schoolnik GK. 2001. Regulation of the Mycobacterium tuberculosis hypoxic response gene encoding alpha-crystallin. Proc. Natl. Acad. Sci. USA 98:7534–39

71) Park H, Guinn KM, Harrell MI, Liao R, Voskuil MI, et al. 2003. Rv3133c/dosr is a transcription factor that mediates the hypoxic response of M. Tuberculosis. Mol. Microbiol. 48:833–43

72) Nathan C. 2002. Inducible nitric oxide synthase in the tuberculous human lung. Am. J. Respir. Crit. Care Med. 166:130– 31

73) Martin E, Davis K, Bian K, Lee YC, Murad F. 2000. Cellular signaling with nitric oxide and cyclic guanosine monophosphate.
Semin. Perinatol. 24:2–6

74) . Zumft WG. 2002. Nitric oxide signaling and NO dependent transcriptional control in bacterial denitrification by members of the FNR-CRP regulator family. J. Mol. Microbiol. Biotechnol. 4:277–86

75) Daigle F, Graham JE, Curtiss R 3rd. 2001. Identification of Salmonella typhi genes expressed within macrophages by selective capture of transcribed sequences (SCOTS). Mol. Microbiol. 41:1211–22

76) macmicking JD, North RJ, lacourse R, Mudgett JS, Shah SK, Nathan CF. 1997. Identification of nitric oxide synthase as a protective locus against tuberculosis.Proc. Natl. Acad. Sci. USA 94:5243– 48

77) Scanga CA, Mohan VP, Yu K, Joseph H, Tanaka K, et al. 2000. Depletion of CD4(C) T cells causes reactivation of murine persistent tuberculosis despite continued expression of interferon gamma and nitric oxide synthase 2. J. Exp. Med. 192:347–58

78) Choi HS, Rai PR, Chu HW, Cool C, Chan ED. 2002. Analysis of nitric oxide synthase and nitrotyrosine expression in human pulmonary tuberculosis. Am. J. Respir. Crit. Care Med. 166:178–86

79) Chan J, Tanaka K, Carroll D, Flynn J, Bloom BR. 1995. Effects of nitric oxide synthase inhibitors on murine infection with Mycobacterium tuberculosis. Infect. Immun. 63:736–40

80) Ehlers S, Kutsch S, Benini J, Cooper A, Hahn C, et al. 1999. NOS2—derived nitric oxide regulates the size, quantity and quality of granuloma formation in Mycobacterium avium-infected mice without affecting bacterial loads. Immunology 98:313–23

81) macmicking JD, North RJ, lacourse R, Mudgett JS, Shah SK, Nathan CF. 1997. Identification of nitric oxide synthase as a protective locus against tuberculosis. Proc. Natl. Acad. Sci. USA 94:5243– 48

82) Shi L, Jung YJ, Tyagi S, Gennaro ML, North RJ. 2003. Expression of Th1-mediated immunity in mouse lungs induces a Mycobacterium tuberculosis transcription pattern characteristic of nonreplicating persistence. Proc. Natl. Acad. Sci. USA 100:241–46

83) Fenhalls G, Stevens L, Moses L, Bezuidenhout J, Betts JC, et al. 2002. In situ detection of Mycobacterium tuberculosis transcripts in human lung granulomas reveals differential gene expression in necrotic lesions. Infect. Immun.70:6330–38

84) Lee BY, Hefta SA, Brennan PJ. 1992. Characterization of the major membrane protein of virulent Mycobacterium tuberculosis. Infect. Immun. 60:2066–74

85) http://www.tballiance.org/downloads/publications/TBA_Annual_2008_web. Pdf

86) Warner D.F., Mizrahi V.: Mycobacterial genetics in target validation. Drug Discovery Today: Technology. (I) 2: 2004

87) Khasnobis S, Escuyer, VE, Chatterjee D: Emerging therapeutic targets in tuberculosis: post-genomic era, Expert Opin. Ther. Targets 2002; 6 (1): 21-40.

88) Anishetty, Mrudula Pulimi and Gautam Pennathur, Potential drug targets in Mycobacterium tuberculosis through metabolic pathway Computational Biology and chemistry Volume 29, Issue 5 , October 2005, Pages 368.

89) Anishetty S, Pulimi M, Pennathur G. Potential drug targets in Mycobacterium tuberculosis through metabolic pathway analysis. Comput Biol Chem. 2005 Oct;29(5):368-78. Epub 2005 Oct 6.

90) Raynaud C, Etienne G, Payron P, Lanelle MA, Daffe M: Extracellular enzyme activities potentially involved the pathogenecity of Mycobacterium tuberculosis. Microbiology 1998; 144: 577-587.

91) Hearth G, Clemens DL, Horwitz MA: Glutamine synthetase of Mycobacterium tuberculosis: Extracellular release and characterization of its enzymatic activity. PNAS 1994; 91: 9342-934

92) Harth G, Horwitz MA: An Inhibitor of Exported Mycobacterium Tuberculosis Glutamine Synthetase Selectively Blocks the Growth of Pathogenic Mycobacteria in Axenic Culture and in Human Monocytes: Extracellular Proteins as Potential as Potential Novel Drug Targets. J. Exp. Med 1999; 189 (9): 1425-1435

93) Hearth G., Zamecnik PC, Tang JY, Tabatadze D, Horwitz MA: Treatment of Mycobacterium tuberculosis with antisense oligonucleotide to glutamine synthetase mrna inhibits glutamine synthetase activity, formation of the poly-L-glutamate /glutamine cell wall structure, and bacterial replication. PNAS 2000; 97: 418-423.

94). Hearth G, Horwitz MA: Inhibition of Mycobacterium tuberculosis Glutamine Synthetase as a Novel Antibiotic Strategy against tuberculosis: Demonstration of Efficacy in Vivo. Infection and immunity 2003; 71(1): 456-464.

95) Tullius MV, Harth G, Horwitz MA: Glutamine Synthetase glna1 Is Essential for Growth of Mycobacterium tuberculosis in Human THP-1 Macrophages and Guinea Pigs Infection Immunity 2003; 71(7): 3927-3936.

96) Gill HS, Pflucgel GMU, Eisenberg D: Multicopy Crystallographic Refinement of a Relaxed Glutamine Synthetase from Mycobacterium tuberculosis Highlights Flexible Loops in the Enzymatic Mechanism and its Regulation. Biochemistry 2002; 41: 9863-72.

97) Wollfolk CA, Shapiro B, Stadtman ER: Regulation of Glutamine synthetase. I. Purification and properties of glutamine synthetase from Escherichia coli. Arch Biochem Biophys. 1966; 116: 177-92

98) Shapiro BM, Stadtman ER: Glutamine synthetase (Escherichia coli). Methods in Enzymology 1970; 17a: 910-922.

99) Singh U,V. Panchanadhikar, Sarkar D: Development of a Simple Assay Protocol for High-Throughput Screening of Mycobacterium tuberculosis Glutamine Synthetase for the Identification of Novel Inhibitors. J Biomol Screen 2005; 10: 725-729.

100) Singh U, Sarkar D: Development of a simple HTS protocol based on biosynthetic activity of Mycobacterium tuberculosis Glutamine synthetase for the identification of novel inhibitors. J Biomol Screen 2006:11; 1125-1129.

101) Woldemichael GM, Gutierrez-Lugo MT, Franzblau SG, Wang Y, Suarez E, Timmermann BN Mycobacterium tuberculosis growth inhibition by constituents of Sapium haematospermum. J Nat Prod. 2004 Apr; 67(4):598-603.

102). Puntumchai A, Kittakoop P, Rajviroongit S, Vimuttipong S, Likhitwitayawuid K, Thebtaranonth Y. Lakoochins A and B, New antimycobacterial stilbene derivatives from Artocarpus lakoocha. J Nat Prod. 2004 Mar;67(3):485-6

103) Parinuch Chumkaew, chatchanok Karalai, Chanita Ponglimanoni, et. Al. Antimicrobial activity of Phorbol Esters from the fruits of Sapium indicum. J Nat Prod. 2003, (66), 540-54

Chapter – 2

Bio-chemical characterization of *Mycobacterium tuberculosis* Glutamine Synthetase and screening of inhouse library

2.1 Introduction

Glutamine synthetase (GS) (EC 6.3.1.2), is a key enzyme in nitrogen metabolism. It has dual functions in two essential biochemical reactions, ammonia assimilation and glutamine biosynthesis (1). It is also one of the few amide synthetases found in the cells. Prokaryotes and eukaryotes were once thought to synthesize different type of GS i.e. 1) GSI for the former and GSII for the latter (2). Glutamine produced by GS is essential for protein synthesis, and its amide nitrogen is donated to synthesize many essential metabolites (2). Thus it is obvious to consider GS, probably indispensable to, all organisms. In view of the central roles played by GS, it is reasonable to believe that the GS gene is extremely old. From the sequence alignment of GSI from *Salmonella typhimurium* and GSII from alfalfa (3), it could be observed that the difference in amino acids between them was 0.75 per site. This value is quite large compared with those for other proteins, suggesting also that the GSI and GSII genes share a very old common ancestor. In enteric bacteria, Glutamate Dehydrogenase can assimilate ammonia directly into glutamate at high concentrations of ammonia (2). However, for bacteria such as *Mycobacterium tuberculosis* which lack Glutamate Dehydrogenase, but GS and Glutamate Synthetase are the sole means of ammonia assimilation (4). Due to its central role in nitrogen metabolism, GS is subject to varied and complex forms of transcriptional and posttranslational regulation as well as feedback inhibition by several products of glutamine metabolism (5, 6). There are at least four major forms of GS (7). In enteric bacteria, a single *glnA* gene encodes a GS type I (GSI) enzyme, and *glnA* null mutants are glutamine auxotrophs (4). Other bacteria have been shown to possess two or three different types of GS. In the case of *Sinorhizobium meliloti* (formerly *Rhizobium meliloti*), all three GS genes must be inactivated to generate the strain that is auxotrophic for L-glutamine (8). *M. tuberculosis* has a *glnA1* gene that encodes a GSI enzyme that is transcriptionally and post-translationally regulated in a manner similar to that of the *Escherichia coli* GS as well as three other *glnA* genes (*glnA2*, *glnA3*, and *glnA4*) that are predicted to encode GSI type enzymes (9, 10). However, it was previously observed that biochemical characterization of the *M. tuberculosis* Glutamine Synthetase (*MtbGS*), GlnA1 seemed to account for the vast majority of GS activity

(10). *MtbGS* was identified as a major component of *M. tuberculosis* culture filtrates and *M. tuberculosis* is quite sensitive to the GS inhibitor L-methionine-*SR*-sulfoximine (L-MSO), particularly in comparison to the nonpathogenic *Mycobacterium smegmatis (*10-13). Like enteric bacteria with *glnA* null mutations and an *M. smegmatis glnA1* mutant, the *M. tuberculosis glnA1* mutant is also a glutamine auxotroph (6, 14). The mutant requires a relatively high level of exogenous L-glutamine for robust growth in vitro and possesses no detectable GS activity. The mutant is attenuated for intracellular growth in differentiated THP-1 cells and is avirulent in guinea pigs infected by the aerosol route, indicating that the *M. tuberculosis* phagosome is limited in L-glutamine and that *glnA1* is essential for *M. tuberculosis* virulence (4).

2.2 Importance of GS for Drug Designing

MtbGS has been classified as essential for optimal growth based on Himar1-based transposon mutagenesis in strain H37Rv (14). Inhibition of the enzyme has a strong impact on growth of the bacterium in *in vitro* as well as *in vivo* systems, such as human macrophages and guinea pigs (4, 12, 15,). The extracellular location means that drugs aimed at GS need not to penetrate the formidable mycobacterial cell wall. The closest human analogue has very low similarity (23% amino acid sequence identity) (16). The combined observations suggest that *MtbGS* is an attractive subject for drug design. However, inhibitors would need to be tight-binding and selective to avoid unwanted interactions with human enzymes (17). Structural studies are expected to play a vital role in finding solutions to such problems. The pioneering work of Eisenberg and coworkers (18-21) has generated a number of GS structures from *Salmonella typhimurium* (StGS) in complex with relevant amino acids (substrates or inhibitors), metals (Mn2+ replacing the biologically relevant Mg 2+ and thallium ions mimicking the ammonium substrate), and nucleotides (AMP or ADP), as well as one with the inhibitor phosphinothricin together with ADP and metals. These represent the ‘‘taut’’ (active) state that exists when multiple metal ions are bound. A more recent structure with bound AMP (22) represents a ‘‘relaxed’’ (inactive) form seen at lower concentrations of metal ions and provides the first GS structure from *M. tuberculosis*.

L-methionine-*S*-sulfoximine (L-MSO) can be phosphorylated by GS to form a transition-state analogue, L-methionine-*S*-sulfoximine phosphate (MSO-P). The highest-resolution GS structure to date and the best-defined ligand complex, it offers several insights into the enzyme's specificity and catalytic activity and a more solid basis for drug design (17).

2.2.1. GS-catalyzed reactions

GS is known to catalyze a variety of reactions summarized in a review by Stadtman and Ginsburg (23). The catalytic activity of bacterial GS is regulated by two types of covalent modification: adenylylation (24), where the type of metal ion and pH play a role in GS activity, and by oxidative modification (25, 26). These regulatory mechanisms influence the following reactions.

a) Transfer reaction -:

The reaction is as follows -:

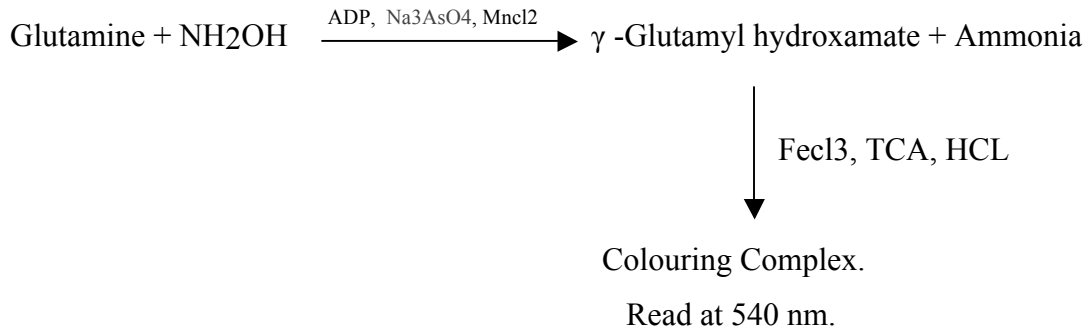

b) Biosynthetic reaction -:

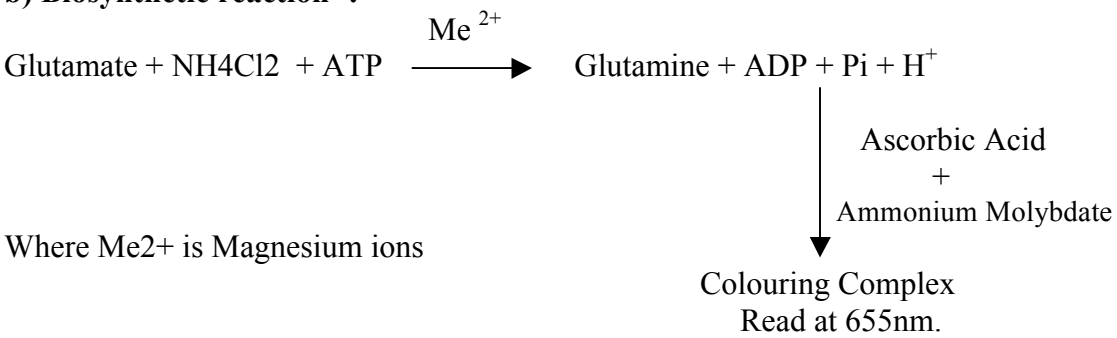

Conventionally, GS activity is monitored by biosynthetic as well as transfer assays (27, 28, 29). The present study evaluates the kinetic properties of *Mtb*GS in transfer assay and biosynthetic assay as well as converts both the assays to a robust high-throughput assay for screening of a large, chemically diverse library.

High-throughput screening (HTS) is a method for scientific experimentation especially used in drug discovery and relevant to the fields of biology and chemistry. Using robotics, data processing and control software, liquid handling devices, and sensitive detectors, High-Throughput Screening or HTS allows a researcher to quickly conduct millions of biochemical, genetic or pharmacological tests. Through this process one can rapidly identify active compounds, antibodies or genes which modulate a particular bio-molecular pathway. The results of these experiments provide starting points for drug design and for understanding the interaction or role of a particular biochemical process in biology (30).

In essence, HTS uses automation to run an assay, or screen, of a library of candidate compounds against a target (31). An assay is a test for specific activity: usually inhibition or stimulation of a biochemical or biological mechanism. Typical HTS screening libraries or "decks" can contain from 100,000 to more than 2,000,000 compounds (32). The term uHTS or *ultra high throughput screening* refers (32) to screening in excess of 100,000 compounds per day.

2.2.3 Recent advances

In March 2010 research was published demonstrating an HTS process allowing 1,000 times faster screening (100 million reactions in 10 hours) at 1 millionth the cost (using 10-7 times the reagent volume) than conventional techniques using drop-based microfluidics (33). Drops of fluid separated by oil replace microplate wells and allow analysis and hit sorting while reagents are flowing through channels.

In 2010 researchers developed a silicon sheet of lenses that can be placed over microfluidic arrays to allow the fluorescence measurement of 64 different output channels simultaneously with a single camera (33). This process can analyze 200,000 drops per second.

Section 2A- Determination of kinetic properties of *Mycobacterium tuberculosis* Glutamine Synthetase and development of transfer assay to adopt it in robust high throughput format.

2.3.1 Introduction

Glutamine synthetase catalyzes the transfer of γ - glutamyl moiety of glutamine to hydroxylamine according to equation - 2. For some studies, the amounts of γ - glutamylhydroxamate formed in this reaction were used to estimate glutamine synthetase activity (34). The γ - glutamylhydroxamate after reaction with ferric chloride (35) was measured spectrophotometrically at 540 nm. The complete assay mixture contained cell extract or purified enzyme, L-glutamine, neutralized hydroxylamine hydrochloride, arsenate, ADP, $MnCl_2$, and imidazole. The use of the transfer assay is a reliable measure of glutamine synthetase activity in crude extracts. The unambiguous demonstration of glutamine synthetase activity in crude extracts is not possible by biosynthetic assay, due to the presence of phosphatase activities that catalyze the liberation of Pi from ATP and thereby causing interference in the biosynthetic assay procedure (36). Among the transfer and biosynthetic reactions of glutamine synthetase, the former was selected first for the development of HTS protocol due to the fast and stable color formation of the assay mixture, which brings flexibility and convenience in screening programs. A robust assay in 96-well format for screening of compounds against *MtbGS* on HTS platform was developed by modifying this classical assay (36). The present assay was developed using purified recombinant *MtbGS* and the composition of the assay mix was optimized based on its K_m values. In order to standardize the assay the K_m value for L-glutamine of the *E. coli* enzymes was also determined.

2.3.2 Results

The purification profile of *MtbGS* in *E. coli* strain YMC21E was evidenced from the SDS-PAGE analysis (Figure - 1). *MtbGS* from *E.coli* YMC21E was purified by modifying a method published earlier (37, 38). Protein purification was divided into six stages. The stages were a) preparation of cell extract, b) Streptomycin Sulfate treatment, c) Acetic Acid precipitation, d) Ammonium sulfate precipitation, e) Ion-Exchange Chromatography and f) Heat treatment. It was important that a rapid, sensitive and specific assay should be available for the detection of protein of interest during purification. The French press technique of cell lysis was found suitable to break the cells and prepare cell extract. Ion exchange chromatography with Unosphere Q beads (anion exchanger) was found to finally purify the enzyme to almost homogeneity level with elution at 1.0 M NaCl, using fast performance liquid chromatography. The final scheme of the purification after optimization of each of these steps is elaborated in materials and methods. This preparation was used for the determination of K_m of all the substrates and cofactors required in the transfer assay. Hanes-Wolf plots were drawn to find out the K_m values of all the constituents of assay mixture (Table-1). All the components were added at the saturating level with respect to their K_m values to get linearity in activity for a longer period of incubation as well as insensitizing the protocol for competitive inhibitors to be picked up during screening. During this standardization stage, we found that divalent cations (Mg^{++}, Co^{++}, Ca^{++}, and Zn^{++}) were not supporting the enzymatic reaction as reported earlier (10).

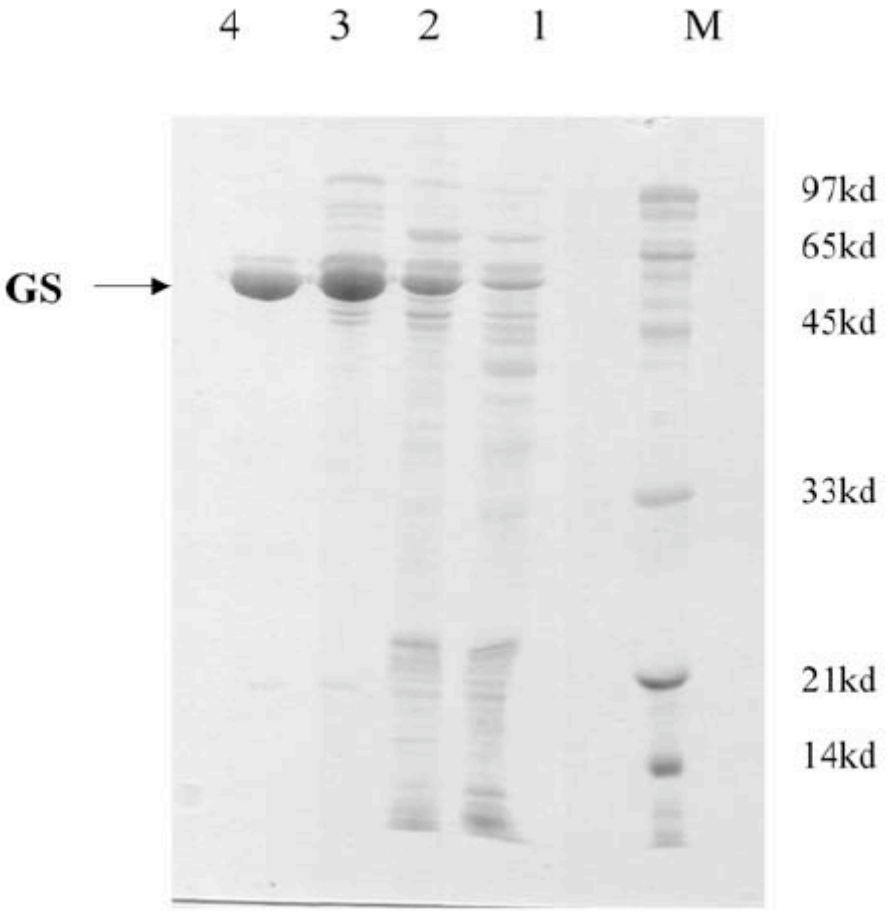

Figure - 1 SDS-PAGE of *Mycobacterium tuberculosis* Glutamine Synthetase at different stages of purification. Equivalent amount of proteins were loaded in lanes as follows: 1) Crude extract 2) AS cut 3) Ion exchange chromatography 4) after heat treatment 5) 6l Markar protein

2.3.3 Transfer assay

The monitoring of γ-glutamylhydroxamate production due to the conversion of L-glutamine and hydroxylamine by glutamine synthetase is called a transfer assay. A modified procedure was followed to carry out *MtbGS* transfer assay as described earlier. K_m values were determined using varied concentrations of L – glutamine (5 - 500 mM), hydroxylamine (0.8 - 200 mM), ADP (0.5 - 20 µM), $MnCl_2$ (2 -320 µM), and Na3AsO4 (1 - 50 µm), keeping other components at a constant level. A Hanes-Wolf plot was drawn from the data point to find out the K_m values of the respective components (Figure –2).

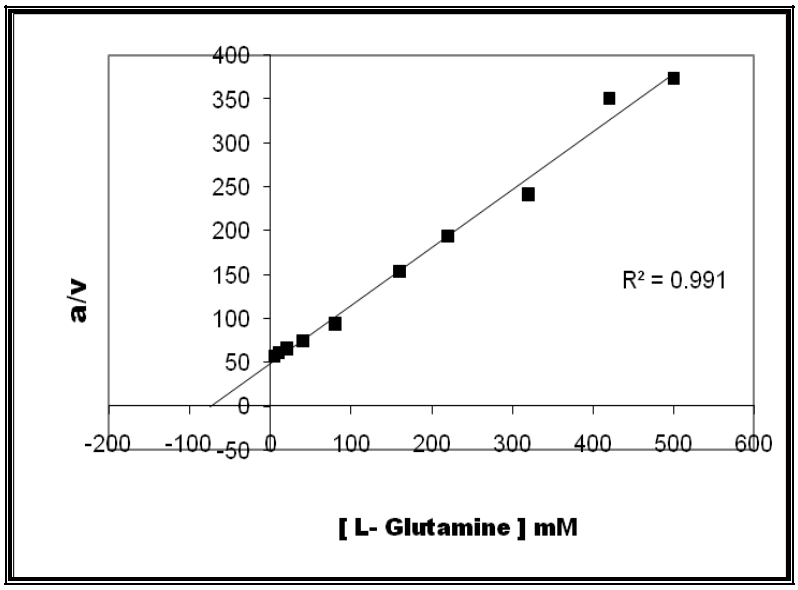

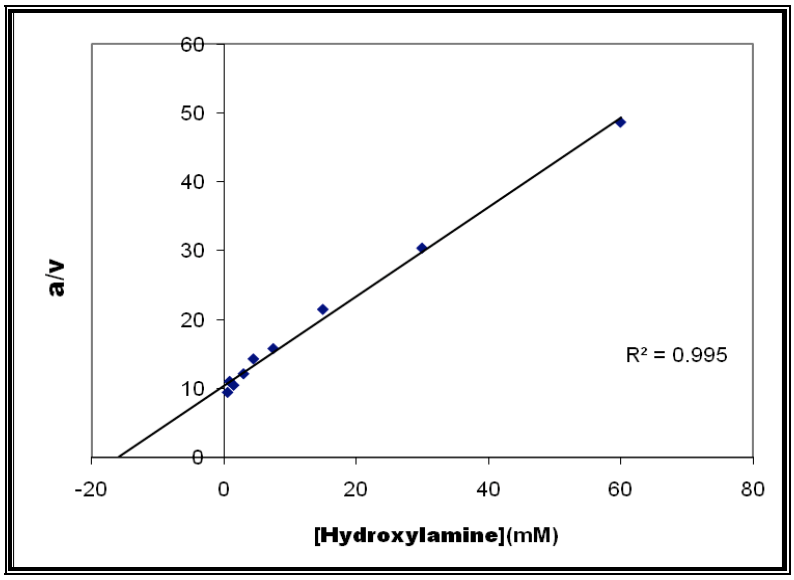

Figure – 2 The graph shows the Hans – Wolf plots drawn by using the data obtained from the experiments mentioned in the materials and methods for determination of K_m. The result is the average of 3 identical experiments

Table 1 – The reaction was carried out with 62.5 µg/ml purified *M. tuberculosis* Glutamine Synthetase in a reaction mix having all other components as mentioned in the materials and methods section with varied concentration of 1) Glutamine 2) Hydroxylamine 3) ADP 4) Arsenate and 5) Mn+. The result is the average of 3 identical experiments

Table 1. K_m of Different Substrates and Cofactors of *Mycobacterium tuberculosis* Glutamine Synthetase Transferase Activity

Substrate Used	*K_m Determined*	*K_m Reported*
L-glutamine	60 mM	2.4 mM
ADP	2 µM	?
Mn^{2+}	25 µM	?
Arsenate	5 µM	?
Hydroxylamine	8.3 mM	?

The final assay mix contained 20 mM imidazole buffer pH 7.0, 300 mM L - glutamine, 20 µM ADP, 60 mM hydroxylamine pH 7.0, 50 µM Na3AsO4, and 250 µM $MnCl_2$. The reaction was started by adding ADP in the reaction mixture and was monitored at 540 nm after addition of stopping reagent. In the classical assay, water was added instead of ADP in the blank. To use the HTS platform more conveniently in the microplate format, EDTA was added in a whole-reaction mix, which serves as a blank. The microplate format assays were carried out using 200 µl reaction mix, and the plates were incubated for 3 hours at 25° C followed by addition of 50 µl stopping reagent to develop color. After adding the stopping reagent, the reading was taken using a 520 nm filter in BMG polar star. To calculate the activity, the reading in the blank well (plus EDTA) was subtracted from the control well unless otherwise mentioned. The Z' factor was determined by following a published procedure (10). L-methionine S-sulfoximine, a known inhibitor of the enzyme, was used to further validate the assay. (4,10,12) The dose-response curve was plotted by using a varied concentration of the inhibitor ranging from 0.25 to 20 mM in the same assay mix. Adoption of the protocol to the Beckman Coulter HTS system was done using SAMI software. The program includes the following

steps: 1) transfer a set of 3 assay plates containing 5 µl of compound solution of 1.25 mg/ml concentrations from Carousal to Biomek 2000, 2) add 175 µl of reaction mix to all wells, 3) start the reaction by adding 20 µl of ADP, 4) move plates to shaker for 30 seconds, 5) move the plates to the carousal again for 3 hours incubation at room temperature, 6) move the plates to Biomek 2000 for addition of 50 µl of stopping reagent, 7) move the plates to the BMG Polar Star for reading, and 8) return the plates to Carousal. The program takes 3 hours, 33 minutes, to complete a screening of 12 plates and 5 hours, 52 minutes, for 60 plates.

Validation

Linearity of the assay, effect of DMSO, and the inhibition of enzyme activity were monitored to validate the HTS format in a 96 - well plate. The activity was monitored for 3 hours at 37° C and 25° C, respectively, to check the linearity of assay (Figure - 3).

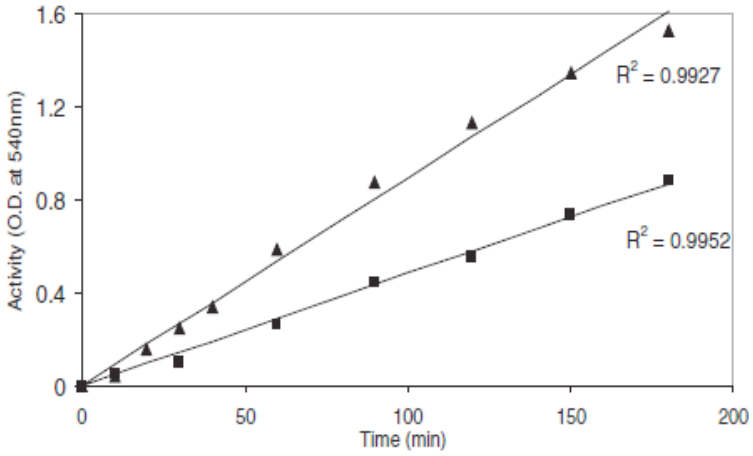

Figure - 3 Time curve of *Mycobacterium tuberculosis* glutamine synthetase activity

1) at 37° C and 2) at 25° C. The reaction was carried out with 0.5 µg/ml of *M. tuberculosis* GS in a reaction mixture containing 300 mM L glutamine, 60 mM hydroxylamine pH 7.0, 20 µM ADP, 50 µM sodium arsenate, and 250 µM $MnCl_2$ at pH 7.1 at temperatures of 37°C (▲) and 25°C (■). The experiment was carried out in a final volume of 200 µl in a 96-well microplate as described in the Materials and Methods section. For each, a blank without ADP was carried out simultaneously. The result is the average of 3 identical experiments

The results indicated that the enzyme activity was found to be linear at least for 3 hours at both the temperatures. When the incubation was extended to 5 hours at 25° C, the linearity was still maintained (data not shown). Similar results were obtained when experiments were carried out without shaking (data not shown). To assess the robustness of the assay protocol in microplate format, the Z factor as well as signal/noise (S/N) ratio was determined with varying assay volumes and enzyme concentrations (Table - 2).

Table -2 The reaction was carried out with the indicated amount of protein in a reaction mixture containing 20 mM imidazole pH - 7.0, 300 mM L-glutamine, 60 mM hydroxylamine pH 7.0, 20 µM ADP, 50 µM sodium arsenate, and 250 µM $MnCl_2$ at 25°C in a 96 - well plate for 3 hours. The rest are described in the Materials and Methods section. The result is an average of 3 identical experiments.

Table 2. Determination of Signal/Noise Ratio and Z′ Factor from 96-Well Plate Format Assays Done at Different Volumes

	Assay Volume					
	Z′ Factor			Signal/Noise Ratio		
Protein Concentration (µg/ml)	100 µl	150 µl	200 µl	100 µl	150 µl	200 µl
0.25	0.71 ± 0.034	0.91 ± 0.019	0.91 ± 0.012	3.2 ± 0.098	5.23 ± 0.088	6.68 ± 0.066
0.50	0.86 ± 0.023	0.93 ± 0.014	0.92 ± 0.011	6.26 ± 0.066	10.19 ± 0.076	12.17 ± 0.092

It was observed that both the Z values as well as the S/N ratio improve with an increase in assay volumes (39). As 0.5 µg/ml protein in 200 µl was showing the best result, the same was used to carry out subsequent assays. It was noted that the color developed in the final assay mix was stable up to 150 minutes (data not shown). The effect of DMSO was checked to decide the volume of compound solution to be used for screening. The results showed that the enzyme activity was not changed significantly even at 10 % DMSO concentration (Figure - 4).

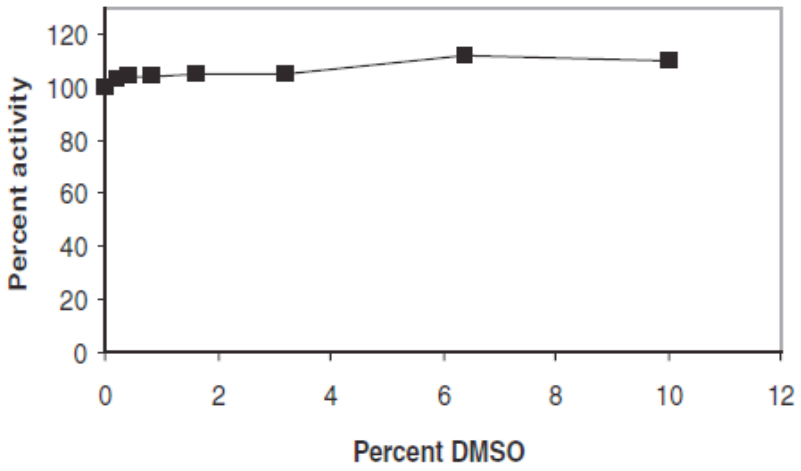

Figure-4. Effect of DMSO on *Mycobacterium tuberculosis* glutamine synthetase. The DMSO concentrations were varied, as indicated in the reaction mixture that contained otherwise all the components mentioned in Figure 2, and incubated at 25°C for 3 hours. The result is the average of 3 identical experiments.

Mixing of reagents for 30 seconds on a shaker is required to obtain uniformity in readings (data not shown). The dose-response effect of L-methionine S-sulfoximine was checked to determine the IC50 value in the standardized protocol (Figure - 5).

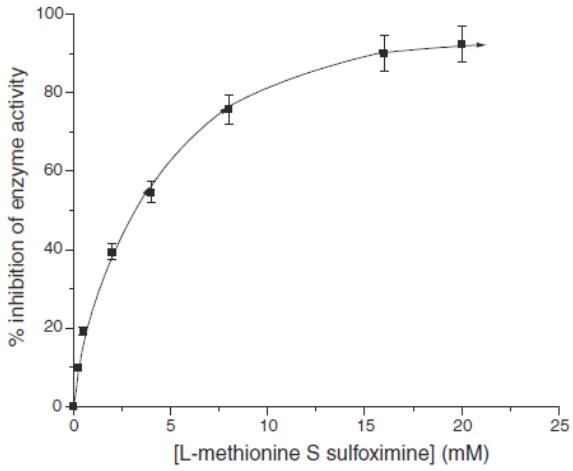

Figure -5 Dose-response curve for L-methionine S-sulfoximine.

L methionine S-sulfoximine concentrations were varied, as indicated (0.25 - 20 mM) in the reaction mixture that contained otherwise all the components described in Figure 2, and incubated at 25°C for 3 h. The result is an average of 3 identical experiments.

The IC_{50} value obtained was 3 mM using a modified protocol. The plate assay also showed an almost similar result as the tube assay, indicative of true adoption of the assay in plate format. When the assay protocol was run on the Beckman Coultier HTS system, it was found that the system would take 3 hours, 33 minutes, for 12 plates. The utilization time for 60 plates using the same program would take 5 hours, 52 minutes, as indicated by SAMI software (data not shown).

2.4 Materials and methods

2.4.1 Materials

All the chemicals were obtained from Sigma. Unosphere 6 column matrix was purchased from BioRad. Beckman Coulter platform integrated with Biomek 2000, ORCA Robot, Thermo Forma CO2 incubator, Shaker, and BMG Polar Star were used to conduct screening of in-house compounds obtained from natural product fractions using SEP BOX from Sepiatek, Germany.

2.4.2 Purification of *M. tuberculosis* Glutamine Synthetase

The enzyme GS was purified to homogeneity by following a modified method published earlier (37). *Escherichia coli* YMC21E culture was grown in LB medium until 1.2 O.D. at 600 nm. The fully-grown culture was centrifuged at 2000 *g* for 10 minutes, and the pellet thus obtained was resuspended in 2 ml of buffer (containing 10 mM imidazole pH 7.0, 10 mM $MnCl_2$, 5 mM PMSF, and 5 mM 2-mercaptoethanol) per gram of wet cell pellet. Then the cell suspension was subjected to lysis using a French press until the O.D. at 600 nm dropped to 90 % of the initial value. It was then centrifuged at 10,860 *g* for 30 minutes. The supernatant was treated with 10 % streptomycin sulfate by 10 % volume of the supernatant and kept for 15 minutes and then centrifuged at 10,860 *g* for 20 minutes. The supernatant was treated with 1 M acetic acid to a pH 5.15 and kept for 15 minutes. Again, the same was centrifuged at 10,860*g* for 20 minutes. The supernatant thus obtained was treated with 100 %

saturated ammonium sulfate 30 % by volume. The pH was adjusted to 4.4 by adding 1 M acetic acid and kept for 15 minutes. It was at 10,860 *g* for 20 minutes. The pellet was resuspended in 5 ml buffer containing 50 mM Hepes buffer pH 7.2, 10 mM MnCl2, and 0.1 M NaCl centrifuged and dialyzed extensively against the same buffer. The dialyzed was centrifuged as mentioned earlier. The supernatant was subjected to ion exchange chromatography by using a Unosphere 6 column. The protein was loaded in the column equilibrated with a buffer consisting of 10 mM imidazole, 10 mM MnCl2, and 100 mM NaCl. *MtbGS* was eluted from the column after applying an isocratic condition with 1.0 M NaCl in the loading buffer. The protein was incubated for 1 minute at 80° C. The whole preparation was centrifuged at 10,860 *g* for 20 minutes to remove the precipitate. The supernatant obtained at this stage contains more than 90 % pure *MtbGS*. The characterization and standardization experiments were carried out using this enzyme preparation. When the preparation was run through a SepharoseHR 6 column, it eluted at 640 kd, indicating dodecamer composition of the protein. The N-terminal sequence of the eluted protein confirmed that it was a glnA1 gene product of *MtbGS* (data not shown).The protein concentration was measured by the Lowry method (40).

.

2.4.3 Enzyme assays

A modified procedure was followed to carry out *MtbGS* transfer assay as described earlier (37, 38). The reaction was started by adding 400 μM ADP in 2 ml of reaction mixture containing 20 mM imidazole buffer pH 7.0, 60 mM hydroxylamine HCl pH 7.0, 3 mM $MnCl_2$, 30 mM glutamine, and 20 mM arsenate with sufficient volume of enzyme. In this reaction, hydroxylamine and L-glutamine were used as substrates in the presence of ADP and arsenate and metal ion as cofactors to yield γ - glutamyl hydroxamate and ammonia. During enzymatic reaction, an unstable intermediate called γ - glutamyl arsenate is formed. It was proposed that arsenate binds the same site as phosphate in the biosynthetic reaction and attacks glutamine through its oxygen to form the intermediate. Subsequently, hydroxylamine binds the ammonium site and attacks the intermediate already bound on the enzyme surface to release γ-glutamylhydroxamate and ammonia (37, 41). The stop reagent, 0.5 ml, containing

$FeCl_3$ (5 %), TCA (24 %), and HCl (0.6 N), was added to stop there action as well as to form the purplish complex between γ-glutamyl hydroxamate and $FeCl_3$ in acidic condition (42). This reaction is being carried out to detect the enzyme activity in crude cell lysate because of its very specific color development, which nullifies the potential of assay artifacts. Incubation of the reaction mixture without ADP served as a blank. The color was monitored at 540 nm in a Cary 50 Bio spectrophotometer. K_m values were determined using varied concentrations of L-glutamine (5-500 mM), hydroxylamine (0.8 - 200 mM), ADP (0.5 - 20 μM), $MnCl_2$ (2-320 μM), and Na3AsO4 (1 - 50 μm), keeping other components at a constant level. A Hanes-Wolf plot was drawn from the data point to find out the K_m values of the respective components. The final assay mix contained 20 mM imidazole buffer pH 7.0, 300 mM L-glutamine, 20 μM ADP, 60 mM hydroxylamine pH 7.0, 50 μM Na3AsO4, and 250 μM $MnCl_2$. The reaction was started by adding ADP in the reaction mixture and was monitored at 540 nm after addition of stopping reagent. In the classical assay, water was added instead of ADP in the blank. To use the HTS plat form more conveniently in the microplate format, EDTA was added in a whole reaction mix, which serves as a blank. The microplate format assays were carried out using 200 μl reaction mix, and the plates were incubated for 3 hours at 25° C followed by addition of 50 μl stopping reagent to develop color. After adding the stopping reagent, the reading was taken using a 520 nm filter in BMG polar star. To calculate the activity, the reading in the blank well (plus EDTA) was subtracted from the control well unless otherwise mentioned. The Z' factor was determined by following a published procedure (39). L-methionine S-sulfoximine, a known inhibitor of the enzyme, was used to further validate the assay (4, 10, 12,). The dose-response curve was plotted by using a varied concentration of the inhibitor ranging from 0.25 to 20 mM in the same assay mix. Adoption of the protocol to the Beckman Coulter HTS system was done using SAMI software. The program includes the following steps: 1) transfer a set of 3 assay plates containing 5 μl of compound solution of 1.25 mg/ml concentrations from Carousal to Biomek 2000, 2) add 175 μl of reaction mix to all wells, 3) start the reaction by adding 20 μl of ADP, 4) move plates to shaker for 30 seconds, 5) move the plates to the carousal again for 3 hours incubation at room temperature, 6) move the plates to Biomek 2000 for addition of 50

µl of stopping reagent, 7) move the plates to the BMG Polar Star for reading, and 8) return the plates to Carousal. The program takes 3 hours, 33 minutes, to complete a screening of 12 plates and 5 hours, 52 minutes, for 60 plates.

2.5 Discussion

A colorimetric assay for HTS is advantageous if the development of color takes place instantaneously and remains stable for a substantial period of time. Among the transfer and biosynthetic reactions of GS, the former was selected for further study for the development of assay format to HTS due to the fast and stable color formation of the assay mixture, which brings flexibility and convenience in screening programs. In addition to GS's playing a major role in *M. tuberculosis* pathogenicity, this enzyme is also found to be associated with certain human brain disorders (43, 44). Considering the possibility of GS's becoming a target in the future and developing new molecules against those diseases, we attempted to provide a screening solution. A simple assay in a 96-well format for HTS of *MtbGS* was developed by modifying a classical assay used earlier to check the enzyme activity in crude cell extract (37). The developed assay is robust and meets all the stringent HTS criteria. The HTS criteria considered here are 1) linearity of enzyme activity for more than 3 hours, 3) DMSO tolerance, 3) reproducible IC50 value for the standard inhibitor, and 4) robustness of the assay protocol (Figs. 2-4, Table 2). The results indicated that the Z′ factor alone is not sufficient for considering the robustness of the assay protocol; the S/N value is also very important. Therefore, along with the quality of the enzyme, optimum concentrations of the reagents and assay volume play important roles in obtaining a better S/N value. The high acidity of the stopping solution in this assay reduces the interference of colored compounds, except for a few, such as tannins (45). The present assay was developed using purified recombinant GS, and the composition of the assay mix was optimized based on its K_m values (Fig. 1, Table 1). The K_m value for L-glutamine of the *E. coli* enzymes was also determined and found that it is giving almost the same value as mentioned earlier (37) (data not shown). This proves the authenticity of our K_m data as well. An S/N ratio of ~10 was obtained using these optimized assay conditions (Table 2). A limited attempt

was made earlier to determine the better inhibitor against this enzyme from structural analogues of L-glutamine (42). Due to the allosteric nature of *MtbGS*, apart from the picking up of competitive inhibitors, there are possibilities to pick up compounds with uncompetitive, noncompetitive, and allosteric inhibitors of the enzyme using this high-throughput assay and diverse chemical library. We have successfully screened ~ 617 natural product fractions, 20 synthetic compounds, and 7 standard antibiotics including rifampicin. The results did not show any plate or distribution effect (data not shown). Further screening is presently under way in our laboratory.

Section 2B - Development **of a high-throughput screening protocol based on biosynthetic activity of *M. tuberculosis* Glutamine synthetase**

2.6 Introduction

The components involved in biosynthetic activity are different from the components of transfer activity of the enzyme. The enzyme participates in biosynthetic activity only under in vivo conditions in which L-glutamic acid, ammonia and adenosine triphosphate (ATP) participate as substrates to generate L-glutamine, adenosine diphosphate (ADP), and Pi (36,37). So, even though L-methionine S-sulfoximine and DL-phosphothriacin inhibit the activities of the enzyme, finding true inhibitors for in vivo efficacy could become very difficult if they are picked up by screening using the transfer assay. Development of a high-throughput screening (HTS) assay protocol based on biosynthetic activity of the enzyme for identifying novel chemical structure against *M. tuberculosis* has immense importance in the current situation. The present study evaluates the kinetic properties of *MtbGS* in biosynthetic activity as well as converts it to a robust high-throughput assay protocol for screening of a chemically diverse synthetic and natural product library.

2.7 Results

Rapid development and stability of color are considered the most valuable aspects in accepting any absorbance-based assay principle for developing a high-throughput assay protocol. The colorimetric estimation of phosphate typically involves the interaction of phosphate, molybdate and reducing agents or dyes to produce a colored complex (46). The reduction of the phosphomolybdate complex in a strong acid solution results in a formation of molybdenum blue. Numerous assays for quantitating phosphate, based on this reaction, have been developed with varying sensitivities and applications, mainly by altering the nature of the reducing agent (47). Similarly, in the glutamine synthetase biosynthetic assay, ferrous sulfate was used conventionally as a reducing agent for Pi detection (37). The crux of the assay system was a continuous increase in color due to the hydrolysis of ATP (46). The major objective during the development of the screening protocol was to control the rate of ATP hydrolysis as well as to increase the sensitivity range with respect to Pi concentration. In this protocol, the reducing agent was changed from FeSO4 to ascorbic acid for rapid development of color in a highly acidic condition. Once the color was developed, sodium citrate was used to control the hydrolysis of ATP. In this process, the increase in color was confined to a negligible extent of 3 % to 4 % up to 50 minutes after the addition of sodium citrate in the reaction mix (Figure - 6).

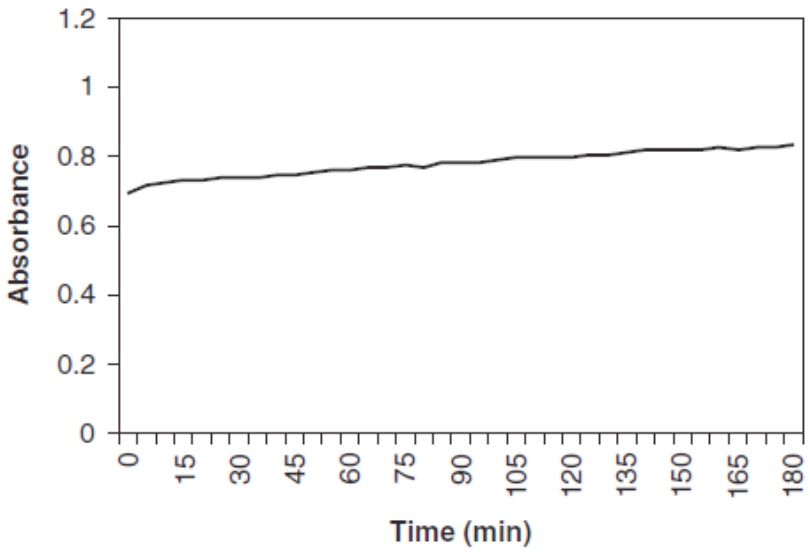

Figure - 6. Kinetics of color development in the assay mix.

Stability profile of the color developed in the final reaction mix. The reaction was carried out with 62.5 µg/ml of *Mycobacterium tuberculosis* glutamine synthetase in a reaction mixture containing 220 mM glutamic acid, 7.5 mM ammonium chloride, 7.6 mM adenosine triphosphate, and 25 mM magnesium chloride at pH 6.8, as described in "Materials and Methods." The development of color was monitored at 655 nm up to 45 minutes at the interval of 2 minutes by using a Cary 50 Bio Spectrophotometer.

Recently, it was clearly shown that the K_m values for all the components of *M. tuberculosis* glutamine synthetase participating in the transfer assay are higher than for other bacterial enzymes (36). The enzyme obtained from other bacterial sources characteristically depends on Mg^{2+} for its biosynthetic activity and mainly on Mn2+ for the transfer activity (37). An earlier report on the enzyme activity purified from extracellular medium of *M. tuberculosis* culture indicated that the optimum pH levels for biosynthetic and transfer activities are 7.5 and 7.0 respectively (10). To get a broader picture of the pattern of substrates and cofactor use by this recombinant *MtbGS*, the K_m values were determined at 4 different pH levels ranging from 8.0 to 6.5 (Table -3).

Table - 3 As described in the "Materials and Methods" section. The ±standard deviation and K_m values are obtained from 3 identical experiments

	Estimated K_m (mM)			
Assay pH	*L-Glutamic Acid*	*Ammonium Chloride*	*Magnesium Chloride*	*Adenosine Triphosphate*
6.5	29 ± 1.41	0.21 ± 0.034	7.5 ± 0.047	0.026 ± 0.026
6.8	22 ± 1.4	0.75 ± 0.017	3.25 ± 0.35	2.5 ± 0.106
7.5	36 ± 2	0.75 ± 0.017	6 ± 0.70	2.6 ± 0.26
8.0	165 ± 2.1	1 ± 0.028	2.5 ± 0.033	4.5 ± 0.036

.

The enzyme was purified from recombinant *E. coli* strain YMC21E by following an earlier published method (36). More than 90 % pure enzyme was used for the determination of K_m of all the substrates and cofactor required in the biosynthetic assay (Figure - 7). Hanes-Wolf plots were drawn to find the K_m values of all the constituents of assay mixture. The results indicated that the affinity for both L-glutamic acid and ATP is highest at pH 6.8. The K_m for other constituents remained within a narrow range with respect to pH, ranging from 6.8 to 8.0. As the pH dropped further to 6.5, the most significant change observed was the dramatic decrease in K_m values of ATP (Table 3). Otherwise, the K_m values for L-glutamic acid and $MgCl_2$ started increasing again when the pH was changed from 6.8 to 6.5. Biosynthetic activity of *MtbGS* is not supported by any other metal ions except Mg^{2+} (data not shown).

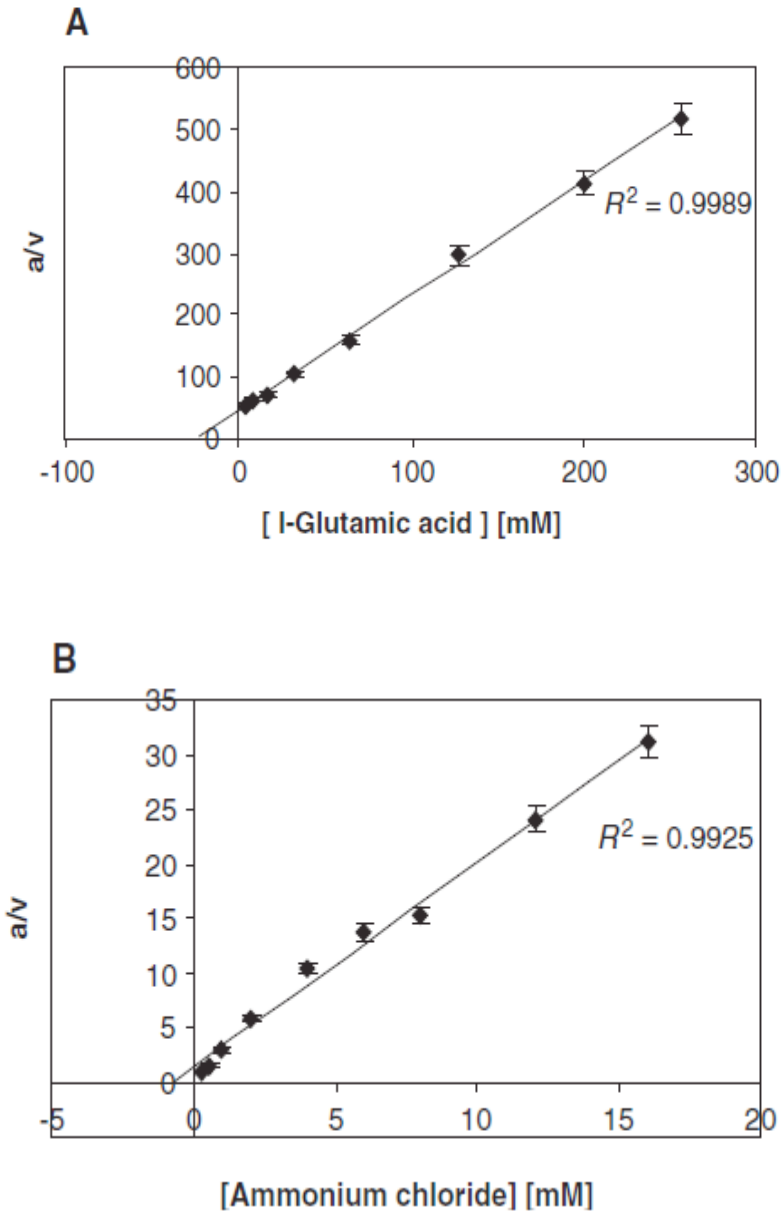

Figure – 7 K_m values determined for different substrates and cofactors of *Mycobacterium tuberculosis* glutamine synthetase in biosynthetic activity at different pH levels. All the experiments were carried out using 62.5 µg/ml of *M. tuberculosis* glutamine synthetase as mentioned in the "Materials and Methods" section. (**A**) Hanes-Wolf plots of initial velocity pattern were drawn for the biosynthetic reaction with varied L-glutamic acid from 4 mM to 256 mM at pH 6.8, keeping ammonium chloride (8 mM), adenosine triphosphate (ATP; 7.6 mM), and magnesium chloride (25 mM) at the saturating level. (**B**) Varying concentrations of ammonium chloride from 0.25 mM to 16 mM were used at the saturating level of L-glutamic acid (220 mM), ATP (7.6 mM), and magnesium chloride (25 mM).

Validation

Linearity of the assay, effect of DMSO and the inhibition of enzyme activity were monitored to validate the HTS format in 96 well plates. The activity was monitored for 3 hrs at 37°C and 25°C respectively to check the linearity of assay (Figure 8). The results indicated that the enzyme activity was found to be linear at least for 3 hrs at 25°C and only 60 minutes at 37°C.

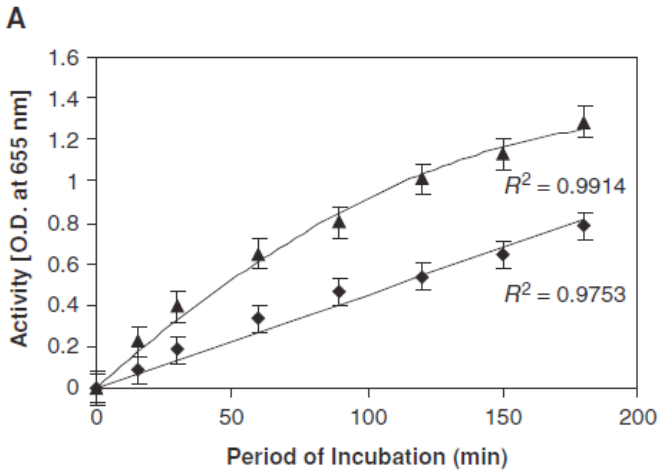

Figure 8 Time curve of *Mycobacterium tuberculosis* glutamine synthetase activity.

The reaction was carried out with 62.5 µg/ml of *Mycobacterium tuberculosis* Glutamine synthetase in a reaction mixture containing 220 mM glutamic Acid, 7.5 mM Ammonium chloride, 7.6 mM ATP and 32.5 mM Magnesium Chloride at pH 6.8 at temperatures of 37°C (▲) and 25° C (■). The experiment was carried out at a final volume of 100µl in a 96 well plate as described in materials and methods section. For each, a blank with 22.5 mM of EDTA was carried out. The results are the average of three identical experiments

In order to assess the robustness of the assay protocol in microtiter plate format, the Z' factors as well as S/N ratio were determined with varying enzyme concentrations (Table 4). The results clearly indicated that the enzyme activity was linearly increasing with respect to enzyme concentration in the assay mix. As 62.5 µg/ml protein in 100 µl volume was showing the best results with respect to Z' factor and S/N ratio, the same was used to carry out screening protocol.

Table – 4 Determination of Signal/Noise ratio and Z' Factor from 96 well plate format assays done at different Volumes. The reaction was carried out with the mentioned amount of protein in reaction mixture containing 50 mM Hepes buffer pH 6.8, 220 mM L-Glutamic Acid pH 6.8, 7.5 mM Ammonium chloride, 32.5 mM Magnesium chloride and 7.6mM ATP (~pH 6.8) at 25 º C in a 96 well plate for 2 hrs as mentioned in materials and methods. The results are the average of three identical experiments.

Protein concentration (µg/ml)	Z' factor	S/N ratio
10.4	0.43±0.066	2.26±0.017
20.8	0.27±0.074	3.37±0.013
41.66	0.58±0.120	4.30±0.016
62.5	0.75±0.031	6.18±0.019

The effect of DMSO was checked to decide the volume of compound solution be used for screening. The results showed that the enzyme activity was not changed significantly even at 10 % DMSO concentration (Figure 8). Mixing of reagents for 30 seconds on a shaker is required to obtain uniformity in readings (data not shown). The dose response effect of L-methionine S sulfoximine and Phosphothriacin was checked to find out IC_{50} values at pH 6.8, 7.5 and 8.0 (Figure 10). The IC_{50} values obtained for both L –methionine S-sulfoximine and DL-Phosphothriacin were found to be 500 µM and 30 µM respectively at pH 6.8. When the same was carried out at pH 7.5 and 8.0 respectively using all the components of the assay mix with respect to their K_m values, the IC 50 values were increasing with pH. This indicated that the affinities of standard inhibitors are also higher at pH 6.8 which might be helpful in identifying even weak

inhibitors from random screening. The plate and tube assay both have showed almost similar result, which is indicative of true adoption of the assay in plate format.

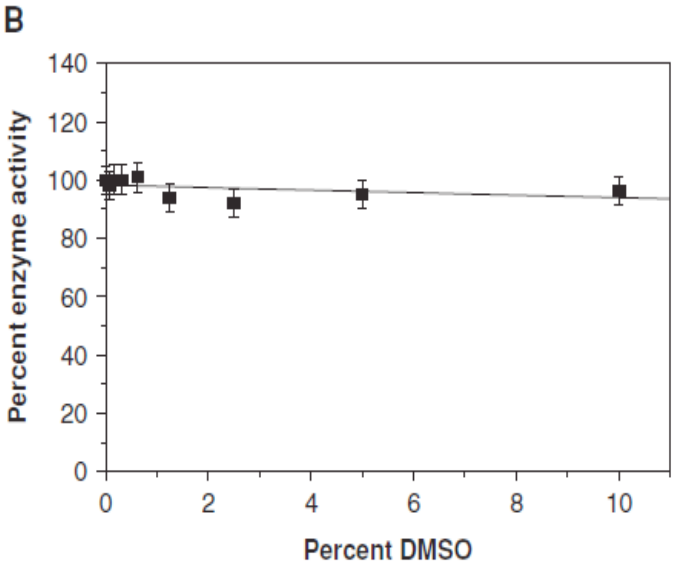

Figure 9. Effect **of DMSO on the biosynthetic activity of *Mycobacterium tuberculosis* glutamine synthetase**. The DMSO concentration were varied, as indicated in the reaction mixture that contained otherwise all the components mentioned in Figure 2, and incubated at 25° C for 2 hrs. The result is the average of 3 identical experiments.

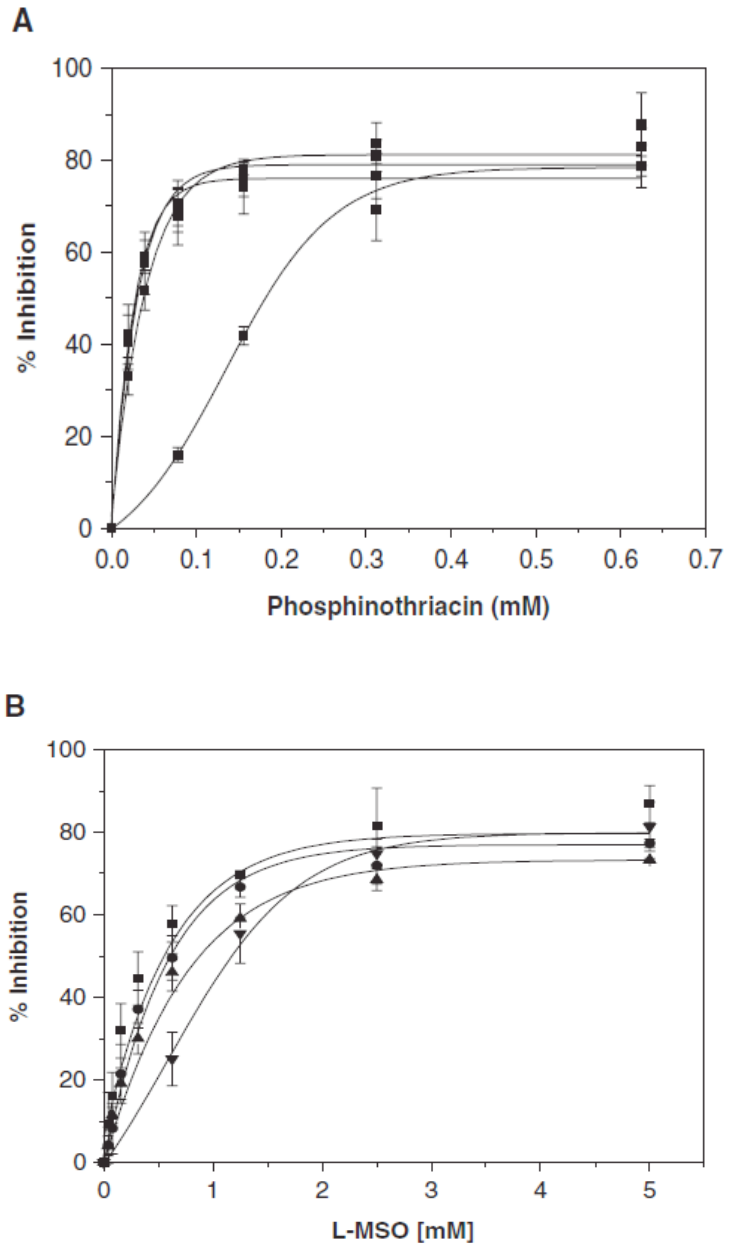

Figure - 10 Dose-response effect of inhibitors on biosynthetic activity of *M. tuberculosis* glutamine synthetase. Varied concentrations of (**A**) L-methionine S-sulfoximine and (**B**) phosphinothricin ranging from 0.25 to 5.0 mM were incubated with 62.5 µg/ml of the enzyme at 25° C for 15 minutes. Then, the reaction was carried out using all the components at saturating level with respect to pH as mentioned in the "Materials and Methods" section.

A chemically diverse library consisting of both extract/fraction from medicinal plants as well as synthetic compounds often either consists of structures that is poorly soluble in aqueous phase or interferes with the absorbance or fluorescence of the analyte in the reaction mixture. In order to avoid this type of color interference, another plate with identical plate map is used where compound is added at the end of the reaction before taking the read out. This calculation makes the procedure very easy to pick up the actives from the natural product/synthetic library with better estimation of inhibition profile (Equation-1). When the assay protocol was run on Beckman Coultier HTS system, it was found that the system would take 2 hrs 47 minutes for 12 plates. The utilization time for 30 assay and replica plates each using the same program would take 5 hrs 09 minutes as indicated by SAMI software (data not shown).

The inhibition profile obtained from the assay plates after screening of 1164 samples was corrected by using the data from replica plates by using a formula (Equation I). Then the inhibition data is shown as scattered plot with respect to the respective compounds (Figure 11). Most of the compounds belong within the range where negligible affect is observed. The histogram of the same data confirmed the earlier observation as well as robustness of the screening protocol (Figure 11). Out of 1164 samples screened, only 29 samples were showing > 40% inhibition (Table-5). The confirmation experiment was carried out using the fresh stock solution of the actives obtained during primary screening of which, 12 samples are identified as confirmed hits.

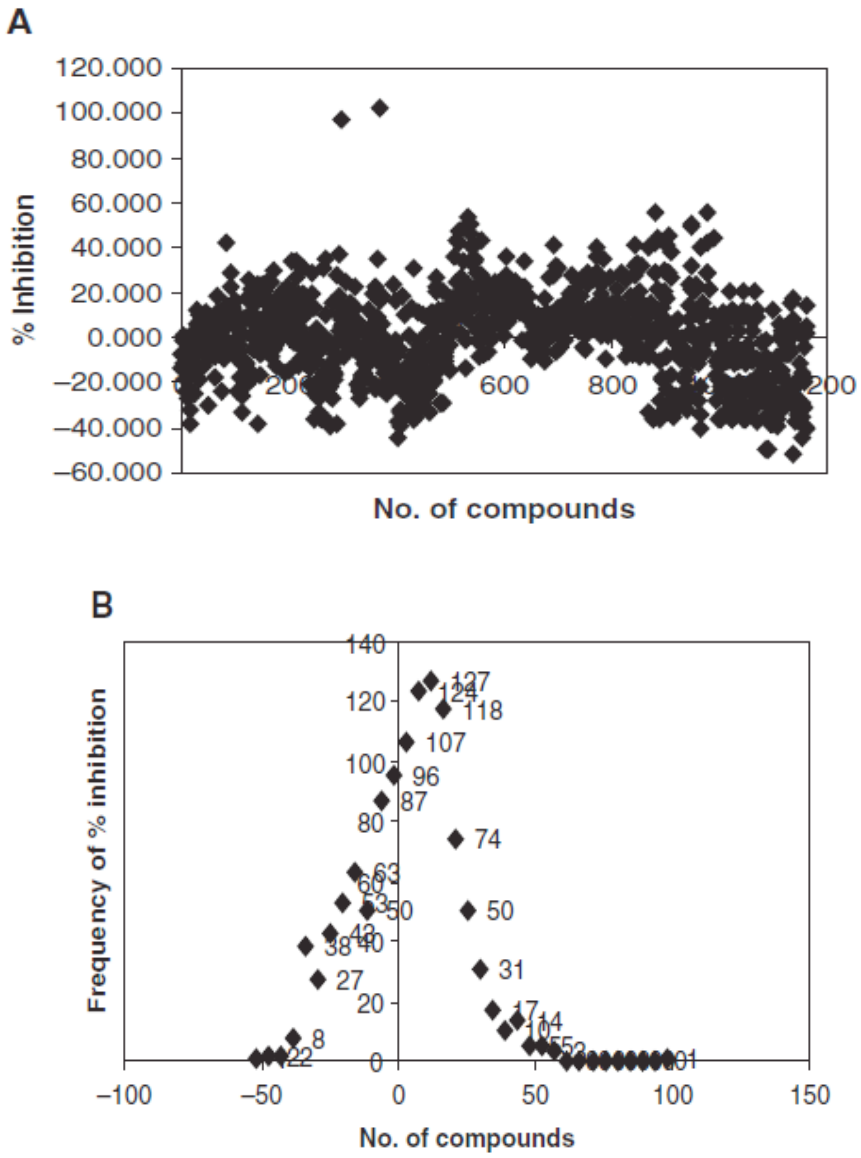

Figure - 11 Analysis of the data obtained from screening of a diverse chemical library on *M. tuberculosis* glutamine synthetase. Samples consisting of extracts and fractions of plants including synthetic compounds were screened at 500 µg/ml concentration using a high throughput protocol for biosynthetic assay of the enzyme as described in the "Materials and Methods" section. (**A**) Scattered plot of percentage inhibition data obtained from screening of the library. (**B**) The histogram of the analyzed screening data mentioned above.

Table -5 The summary of screening results on *Mycobacterium tuberculosis* glutamine synthetase

Samples screened	Actives showing >40 % activity	Actives confirmed
1164	29	12

2.8 Materials and Methods

2.8.1 Materials

All the chemicals were obtained from Sigma. Beckman Coulter platform integrated with Biomek 2000, ORCA Robot, Thermo Forma CO 2 incubator, Shaker, and BMG Polar Star were used to conduct screening of in-house library obtained from natural products fractions using SEP BOX from Sepiatek, Germany and synthetic compounds from in-house depository. Cary 50 bio Spectrophotometer was used to carry out the initial standardization of biosynthetic experiments.

2.8.2 Purification of the enzyme

The enzyme was purified from recombinant *E. coli* strain YMC21E by using a modified method (36). The enzyme preparation was used for further standardization and characterization of the enzyme for biosynthetic activity of the enzyme as well as development of the HTS screening protocol.

2.8.3 Transfer assay

The transfer assay was carried out using 20 mM imidazole buffer pH 7.0, 300 mM L-glutamine, 60 mM Hydroxylamine, 20 µM ADP, 50 µM Na3AsO4 and 250 µm $MnCl_2$. The stop reagent, containing FeCl3 (5%), TCA (24%) and HCL (0.6 N) was added to stop the reaction as well as to form the purplish complex between γ – glutamylhydroxamate and $FeCl_3$ in acidic condition (39)

2.8.4 Biosynthetic assay

A modified protocol was followed to carry out *MtbGS* biosynthetic assay as described earlier (48, 49). The reaction was started by adding 7.6 mM of ATP, in 200 µl of reaction mixture containing 20 mM Imidazole buffer pH 7.0, 100 mM $NH_3CO_2C_3H_5COOH$, 50 mM $MgCl_2$, 50 mM NH_4Cl and sufficient volume of enzyme (48, 49). In this reaction, Ammonium Chloride, L-Glutamic Acid and ATP were used as substrate and Mg_{2+} ion as cofactor to yield inorganic phosphate, glutamine and ammonia. To stop the reaction 12 % w/v L-Ascorbic Acid in 1N HCL and 2 % w/v Ammonium Molybdate in ddH2O were mixed in 2:1 proportion, and 600 µl of that is added to 200 µl of reaction mixture and mixed well to developed immediately the blue color (46-50). To get the fully developed color, it was incubated for 7 minutes. After that 600 µl of 1% sodium citrate tribasic dihydrate in 1% acetic acid in ddH2O should be added in the reaction mixture, to restrict the further development of color due to hydrolysis of ATP (46-50). Incubation of the reaction mixture with 22.5 mM EDTA is served as blank. Using Cary 50 Bio Spectrophotometer monitored the color at 655 nm after 30 minutes incubation.

K_m values were determined using varied concentrations of L Glutamic acid (4.0 – 256 mM), Ammonium chloride (0.25-16.0 mM), ATP (0.5-25.0 mM) and $MgCl_2$ (0.8-20.0 mM), Keeping other components at a constant level. The K_m values were determined at three different pH's taking a range from 6.8, 7.5 and 8.0. Hanes-wolf plot was drawn from the data point to find out the K_m values of the respective components separately at all three different pH as mentioned earlier. Considering the physiological relevance and determined K_m values it was decided to take pH 6.8 for final assay protocol.

The final assays mix contained 50 mM Hepes buffer pH 6.8, 220 mM L-Glutamic acid pH 6.8, 7.5 mM NH_4Cl and 32.5 mM $MgCl_2$ and. The reaction was started by adding 7.6 mM ATP ~ pH 6.8 in the reaction mixture and incubated for 2hrs at 25^oC. Adding stop reagent terminated the reaction and subsequently citrate was added within 10

minutes. The whole mixture was kept at room temperature for another 30 minutes to take the read out using 620 nm filter.

2.8.5 High throughput screening protocol

The assay plates were made by adding 5 µl of samples in DMSO at10mg/ml concentration to the respective wells according to the format. 5 µl DMSO should be added to the control and blank wells. 5 µl of 420 mM EDTA is added in the blank wells. Same volume of water should also be added in other wells and then 80 µl reaction mix was added to all the wells. The plate is kept on shaker for 2 minutes for proper mixing. Then adding 10 µl of ATP to all wells started the reaction. After incubation, 75 µl stop reagent was added and allow it to develop the color for ~7 minutes. The reading was taken after 30 minutes of addition of 75 µl sodium citrate in the reaction mix using 620 nm filters in BMG polar star. The Z' factor was determined by following a published procedure (32). L–Methionine S–sulfoximine and DL-Phosphothriacin are two known inhibitors, which were used to further validate the assay. Using a varied concentration of the inhibitor ranging from 0.125 mM to 5 mM dose response curves are plotted at different pHs mentioned earlier. 1070 natural products, 94 synthetic compounds including 7 standard antibiotics including Rifampicin were screened as single point data using 0.5 mg/ml concentrations in the final assay mix.

Adoption of the protocol to the Beckman Coulter HTS System was done using SAMI software. The program includes the following steps, a) Transfer a set of three assay plates containing 5µl of compound solutions of 10 mg/ml concentration/DMSO/EDTA/water from Carousal to Biomek 2000, b) Add 80 µl of reaction mix to all wells, c) Start the reaction by adding 10 µl of ATP, d) Move plates to shaker for 30 seconds, e) Move the plates to the carousal again for 2hrs incubation at room temperature, f) Move the plates to Biomek 2000 for addition of 75 µl of stop reagent, and g) followed by moving plates to BMG Polar star for reading, h) Return the

plates to Carousal. The program takes 2 hrs 47 minutes to complete screening of 12 plates and 5 hrs 09 minutes for 60 plates.

2.8.6 Replica Plate

Apart from addition of samples after termination of the reaction in replica plates, the protocol followed in the replica plates is otherwise identical. Following formula was used for the normalization of the data obtained in assay plate.

$$\text{Percent inhibition} = 100 - \frac{[(S)\,A - \{(C)\,R - (S)\,R\}]}{(C)\,A} \times 100 \quad \text{---------- (Equation -I)}$$

Where, (S) A is sample reading in assay plate,
(S) R is sample reading in replica plate,
(C) R is reading of control in replica plate,
(C) A is reading of control in assay plate.

2.9 Discussion

The major challenge in biosynthetic assay was to substantially protect the rapid increase in color due to ATP hydrolysis under the reaction condition used. It was clearly shown in this study that addition of citrate in the assay mix has blocked further increase of color (Figure 1). Many coupled assays were designed earlier to carry out screening of chemical library because of mainly the inability to stop this continuous increase in color (46-50). In earlier studies it was reported that the activity of this enzyme from other bacterial sources was seen to be optimum at pH 7.5 (48, 49). *Mycobacterium tuberculosis* enzyme clearly showed that the affinity for the substrates is highest at pH 6.8 (Table-I). Optimum enzyme activity at pH 6.8 supports its physiological relevance for the extracellular function of the enzyme. So, the screening of a chemical library on biosynthetic activity at pH 6.8 has better prospect to get an

antitubercular Glutamine synthetase inhibitor than at any other pH. The results also indicated that the assay protocol is robust for high throughput screening (Figure 3) (table II).

The HTS criteria considered here were 1) linearity of enzyme activity for more than 2 hrs, 2) DMSO tolerance and 3) reproducibility of IC50 value for the standard inhibitor (Figure 2-4 and Table II). The assay protocol needed to successfully overcome one more validation step using a library mainly consisting of extracts and fractions from medicinal plants along with synthetic compounds. It was observed that many a samples from natural product and synthetic library consists of colored molecules having poor solubility in aqueous solution. These samples cause interference in the read out during screening which increases the number of false positive and false negatives. In order to overcome this bottleneck, replica plates were used to get a more accurate estimate about the interference in the read out caused by the extract or fractions. After correction in the reading, 29 samples were picked up from a set of 1164 for further confirmation studies (Equation-I, Table-III). Without this correction, it was not possible to identify even a single extract/fraction as true inhibitor of the enzyme. Mainly two reasons were considered in deciding the cut off as 40 % inhibition, 1) very low quantity of the active ingredient may be present in the crude extracts of the plants used and 2) the enzyme is allosteric in nature. The scattered plot and histogram of screening data clearly indicated that the protocol was robust in screening any chemical library (Figure 5-6). Finally, 12 samples were identified as confirmed hits. Currently the chromatographic separations are being carried out guided by its inhibition on *MtbGS* to identify the molecule.

2.10 References

1) Wojciech W. Krajewski, T. Alwyn Jones, and Sherry L. Mowbray. Structure of *Mycobacterium tuberculosis glutamine synthetase* in complex with a transition-state mimic provides functional insights. PNAS. 2005 vol. 102 (30) 10499–10504.

2) Y. KUMADA, D. R. BENSON, D. HILLEMANN, T. J. HOSTED, D. A. ROCHEFORT, C. J. THOMPSON, W. WOHLLEBEN, Y. TATENOVII, Evolution of the glutamine synthetase gene, one of the oldest existing and functioning genes. Proc. Natl. Acad. Sci. USA. Vol. 90, pp. 3009-3013, April 1993

3) Eisenberg, D., Almassy, R. J., Janson, C. A., Chapman, M. S., Suh, S. W., Cascio, D. & Smith, W. W. (1987) Some Evolutionary Relationships of the Primary Biological Catalysts Glutamine Synthetase and RuBisCOCold Spring Harbor Symp. Quant. Biol. 52, 483-490.

4) Michael V. Tullius, Gu¨nter Harth, and Marcus A. Horwitz Glutamine Synthetase GlnA1 Is Essential for Growth of *Mycobacterium tuberculosis* in Human THP-1 Macrophages and Guinea Pigs. INFECTION AND IMMUNITY, July 2003, p. 3927–3936

5) Dall'Asta, V., P. A. Rossi, O. Bussolati, and G. C. Gazzola. 1994. Regulatory volume decrease of cultured human fibroblasts involves changes in intracellular amino-acid pool. Biochim. Biophys. Acta 1220:139–145.

6) Reitzer, L. J. 1996. Ammonia assimilation and the biosynthesis of glutamine, glutamate, aspartate, L-alanine, and D-alanine, p. 391–407. *In* F. C. Neidhardt and R. Curtiss (ed.), *Escherichia coli* and *Salmonella typhimurium*, 2nd ed. ASM Press, Washington, D.C.

7) Merrick, M. J., and R. A. Edwards. 1995. Nitrogen control in bacteria. Microbiol. Rev. 59:604–622.

8) Shatters, R. G., Y. Liu, and M. L. Kahn. 1993. Isolation and characterization of a novel glutamine synthetase from *Rhizobium meliloti*. J. Biol. Chem. 268:469–475.

9) Cole, S. T., R. Brosch, J. Parkhill, T. Garnier, C. Churcher, D. Harris, S. V. Gordon, K. Eiglmeier, S. Gas, C. E. Barry III, F. Tekaia, K. Badcock, D. Basham, D. Brown, T. Chillingworth, R. Connor, R. Davies, K. Devlin, T. Feltwell, S. Gentles, N. Hamlin, S.

Holroyd, T. Hornsby, K. Jagels, B. G. Barrell, et al. 1998. Deciphering the biology of *Mycobacterium tuberculosis* from the complete genome sequence. Nature 393:537–544

10) Harth, G., D. L. Clemens, and M. A. Horwitz. 1994. Glutamine synthetase of *Mycobacterium tuberculosis*: extracellular release and characterization of its enzymatic activity. Proc. Natl.Acad. Sci. USA 91:9342–9346.

11) Harth, G., and M. A. Horwitz. 1997. Expression and efficient export of enzymatically active *Mycobacterium tuberculosis* glutamine synthetase in *Mycobacterium smegmatis* and evidence that the information for export is contained within the protein. J. Biol. Chem. 272:22728–22735..

12) Harth, G., and M. A. Horwitz. 1999. An inhibitor of exported *Mycobacterium tuberculosis* glutamine synthetase selectively blocks the growth of pathogenic mycobacteria in axenic culture and in human monocytes: extracellular proteins as potential novel drug targets. J. Exp. Med. 189:1425–1436.

13) Tullius, M. V., G. Harth, and M. A. Horwitz. 2001. High extracellular levels of *Mycobacterium tuberculosis* glutamine synthetase and superoxide dismutase in actively growing cultures are due to high expression and extracellular stability rather than to a protein-specific export mechanism. Infect. Immun. 69:6348–6363.

14) Sassetti, C. M., Boyd, D. H. & Rubin, E. J. (2003) Genes required for mycobacterial growth defined by high density mutagenesi*Mol. Microbiol.* 48, 77–84.

15) Harth, G., Zamecnik, P. C., Tang, J. Y., Tabatadze, D.&Horwitz, M. A. Structure of Mycobacterium tuberculosis glutamine synthetase in complex with a transition-state mimic provides functional insights (2000) *Proc. Natl. Acad. Sci. USA* 97, 418–423.

16) Harth, G. & Horwitz, M. A. Inhibition of *Mycobacterium tuberculosis* Glutamine Synthetase as a Novel Antibiotic Strategy against Tuberculosis: Demonstration of Efficacy In Vivo (2003) *Infect. Immun.* 71, 456–464.

17) Wojciech W. Krajewski, T. Alwyn Jones, and Sherry L. Mowbray, Structure of Mycobacterium tuberculosis glutamine synthetase in complex with a transition-state mimic provides functional insights. PNAS (2005) vol. 102(30) 10499–10504

18) Yamashita, M. M., Almassy, R. J., Janson, C. A., Cascio, D. & Eisenberg, D. Refined atomic model of glutamine synthetase at 3.5 A resolution. (1989) *J. Biol. Chem.* 264, 17681–17690.

19) Liaw, S. H., Pan, C. & Eisenberg, D. Feedback inhibition of fully unadenylylated glutamine synthetase from Salmonella typhimurium by glycine, alanine, and serine (1993) *Proc. Natl. Acad. Sci. USA* 90, 4996–5000.

20) Liaw, S. H., Jun, G. & Eisenberg, D. Structural model for the reaction mechanism of glutamine synthetase, based on five crystal structures of enzyme-substrate complexes (1994) *Biochemistry* 33, 11184–11188.

21) Gill, H. S. & Eisenberg, D. The Crystal Structure of Phosphinothricin in the Active Site of Glutamine Synthetase Illuminates the Mechanism of Enzymatic Inhibition (2001) *Biochemistry* 40, 1903–1912.

22) Gill, H. S., Pfluegl, G. M. & Eisenberg, D. Multicopy Crystallographic Refinement of a Relaxed Glutamine Synthetase from *Mycobacterium tuberculosis* Highlights Flexible Loops in the Enzymatic Mechanism and Its Regulation (2002) *Biochemistry* 41, 9863–9872.

23) E.R. Stadtman, A. Ginsburg, in: P.D. Boyer (Ed.), The Enzymes, Vol. 10, Academic Press, New York, 1974, pp. 755 -807

24) A. Ginsburg, Adv. Protein Chem. 26 (1972) 1-76.

25) R.L. Levine, L. Mosoni, B.S. Berlett, E.R. Stadtman, Methionine residues as endogenous antioxidants in proteins Proc. Natl. Acad. Sci. USA 93 (1996) 15036-15040.

26) S.H. Liaw, J.J. Villafranca, D. Eisenberg, A model for oxidative modification of glutamine synthetase, based on crystal structures of mutant H269N and the oxidized enzyme Biochemistry 32 (1993) 7999 - 8003

27) M. Yamashita, R. Almassy, C. Janson, D. Cascio, D. Eisenberg, Refined atomic model of glutamine synthetase at 3.5 A resolution. J. Biol. Chem. 264 (1989) 17681 - 17690.

28) F.R. Bloom, M.S. Levin, F. Foor, B. Tyler, Regulation of glutamine synthetase formation in Escherichia coli: characterization of mutants lacking the uridylyltransferase J. Bacteriol. 134 (1978) 569 -577.

29) H. Gill, G.M.U. Pfluegl, D. Eisenberg, Preliminary crystallographic studies on glutamine synthetase from *Mycobacterium tuberculosis* Acta Cryst. D 55 (1999) 865-868.

30) http://en.wikipedia.org/wiki/High-throughput_screening

31) Hann MM, Oprea TI (June 2004). "Pursuing the leadlikeness concept in pharmaceutical research". *Curr Opin Chem Biol* 8 (3): 255–63

32) Agrestia JJ, Antipovc E, Abatea AR, Ahna K, Rowata AC, Barete JC, Marquezf M, Klibanovc AM, Griffiths AD, Weitz DA (2010). "Ultrahigh-throughput screening in drop-based microfluidics for directed evolution". *Proceedings of the National Academy of Sciences* 107 (9): 4004–4009.

33) Ethan Schonbrun, Adam R. Abate, Paul E. Steinvurzel, David. A. Weitz and Kenneth B. Crozier (2010). "High-throughput fluorescence detection using an integrated zone-plate array. *Lab on a Chip* 10 (7): 852-856.

34) S.H. Liaw, D. Eisenberg, Structural model for the reaction mechanism of glutamine synthetase, based on five crystal structures of enzyme-substrate complexesBiochemistry 33 (1994) 675-681.

35) A. Meister, in: Glutamine: Metabolism, Enzymology and Regulation, Academic Press, New York, 1980, pp. 140.

36) Upasana Singh, Vinita Panchanadikar and Dhiman Sarkar Development of a Simple Assay Protocol for High-Throughput Screening of *Mycobacterium tuberculosis* Glutamine Synthetase for the Identification of Novel Inhibitors *J Biomol Screen* 2005; 10; 725

37) Wollfolk CA, Shapiro B, Stadtman ER: Regulation of glutamine synthetase: I. Purification and properties of glutamine synthetase from *Escherichia coli*. *Arch Biochem Biophys* 1966;116:177-192.

38) Shapiro BM, Stadtman ER: Glutamine synthetase (*Escherichia coli*). *Methods Enzymol* 1970;17a:910-922

39) Zhang JH,ChungTDY, OldenburgKR: A simple statistical parameter for use in evaluation and validation of high-throughput screening assays. *J Biomol Screen* 1999;4:67-73.

40) Lowry OH, Rosebrough NJ, Farr AL, Randall RJ: Protein measurement with Folin phenol reagent. *J Biol Chem*1951;193:265-275.

41) Eisenberg D, Gill SH, Pfluegl GMU, Rotstein SH: Structure-function relationships of glutamine synthetase. *Biochemica et Biophysica Acta* 2000;1477:122-145.42)

Lipmann F, Tuttle CL: A specificmicro method for the determination of acyl phosphatase. *J Biol Chem*1945;159:21.

43) Gunnersen D, Haley B: Detection of glutamine synthetase in the cerebrospinal fluid of diseased patients: a potential diagnostic biochemical marker. *Proc Natl Acad Sci U S A* 1992;89:11949-11953.

44) Tumani H, Shen GQ, Peter JB, Bruck W: Glutamine synthetase in cerebrospinal fluid, serum and brain: a diagnostic marker for Alzheimer disease. *Arch Neurol* 1999;56:1241-1246.

45) Carter JM: *A Guide to Assay Development*. Westborough, MA: D & MD; 2003.

46) Gawronski JD, Benson DR: Microtiter assay for glutamine synthetase biosynthetic activity using inorganic phosphate detection. *Anal Biochem* 2004;327:114-118.

47) Romo G, Nieto SS, Ruiz MG: A modified colorimetric method for the determination of orthophosphate in the presence of high ATP concentration. *Anal Biochem* 1992;200:235-238.

48) Romo G, Nieto SS, Ruiz MG: A modified colorimetric method for the determination of orthophosphate in the presence of high ATP concentration. *Anal Biochem* 1992;200:235-238.

49) Black MJ, Jones EM: Inorganic phosphate determination in the presence of labile organic phosphate: assay for carbamyl phosphate phosphatase activity. *Anal Biochem* 1983;135:233-

Chapter – 3

Activity guided purification of active principle from *Byttneria species*

3.1 Introduction

For a long period of time, plants have been a valuable source of natural products for maintaining human health. Natural products played a prominent role in ancient traditional medicine systems, such as Ayurveda, Chinese and Egyptian, which are still in common use today. More intensive studies of natural therapies actually started in the last decade. Natural products so far remained the single most productive source of lead molecules for the development of drugs. Over 100 new products, particularly as anti-cancer agents and anti-infectives were in clinical development (1). According to the World Health Organization (WHO), 75% of people rely on plant-based traditional medicines for primary health care globally (2). Several modern drugs (~ 40 % of the modern drugs in use) were developed from natural products (2). The largest parts of the world medicine treasure were directly or indirectly obtained from natural products, which are compounds from medicinal plants.

In more recent history, the use of plants as medicines has turned into the isolation of active compounds, beginning with the isolation of morphine from opium in the early 19th century (3, 4). Drug discovery from medicinal plants led to the isolation of early drugs such as cocaine, codeine, digitoxin and quinine, in addition to morphine, of which some are still in use (4 - 6). Isolation and characterization of pharmacologically active compounds from medicinal plants continue today. Phytochemists (natural product chemists) prepare extracts from the plant materials, subject these extracts to biological screening in pharmacologically relevant assays, and commence the process of isolation and characterization of the active compound(s) through bioassay-guided fractionation.

Numerous methods have been utilized to acquire compounds for drug discovery including isolation from plants and other natural sources, synthetic chemistry, combinatorial chemistry, and molecular modeling (7 - 9). Despite the recent interest in molecular modeling, combinatorial chemistry and other synthetic chemistry techniques by pharmaceutical companies and funding organizations, natural products and particularly medicinal plants, remain an important source of new drugs, new drug leads, and new chemical entities (NCEs) (5 , 6). In both 2001 and 2002, approximately one quarter of the bestselling drugs worldwide were natural products or derived from

natural products (6). There are also four new medicinal plant-derived drugs that have been recently introduced to the U.S. market. Natural products have played an important role as new chemical entities (NCEs) — approximately 28% of NCEs between 1981 and 2002 were natural products or natural product-derived (10). Another 20% of NCEs during this time period were considered natural product mimics, meaning that the synthetic compound was derived from the study of natural products (10). Combining these categories, research on natural products accounts for approximately 48% of the NCEs reported from 1981–2002. Natural products provide a starting point for new synthetic compounds, with diverse structures and often with multiple stereocenters that can be synthetically challenging (11 - 14). Many structural features common to natural products (e.g., chiral centers, aromatic rings, and complex ring systems, degree of molecule saturation, and number and ratio of heteroatoms) have been shown to be highly relevant to drug discovery efforts (15 - 17). Furthermore, since the escalation of interest in combinatorial chemistry and the subsequent realization that these compound libraries may not always be very diverse, many synthetic and medicinal chemists are exploring the creation of natural product and their analogues in the libraries that combine the structural features of natural products with the compound-generating potential of combinatorial chemistry (18 - 22). Drugs derived from medicinal plants can serve not only as new drugs themselves but also as drug leads suitable for optimization by medicinal and synthetic chemists. The design, determination, and implementation of appropriate, clinically relevant, high-throughput bioassays are a difficult process for all drug discovery programs (23). Screening of extract libraries can be problematic, but new techniques, including pre-fractionation of extracts, can alleviate some of these issues (6, 14). Challenges in bioassay screening remain an important issue in the future of drug discovery from medicinal plants. We have developed an HTS assay targeting *Mycobacterium tuberculosis* Glutamine synthetase (*MtbGS*), which is capable of screening of natural products. After successful screening of 2500 samples, 12 samples confirmed as hits and one natural product extract was pursued further. In the present study, active principle exhibiting tuberculostatic activity from the plant *Byttneria herbecea (family – Sterculiaceae)* is discussed. The compound exhibits anti-tubercular activity against actively growing mycobacterium bacilli by targeting the enzyme

MtbGS. Methanol extracts of the aerial part of *Byttneria herbecea* exhibited activity against *MtbGS* in primary screening of biosynthetic assay. The major advantage of the present study is that the mode of action of the compound is known, which increases the potential of *Byttneria herbecea* becoming an anti-tubercular herbal drug.

3.2 Results

The results indicated that the crude extracts of *Byttneria herbecea* showed antibacterial activities towards *M. bovis* BCG culture. The problem of natural product inhibitors is the non specificity of the compound. But in the present study the target was known because *MtbGS* was inhibited by the compound. After screening of 2500 samples against biosynthetic activity of *MtbGS*, methanolic extract of *Byttneria herbecea* was identified as a confirmed hit. Bioactivity was determined against biosynthetic reaction catalyzed by *MtbGS*, using the optimized method mentioned in the section 3.2.2. The 4th fraction and the 11th fraction were found active against *MtbGS* (Table-III) in the first chromatographic separation. The yield of the 4th fraction was extremely less, so the 11th fraction was further pursued.

Table – III. Comparison of bioactivity between two fractions identified in the first chromatography.

Srl. no	**Fractions**	**% Inhibition found on enzyme *Mycobacterium tuberculosis* Glutamine Synthetase**			
		7.5 mg/ml		**15mg/ml**	
1	Original MeoH Extract	37 %		71 %	
2	1st Chromatographic fractionation	Fraction D	Fraction K	Fraction D	Fraction K
		74.2 %	44.5 %	100 %	80.63 %

Dose - response effect of fraction K on biosynthetic activity of *MtbGS* was determined by applying varying concentrations of fraction K from 0.25 mg/ml to 15 mg/ml (Figure -3 A). The determined IC50 value from the dose response curve is 4.5 mg/ml. The IC50 value for *M. bovis* BCG is 1.56 µg/ml (Figure -3.3 B).

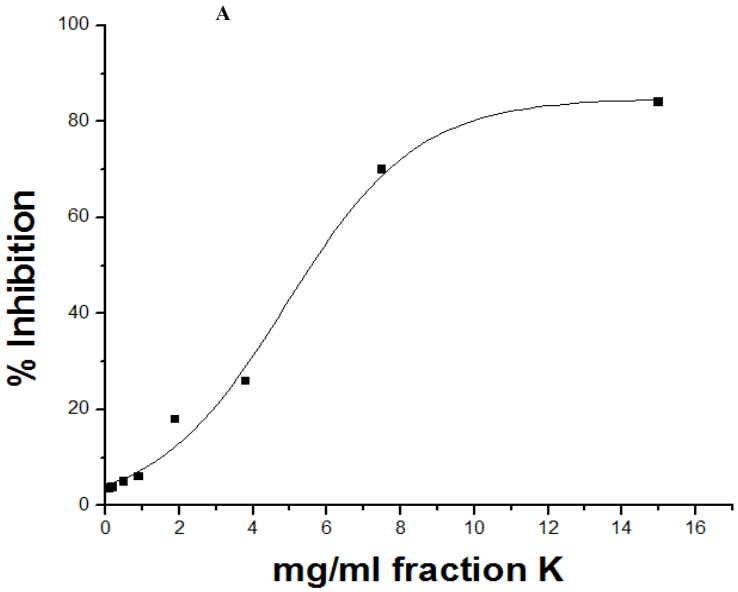

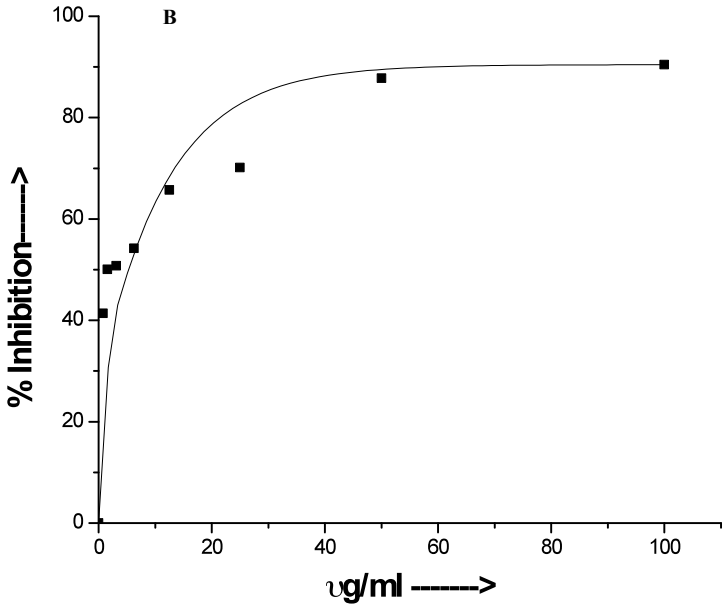

Figure - 3 Dose response curve of fraction K against purified *Mycobacterium tuberculosis* Glutamine Synthetase enzyme activity (A) and growth of *M. bovis* BCG (B) culture. 0.25 mg/ml -15 mg/ml of fraction K was applied on *MtbGS* (A) and 1.0 µg/ml – 100 µg/ml for *M. bovis* BCG (B) culture. The details of the experiments are explained in 'Materials and Methods'. The plots were drawn from the average values of 3 separate experiments under identical condition

Hits should be evaluated in terms of its cytotoxicity on mammalian cells particularly the host cell line before taking them ahead into the lead stage in discovery chain. Here, cytotoxicity of the hits was estimated against the HL-60 cell line by using standard cell proliferation assay. It was observed that there was no significant effect on proliferation of HL-60 cell line at 10 X MIC levels of the hits (Table - IV). This data indicated that these compounds could be initially considered safe from *in vitro* toxicity data.

Table – IV Cytotoxicity profile of fraction K against macrophage cell line. Three concentrations of fraction K were applied on the HL-60 cell line to determined the cytotoxicity.

Srl.No.	Fractions	% Inhibition on HL60 Cell lines		
		7.5 mg/ml	3.75 mg/ml	1.875 mg/ml
1.	K	-19	-31	-11
2.	D	-27	-24	-7

Two major peaks were observed in the HPLC profile K1 fraction and these two peaks were separated by preparative HPLC (Figure – 4). Bioactivities of these two samples were determined. Purity for the active compound was achieved by more than 95% using preparative HPLC (Figure – 5).

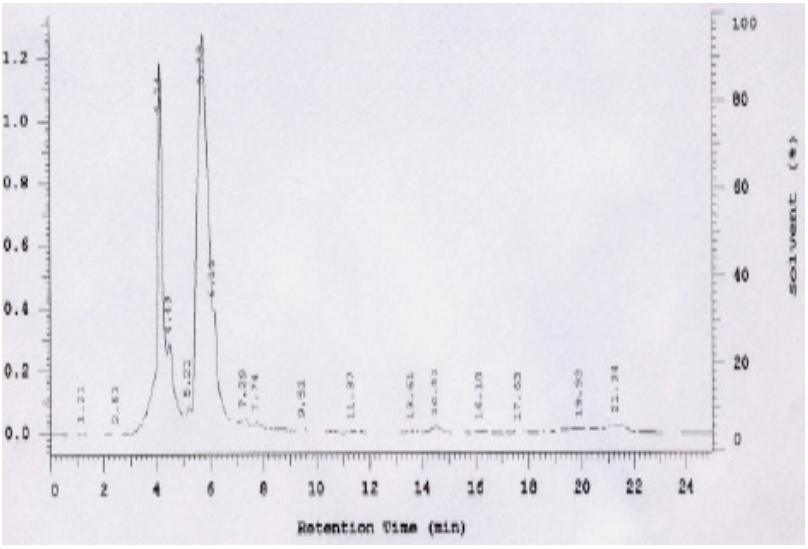

Figure – 4 Chromatogram of fraction K1 after vacuum chromatography over RP C18 silica gel. Mobile phase was 10:90 Methanol: Water.

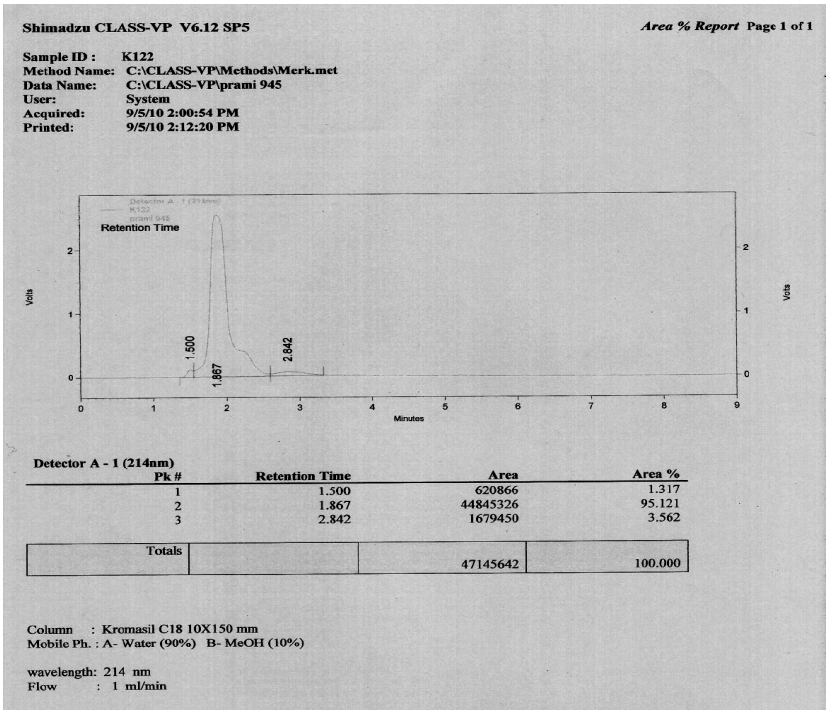

Figure – 5 Chromatogram of fraction K 122 which was separated by preparative HPLC

The mobile phase was 10: 90 methanol: water and Kromasil C_{18} column was used for analytical HPLC.

.

3.3 Materials and Methods

3.3.1 Purification of the enzyme

The enzyme was purified from recombinant *Escherichia coli* strain *YMC21E* by using a modified method (24). The enzyme preparation was used for the HTS screening of 2500 compounds and for the determination of bioactivity.

3.3.2 Assay of the enzyme

A protocol, which can identify inhibitors of *MtbGS* was used to screen the samples (25). The assay mix contained 50 mM HEPES buffer with pH 6.8, 220 mM L-glutamic acid (pH adjusted to 6.8), 7.5 mM NH_4Cl, 32.5 mM $MgCl_2$, and 62.5 µg/ml enzyme. 85

µl of the reaction mix was added with 5 µl of sample. In the control, 5 µl of DMSO was added and 5 µl of 420 mM EDTA was added in the blank. The reaction was started by adding 7.6 mM ATP (pH adjusted ~ 6.8) in the reaction mixture and incubated for 2 hours at 25°C. The reaction was terminated by adding a stop reagent followed by addition of citrate to block the further hydrolysis of ATP. The whole mixture was kept at room temperature for another 30 minutes to read the color at 655 nm by spectramax plate reader.

3.3.3 High throughput screening protocol

The assay plates were made by adding 5 µl of samples in DMSO at 10 mg/ml concentration to the respective wells. 5 µl of DMSO was added to the control and blank wells. 5 µl of 420 mM EDTA was added to the blank wells. The same volume of water was added to the other wells, and then 80 µl of the reaction mix was added to all the wells. The plate was kept on the shaker for 2 minutes for proper mixing. Then, 10 µl of 76 mM working solution of ATP was added to all the wells to start the reaction. After incubation, 75 µl of the stop reagent was added and allowed to develop the color for approximately 7 minutes. The reading was taken after 30 min of the addition of 75 µl sodium citrate in the reaction mix using 655 nm by spectramax plate reader (24).

3.3.4 Plant materials

The leaves of *Byttneria herbecea* were collected from various places of the North eastern parts of India. Samples were identified by botanists at Botanical Survey of India.

3.3.5 Preparation of extracts

Each batch of plant material (aerial part) was air dried and powdered. Approximately 60 grams of the powder were then extracted with 500 ml methanol, at room temperature

and with constant shaking, for 24 hours. The extract was filtered and concentrated to dryness under reduced pressure.

3.3.6 Column chromatography of Methanol extract

Methanol extract was obtained as light brown powder. 19 gms of the sample were subjected to chromatography over silica gel (100 - 200 mesh) using mobile phase gradient (Table-1). TLC of all the collected fractions was carried out using 5:95 MeOH: CHCl3 developing phase. Fractions showing similar TLC (Figure-1) pattern were combined to obtain 11 fractions (A, B, C, D, E, F, G, H, I, J, K). After removal of the solvent, these fractions were evaluated for their bioactivity using the protocol mentioned in section (A). Fractions D (4th fraction) and K (11th fraction) are found to exhibit activity against *MtbGS* (Table-II).

Table – I Solvent gradient for first chromatography was given using chloroform, Methanol and water over silica gel.

Steps	Choloform %	Methanol %	Water %	Volume ml
1.	98	2	-	1000
2.	95	5	-	1000
3.	90	10	-	1000
4.	85	15	-	1000
5.	80	20	-	1000
6.	-	100	-	1000
7.	-	50	50	500

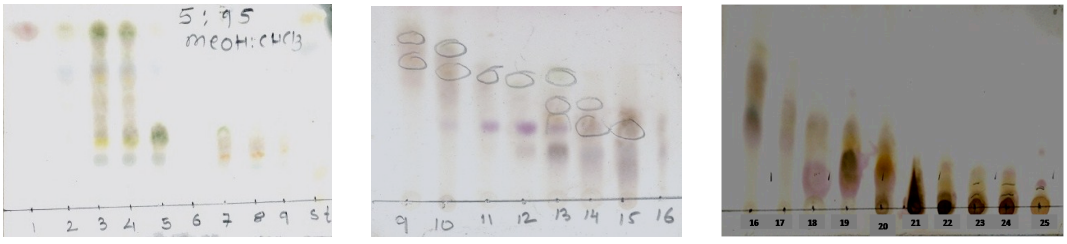

Figure –1 TLC profile of all fractions collected in the chromatography where mobile phase was 5 : 95 Methanol : Water. Similar fractions were pulled together and bioactivity was determined.

3.3.7 Dose response curve of fraction for the purified enzyme

Bioactivity was determined against biosynthetic reaction, using the optimized method mentioned in the section 3.2.2. Dose-response effect of fraction K on biosynthetic activity of *MtbGS* was determined by applying varying concentrations of fraction K from 0.25 mg/ml - 15 mg/ml.

3.3.8 Determination of anti-tubercular activity of the fraction K1 against active replicating bacilli

A protocol, which can identify inhibitors of active tubercle bacilli, was used to screen the fractions. Absorbance of the culture at 620 nm was used to represent the actively growing stage of the bacilli in this screening protocol. 2.5 µl of compound solution with varied concentration from 0.78 – 100 µg/ml in DMSO was aseptically transferred to individual wells of sterile 96-well plates. 247.5 µl of *M. bovis* BCG culture containing ~105cells/ml, supplemented with L-Glutamic acid as nitrogen source in *M. pheli* medium, were aseptically transferred to each well to make up the total volume to 250 µl and the plate was covered with a sealer. Space of 125 µl was left in each well to make the headspace to culture volume ratio exactly 0.5. After sealing, these culture plates were incubated at 37^0C in an incubator. After 8 days of incubation, culture OD was read at 620 nm.

3.3.9 Further Purification of the Fraction K (11th fraction)

9 gms of fraction K were subjected to vacuum liquid chromatography over RP C4 silica gel using Methanol: Water (50:50) as mobile phase. Solvent was evaporated from 25 fractions and bioactivity was determined against biosynthetic assay. Fractions K1 - K19 were found active against *MtbGS*. Considering the efficiency of bioactivity Fraction K1 was further separated by using RP C18 column. Fraction K1 was subjected to vacuum chromatography using mobile phase as described in Table II and 20 fractions were

collected. The purity was assessed by RP C18 Glass TLC plates (Figure – 2) using Methanol : Water (10 : 90) mobile phase. First four fractions were found active against the enzyme and were further separated by preparative HPLC.

Table -II Solvent gradient for third chromatography was given using Methanol and Water over RP C_{18} silica gel.

Steps	Methanol	Water	Volume In mls
1.	-	100	100
2.	10	90	100
3.	20	80	100
4.	30	70	100
5.	40	60	100
6.	60	40	100
7.	70	30	100
8.	80	20	100
9.	90	10	100
10.	200	-	200

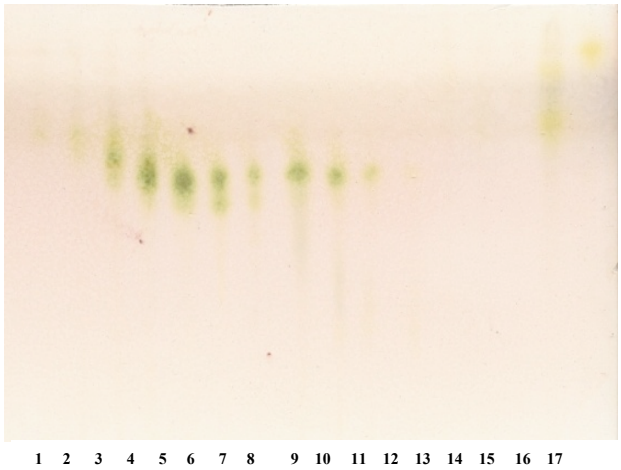

Figure – 2 RP C_{18} TLC plate was used for the fractions collected in the third chromatography where mobile phase was 50 : 50 Methanol : Water.

3.3.10 Preparative HPLC

The first four fractions of K1 sample were separated by preparative HPLC using a mobile phase composed of DI Water : Methanol 90 :10 (v/v) delivered at 1.0 ml /min. The column used was X Bridge lichrosphere RP C_{18} (250 - 4 mesh) 5 micron column (250 x 10 mm) (The column was purchased from Merck). The column was washed with Water : Methanol 90 :10 (v/v) for 30 minutes. The separation was achieved using a Shimadzu preparative instrument controller (Model no – SCL-10 AVP, catalogue no. – 2228 – 34350 – 38) and Pump (Model no. LC 10 AT VP) as well variable wavelength detector (model no. SPD -10AVP) operated at 214 nm to detect the peaks. The injection volume was 50 µl and the column was re-equilibrated by Water : Methanol 90 : 10 (v/v). Three fractions from each sample were collected from preparative HPLC. Approximately 100% inhibition was observed by the first two fractions collected from HPLC of three samples. The purified *MtbGS* was 100 % inhibited by the first two samples at 25 µg/ml concentration which were separated by HPLC.

3.3.11 Cytotoxicity against the human cell line (HL-60)

Cytotoxicity of the active compound was determined by its dose dependent effect on proliferation of Human promyelocytic leukemia cells (HL-60) cell lines. These cells were incubated with the compound upto 50 fold higher concentration of their MIC. Approximately 100000 cells per ml were seeded in MEM medium containing 10 % heat inactivated fetal bovine serum along with 100 µg/ml each of streptomycin and ampicillin respectively. 100 µl of this cell suspension was added to each well of sterile 96-well plate and compound was added in the wells at the time of inoculation in a dose dependent manner. 10 µl of MTT dye solution (5 mg/ml) was added after 72 hours of incubation and was incubated for another 1 hours. After another 4 hours of incubation, 200 µl of isopropanol was added to the culture to read the absorbance at 490 nm to examine its effect on proliferation.

3.4 Discussion

Medicinal plants offer a great hope to fulfill the need of anti-tubercular drugs and have been used for curing diseases for many centuries. Medicinal plants have been used extensively as drugs in the form of pure compounds or as a crude material (26). In the present study, methanol extracts of *Byttneria herbecea* were observed to have anti-tubercular activity against *M. bovis* BCG culture. As inhibition of growth by semi-purified principle was observed in *M. bovis* BCG as well as in bioactivity of *MtbGS*, its anti-tuberculous activity appears to be meaningful. However, more studies using other strains of *M. tuberculosis* are needed to conclude about the anti-tuberculous potential and promise of these plants for their ultimate use in the treatment of tuberculosis. So far, many plants have been tested against mycobacteria and a few plants which showed anti-tubercular activity were *Salvia hypargeia, Euclea natalensis*, etc (27-31). There are reports about anti-tuberculous activity of *A. vera (32-36)* against reference susceptible strain H37Rv while *A. vasica* (32, 33) and garlic (34, 35) have been tested against clinical isolates which were resistant to streptomycin and isoniazid, respectively. In addition, anti-TB activity of *Byttneria herbecea* is being reported for the first time. Further studies should be carried out using various fractions of crude extracts of other species of this plants as well as their semi-purified/purified principle responsible for anti-tubercular activity (specially against MDR and XDR isolates of *M. tuberculosis*) to find out the minimum inhibitory concentration (MIC) in suitable broth based media as MICs defined in broth are more accurate. We did not find any cytotoxicity of these extracts against the human (HL-60) cell line. The inhibitory activity of the active principle against *MtbGS* assigns its mode of action. So, the active principle is not a non specific inhibitor. However, more studies can be done on its biochemical characterization as well as elucidation of the chemical structure.

3.5 References

1) WHO traditional medicine strategy 2002 -2005. http: //whqlibdoc. who.int/hq/ 2002/WHO _EDM_TRM_2002.1.pdf

2) SATYAJIT D. SARKER, ZAHID LATIF, ALEXANDER I. GRAY , Natural Product Isolation (Book) 2005.

3) Kinghorn, A.D., 2001. Pharmacognosy in the 21st century. Journal of Pharmacy and Pharmacology 53 (2), 135–148.

4) Samuelsson, G., 2004. Drugs of Natural Origin: a Textbook of Pharmacognosy, 5th Swedish Pharmaceutical Press, Stockholm.

5) Newman, D.J., Cragg, G.M., Snader, K.M., 2000. The influence of natural products upon drug discovery. Natural Product Reports 17 (3), 215– 234.

6) Butler, M.S., 2004. The role of natural product chemistry in drug discovery. Journal of Natural Products 67 (12), 2141– 2153.

7) Ley, S.V., Baxendale, I.R., 2002. New tools and concepts for modern organic synthesis. Nature Reviews Drug Discovery 1 (8), 573– 586.

8) Geysen, H.M., Schoenen, F., Wagner, D., Wagner, R., 2003. Combinatorial compound libraries for drug discovery: an ongoing challenge. Nature Reviews Drug Discovery 2 (3), 222– 230.

9) Lombardino, J.G., Lowe III, J.A., 2004. The role of the medicinal chemist in drug discovery—then and now. Nature Reviews Drug Discovery 3 (10), 853–862.

10) Newman, D.J., Cragg, G.M., Snader, K.M., 2003. Natural products as sources of new drugs over the period 1981–2002. Journal of Natural Products 66 (7), 1022–1037.

11) Clardy, J., Walsh, C., 2004. Lessons from natural molecules. Nature 432 (7019), 829– 837.

12) Nicolaou, K.C., Snyder, S.A., 2004. The essence of total synthesis. Proceedings of the National Academy of Sciences of the United States of America 101 (33), 11929–11936.

13) Peterson, E.A., Overman, L.E., 2004. Contiguous stereogenic quaternary carbons: a daunting challenge in natural products synthesis. Proceedings of the National Academy of Sciences of the United States of America 101 (33), 11943– 11948.

14) Koehn, F.E., Carter, G.T., 2005. The evolving role of natural products in drug discovery. Nature Reviews Drug Discovery 4 (3), 206– 220.

15) Lee, M.L., Schneider, G., 2001. Scaffold architecture and pharmacophoric properties of natural products and trade drugs: application in the design of natural

product-based combinatorial libraries. Journal of Combinatorial Chemistry 3 (3), 284–289.

16) Feher, M., Schmidt, J.M., 2003. Property distributions: differences between drugs, natural products, and molecules from combinatorial chemistry. Journal of Chemical Information and Computer Sciences 43 (1), 218– 227.

17) Piggott, A.M., Karuso, P., 2004. Quality, not quantity: the role of natural products and chemical proteomics in modern drug discovery. Combinatorial Chemistry and High Throughput Screening 7 (7), 607– 630.

18) Hall, D.G., Manku, S., Wang, F., 2001a. Solution- and solid-phase strategies for the design, synthesis, and screening of libraries based on natural product templates: a comprehensive survey. Journal of Combinatorial Chemistry 3 (2), 125– 150.

19) Eldridge, G.R., Vervoort, H.C., Lee, C.M., Cremin, P.A., Williams, C.T., Hart, S.M., Goering, M.G., O'Neil-Johnson, M., Zeng, L., 2002. High-throughput method for the production and analysis of large natural product libraries for drug discovery. Analytical Chemistry 74 (16), 3963–3971.

20) Burke, M.D., Berger, E.M., Schreiber, S.L., 2004. A synthesis strategy yielding skeletally diverse small molecules combinatorially. Journal of the American Chemical Society 126 (43), 14095–14104.

21) Ganesan, A., 2004. Natural products as a hunting ground for combinatorial chemistry. Current Opinion in Biotechnology 15 (6), 584– 590.

22) Tan, D.S., 2004. Current progress in natural product-like libraries for discovery screening. Combinatorial Chemistry and High Throughput Screening 7 (7), 631–643.

23) Knowles, J., Gromo, G., 2003. Target selection in drug discovery. Nature Reviews Drug Discovery 2 (1), 63– 69.

24) Singh U, Sarkar D: Development of a simple assay protocol for high throughput screening of *Mycobacterium tuberculosis* glutamine synthetase for the identification of novel inhibitors. *J Biomol Screen* 2005;10: 725-729.

25) Singh U, Sarkar D Development of a Simple High-Throughput Screening Protocol Based on Biosynthetic Activity of *Mycobacterium tuberculosis* Glutamine Synthetase for the Identification of Novel Inhibitors *J Biomol Screen* 2006; 11; 1035

26) Renu Gupta, Bandana Thakur, Pushpendra Singh, H.B. Singh, V.D. Sharma, V.M. Katoch ,& S.V.S. Chauhan Anti-tuberculosis activity of selected medicinal plants against multi-drug resistant *Mycobacterium tuberculosis* isolates.

27) Ulubelen A, Euren N, Tuzlaci E, Johanson. Source of antimycobacterial agents. *J Ethnopharmacol* 2007; *110* : 200-34.

28) Newton SM, Lau C, Wright CW. A review of antimycobacterial 7. natural products. *Phytother Res* 2000; *14* : 303-22.

29) Newton SM, Lau C, Gurcha SS, Besra GS, Wright CW. 8. The evaluation of forty-three plant species for *in vitro* antimycobacterial activities: isolation of active constituents from *Psoralea corylifolia* and *Sanguinaria canadensis*. *J Ethnopharmacol* 2002; *79* : 57-67.

30) Ulubelen A, Euren N, Tuzlaci E, Johanson C. Diterpenoids 9. from the root of *Salvia hypergeia*. *J Nat Prod* 1988; *51* : 1178-83.

31) Lall N, Me10. yer JJ. Inhibition of drug-sensitive and drug-resistant strains of *Mycobacterium tuberculosis* by diospyrin, isolated from *Euclea natalensis. J Ethnopharmacol* 2001; *78* : 213-6.

32) Grange JM, Snell NJ. Activity of bromhexine and ambroxol, 11. semi-synthetic derivatives of vasicine from the Indian shrub *Adhatoda vasica* against *Mycobacterium tuberculosis in vitro*. *J Ethnopharmacol* 1996; *50* : 49-53.

33) Gupta KC, Chopra IC. Anti-tubercular action of 12. *Adhatoda vasica* (N.O. acanthacea). *Indian J Med Res* 1954; *42* : 355-8.

34) Jain RC. Antitubercular activity of garlic oil. 13. *Indian drugs* 1993; *30* : 73-5.

35) Ratnakar P, Murthy PS. Preliminary studies in the antitubercular 14. activity and the mechanism of action of water extract of garlic and its two partially purified proteins. (garlic defensins?). *Indian J Clin Biochem* 1996; *11* : 37-41.

36) Bruce WGG. Investigations of antibacterial activity in the 15. *aloe*. *S Afr Med J* 1967; *41* : 984.

Chapter - 4

Kinetics studies on the interaction between L-Methionine sulfoximine and *Mycobacterium tuberculosis* Glutamine Synthetase

4.1. Introduction

In the active state, bacterial Glutamine Synthetase (GS) catalyzes the ATP dependent condensation reaction of ammonium and glutamate to form glutamine, ADP, phosphate, and a hydrogen ion (a process termed as the `biosynthetic reaction`) (1,2). To be in this active state, GS requires two enzyme-bound divalent cations, either magnesium or manganese ions, which play both structural and catalytic roles (3, 4, 5). These metal ion binding sites are termed the n1 and n2 sites. The reaction proceeds as an ordered and sequential two-step mechanism (6-10). In the first step, a tightly bound, activated intermediate γ - glutamyl phosphate (Glu~P) is formed as the terminal phosphate of ATP is transferred to the carboxylate side chain of the substrate glutamate (*9*). In the second step, an enzyme-bound ammonium ion is de-protonated, forming ammonia that attacks the carbonyl carbon of Glu~P to form a tetrahedral intermediate at the transition state. The enzyme subsequently releases free phosphate to yield glutamine (*9*). The structure of GS from a mutant *Salmonella typhimurium* strain, unable to adenylylate GS (*11*), was initially determined to 3.5 Å resolutions by X-ray crystallography (*12*). The structure has been subsequently refined and the resolution extended to 2.5 Å (*13*, *14*). *Salmonella* GS has a molecular mass of 620 kDa and is a dodecamer with 622 symmetry (*12*, *15*), formed from two hexameric rings stacked face to face. Each of the 12 active sites is formed between two adjacent subunits within a ring and is described as a `bi-funnel`. ATP enters the bi-funnel from the exposed outer surface of the dodecamer, near the 6-fold axis of symmetry. Glutamate enters the opposite end of the bi-funnel, at the interface of the hexamric rings, near the 2-fold axis. The n1 and n2 binding sites are located at the joint of the bi-funnel.

The crystal structure of glutamine synthetase (GS) from *Mycobacterium tuberculosis* determined at 2.4 Å resolution reveals citrate and AMP bound in the active site (12). The structure of *MtbGS* in complex with MSO-P (L-Methionine Sulfoximine Phosphate) and MgADP was solved by molecular replacement using a subunit from the MtbGS/citrate/MnAMP model reported earlier (14) as a probe; it was ultimately refined to 2.1-Å resolution. The final model consists of six subunits that constitute one hexameric ring (Figure -1). The biologically relevant dodecamer is formed as the result

of a crystallographic two-fold axis that places the second hexamer ring behind the first (12). In the course of model building, the MtbGS/MSO-P/MgADP structure was re-numbered according to the actual *MtbGS* sequence, instead of referencing to the *Salmonella* structure as used earlier (12). In the final refined model, all residues of each subunit are supported by good electron density, beginning with Lys-4 and ending with Val-478 of the native sequence. Pair wise comparisons of the various subunits show them to be very similar, with rms distances in the range of 0.1 – 0.3 Å (12).

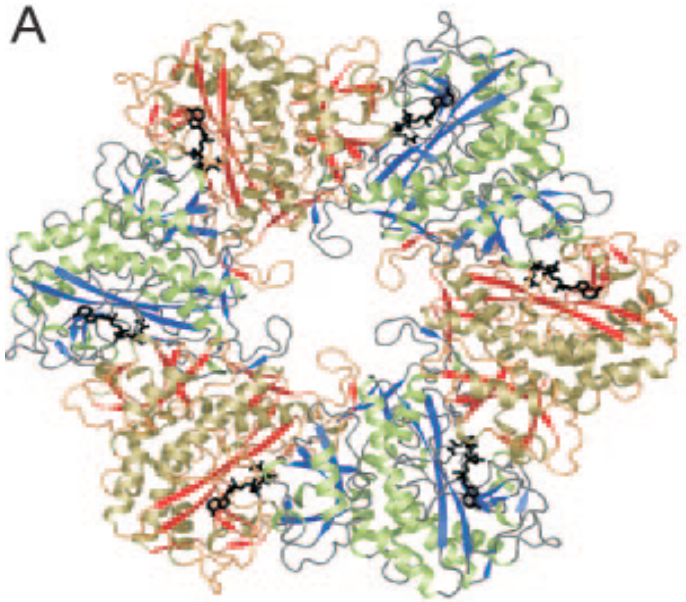

Figure 1. Overall Structure of *Mycobacterium tuberculosis* Glutamine Synthetase

The subunits of the MtbGS hexamer are colored either gold/red or green/blue. Ball-and-stick representations of MSO-P and ADP (black) show the location of the active sites at subunit–subunit interfaces (The picture is extracted from reference number 12).

In vivo, GS activity is controlled in a number of ways, including reversible covalent modification. Adenylylation catalyzed by one domain of GlnE reduces GS activity, whereas deadenylylation performed by the other domain of GlnE activates the enzyme (15). The electron density of the relevant side chain in the present *MtbGS* structure (Tyr-406) clearly shows that it is unmodified, allowing it to occupy a position that is buried within the protein, inaccessible to GlnE. Thus, the structure represents an active enzyme. Interestingly, the only significant conformational differences between the six

subunits in the asymmetric unit are rearrangements in the adjacent 407–415 loop (12). The conclusion is that this portion of the structure has some inherent flexibility, as would be needed if the tyrosine were to be available to modifying enzymes with the required frequency (12). Crystallographic studies using L-MSO (L-Methionine Sulfoximine) phosphate a proposed transition state analogue clearly indicated a non-covalent interaction with the enzyme which leads to the conclusion of a tight binding mechanism (12). In fact, there was no other experimental proof available in favor of this conclusion. In absence of any biochemical or kinetic data, it could not gain the interest to the drug developers from pharmaceutical industry. The detail biochemical characterizations of *MtbGS* remained unexplored due to limitation in phosphate estimation procedure. Probably this was the major reason for the absence of any kinetic data for the inhibition of this enzyme using L-MSO. In our previous study, this problem was rectified and it has become possible to determine the inhibition kinetics of L-MSO for *MtbGS.*

Considering the importance of the glutamine biosynthetic pathway and its inhibition by L-Methionine Sulfoximine under in vivo conditions, it could be interesting to study the inhibition kinetics of L-Methionine Sulfoximine in greater detail. The kinetic analysis of our biochemical studies clearly indicated that L-Methionine Sulfoximine forms a covalent linkage with the enzyme by following mechanism based enzyme inhibition kinetics

4.2 Results

The efficiency of enzyme inhibitor is frequently quantified from its IC_{50} values (19). While this is a suitable parameter for reversible inhibitors, concerns arise when dealing with tight binding and irreversible or mechanism-based inhibitors (MBEI) (19). IC_{50} values of MBEI are time-dependent, causing serious problems when aiming to ranking different compounds with respect to their inhibitory potential. As a consequence, most studies and ranking schemes related to MBEI rely on the inhibition constant (K_I) and the rate of enzyme inactivation (kinact) rather than on IC_{50} values. L-MSO is a well-characterized inhibitor of prokaryotic and eukaryotic glutamine synthetase (GS) (20).

MtbGS was found more sensitive to L-MSO by one to two orders of magnitude than mammalian GS and also found to be selectively inhibiting the growth of pathogenic mycobacteria (6). Apart from the indication from crystallographic experiments, our data along with others also clearly established that there is a significant difference between the enzyme inhibitions with the whole cell growth inhibition (Chapter -5). Hence, it was necessary to characterize the nature of interaction between *MtbGS* and L-MSO. The assay developed in our laboratory clearly became an advantage to carry out few fact finding experiments.

4.2.1 Determination of IC50 of standard inhibitors against purified *Mycobacterium tuberculosis* glutamine synthetase

Initially, dose-response curves obtained from inhibition of L-MSO, Phosphinothriacin and L-methionine sulfone (Figure 2). The IC_{50} values obtained for L -methionine S-sulfoximine, DL-phosphothriacin and L-Methionine Sulfone were found to be 500 µM, 30 µM and 24 mM respectively under the said condition. The results clearly indicated that the inhibition efficiency of DL-phosphothriacin and L-Methionine S-sulfiximine was significantly better than L-Methionine sulphone.

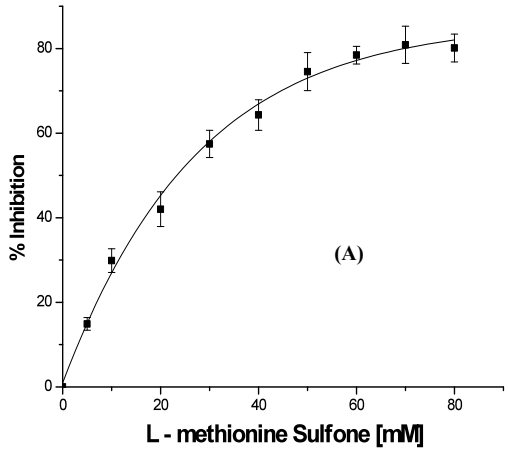

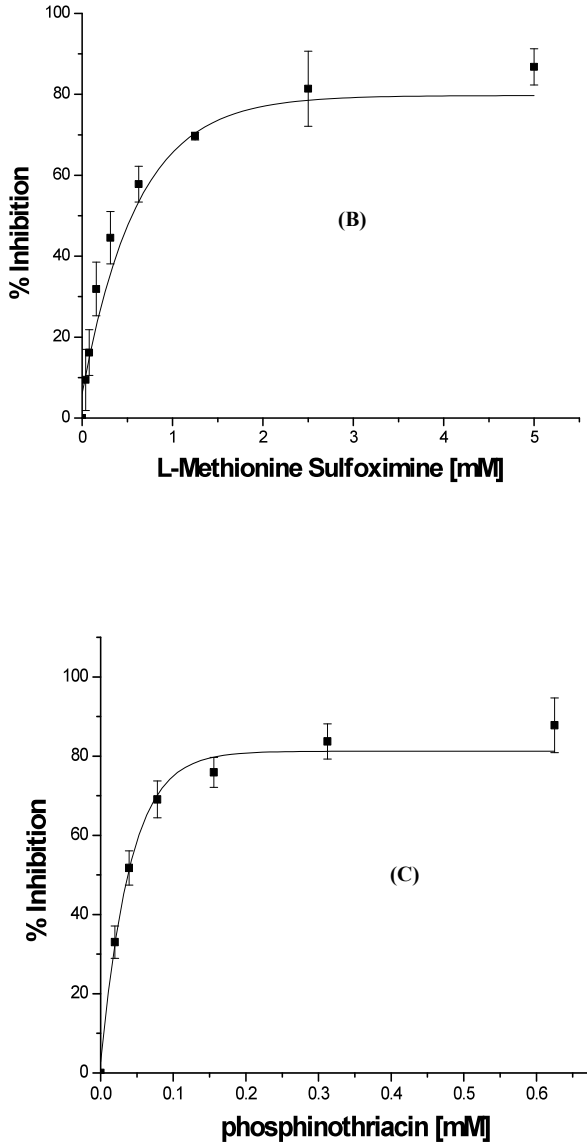

Figure – 2 Determination of IC_{50} values of the standard inhibitors

Varied concentrations of (**A**) L-Methionine S-sulfone (5 to 80 mM) (**B**) L-Methionine S-sulfoximine (0.25 to 5.0 mM) and (C) phosphinothricin (0.25 to 5.0 mM) were incubated with 62.5µg/ml of the enzyme at 25° C for 15 minutes. Then, the reaction was carried out using all the components at saturating level as mentioned in `Materials and Methods`. The plots were drawn from the average values of 3 separate experiments under identical condition.

4.2.2 Time Dependent Inhibition of *Mycobacterium tuberculosis* glutamine synthetase

Generally, the tight binding inhibitors apparently follow a time dependent kinetics of enzyme inhibition (17). A time dependent inactivation of the enzyme could potentially be the very initial steps in characterizing the nature of interaction between L-Methionine Sulfoximine and/or Phosphinothriacin and MtbGS. (Figure -3). The results indicated that L-MSO and Phosphinothriacin inhibition of *MtbGS* increased in a time-dependent manner. In contrast, inhibition by L-methionine sulfone was clearly not dependent on the preincubation with enzyme. L- Methionine ulfoximine was taken up for further studies because of the availability of related research carried out till date. It was also observed that this inhibition actually happened in presence of ATP and $MgCl_2$ only. In the presence of other components, this inhibition was not observed (Figure – 4). This loss of activity was of first-order and followed saturation kinetics which is explained in the next section.

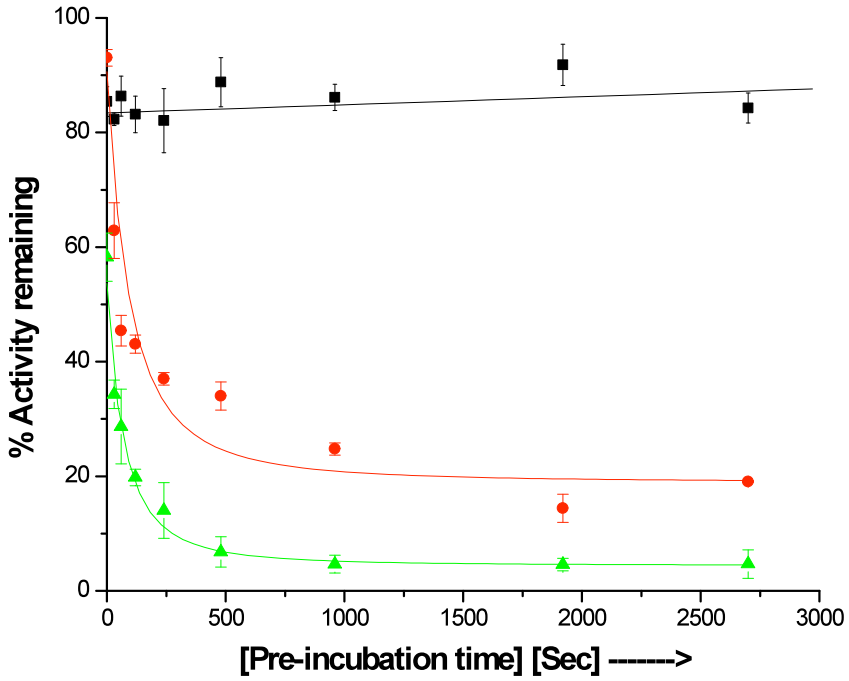

Figure –3 Time dependent inhibition of *Mycobacterium tuberculosis* Glutamine Synthetase by L-MSO, Phosphinothriacin and L-Methionine Sulfone. The 62.5mg/ml of the enzyme was preincubated with 500 µM L-MSO (▲), 30 µM Phosphinothriacin (●) and 24 mM of L-methionine sulfone (■) at room temperature. Fixed aliquots were taken out of the tubes were taken out and mixed in large volume of stopping buffer. The details of the experiment are described in `Materials and Methods` (section 4.3.4). The plots represent average of the data obtained from three identical experiments ±standard deviation.

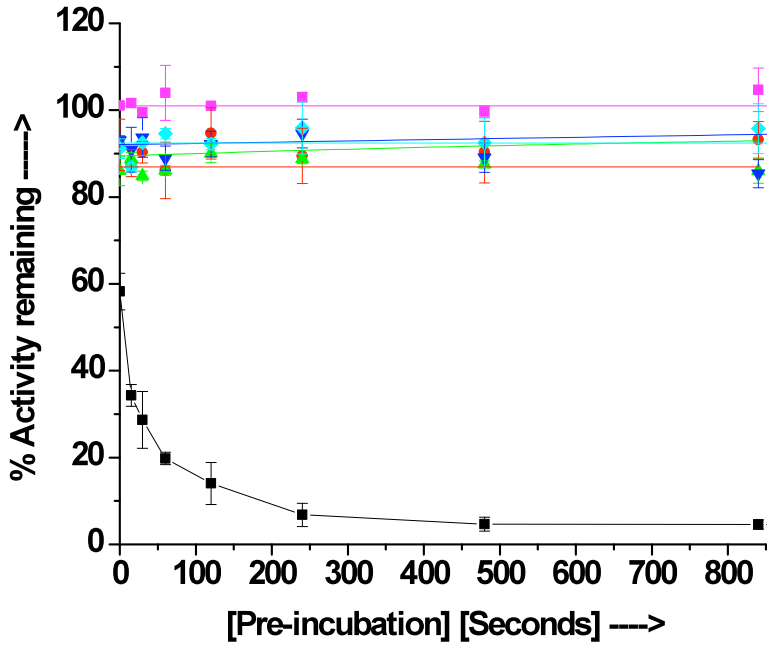

Figure–4 Time dependent inhibition of purified recombinant *Mycobacterium.tuberculosis* Glutamine Synthetase by L-Methionine Sulfoximine. The enzyme (62.5µg/ml) and L-MSO (500µM) was separately preincubated with each of 25 mM EDTA and 76 mM ATP (■), 220 mM Glutamic acid (●), 50 mM Ammonium Chloride (▲), with none (▼), 50 mM Magnesium Chloride (♦) and 76 mM ATP & 50 mM $MgCl_2$ (▪). The details of the experiment are described in `Materials and Methods` (section 4.3.5). The plots represent average of the data obtained from three identical experiments ± standard deviation.

4.2.3 Basic Kinetics of mechanism based Enzyme Inactivators

A mechanism-based enzyme inactivator (MBEI) requires a step to convert the compound to the inactivating species (k_2), as shown in Scheme – 1 (17). This step, which is generally responsible for the observed time dependence of the enzyme inactivation, is usually irreversible and forms a new complex (E- MBEI') which can have three fates: (1) if MBEI' is not reactive, but forms a tight complex with the enzyme, then the inactivation may be the result of a non-covalent tight-binding

complex (E-MBEI'); (2) if MBEI' is a reactive species (17), then a nucleophilic, electrophilic, or radical reaction with the enzyme may ensue (k_4) to give the covalent complex E-MBEI"; or (3) the species generated could be released from the enzyme as a product (k_3). Most often these inactivators result in covalent bond formation with the enzyme, and, therefore, dialysis or gel filtration does not restore enzyme activity.

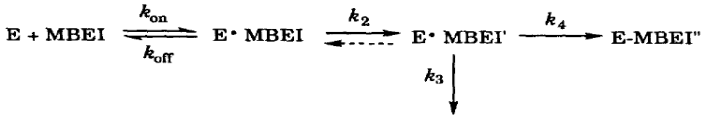

---------- **Scheme – 1**

The two principal kinetic constants that are useful in describing mechanism-based enzyme inactivators are K_{inact} and K_I. Based on Scheme - 1, K_{inact} is a complex mixture of k_2, k_3, and k_4 [Eq. (I)], and K_I is a

$$k_{inact} = k_2k_4/(k_2 + k_3 + k_4) \quad \text{----------(I)}$$

complex mixture of k_{on}, k_{off}, k_2, k_3, and k_4 [Eq. (2)] (21). Only if k_2 is rate determining ($k_2 < k_4$) and k_3 is 0 (or nearly 0), will $K_{inact} = k_2$.

$$K_I = [(k_{off} + k_2)/k_{on}][(k_3 + k_4)/(k_2 + k_3 + k_4)] \quad \text{----------(2)}$$

Values given for K_{inact} are assumed to represent the inactivation rate constants at infinite concentrations of inactivator. An expression can be derived (22) that relates the enzyme concentration (E), the inactivator concentration (I), K_{inact}, and K_I [Eq. (3)].

$$\frac{\partial \ln E}{\partial t} = \frac{k_{inact}I}{K_I + I} \quad \text{----------(3)}$$

The half-life for inactivation ($t_{1/2}$), then, is described by Eq. (4).

$$t_{1/2} = \frac{\ln 2}{k_{inact}} + \frac{\ln 2\, K_I}{k_{inact}\, I} \quad \text{----------(4)}$$

Extrapolation to infinite inactivator concentrations reduces Eq. (4) to $t_{1/2} = \text{In } 2/ K_{inact}$. These are the basic equations needed for typical mechanism-based enzyme inactivators (23, 24, 25).

Formation of the E. MBEI complex occurs rapidly (Scheme – 4), and the rate of inactivation is proportional to added inactivator until sufficient inactivator is added to saturate all of the enzyme molecules. Then there is no further increase in rate with additional inactivator, that is, saturation kinetics is observed. From Figure – 5 (A) & (B) the determined K_{inact} is 0.158 m-1and K_1 is 161.29 mM. Mechanism-based enzyme inactivators act as modified substrates for the target enzymes and bind to the active site. Therefore, addition of Glutamic acid slows down the rate of enzyme inactivation. This is referred to as substrate protection of the Enzyme (Figure -6). Most cases of mechanism-based inactivation result in the formation of covalent irreversible adduct. Consequently, dialysis or gel filtration does not restore enzyme activity. A permanent loss of enzyme activity was observed when the enzyme was incubated with L-MSO for 30 minutes.

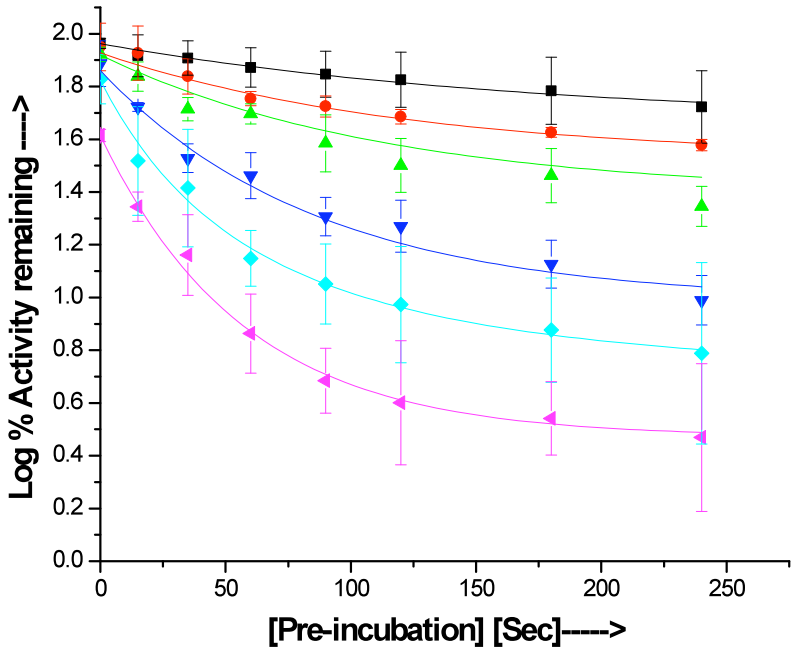

Figure – 5 (A) Effect of different L-MSO concentrations on pre-incubation with purified *Mycobacterium tuberculosis* Glutamine Synthetase

0.15 mg/ml enzyme was pre-incubated with different concentrations of L-MSO for indicated time before initiation of the reaction by micro-dilution. The different concentration of LMSO used for the experiment are 10 µM (■), 31.25 µM (●), 62.5 µM (▲), 150 µM (▼), 1000 µM (♦) and 9600 µM (◄). The logarithm of the percentage of the remaining enzyme activity relative to the inactivated control is plotted against time of pre-incubation. The details of the experiment are described in 'Materials and Methods' (section 4.3.5). The plots represent average of the data obtained from three identical experiments ± standard deviation.

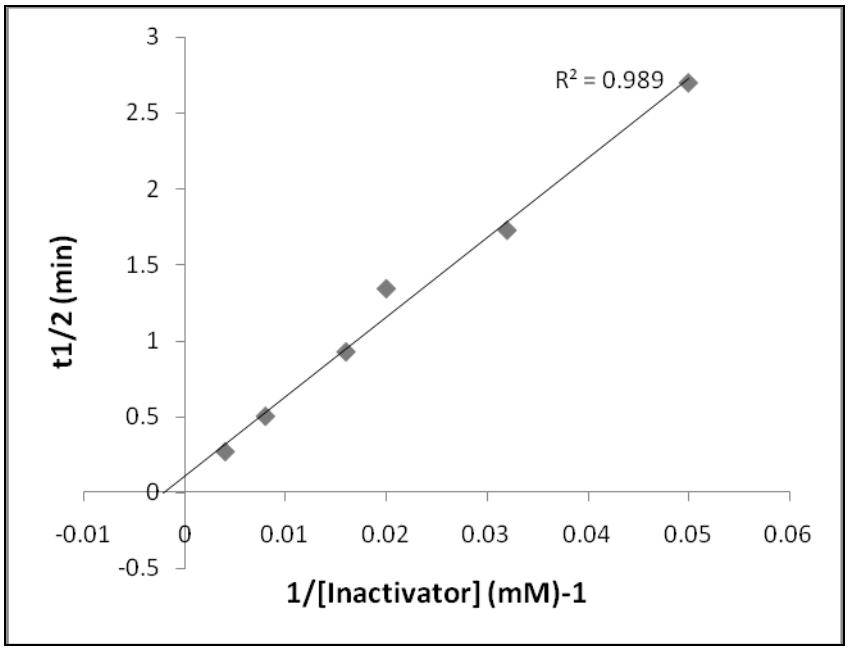

Figure –5 (B) Determination of K_I and K_{inact} of L-MSO for *Mycobacterium tuberculosis* Glutamine Synthetase by using Kitz and Wilson plot.

Kitz and Wilson plot is a replot of the half life of enzyme inactivation as a function of reciprocal of the mechanism based in-activator concentration. Saturation is indicated by the intersection of the experimental line at the positive 'y' axis. When that occurs, then there is a finite rate of inactivation at infinite in-activator concentration is observed. The point of intersection at the y axis is In 2/kinact, from which the value of K_{inact} can be determined. The extrapolated negative x axis intercept is *-1/KI.* The calculated K_{inact} is 0.158 $m^{-1}$and K_I is 161.29 mM

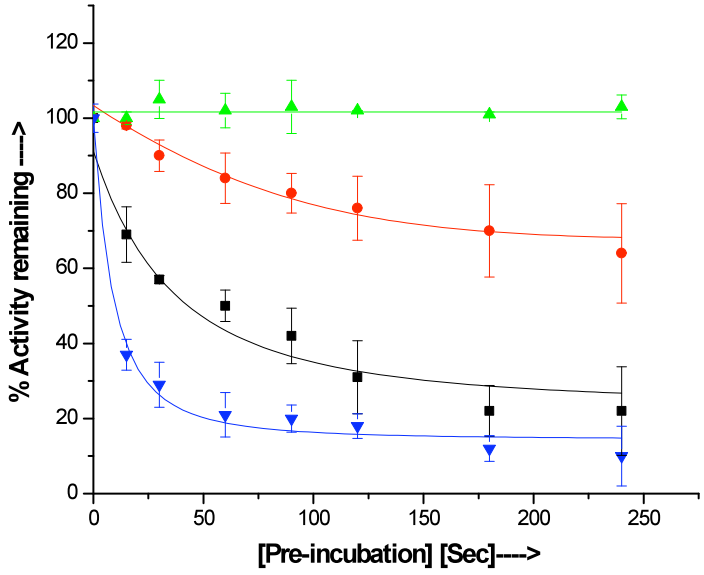

Figure – 6 Substrate protection of *Mycobacterium tuberculosis* Glutamine Synthetase from inactivation by L-MSO The enzyme (0.15mg/ml) was incubated with 500 µM L-MSO at 25 °C with (a) no Glutamic acid (▼), b) 15 mM Glutamic acid (■), c) 22 mM Glutamic acid (●), and d) 220 mM Glutamic acid (▲).The details of the experiment are described in `Materials and Methods` (section 4.3.7). The plots represent average of the data obtained from three identical experiments ±standard deviation.

4.2.4 Irreversibility of the inhibitor binding

After inactivation is complete, the enzyme is subjected to gel filtration at 25°C to remove any reversibly bound inactivator molecules. A non inactivated enzyme control was run simultaneously and carried through the same operations as the inactivated enzyme. This control is required to show that under the conditions of the experiment the enzyme would still be active if it were not treated with the inactivator, and the control enzyme activity is set to 100% for comparison. The inactivated enzyme complex was marginally stable and gel filtration at room temperature does not restore the enzyme activity (Table –I). To confirm the irreversibility of the inhibitor binding radiolabeled L-MSO was incubated with the enzyme and the same sample was divided into two equal volumes. One aliquot was treated with 1% SDS and another was served

as control. SDS added sample was incubated for 20 minutes with occasionally gentle stirring. Both the samples were extensively dialyzed against 50 mM HEPES buffer. It was observed that the radioactivity is restored in the dialysis bag with the protein for both the samples, which confirms the irreversible binding of L-MSO with *MtbGS* (Table –II).

Table -I Recovery of percent activity of the enzyme eluted from Gel filtration column

MtbGS (62.5 µg/ml) was incubated with 500 µM L-Methionine sulfoximine, 76 mM ATP and 50 mM $MgCl_2$ for 15 minutes at 25 ^{O}C. A similar reaction mixture was prepared as control, where L-MSO was not added. After pre-incubation 100 µl of the reaction mixture was diluted by adding 500 µl of 50 mM Hepes buffer. The samples were loaded in the gel filtration column and the enzyme activity was determined in the eluted fractions. The activity of the inhibitor-treated enzyme samples was not restored. The samples which were not treated by the inhibitor were active and assumed as controls for percentage calculation. The data was obtained from three identical experiments.

% Activity of Enzyme eluted from gel filtration column	% Activity of Inhibited Enzyme Eluted From gel filtration column
100 %	**3%**

Table –II Recovery of radioactivity incorporated in the enzyme after extensive dialysis

The enzyme was incubated with 500 µM cold L-MSO and 2 µM S^{35} L-MSO along with 76 mM ATP and 50 mM $MgCl_2$. The sample was divided into two parts and one part was treated with 1% SDS. Both are extensively dialyzed and the incorporation of radioactivity was measured. The data was obtained from three identical experiments.

Inhibited enzyme (SDS not added) % Recovery after dialysis	Inhibited enzyme (SDS added) % Recovery after dialysis
~ 94.4 % radioactivity retained	**~100% radioactivity retained**

4.2.5 Stoichiometry of binding inactivator with the enzyme

When a Radiolabelled S^{35} Methionine Sulfoximine is used, it is possible to measure the number of inactivator molecules attached per enzyme molecule. For this, we followed the decrease in remaining activity of the enzyme with simultaneous incorporation of the radioactivity (Figure- 7). There was a linear relationship between losses of enzymatic activity and incorporation of S^{35} labelled L-MSO which indicated that the nature of inactivation is mechanism-based. In this case, enzymatic activity (abscissa) declined exponentially as a function of EMBI'' complex formation during the initial incubation with L-MSO. The activity did not decline to zero but reached a plateau at 5% of the initial level, suggesting that individuals display variable susceptibility to mechanism based inactivation. A 1:1 stoichiometry of binding was observed by calculating the pmoles of S35 labelled L-MSO incorporated into pmoles of enzyme used in the assay. 75 pmoles of protein was used in the reaction and 66 pmoles of L-MSO was found to incorporate in the protein to bring complete inactivation of the holoenzyme.

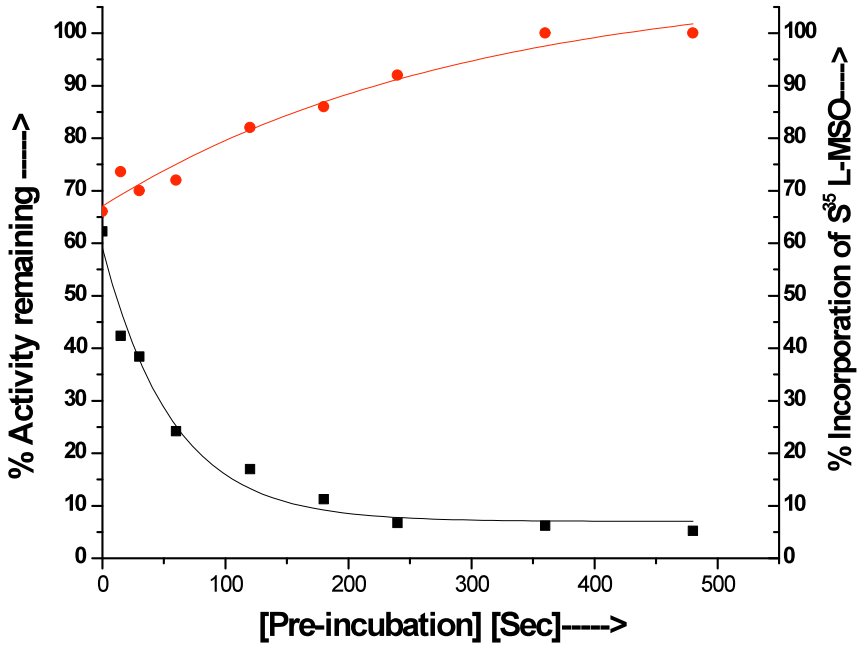

Figure –7 Relationship between incorporation of S^{35} labeled L-MSO and remaining activity of *Mycobacterium tuberculosis* Glutamine Synthetase.

MtbGS (62.5 µg/ml) was incubated with S^{35} labeled L-MSO, 500 µM cold L-MSO, 76 mM ATP and 50 mM MgCl2. From the reaction mix aliquots were removed and added in 25 mM EDTA to stop the reaction (●). All the samples were extensively dialyzed against distilled water and counts were taken by Hidex scintillation counter. The remaining activity (■) was determined as explained in 'Materials and Methods' (section 4.3.5). The plots represent average of the data obtained from three identical experiments ±standard deviation.

4.2.6 Autoradiogram

In order to confirm the covalent binding of L-MSO to MtbGS, we developed the autoradiogram of the labeled protein sample along with a control enzyme sample having modified with cold L-MSO along with marker proteins (Figure 8). The SDS-PAGE data clearly showed the presence of thick bands at the respective molecular weight of MtbGS but the autoradiogram indicated only a super imposable protein band

in the lane where labeled protein was loaded. This finding confirmed that *MtbGS* was covalently modified by L-MSO.

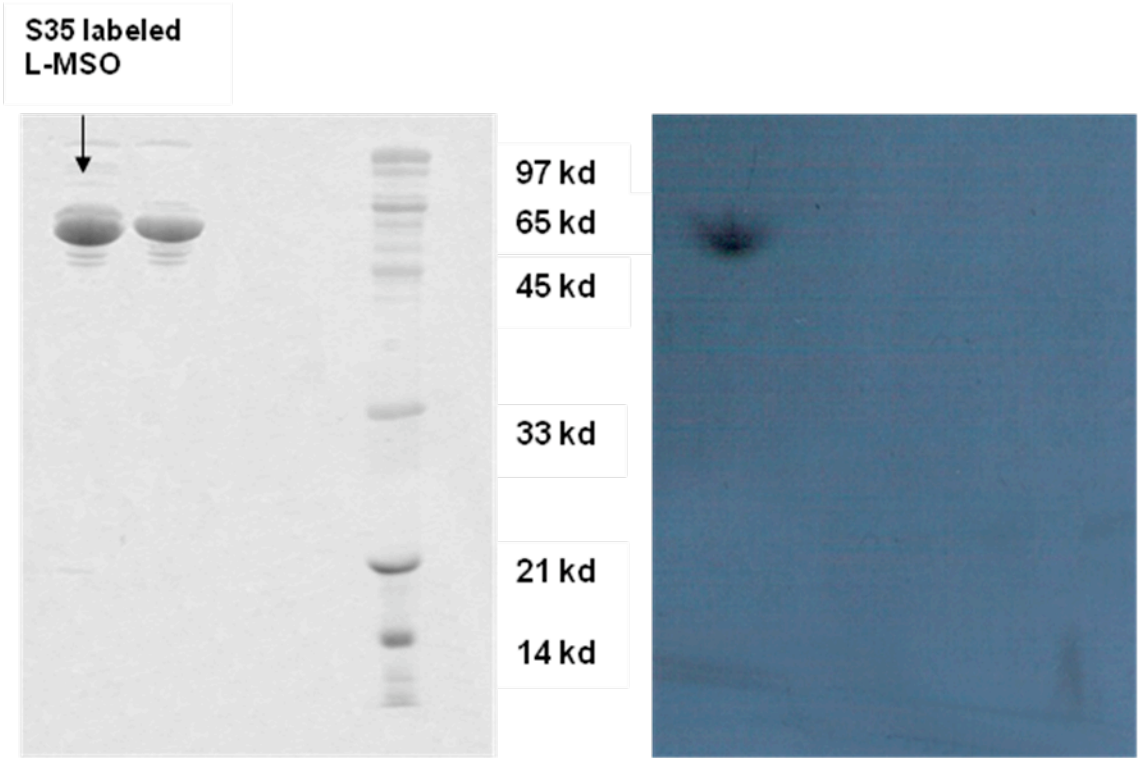

Figure –8 SDS-polyacrylamide gel electrophoresis and autoradiography of radiolabelled L-MSO incorporated *Mycobacterium tuberculosis* Glutamine Synthetase

(A) SDS-PAGE of standard proteins of known molecular weights as well as purified MtbGS suspension inactivated by 5 µM cold and S^{35} labelled L-MSO separately. The regions in the vicinity of *M,* 97,000, 65,000, 45,000, 33,000, 21,000 and 14,000 are bands as indicated. (B) Autoradiogram of *MtbGS* which had been incubated with 5 µM S35 labelled L-MSO before electrophoresis.

4.3. Materials and Methods

4.3.1 Materials

All the chemicals were obtained from Sigma. Unosphere 6 column matrix was purchased from BioRad. S35 labelled L-Methionine Sulfoxamine was custom synthesized by BRIT, Mumbai, India. Other radio-labeled chemicals were obtained from BRIT, Hyderabad, India. All chemicals used were of analytical grade. A Cary 50 Bio Spectrophotometer was used to carry out the initial experiments of biosynthetic assay. A Hidex 50 scintillation counter is used for radioactive studies.

4.3.2 Purification of Protein

The enzyme was purified from recombinant *Escherichia coli* strain *YMC21E* by using the method explained in chapter 2.

4.3.3 Enzyme Assay

A modified protocol was followed to carry out *M. tuberculosis* glutamine synthetase biosynthetic assay, as described earlier (16). The reaction was started by adding 7.6 mM of ATP in 200 µl of reaction mixture containing 200 mM Hepes buffer with pH 6.8, 100 mM L-glutamic acid, 50 mM $MgCl_2$, 50 mM NH_4Cl and 62.5 µg/ml of enzyme, in a test tube. In this reaction, ammonium chloride, L-glutamic acid, and ATP were used as substrate and Mg^{2+} ion as a cofactor to yield inorganic phosphate, glutamine, and ammonia. In the modified protocol, to stop the reaction, 12 % w/v L-ascorbic acid in 1 N HCL and 2% w/v ammonium molybdate in ddH_2O were mixed in a 2:1 proportion, and 600 µl of that was added to 200 µl of reaction mixture and mixed well to develop a blue color immediately. It was incubated for 7 minutes to get the fully developed color. After that, 600 µl of 1% sodium citrate tribasic dihydrate in 1% acetic acid in ddH_2O was added to the reaction mixture to restrict the further development of color due to hydrolysis of ATP. Incubation of the reaction mixture with 22.5 mM

EDTA served as the blank. A Cary 50 Bio Spectrophotometer was used to monitor the color at 655 nm after 30 minutes of incubation.

4.3.4 Inhibition of *Mycobacterium tuberculosis* Glutamine Synthetase by its standard inhibitors

Dose-response curves were plotted for L-MSO and phosphothriacin using a varied concentration of the inhibitor ranging from 0.125 mM to 5 mM. Whereas 5 mM to 80 mM of concentration was used for L-methionine Sulfone to get the dose response curves. The inhibitors were incubated for 15 minutes with 62.5 µg/ml enzyme and the assay was done using the same protocol described in the section 4.2.3.

4.3.5 Time Dependence of Inhibition

Inactivation experiment using 500 µM L-MSO was performed by incubating 0.15 mg/ml enzyme, 160 mM $MgCl_2$ and 7.6 mM ATP in 50 mM Hepes buffer with pH 6.8. The temperature of the pre-incubation reaction mixture was 25 °C. Sufficient enzyme for 6 -10, assays was added into the pre-incubation reaction mixture to prepare a solution at least 50 times higher than the concentration necessary for a standard assay of enzyme activity. Once the solution has been mixed, 4 µl of pre-incubation mixture (196 µl) was removed at different time intervals and was added into the enzyme assay mixture containing the substrate at saturating concentration. Then the assay was carried out at 37 °C. Two structural analogs of L-MSO i.e. L-methionine Sulfone and Phosphinothriacin were also taken for time dependent experiments. The enzyme in the pre- incubation mix was periodically removed in identical aliquots and diluted as mentioned above for carrying out the assay. The inhibition experiment was repeated with a series of inhibitor concentrations starting from 10 µM to 9600 µM of L-MSO. Loss of enzyme activity was monitored until saturation in inhibition was observed. All inhibition experiments were monitored relative to a control sample where buffer was added instead of inhibitor solution. The enzyme activity obtained in control was set to 100% at each time point. Once the data was collected, the logarithm of the percentage

of enzyme activity remaining relative to the un-inhibited control was plotted against the time of pre-incubation.

4.3.6 Saturation and Determination of K_I and K_{inact}

Saturation was demonstrated by carrying out the time-dependent experiment described at six (10 μM, 31.25 μM, 62.5 μM, 150 μM, 1000 μM and 9600 μM) different inhibitor concentrations at a fixed enzyme concentration (17). The half-life for inhibition (t1/2) at each inhibitor concentration was plotted against I/[inactivator] (known as a Kitz and Wilson plot (17). Saturation could be interpreted by the intersection of the experimental line at the positive y axis. This indicated that we will still get a finite rate of inhibition at infinite inhibition (L-MSO) concentration. The point of intersection at the y axis is In 2/kinact from which the value of *K*inact can be determined. The extrapolated negative X - axis intercept is (*-) 1/KI.* The value of *K*inact and the K1 are determined from the plot (17).

4.3.7 Substrate Protection of the enzyme activity against inhibition

In order to check that inhibition was occurring due to binding of L-MSO at the active site of the enzyme, the experiment described in section 4.2.4 was repeated under identical conditions 1) in the presence and 2) in the absence of substrates like L-Glutamic Acid, ATP, and Hydroxyamine which are known substrates for the enzyme. The experiment was done at several different fixed concentrations of substrate. The percent activity remaining was plotted against time of pre-incubation of the enzyme with L-MSO. Here, the positive control did not have any substrate along with the enzyme at the time of pre-incubation.

4.3.8 Nature of binding

The reversibility of MtbGS inhibition was carried out by following an earlier established method (25). Initially, 0.15 mg/ml of the enzyme was incubated with 500

µM L-MSO, 160 mM $MgCl_2$ and 7.6 mM ATP in 50 mM Hepes buffer with pH 6.8 for 30 minutes to obtain complete inhibition. Then, the reaction mix was subjected to gel filtration by using PD10 (GE Healthcare Life Sciences) column at 25ºC to remove any free inhibition molecules. An enzyme control without inhibitor was run simultaneously and carried through identical procedure as the inhibited enzyme. The control enzyme activity was assumed as 100% for comparison with the inhibited samples.

In order to confirm the nature of binding, radiolabelled S35 -Methionine Sulfoximine having specific activity of ~ 5mci/ml was used. 500 µM cold & 2 µM S^{35} labelled L-MSO were mixed with 160 mM $MgCl_2$ and 7.6 mM ATP in 50 mM Hepes buffer with pH 6.8 and incubated with 0.15 mg/ml enzyme for 30 minutes. The sample was then divided into two and in one sample 1% SDS was added. SDS added sample was incubated for 20 minutes with occasionally gentle stirring. Both the samples were extensively dialyzed against 50 mM HEPES buffer using dialysis tubing cellulose membrane avg. flat width 10 mm (Sigma). The dialysis bag was opened and placed in a scintillation vail. 8 ml of scintillation fluid (PerkinElmer OptiPhase SuperMix) was added in vail and counts were taken by using Hidex scintillation counter.

4.3.9 The kinetics of S^{35} L- MSO Incorporation with the enzyme

The kinetics of inhibitor binding to the enzyme was monitored by following the radiolabelled L-MSO incorporation. For this, 500 µM of cold L-MSO was mixed with 2 µM S^{35} labelled L-MSO and then incubated with 0.15 mg/ml enzyme in 50 mM Hepes buffer with pH 6.8 containing, 160 mM $MgCl_2$ and 7.6 mM ATP. Periodically, 4 µl aliquots were removed and added in 50µl of 25 mM EDTA to stop the reaction. All the samples were then extensively dialyzed against distilled water. Then, the dialysis bag was opened and transferred to a scintillation vial. 8 ml of scintillation fluid (PerkinElmer OptiPhase SuperMix) was added into the vials and counts were taken by Hidex scintillation counter. Similar experiment was carried out with 500 µM of cold L-MSO and the remaining activity was determined by following the protocol explained in the section 4.2.5.

4.3.10 Autoradiography of the modified glutamine synthetase

Autoradiography of the enzyme was carried out by following an earlier method (18). Briefly, 62.5 µg/ml of purified protein along with 76 mM ATP and 160 mM $MgCl_2$ was incubated with 5 µM S^{35} labelled L-MSO (Specific activity = 5mCi/ml) and 5 µM cold L-MSO separately for ~10 hours in 50 mM Hepes buffer with pH 6.8 to achieve maximum incorporation of radioactivity with the enzyme. The samples were washed 5 times with ddH_2O by using 10K Nanosep Centrifugal Devices from Pall life sciences. Then, the modified enzymes were subjected to SDS polyacrylamide gel electrophoresis. Identical quantities of these modified proteins were placed in adjacent slots of slab gels. Gels were calibrated using proteins of known *Molecular Weight*. Following electrophoresis, gels were stained with Coomassie Blue, dried and subjected to autoradiography using Kodak Exomat XRP-1 film at -20ºC for 8 days (18).

4.4 Discussion

Glutamine synthetase was found among the 11 proteins, which were released, extracellularly in great abundance by *M. tuberculosis* (26). The belief in targeting glutamine synthetase for drug development increased further when L-methionine sulfoximine blocked the multiplication of the pathogen in axenic culture as well as in human mononuclear phagocytes (27). The blockage of growth was correlated with marked reduction in the synthesis of poly L- Glutamate-glutamine complex in the cell wall of virulent mycobacteria. Hence, it indicated toward the importance of extracellular function of the enzyme. In spite of its importance as an excellent target, very little work was done to validate the observation made from crystallographic studies. Our initial experiments clearly indicated that DL-Phosphothriacin and L-MSO was significantly inactivating the enzyme whereas L-Methionine sulphone was simply a reversible inhibitor (Figure 2-3). This observation also supported the conclusion made from crystal structure data that L-MSO is basically a tight binding inhibitor of the enzyme obtained by co-crytallization of L-MSO~P and MtbGS (12). Tight binding inhibitors belong to the same category of "mechanism based enzyme inhibitors

(MBEI)" where eventually three different fates of the actual inhibitor has been described at the end of the reaction (21). So, in order to check the mechanism of enzyme – inhibitor interaction as MBEI, Kitz and Wilson plot was drown and found that a very straight line has been generated from the inactivation kinetics of enzyme (Figure -5). This is supported by the specific interaction of the inhibitor with the enzyme in presence of ATP and $MgCl_2$ resulting in the formation of an irreversibly inhibited complex E'MBI'' (Scheme 1). The kinetic parameters for this process, Ki and kinact, were evaluated from the Kitz and Wilson plot (Figure- 5). The kinetics of the inactivation showed saturation with respect to L-MSO and protection against inactivation by L-Glutamic Acid indicating probable complex formation at the active site prior to inactivation (Figure - 6). In this context, it was very surprising to get 1:1 stochiometry of the inactivator with the holoenzyme because the binding of inactivator is dependent on the number of active sites. As the enzyme has 12 identical subunits, like the crystal data, it should have indicated binding of the inhibitor at 1:1 with respect to the enzyme subunit. In fact, there is no direct proof of 12 active sites in the whole enzyme except binding of crystal structure report. Possibly the first step of the reaction starts before binding of the second inhibitor and the modified active site brings a major conformational change within the holoenzyme preventing the entry of the substrates towards other active sites which needs to be proved. This major conformational change only could be induced if the binding of inactivator and enzyme is covalent in nature. The data extracted from the experiments of microdilution, gel filtration, SDS denaturation with subsequent dialysis and autoradiogram of modified enzyme clearly confirmed formation of covalent bond between L-MSO and MtbGS (Table 1-2 and Figure - 8). Mechanism-based enzyme inactivation is a powerful tool for studies of enzyme mechanisms and mechanisms of enzyme inactivation by small molecules. Mechanistic hypothesis can be tested on *MtbGS* by appropriate molecular design, utilizing isotopically labeled analogs to permit the elucidation of structures of metabolites produced and to determine what portions of the mechanism-based inactivators become covalently attached to the target enzyme. The use of mechanism-based enzyme inactivators is yet another of the very important methods in enzymology.

In conclusion *MtbGS* is identified as an essential component of tuberculosis and its inhibitor L-MSO is proved as a Mechanism based inhibitor.

4.5 References

1. Ginsburg, A. Glutamine synthetase of Escherichia coli: some physical and chemical properties (1972) *Ad*V. *Protein Chem. 26*, 1-79.

2. Krishnaswamy, P., Pamiljans, V., and Meister, A. Studies on the mechanism of glutamine synthesis: evidence for the formation of enzyme-bound activated glutamic acid (1962) *J. Biol. Chem. 237*, 2932-2940.

3. Midelfort CF, Rose IA. A stereochemical method for detection of ATP terminal phosphate transfer in enzymatic reactions. Glutamine synthetase. *J Biol Chem.* 1976 Oct 10; 251(19):5881–5887

4. Meek, T. D., and Villafranca, J. J. Kinetic mechanism of Escherichia coli glutamine synthetase (1980) *Biochemistry 19*, 5513- 5519.

5. Meister, A. (1980) Catalytic mechanism of glutamine synthetase; overview of *glutamine metabolism*. In *Glutamine*: *Metabolism*, *Enzymology, and Regulation of Glutamine Metabolism*, pp 1-40, Academic Press, New York.

6. Liaw, S. H., and Eisenberg, D. Structural model for the reaction mechanism of glutamine synthetase, based on five crystal structures of enzyme-substrate complexes (1994) *Biochemistry 33*, 675- 681.

7. Bancroft, S., Rhee, S. G., Neumann, C., and Kustu, S. Mutations that alter the covalent modification of glutamine synthetase in Salmonella typhimurium (1978) *J. Bacteriol. 134*, 1046-1055.

8. Almassy, R. J., Janson, C. A., Hamlin, R., Xuong, N., and Eisenberg, D. Novel subunit-subunit interactions in the structure of glutamine synthetase (1986) *Nature 323*, 304-309.

9. Yamashita, M., Almassy, R., Janson, C., Cascio, D., and Eisenberg, D. Refined atomic model of glutamine synthetase at 3.5 A resolution (1989) *J. Biol. Chem. 264*, 17681-17690.

10. Gill, H. S., and Eisenberg, D. (2001) The Crystal Structure of Phosphinothricin in the Active Site of Glutamine Synthetase Illuminates the Mechanism of Enzymatic Inhibition *Biochemistry 40*, 1903- 1912.

11.Valentine, R. C., Shapiro, B. M., and Stadtman, E. R. Regulation of glutamine synthetase XII. Electron microscopy of enzyme from E. *coli.* (1968) *Biochemistry 7*, 2143-2152.

12. Wojciech W. Krajewski, T. Alwyn Jones, and Sherry L. Mowbray, Structure of Mycobacterium tuberculosis glutamine synthetase in complex with a transition-state mimic provides functional insights. PNAS 2005 vol. 102 no. 30 10499–10504.

13. Gill, H. S., Pfluegl, G. M. & Eisenberg, D. (2002) Multicopy Crystallographic Refinement of a Relaxed Glutamine Synthetase from *Mycobacterium tuberculosis* Highlights Flexible Loops in the Enzymatic Mechanism and Its Regulation *Biochemistry* 41, 9863–9872.

14. Jaggi, R., van Heeswijk, W. C., Westerhoff, H. V., Ollis, D. L. & Vasudevan, S. G. The two opposing activities of adenylyl transferase reside in distinct homologous domains, with intramolecular signal transduction (1997) *EMBO J.* 16, 5562–5571.

15. Upasana Singh, Vinita Panchanadikar and Dhiman Sarkar Development of a Simple Assay Protocol for High-Throughput Screening of *Mycobacterium tuberculosis* Glutamine Synthetase for the Identification of Novel Inhibitors *J Biomol Screen* 2005; 10; 725

16. UPASANA SINGH, DHIMAN SARKAR, Development of a Simple High-Throughput Screening Protocol Based on Biosynthetic Activity of *Mycobacterium tuberculosis* Glutamine Synthetase for the Identification of Novel Inhibitors. *J Biomol Screen* 2006; 11; 1035

17. RICHARD B. SILVERMAN, Mechanism-Based Enzyme Inactivators METHODS IN ENZYMOLOGY, VOL. 249 p 240-283

18. Marc R. Hammerman and Jame R. Gavin Binding of Insulin-like Growth Factor and Multiplication-stimulating Activity-stimulated Phosphorylation in Basolateral Membranes from Dog Kidney, *J. Biol. Chem* Vol. 259, No. 21, pp. 13511-13517,1984

19. *David C. Swinney,* Applications of Binding Kinetics to Drug Discovery, Pharm Med 2008; 22 (1): 23-34

20. Manning, J.M., S. Moore, W.B. Rowe, and A. Meister. 1969. Identification of L-methionine-*S*-sulfoximine as the diastereomer of L-methionine-*S, R*-sulfoximine that inhibits glutamine synthetase. *Biochemistry* 8: 2681-2685

21. S. G. Waley, Kinetics of suicide substrates *Biochem. J.* 185, 771 (1980); S. G. Waley, *Biochem. J.* 227, 843 (1985).

22. Jung MJ, Metcalf BW. Catalytic inhibition of gamma-aminobutyric acid - alpha-ketoglutarate transaminase of bacterial origin by 4-aminohex-5-ynoic acid, a substrate analog. *Biochem Biophys Res Commun.* 1975 Nov 3;67(1):301–306

23. Armand W. J. W. Tepper, Luigi Bubacco, and Gerard W. Canters, Stopped-flow Fluorescence Studies of Inhibitor Binding to Tyrosinase from *Streptomyces antibioticus.* THE JOURNAL OF BIOLOGICAL CHEMISTRY Vol. 279, No. 14, , pp. 13425–13434, 2004

24. T. Funaki, S. Ichihara, H. Fukazawa, and I. Kuruma, The behaviour of remaining enzyme activity in a suicidal enzyme system. *Biochim. Biophys. Acta* 1118, 21 (1991).

25. D. J. Kuo and F. Jordan, Active site directed irreversible inactivation of brewers' yeast pyruvate decarboxylase by the conjugated substrate analogue (E)-4-(4-chlorophenyl)-2-oxo-3-butenoic acid: development of a suicide substrate *Biochemistry* 22, 3735 (1983).

26. GUNTER HARTH, DANIEL L. CLEMENS, MARCUS A. HORWITZ, Glutamine synthetase of Mycobacterium tuberculosis: Extra-cellular release and characterization of its enzymatic activity, PNAS. Vol. 91, pp. 9342-9346.

27 Michael V. Tullius, Gunter Harth, and Marcus A. Horwitz Glutamine Synthetase GlnA1 Is Essential for Growth of *Mycobacterium tuberculosis* in Human THP-1 Macrophages and Guinea Pigs. INFECTION AND IMMUNITY, July 2003, p. 3927–3936

Chapter -5

Studies on utilization of amino acids as nitrogen source of *M.tuberculosisH37ra* as well as regulator of Glutamine synthetase

5.1 Introduction

Nitrogen incorporated into glutamate and glutamine which actually serve as the major biosynthetic donors for all other nitrogen containing components in a cell. Glutamine is a source of nitrogen for the synthesis of purines, pyrimidines, a number of amino acids, glucosamine and ρ-benzoate, whereas glutamate provides nitrogen for most transaminases (1) and is responsible for 85% of nitrogenous compounds in a cell (2). In most prokaryotes, there are two major routes for ammonia assimilation. In the first one, tglutamine synthetase (GS) and glutamate synthase (GOGAT) cyclic mechanism is largely active when exogenous nitrogen concentrations are limiting and due to the high affinity of GS for ammonium, it is able to trap ammonium nitrogen very easily. This pathway utilizes approximately 15% of the cell's ATP requirement (1) for the production of glutamine and its activity is, therefore, strictly regulated at both transcriptional and post-translational levels to prevent wastage of energy (Figure 1A). Under conditions of excess nitrogen, glutamine synthetase activity is reduced via adenylylation by the adenylyltransferase GlnE (3, 4) and under these conditions glutamate dehydrogenase (GDH) with low ammonium affinity plays a major assimilatory role with comparatively lower demand for associated energy (5). GDH enzymes catalyze the reversible amination of α-ketoglutarate to form glutamate with concomitant reduction of NAD(P)H (Figure 1B). They also serve as metabolic branch enzymes as the GDH enzymes are involved in anapleurotic processes which regulate the flux of intermediates such as α- ketoglutarate between the Krebs cycle and nitrogen metabolism (6). The GDH enzymes identified in prokaryotes usually function in association with either $NADP^+$ (EC 1.4.1.4) or NAD^+ (EC 1.4.1.2) as co-factors whilst in higher eukaryotes the enzymes have dual co-factor specificity (EC 1.4.1.3). $NADP^+$ specific enzymes are normally involved in the assimilation of nitrogen via amination of α-ketoglutarate (7) and may be transcriptionally regulated

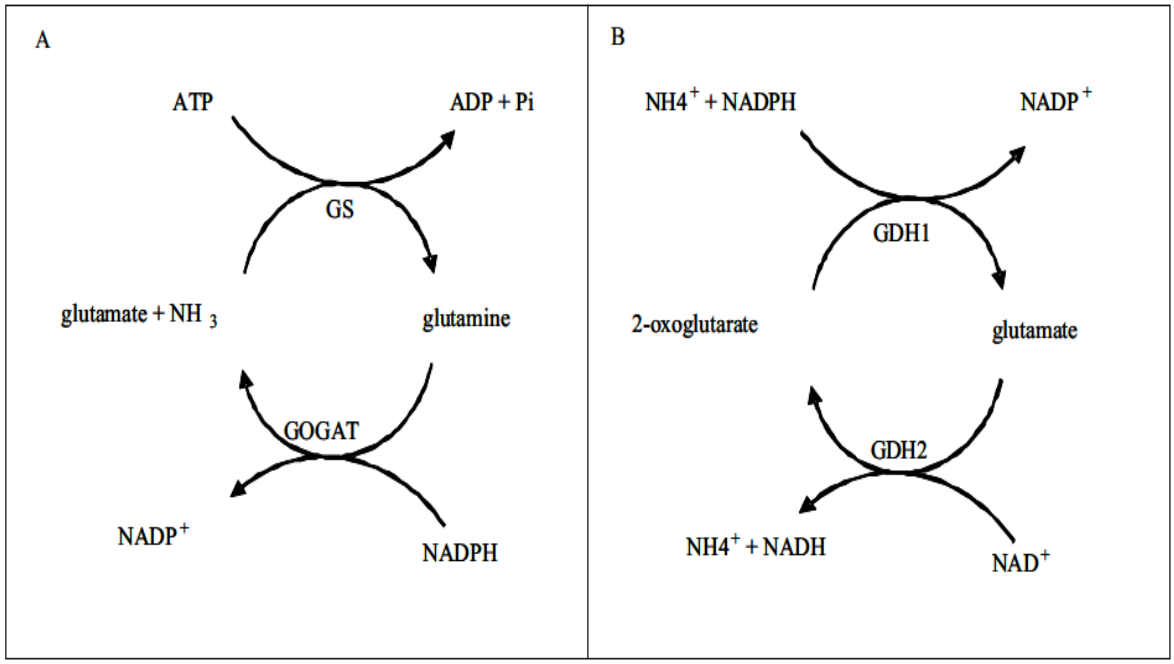

Figure 1 Assimilation of nitrogen by (A) GS and GOGAT; (B) $NADP^+$ - dependant-glutamate dehydrogenase (GDH1) and NAD^+-dependant glutamate dehydrogenase (GDH2).

by a variety of growth conditions, including carbon and nitrogen limitation (8-11). In contrast, NAD^+ specific GDH enzymes are thought to be largely involved in glutamate catabolism (deamination) (12-14) and do not appear to be regulated in response to ammonium limitation (15,16). GDH enzymes described till date are oligomeric structures and can be grouped into three subgroups according to subunit composition. Many $NADP^+$ and NAD^+GDH enzymes from a number of organisms are hexameric structures made up of subunits that are approximately 50 kDa in size [6]. The second GDH class comprises NAD^+ specific GDH enzymes with tetrameric structures whose subunits have a molecular mass of approximately 115 kDa (17). Recently, a third class of oligomeric NAD^+ specific GDH enzymes whose subunits are approximately 180 kDa in size was defined (18-20). Information regarding nitrogen metabolism and its regulation in the mycobacteria is relatively limited. Glutamine synthetase (encoded by *glnA1*) has traditionally formed an isolated focal point of study with regard to nitrogen metabolism in the mycobacteria as it has been associated with *Mycobacterium tuberculosis* virulence and pathogenicity (21, 22). It has previously been demonstrated

that GS from pathogenic mycobacterial species such as *M. tuberculosis* and *M. bovis* is exported, (23) yet the reasons for this phenomenon and the mechanism of export remain controversial (24). It has been speculated that extracellular GS may play a role in the production of poly- L-glutamine-glutamate complex, a polymer found only in pathogenic mycobacterial cell walls, and/or that extracellular GS activity may modulate phagosome pH and thereby prevent phagasome-lysosome fusion (23 - 25). Comparatively little is known about GS in other mycobacterial species, such as *Mycobacterium smegmatis*, or GDH in the mycobacteria as a whole. The *M. smegmatis* genome encodes for a variety of putative glutamine synthetase enzymes which encode for each of the four possible classes of GS proteins, many of which serve unknown functions (26). Of these homologs, *msmeg_4290* has the greatest amino acid identity to *glnA1* in *M. tuberculosis*, which encodes for a GS type 1 ammonium assimilatory enzyme (27). The *M. smegmatis* GS seems different to *M. tuberculosis* GS in that it does not appear to be expressed at such a high level, nor does it appear to be exported to the extracellular milieu (23, 24). The *M. smegmatis* genome also encodes for an $NADP^+$GDH (*msmeg_5442*) which was isolated by using a reported protocol; an L_180 class NAD^+GDH (*msmeg_4699*) as well a second putative NAD^+GDH enzyme (*msmeg_6272*) (28,29). In contrast, the *M. tuberculosis* genome only encodes for a single putative NAD^+ specific GDH (*Rv2476c*) whose activity was detected in culture filtrates by Ahmad *et al* (30). The enzyme shares a 71% amino acid identity with MSMEG_4699 and may also belong to the L_180 class of NAD^+-GDH (18, 29). NAD^+ specific glutamate dehydrogenases belonging to the L_180 class have been characterized in four organisms to date, namely *Streptomyces clavuligerus* (18), *Pseudomonas aeruginosa* (20), *Psychrobacter* sp. TAD1 (31) and *Janthinobacterium lividum* (19). However, little functional work has been done on these enzymes. It has very recently been found that the NAD^+GDH (MSMEG_4699) isolated from *M. smegmatis* may belong to this class and that its activity is affected by the binding of a small protein, GarA. This small protein is highly conserved amongst the actinomycetes and was given the name glycogen accumulation regulator (GarA) due to its observed effects on glycogen metabolism in *Mycobacterium smegmatis* (32), however its precise function remained unclear till date. GarA has a fork-head associated (FHA) domain

which is able to mediate protein-protein interactions as well as a highly conserved N-terminal phosphorylation motif. In this, a single threonine residue may be phosphorylated by either serine/threonine kinase B (PknB) (33) or serine/threonine kinase G (PknG) (29) thereby presumably playing a role in phosphorylation-dependant regulation mechanisms (34). It has been shown that Odh1 (the GarA ortholog in *C. glutamicum*; 75 % amino acid identity) is able to bind 2-oxoglutarate dehydrogenase, a key TCA cycle enzyme, and cause a reduction in its activity. This inhibition of enzyme activity was removed by phosphorylation of Odh1 by PknG (35). A similar phenomenon has been observed in *M. smegmatis* with regard to the modulation of NAD^+GDH by GarA. Native or unphosphorylated GarA has been shown to interact with NAD^+GDH causing a reduction in NAD^+GDH activity by altering the affinity of the enzyme for its substrate (29). This binding, however, is prevented by the phosphorylation of GarA (29) by PknG. The conditions under which PknG is stimulated to phosphorylate or dephosphorylate GarA have not yet been investigated and it is not clear how the relationship between GarA, NAD^+GDH and PknG may impact nitrogen metabolism in the mycobacteria.

In bacteria, externally available amino acids can be used directly for protein synthesis and can be catabolized as well, serving as a nitrogen source. The intracellular function of GS could play an important role for survival of this pathogen in case when only those nitrogen sources are available which require GS for assimilation. Thus, it became interesting to find the nitrogen sources which require GS for bacterial assimilation. L-methionine sulfoxamine (L-MSO) is a well-characterized inhibitor of prokaryotic and eukaryotic glutamine synthetase (GS). The function of GS in nitrogen rich condition could be dispensable as other alternative pathways, which do not require GS for their assimilation, may become useful. So it has become essential to understand the role of GS during survival of intracellular tubercular bacilli. Hence, all 20 amino acids were applied on the biosynthetic activity of the enzyme and on *in vitro* growth of the bacilli. The utilization of nitrogen sources like nitrate, nitrite, ammonia and amino acids during growth of mycobacteria was checked in presence of L-MSO. In order to define the role of intracellular GS, the dose dependent effect of L- MSO on growth for all three species

was compared for enriched and minimal media containing nitrate as the sole nitrogen source. (Section - A of chapter 5) But the major challenge was to identify the nitrogen sources utilized by mycobacteria during its survival under anaerobic environment. The growth of mycobacterium in different nitrogen sources and their utilization was monitored using *M. pheli* medium. The *M. pheli* medium is a minimal medium in which the different nitrogen sources can be used. The major problem related to the study of utilization of amino acids was the lack of a viability assay for the assessment of aerobic as well as anaerobic mycobacteria. The problem of using agar plate based *cfu* estimation was the variance in the extent of aggregations of mycobacterial cell in presence of different amino acids in the medium. Hence a whole cell based XTT reduction assay is developed. (Section - B of chapter 5).

Section 5A- Role of intracellular Glutamine Synthetase (GS) in growth and survival of *M. tuberculosis* during active and hypoxic dormant stage

L- methionine sulfoxamine (L-MSO) inhibited extracellular glutamine synthetase in concentration dependent manner but had minimal effect on cellular glutamine synthetase of *M. tuberculosis* (36). In the present study it was observed that L-MSO could inhibit the assimilation of nitrate as sole nitrogen source, which indicated that intracellular GS could also play important role in the survival of the organism (37).

5.2 Results

5.2.1 Comparison of growth and effect of L-MSO for enriched and minimal medium

L-MSO is a well-characterized inhibitor of prokaryotic and eukaryotic glutamine synthetase (GS) (38). *M. tuberculosis* GS was found more sensitive by one to two orders of magnitude to L-MSO than mammalian GS and was also found to selectively block the growth of pathogenic mycobacteria (39). Though the GS present inside the cell was identical to the enzyme present outside the cell, it has been reported earlier that the effect of L-MSO on the growth and survival of *M. tuberculosis* is only due to

inhibition of extracellular activity (36). It is difficult to assume that the same enzyme present inside the cell is not inhibited by this inhibitor. Moreover these results were based on *in vitro* studies where multiple nitrogen sources were provided by using enriched medium for the growth of the organism (36). Thus the function of GS in this nitrogen rich condition could be dispensable as other alternative pathways, which do not require GS for their assimilation, may become available. So the evaluation of intracellular function of GS and its role in growth and survival was done in defined nutrient condition where a single nitrogen source at a time is provided for the growth. Functional nitrate assimilation pathway allowed us to take nitrate as the sole nitrogen source in the defined media. Growth in this defined media was then compared with growth in enriched complex media for *M. smegmatis*, *M. bovis* BCG and *M. tuberculosis* (Fig. 1A and B). All three species could grow in this defined media and their growth was quite comparable with growth in enriched media. In order to define the role of intracellular GS, dose dependent effect of GS inhibitor L- MSO on growth for all three species was compared for enriched and minimal media (Figure - 2A and B). L-MSO completely blocked the growth of all three species at a very low concentration of 2.0 µg/ml in the defined medium where nitrate was used as the sole nitrogen source. In contrast, effect of L- MSO on growth of above species in enriched medium was found sub inhibitory even up to 20.0 µg/ml. Complete inhibition of growth in defined medium where nitrate was used as nitrogen source could be explained by the fact that GS located in the cytoplasm, which allows the assimilation of nitrate, becomes compulsory for growth. Inhibition of this intracellular function led to the cessation of growth since apart from nitrate no other nitrogen source was provided in the medium. The enriched medium contains multiple nitrogen sources and the presence of any nitrogen source, which does not depend on the intracellular function of GS, may allow the growth of the organism even if GS inhibitor L-MSO is applied. Thus the little effect of L-MSO on growth seen in the enriched medium must be because of inhibition of extracellular GS function.

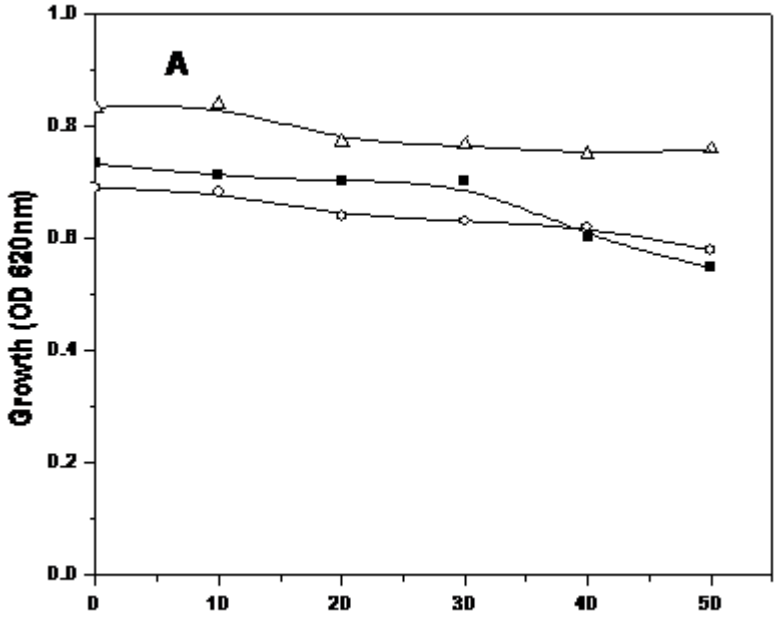

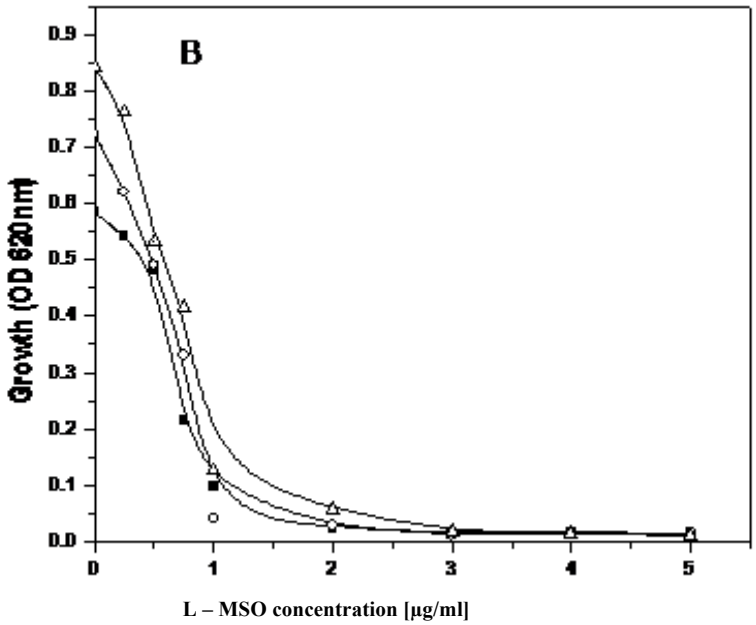

Figure 2. Dose dependent effect of L- MSO on growth of different Mycobacterial cultures

M. tuberculosis (■), M. bovis BCG (○), M. smegmatis (Δ), in enriched (A) and minimal medium (B). Enriched medium contained multiple nitrogen sources whereas 10 mM of sodium nitrate was used as sole nitrogen source in the minimal medium. L- MSO was added at the time of inoculation and growth was measured after 8 days of incubation time. The experiments were carried out more than three times

5.2.2 Requirement of GS in dormant phase

Though the results clearly indicated that many of the nitrogen sources could be assimilated only when GS is functional, yet these results are observed for aerobic replicating phase where the organism can multiply. In the dormant phase of the bacilli where it cannot multiply, the requirement of nitrogen source to remain viable has still remained an unexplored area. Since GS is required for assimilation of some of the nitrogen source, inhibitor of GS could be used to predict whether nitrogen metabolism is active during dormant phase. All three mycobacterial cultures were grown in Wayne's 0.5 HSR *in vitro* dormancy model with a single nitrogen source, which required GS for its assimilation (40). Once the cultures reached the dormant phase, L-MSO was added to the culture by a syringe. The effect of MSO on the viability of the dormant bacilli was determined by taking plate counts of the bacilli after 48 and 96 hours of incubation (Figure 3A). A significant reduction in viability of the dormant bacilli of all three species was seen in presence of L-MSO when nitrate used as the sole nitrogen source. The effect of L-MSO was negligible on the dormant bacilli of these cultures in the medium where asparagine was provided as the sole nitrogen source, which does not rely on GS for its assimilation (Figure 3B). These results have two implications; 1) nitrogen assimilation continues in dormant phase since inhibition of GS leads to the death of dormant bacilli and 2) extracellular GS function is not indispensable for survival of dormant bacilli since dormant bacilli survived in presence of MSO in a medium supplemented with a nitrogen source, which does not require GS for its assimilation.

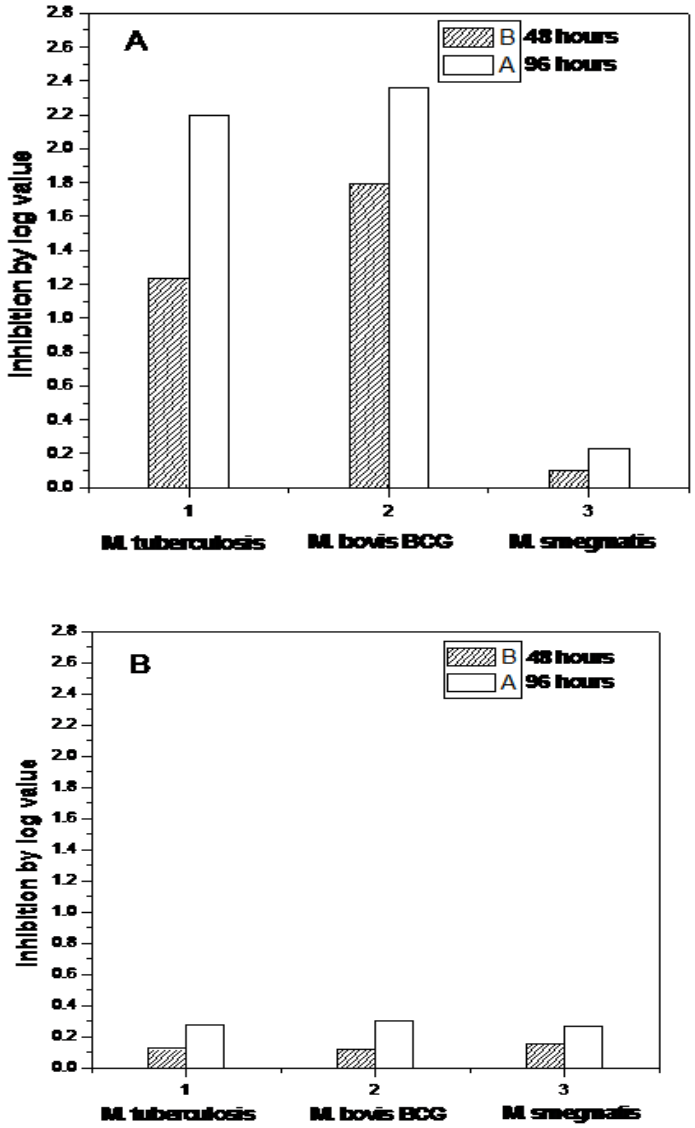

Figure - 3 Effect of L-MSO on the viability of mycobacteria under hypoxia induced dormant stage.

Effect of L-MSO (2 ug/ml) on viability of dormant bacilli of *M. tuberculosis*, *M.bovis* BCG, *M. smegmatis* after 48 (dark bars) and 92 hours (light bars) of incubation period when grown in minimal medium with glutamine (A) and asparagine (B) as sole nitrogen source. Inhibition by log value was calculated by deducting the log cfu/ml in presence of L- MSO from control log cfu/ml. L-MSO was added to an 8 days old culture of *M.tuberculosis* and *M.bovis* BCG but for *M.smegmatis* it is 4 days when all the cells reached the dormant stage. The experiments were carried out more than three times.

5.3 Materials and Methods

5.3.1 Bacterial strains

M. bovis BCG (ATCC 35745), *M. smegmatis* (ATCC607) were obtained from AstraZeneca, India and *M. tuberculosis* H37Ra (ATCC 25177) was obtained from MTCC, India.

5.3.2 Chemicals and media

All the chemicals were purchased from Sigma, USA unless mentioned. A defined medium containing 0.5 gm KH_2PO_4, 0.2 gm sodium citrate, 60 mg $MgSO_4$, 0.5 gm asparagine and 2 ml glycerol in 100 ml of distilled water with pH 6.6 was used throughout the whole study as a minimal medium. Asparagine was replaced by other nitrogen sources according to the experimental requirement.

5.3.3 Cultivation of aerobic and dormant bacilli

For aerobic cultivation of the bacilli 5 ml of the culture was added to a 25 ml capacity tube containing 8mm magnetic bar and was then incubated at 37^0C on a magnetic stirrer rotating at 100 rpm. Inoculums was prepared by first allowing the organism to grow upto the stationary phase in minimal medium without nitrate/nitrite and then palleting the cells aseptically in a centrifuge at 10000 rpm for 10 minutes. Cell pallet was then suspended to equal volume of the minimal medium without any nitrogen source. 1% of this suspension was used as inoculum size for each experiment yielding approximately 10^5 cells per ml.

To cultivate the anaerobic bacilli, Wayne's 0.5 HSR tube model was followed, using 20 x 125 mm tubes with a total volume of 25.5 ml (37). Inoculum size used here was about 10^5 cells per ml by diluting the culture upto 0.008 A_{620}. The tubes containing 8 mm magnetic spin bars were made airtight by using rubber septa. The cultures were gently stirred at 100 rpm on a magnetic stirring platform.

5.3.4 Measurement of growth

Growth of the organism was measured by reading absorbance of culture at 620nm following an earlier described method (37). Viability of dormant bacilli was determined by plating different dilutions of the culture on Dubos agar plates and counting the colonies appeared (37).

5. 4 DISCUSSION

As it was discussed in earlier chapters, extracellular release and characterization of its activity could identify it as one of the important determinants of pathogenecity of *M. tuberculosis* (39). This was based on the facts of the enzyme's 1) central role in nitrogen metabolism (43); 2) influence on ammonia level within infected host cells to inhibit phagosome lysosome fusion and phagosome acidification (44); 3) extracellular catalysis of synthesis of the cell wall structure poly L- Glutamate-glutamine which is present in pathogenic bacilli but not in non pathogenic mycobacteria (36,45). The surprising factor here was that this enzyme is found only in the cytoplasmic milieu in other bacterial systems (43).

The blockage of growth was again found correlated with marked reduction in the amount of virulence associated with cell wall component poly L- Glutamate-glutamine. The results were further confirmed when application of antisense (PS-ODN) against mRNA of *M. tuberculosis* GS reduced its growth by 0.75 to 1.25 logs (46). Gene disruption studies also showed that glutamine synthetase is essential as *GlnE* (regulator of GS-1) mutant could not grow and *GlnA1* (GS-1) mutant became attenuated for intracellular growth in THP-1 macrophage (48, 49). Since L-MSO is assumed as not being able to cross the mycobacterial cell wall and a decreased amount of poly L-glutamate- glutamine complex in GlnE and GlnA1 mutant of *M. tuberculosis* was observed correlated with their reduced virulence, it could be predicted that disruption of extracellular GS is responsible for the blockage of growth (47, 50). Thus, the effect of L-MSO seen on growth is only because of inhibition of the extracellular function of this enzyme as the same enzyme is catalyzing these two different functions. High

extracellular amount of this enzyme was due to the high expression and extracellular stability rather than to protein specific export mechanism (51). It was also suggested that the release of protein was due to the increased rate of autolysis in *M. tuberculosis* when compared to other bacteria (51). Thus, it became essential to analyze the function of this enzyme more precisely in order to validate the target finally. In order to clarify whether intracellular function of the enzyme is at all important, we designed the experiments in growth conditions where certain nitrogen sources were used one by one each time. This was essential as availability of multiple nitrogen sources could make the organism's other pathways available, which may not require glutamine synthetase for assimilation of nitrogen. Thus, a single nitrogen source at a time in a defined medium was used to evaluate the intracellular function of GS in mycobacteria for different nitrogen sources (40). The intracellular function of GS gained more importance when the dose dependent effect of GS inhibitor L-MSO on growth was compared between a nitrogen rich medium and a single nitrogen source defined medium which requires GS for its assimilation (Figure. 2). L-MSO could completely inhibit the growth of both *M. bovis* BCG and *M. tuberculosis* at very low concentration of 2.0 µg/ml when glutamine was used as sole nitrogen source in defined medium. In contrast, the effect of L-MSO was found only sub inhibitory even upto 20 µg/ml for both *M. bovis* BCG and *M. tuberculosis* when they were grown in an enriched medium containing multiple nitrogen sources. Though these results suggest that intracellular function could become more important than extracellular function of GS for survival of the pathogen, it depends more importantly on the availability of nitrogen sources. In a different perspective of evaluating this enzyme's importance during the so called latent stage, we used hypoxia- induced dormancy model. We observed that L-MSO reduced the viability by almost 2 logs for both *M. bovis* BCG and *M. tuberculosis* when a nitrogen source was used which requires GS for assimilation (Fig. 4). In contrast L-MSO did not have any significant effect on the viability of dormant bacilli when a nitrogen source which does not require GS for assimilation was used as the sole nitrogen source in the medium. Results showed that GS was even required in the dormant stage of the pathogen where it was not multiplying though it was also dependent on the available nitrogen sources. Thus, it can be concluded that

intracellular function of GS might play a much more important role than its extracellular function during survival of *M. tuberculosis* and most importantly this enzyme can be a good drug target for latent phase as well.

Section 5B Development of a simple and robust assay that allows more rapid determination of the susceptibility of all the three species of mycobacterium, as well as investigation of catabolic regulation of amino acids

In order to develop antitubercular screening assays many attempts were made using redox dyes like alamar blue/resazurin, tetrazolium, etc. on aerobic cultures of mycobacterium (52, 53, and 54). The search for drugs targeting mycobacterium is delayed because of either continuing CFU or following unexpectedly longer incubation with the dye as the main assessment technique, both of which are primarily designed for very low throughput screening. Apart from these disadvantages, incubation of the dye for longer period could result in changes in metabolic and physiological status of the bacilli under investigation. Currently available assays are not capable enough to identify inhibitors of dormant stage mycobacteria. In one of our earlier attempts, an *in vitro* whole cell based assay was developed to make the screening process convenient and applicable on dormant culture (40). Normally, NarGHJI (an operon which codes for a respiratory type of nitrate reductase) activity should not be seen in aerobic culture but *M. tuberculosis* culture reduces substantial amount of nitrate to nitrite (40). Due to this higher level of basal nitrate reduction, its use in anti-tubercular screening remained limited to *M. bovis* BCG.

The present study described the application of tetrazolium salt XTT along with menadione to estimate viable bacilli during screening of chemical libraries. Due to addition of menadione in this assay, superoxide was generated in the bacilli which rapidly reduce XTT to produce the color. Hence, XTT reduction assay was carried out on bacilli obtained from Wayne's dormancy model to develop a robust whole cell assay to screen anti-tubercular compounds against all possible physiological stages of bacilli (55). However, the use of tetrazolium salts is a well known method for analyzing *Mycobacterium tuberculosis* strains while the addition of menadione is a new development in this context (56, 57).

5.5 Results

The major obstacles in developing a simple protocol for drug screening were the varying aggregation, generation time and metabolic activity between replicate and dormant stage of different mycobacterium bacilli. The screening protocol earlier developed by our group using *M. bovis* BCG clearly demonstrated the establishment of culture conditions for both dormant and replicate stage of the bacilli. This microplate format provided a platform which could be coupled with different detection techniques to obtain better results in the screening of anti-mycobacterial compounds. In the present study, the assay was modified by using XTT to monitor the viability of the bacilli irrespective of its replicate or non-replicate stage. The water solubility and colorimetric detection of XTT at 470 nm have also made the method more convenient to rapidly carry out the screening program (57, 58). The earlier reports as well as our present study indicated that mycobacterium cultures were very poor reducers of tetrazolium dyes (Figure-1) (56, 57). For this reason, we included menadione into this assay to enhance XTT reduction, so that its detection could be faster and easier. Therefore, the effect of menadione was checked to test this hypothesis.

5.5.1 Menadione concentration

Initially, a dose response experiment was carried out to find the sensitivity of menadione towards XTT reduction and finally three different concentrations were selected for kinetic studies (Figure–4). The kinetic data observed from XTT reduction using *M. smegmatis* cells indicated that maximum reduction was attained within 30 minutes of incubation in presence of 60 μM of menadione. Molar extinction coefficient ($\Delta\lambda$) of XTT reduction was around 8.3 x 104 M^{-1s-1} (59). In this experiment, it was observed that XTT reduction was directly proportional to the concentration of menadione applied. The linearity of XTT reduction at lower concentrations of menadione was maintained beyond 30 minutes of incubation. The linearity of the same was terminated within 10 minutes when 80 μM of menadione was added. As 60 μM

was the maximum concentration where the linearity was maintained up to a substantial period of time along with the acceptable rate of XTT reduction, this concentration was accepted as convenient for carrying out subsequent experiments.

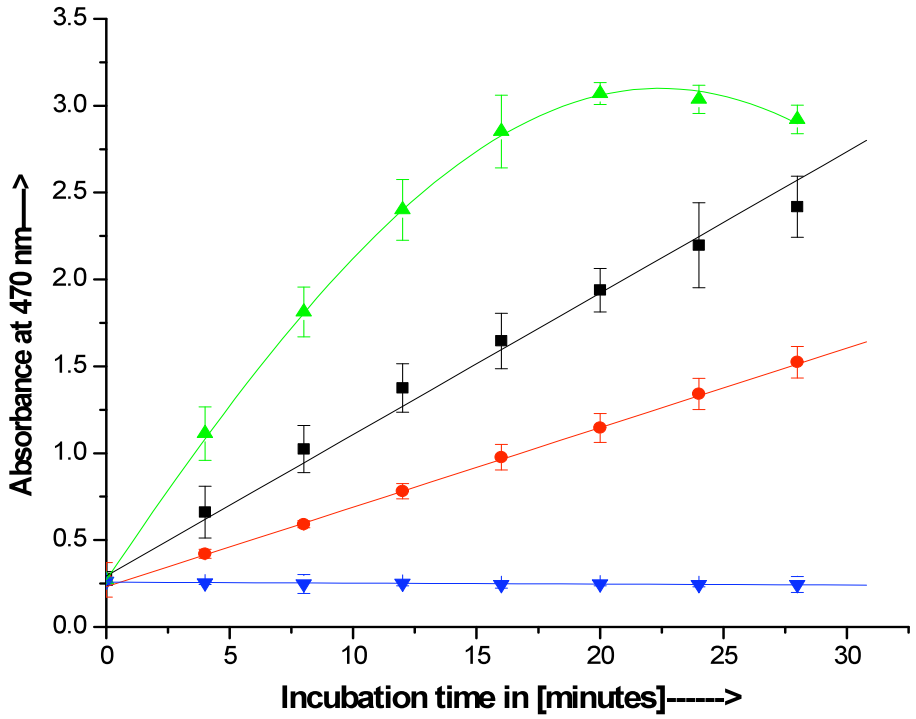

Figure 4. Kinetics of XTT reduction in presence of varying menadione concentrations on *M. Smegmatis.* The cell suspensions with ~0.2 $O.D_{620}$ of density were separately treated with 30 µM (●), 60 µM (■), 80 µM (▲) and none (▼) of menadione along with 200 µM XTT. The O.D470 read outs were taken at intervals of 4 minutes in the kinetic mode of the plate reader. The results for each data point were obtained from 8 identical wells from the same plate. Further details of the experiment were mentioned in 'Materials and Methods' section. The plots were drawn from average values obtained for each data point from 4 such identical experiments.

5.5.2 Incubation Time

Even though the XTT reduction continued for 30 minutes, the result indicated that it maintained the linearity till 20 minutes after the addition of menadione when *M. smegmatis* cell suspension was used (Figure–5). Hence, incubation time for *M. smegmatis* was fixed at 20 minutes. Identical protocol was used to compare the kinetics of XTT reduction by *M. tuberculosis* and *M. bovis* BCG (Figure-4). The results also indicated that the extent of XTT reduction by *M. smegmatis* was ~3.5 X greater than *M. tuberculosis* and *M. bovis* BCG. Therefore, reduction of XTT occurs significantly faster in *M. smegmatis* than *M. tuberculosis* and *M. bovis* BCG. Linearity was grossly maintained for *M. bovis* BCG and strictly for *M. tuberculosis* till 45 minutes of incubation with menadione. Hence, the incubation time for both *M. tuberculosis* and *M. bovis BCG* cells were fixed at 40 minutes before taking the read out at 470 nm.

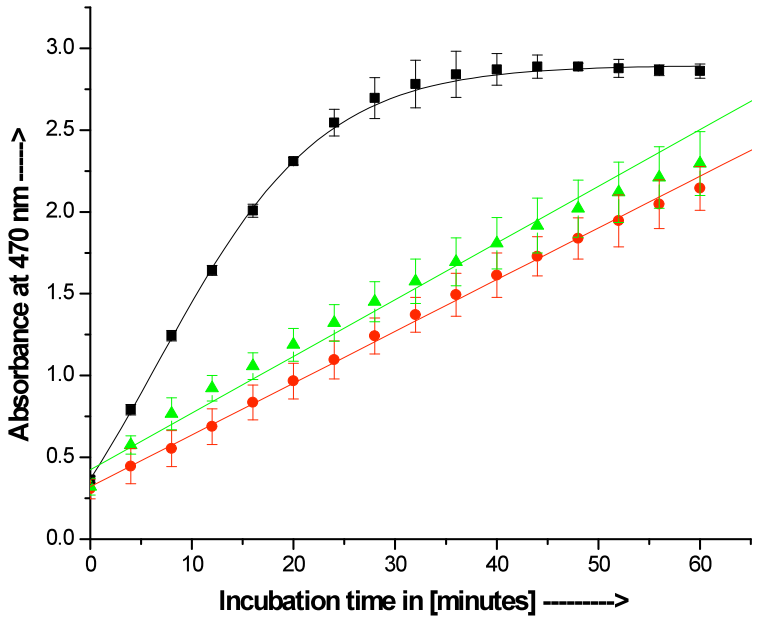

Figure–5 Comparative reduction kinetics of XTT by *M. smegmatis, M. tuberculosis and M. bovis* BCG. *M. smegmatis* (■), *M. tuberculosis* (▲) and *M. bovis BCG* (●) cell suspensions at ~0.25 O.D620 were incubated with 60 µM menadione and 200 µM

XTT. The $O.D_{470}$ read outs were taken in the kinetic mode at intervals of 4 minutes immediately after addition of menadione. The results for each data point were obtained from 8 identical wells from the same plate. Further details of the experiment were mentioned in 'Materials and Methods' section. The plots were drawn from average values obtained for each data point from 4 such identical experiments.

5.5.3 Cell density for aerobic cultures

As observed earlier, it became essential to get the linearity in XTT reduction with respect to cell density at least up to 0.25 $O.D_{620}$ of culture density (40). Initially, aerobic cultures from *M. smegmatis*, *M. bovis* BCG and *M. tuberculosis* were taken at different concentrations to check the linearity of XTT reduction (Figure -6). For *M. smegmatis,* the cell suspension was incubated for 20 minutes whereas for *M. tuberculosis* and *M. bovis* BCG, it was incubated for 40 minutes. The results indicated that all three mycobacterium cultures were showing linearity in XTT reduction with the increase in $O.D_{470}$ of the culture taken. The XTT reductions in all these cultures were directly proportional to the cell density.

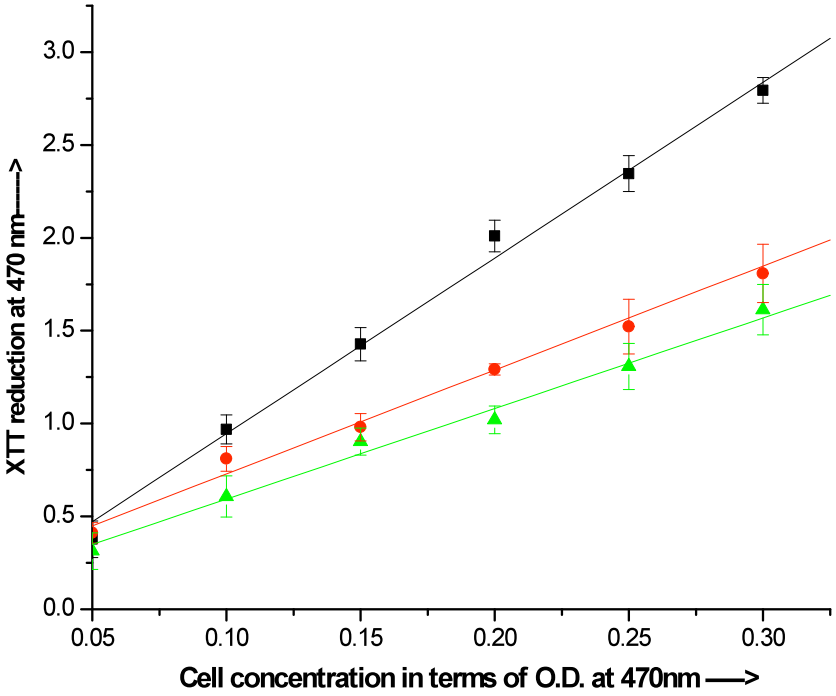

Figure 6 XTT reduction as a function of cell density for aerobically grown *M. smegmatis*, *M. tuberculosis and M. bovis* BCG. Aerobic cell suspensions of all three different bacilli were incubated with 200 μM of XTT and 60 μM of menadione to measure the read outs of XTT reduction at 470 nm. *M. smegmatis* (■) cells were incubated for 20 minutes whereas *M. tuberculosis* (●) and *M. bovis* BCG (▲) were incubated for 40 minutes after addition of Menadione. The results for each data point were obtained from 8 identical wells. Further details of the experiment were mentioned in 'Materials and Methods' section. The plots were the average of 4 such identical experiments.

5.5.4 Cell density for anaerobic cultures

In order to understand the pattern of XTT reduction, anaerobic cultures of different mycobacterium bacilli grown in Wayne's 0.5 HSR model were immediately used in the same assay protocol (Figure - 7). Our unpublished observation suggested that these

hypoxia induced dormant bacilli when exposed to air do not revert to metabolically active stage at least within 2 hrs. Interestingly, though the linearity in XTT reduction was maintained in all the cultures used, the extent of reduction was significantly dissimilar with their respective aerobic cultures. The extent of XTT reduction in all these cultures was directly proportional to the culture density.

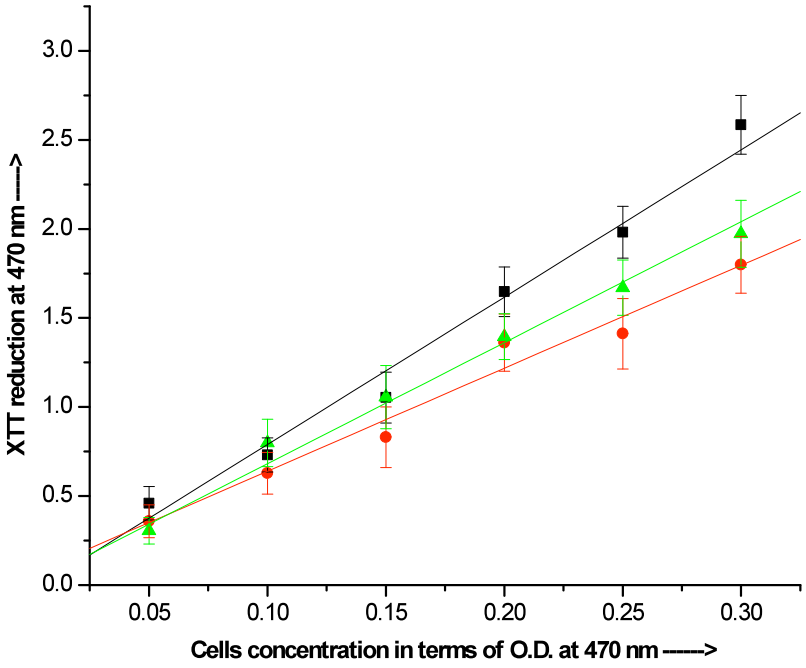

Figure 7 XTT reduction as a function of cell density for anaerobic *M. smegmatis, M. tuberculosis and M. bovis* BCG

Anaerobic cell suspensions of all three different bacilli were incubated with 200 μM of XTT and 60 μM of menadione to measure the read outs of XTT reduction at 470 nm. *M. smegmates* (■) cells were incubated for 20 minutes whereas *M. tuberculosis* (●) and *M. bovis* BCG (▲) were incubated for 40 minutes after addition of Menadione as described in Figure-3. The results for each data point in both the experiments were obtained from 8 identical wells. Further details of the experiment were mentioned in 'Material and Method' section. The plots were the average of 4 such identical experiments.

5.5.5 Z ` factor and statistical analysis for quality assessment

S/N ratio and Z' factor were the two essential components considered during the development of a robust assay protocol for rapid screening of inhibitors (60). When the values were derived for *M. smegmatis* cells using the optimized assay protocol, the S/N ratio values obtained were found to have varied between 8.0 – 10.0. The Z' values for *XRMA* were found to be ~0.9 for the whole range of cell density evaluated (Table-1). The determined S/N ratios were > 6.0 for *M. tuberculosis* and > 5.0 for *M. bovis* BCG respectively. The Z' factor values obtained from similar experiments using *M. tuberculosis* and *M. bovis BCG* were varying around 0.80 and 0.90 respectively. The S/N ratio and Z' factor values obtained from the experiments using the optimized conditions indicated that the protocol was robust for carrying out high throughput screening of the compound library.

Table – 1 S/N ratio and Z factor for *M. smegmatis* –Varying concentrations of *M. smegmatis* were incubated with 200 µM of XTT followed by addition of 60 µM of menadione. The S/N ratio and Z' factors of *M. smegmatis* cells were determined using the data points of 20 minutes after addition of menadione. The results were the average of 4 identical experiments and standard deviation. The results for each data point in both the experiments were obtained from 8 identical wells.

Serial Number	Cell O.D	S/N Ratio	Z' Factor
1.	**0.07**	**9.4 ± 0.049**	**0.95 ± 0.049**
2.	**0.11**	**9.7 ± 0.072**	**0.96 ± 0.120**
3.	**0.15**	**9.3 ± 0.054**	**0.85 ± 0.054**
4.	**0.20**	**9.5 ± 0.096**	**0.86 ± 0.096**
5.	**0.25**	**9.3 ± 0.026**	**0.76 ± 0.026**
6.	**0.31**	**9.0 ± 0.035**	**0.67 ± 0.035**

Table - 2 S/N ratio and Z factor for *M. bovis* BCG – Varying concentrations of *M. bovis* BCG was incubated with 200 µM of XTT followed by addition of 60 µM menadione. The S/N ratio and Z' factors of *M. bovis* BCG cells were determined using the $O.D_{470}$nm read outs at 40 minutes after addition of menadione. The results were the average of 4 identical experiments with ±standard deviation. The results for each data point in both the experiments were obtained again from 8 identical wells.

Serial Number	Cell O.D	S/N Ratio	Z' Factor
1.	**0.07**	5.97 ± 0.071	0.80 ± 0.096
2.	**0.11**	5.0 ± 0.068	0.81 ± 0.064
3.	**0.15**	5.3 ± 0.018	0.92 ± 0.012
4.	**0.20**	5.6 ± 0.015	0.84 ± 0.077
5.	**0.25**	5.2 ± 0.077	0.80 ± 0.082
6.	**0.31**	5.4 ± 0.065	0.83 ± 0.094

Table – 3 S/N ratio and Z' factor for *M. tuberculosis* – Varying concentrations of *M. tuberculosis* were incubated with 200 µM of XTT followed by addition of 60 µM menadione. The S/N ratio and Z' factors of *M. tuberculosis* cells were determined using the $O.D_{470}$nm read outs at 40 minutes after addition of menadione. The results were the average of 4 identical experiments ± standard deviation. The results for each data point in both the experiments were obtained again from 8 identical wells.

Serial Number	Cell O.D	S/N Ratio	Z' Factor
1.	**0.07**	6.0 ± 0.055	0.950 ± 0.048
2.	**0.11**	6.9 ± 0.017	0.80 ± 0.0205
3.	**0.15**	6.7 ± 0.018	0.960 ± 0.072
4.	**0.20**	6.2 ± 0.073	0.80 ± 0.088
5.	**0.25**	6.7 ± 0.035	0.90 ± 0.053
6.	**0.31**	6.7 ± 0.060	0.89 ± 0.160

5.7.6 Validation with standard inhibitors

The MIC values were determined by using the calculations mentioned in Equation-1. 10 antimycobacterial agents including rifampin, streptomycin, isoniazid, ethambutol and pyrazinamide were used to determine the MIC values using this protocol. All these inhibitors are specific to the aerobic stage of the bacilli. The major obstacle for validation with anaerobic cells is the unavailability of latent stage specific inhibitors in the literature. Briefly, 2.5 µl of compound solutions were added in a total volume of 250 µl. The incubation was terminated on the 4th and 8th day for *M. smegmatis* and *M. tuberculosis*/*M. bovis BCG* cultures respectively. The XRMA was then carried out to estimate viable cells present in different wells of the assay plate. Growth inhibition of

the bacilli was calculated by following equation-1. The concentration of inhibitor at which > 90% inhibition of growth was seen was considered as the MIC value of the respective anti-tubercular compound. The calculated MIC values were found to be fairly consistent with the reported MIC values using CFU, REMA and NR assays.

Table - 4 Comparative MIC values of 8 antitubercular drugs against *M. tuberculosis*, *M. bovis* BCG and *M. smegmatis* determined by *XRMA assay with* REMA and *CFU* under aerobic condition. MIC was defined as lowest concentration of the drug/test compound that results in ≥ 90% inhibition of viability by REMA assay and ≥ 99 % loss of viability by the CFU technique.

ND* = Not done and NH* = No inhibition

Drugs Names	MIC in μg/ml											
	M. tuberculosisH37ra				*M. bovis* BCG				*M. smegmatis*			
	XRMA	**REMA**	**CFU**	**NR assay**	**XRMA**	**REMA**	**CFU**	**NR assay**	**XRMA**	**REMA**	**CFU**	**NR assay**
1. Rifampin	**0.0019**	0.002	0.002	0.05	**0.0019**	0.002	0.004–0.008	0.05	**0.5**	0.5–1	0.25–1	0.3
2. Isoniazid	**0.125**	0.125	>0.031	0.05	**0.015**	0.063	0.015	0.05	**5**	4	>0.06–0.125	0.2
3. Ethambutol	**0.8**	1	0.5–0.25	2	**0.5**	0.5	0.5	3	**0.5**	0.5–2	> 4–5	4
4. Pyrazinamide	**>10**	ND*	-	>10	**>100**	ND*		>10	**NH***	ND*		>10
5.4-amino Salicylic Acid (PASA)	**1**	1	4	1	**1**	1	4	5	**>10**	256–512	0.5–.2	>10
6. Streptomycin	**0.138**	0.125	> 0.03	0.15	**0.25**	0.25	0.25–0.5	0.2	**0.25**	0.5–1	0.25–1	0.2
7. Ofloxacin	**0.25**	0.25	0.25	1	**0.5**	0.5	0.5	2	**1**	0.5–1	0.5–1	3
8. Vancomycin	**>10**		-	>10	**>10**			>10	**>10**			>10

5.5.7 Nitrogen sources utilized/not utilized by mycobacterial cells

Those nitrogen sources, which did not allowed the growth, were identified as unutilizable nitrogen sources (Table -5). L- Glutamine, L-Arginine and L –Tryptophan do not support growth of *M. tuberculosis* in any stage of growth. L- Aspargine, L-Aspartic acid, L-Glutamic acid, L-Glycine , L-Alanine, L-leucine, L-Isoleucine, L-Serine, L-Proline, L-Threonine, L-Cystine, L-Methione and L-Lysine are utilized by *M. tuberculosis* in both the stages. L- Histidine and L-phenylanaline are poorly utilized in both the stages. On the other hand L-Valine is utilized poorly in aerobic stage but does not support the growth in anaerobic stage. Tyrosine and Hydroxyproline don't support growth in aerobic stage but poorly supports growth in anaerobic stage.

Table – 5 Investigation of catabolic regulation of amino acids in *M. tuberculosis* Each amino acid was served as sole nitrogen source separately to support the growth of *M. tuberculosis*

Srl. No.	***Name of the amino acid***	***Growth in Presence of Amino acids Detected by XTT Menadione assay In terms of % Activity with reference to Asperagine Cells***	
		Aerobic Cells	***Anaerobic Cells***
1.	***L-Aspargine***	***100***	***100***
2.	***L- Aspartic acid***	***205***	***519***
3.	***L-Glutamine***	***-7***	***-21***
4.	***L-Glutamic acid***	***219***	***634***
5.	***L-Glycine***	***196***	***417***
6.	***L-Alanine***	***327***	***815***
7.	***L-Arginine***	***19***	***-50***
8.	***L-Leucine***	***124***	***527***
9.	***L-Isoleucine***	***173***	***400***
10.	***L-Serine***	***194***	***427***
11.	***L-Tryptophan***	***-5***	***-5***
12.	***Histidine***	***68***	***57***
13.	***Proline***	***147***	***249***
14.	***Valine***	***26***	***-64***
15.	***Phenylalanine***	***61***	***59***
16.	***Threonine***	***103***	***125***
17.	***Tyrosine***	***-29***	***72***
18.	***Hydroxyproline***	***-42***	***12***
19.	***Cystine***	***592***	***524***
20.	***Methionine***	***115***	***199***
21.	***Lysine***	***150***	***361***

.

5.5.8 Effects of amino acids against *Mycobacterium yuberculosis* Glutamine Synthetase

Table - 6 summarizes data illustrating the differences in response to effectors of glutamine synthetase preparations in biosynthetic assay. In case of *MtbGS* three different amino acids are identified as allosteric effectors (Table -7). For *MtbGS* the other end products like CTP and ADP are also identified as allosteric effector. The allosteric property was not observed in the enzyme when it was purified from *YMC21E*, because the enzyme was not an adenylated one. In *E. coli* the unadenylated enzyme was inhibited by Glycine, Serine and Alanine by interfering at the substrate-binding site. Our data reported in this thesis was in accordance with the previous observation on *E. coli* enzyme. Inhibition by Glycine was highest and inhibition by Serine was lowest, which indicated a similar structure of the mycobacterial enzyme with the *E. coli*. Alanine binds in Mg^{++} binding site in *E. coli* enzyme. As the inhibition was found maximum among all other, it was decided to carry on preliminary experiments using Glycine as inhibitor. ADP, CTP, NAD^{+} and NADPH were the allosteric effectors which were reported earlier in *E. coli* and *Salmonella typhumurium*, but interestingly here inhibition was found by ADP and CTP.

Table – 6 *M.tuberculosis* Glutamine synthetase was inhibited by L-Glycine, L-Alanine and L- Serine

Srl. No.	*Name of the amino acid (10 mM concentration)*	*Percentage Inhibition*
1.	*L-Aspargine*	*6.3*
2.	*L- Aspartic acid*	*7.8*
3.	*L-Glutamine*	*6.6*
4.	*L-Glycine*	***78.8***
5.	*L-Alanine*	***54.4***
6.	*L-Arginine*	*11.4*
7.	*L-Leucine*	*2.7*
8.	*L-Isoleucine*	*2.3*
9.	*L-Serine*	***51.4***
10.	*L-Tryptophan*	*-5.2*
11.	*Histidine*	*-7.5*
12.	*Proline*	*3.0*
13.	*Valine*	*3.5*
14.	*Phenylalanine*	*-2.9*
15.	*Threonine*	*2.5*
16.	*Tyrosine*	*-7.0*
17.	*Hydroxyproline*	*-2.7*
18.	*Cystine*	*2.9*
19.	*Methionine*	*2.7*
20.	*Lysine*	*8.7*

Table - 7 *M. tuberculosis* Glutamine synthetase was inhibited by ADP and CTP

Srl . No.	**Allosteric effectors**	**Percentage Inhibition**	
		Concentration of L-Glutamic Acid	
		100 mM	**20 mM**
1.	**ADP**	**82.6**	**86.18**
2.	**CTP**	**73.71**	**81.74**
3.	**NAD +**	**2.91**	**-2.68**
4.	**NADPH**	**-10.25**	**-30.23**

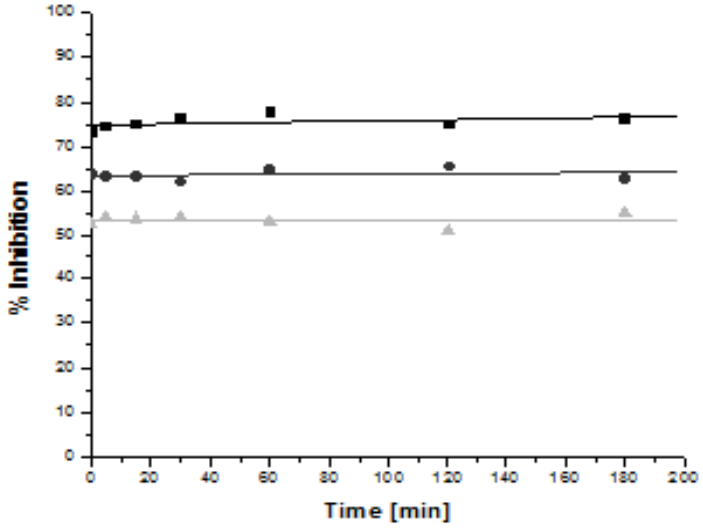

Figure – 8 Time curve in presence of Glycine, Alanine and Serine.

The 62.5mg/ml of the enzyme was preincubated with 10 mM L-Glycine (▲), 10 mM L-Alanine (●) and 10 mM of L-Serine (■) at room temperature. Fixed aliquots were taken out and mixed in large volume of stopping buffer. The details of the experiment are described in `Materials and Methods'. The plots represent average of the data obtained from three identical experiments ±standard deviation.

5.6 Materials and Methods

5.6.1 Bacterial strains and growth conditions

In order to prepare the stock cultures, *Mycobacterium tuberculosis* H37Ra (ATCC 25177), *M. bovis* BCG (ATCC 35755) and *M. smegmatis* mc2 (ATCC 607) were grown to logarithmic phase ($O.D._{595}$ ~ 1.0) in a defined medium (*M. pheli* medium) containing 0.5 gm KH_2PO_4, 0.2 gm sodium citrate, 60 mg $MgSO_4$, 0.5 gm asparagine and 2 ml glycerol in 100 ml of distilled water with pH 6.6 following a described method (40). The stock culture was maintained at -70^{0}C and sub cultured once in *M. pheli* medium before inoculation into experimental culture. The bacterial stock was sub-cultured in *M. pheli* medium under aerobic conditions, shaking it at 150 rpm at 37^{o}C within an incubator shaker till logarithmic phase ($O.D._{595}$ ~ 1.0) was reached (Thermo Electron

Corporation Model 481). After growth, the culture was sonicated for 2 minutes using a water bath sonicator (BANDELYN electronic Model RK 1028c).

For the cultivation of anaerobic dormant bacilli, Wayne's 0.5 HSR tube model was followed wherein 20 x 125 mm tubes with 17 ml of the medium which was inoculated with 1% v/v of (O.D.595 ~ 1.0) (40). The culture tubes were incubated at 37^{o}C within an incubator for 12 days in case of *M. tuberculosis* and *M. bovis* BCG and for 5 days of *M. smegmatis* after making the tubes air tight with rubber septa. In these tubes, 8 mm magnetic spin bar were already placed and gently stirred at 100 rpm on a magnetic stirrer. Viable cells were counted by the method described earlier (40). For aerobic cells, 50 ml of *M. pheli* medium was inoculated with 1% v/v log phase culture of the bacilli. For initial optimization the cells were grown in identical conditions as mentioned above for both aerobic and anaerobic bacilli. Generally, O.D.470 ~ 0.25 cells were taken for initial optimization unless otherwise mentioned. Dilutions of the cells were done by using sterile *M. pheli* medium.

5.6.2 Drug and Reagent preparation

Rifampicin, Streptomycin, Ethambutol, Isoniazid, Pyrazinamide, Ofloxacin, p-aminosalicylic acid, Vancomycin, Clotrimazole and Fluconazole were procured from Sigma. Drugs were solubilized according to the manufacturer's recommendations and were stored in aliquots at -20^{0}C. XTT sodium salt powder (Sigma) was prepared as a 1.25 mM stock solution in sterile 1 x PBS which was stored at - 20^{0}C, for not more than 10 days. Menadione (Sigma) was prepared as a 6 mM solution in DMSO and was stored at room temperature for two weeks.

5.6.3 Reduction of 2, 3-bis [2-methyloxy-4-nitro-5-sulfophenyl]-2H-tetrazolium-5-carboxanilide by *M. smegmatis*

For optimization of XTT and menadione concentrations, cells were sonicated for 2 minutes and 250 µl of cells were taken in sterile 96 well plates. Cells in *M. pheli* medium with quadruplicate wells were used for each of the experimental conditions. Unless otherwise mentioned, XTT was added at 200 µM final concentration and incubated for 20 minutes. At the end of 20 minutes incubation, different concentrations (30 µM, 60 µM & 80 µM) of menadione were added and the increase in optical density was observed with continuous mixing at the interval of 30 seconds in a plate reader (Spectramax plus 384 from Molecular Devices Inc). The absorbance was taken at 470 nm. In blank wells, XTT and menadione were added in *M. pheli* medium.

5.6.4 In vitro culture of anaerobic and aerobic cells in micro plate

In order to avail of aerobic as well as hypoxic bacilli in micro plate format, a modified method reported earlier was followed (40). Mycobacterium cells were mostly remained aggregated under aerobic condition in the *M. pheli* medium. Before inoculation, the log phase cells were sonicated at 50 KHz for 2 minutes in water bath sonicator. These sonicated cells were used for inoculation in micro plate wells. 250 µl of the culture containing ~105 cells/ml was added to each well of 96 well plates and thus exactly maintaining the head space to culture volume ratio at 0.5. The air supply of the culture in the micro plate was blocked by applying a micro plate sealer (Nunc Inc.). Then, the plates were incubated in a CO2 incubator at 37°C.

5.6.5 Final XTT Reduction Menadione Assay (XRMA) protocol

5.6.5 (a) M. tuberculosis and M. bovis BCG

For XRMA against aerobic culture, the plates were taken out on the 8th day of incubation to remove the seal and to measure the viable cell counts. The optical density

of the culture was measured before addition of XTT at 470 nm which was served as a blank for the MIC calculations using equation -1. 200 µM XTT is added and incubated for 20 minutes at 37^0C after shaking for 1 minute. After 20 minutes incubation 60 µM of menadione was added and incubated at 37ºC for 40 minutes after mixing for 1 minute. Finally, the optical density of the suspension was measured at 470 nm by using a plate reader.

For XRMA against hypoxia induced dormant culture, the plates were taken out on the 12th day of incubation to remove the seal and to measure the viable cell counts. As mentioned earlier, the optical density was measured before addition of XTT at 470 nm and a similar method was repeated as mentioned above.

5.6.5 (b) M. smegmatis

For XRMA on the 3rd day of incubation, the plate was taken out to remove the seal and measure the viable cells. Optical Density was measured before the addition of XTT at 470 nm. 200 µM XTT was added and incubated for 20 minutes at 37^0C after shaking of 1 minute. After 20 minutes incubation 60 µM of menadione was added and mixed for 1 minute and then incubated at 37ºC for another 20 minutes. The optical density was measured at 470 nm by using a micro plate reader. For Hypoxia induced XTT reduction microplate assay (HXRMA) on the 7th day of incubation, the plates were taken out and the seal was removed. A similar protocol was repeated as mentioned above.

5.6.6 Calculation for determination of MIC

The MIC was defined as the lowest drug concentration effecting growth inhibition of ≥ 90% relative to the growth for the drug-free controls. The MICs were numerically extrapolated from transformed inhibition-concentration plots derived from the equation as follows –

$$\% \text{ Inhibition} = 100 - \left(\frac{(A1 - \text{Blank})}{(A2 - \text{Blank})} \right) X100 \quad \text{---------- Equation -1}$$

where,

A1= Culture absorbance at 470 nm in presence of the compound after addition of menadione

A2= Culture absorbance at 470 nm (DMSO solvent control) after addition of menadione

Blank = Culture absorbance at 470 nm of the respective data points before addition of XTT/menadione

Briefly, the numeric approach uses Origin 6.1 software to calculate the average difference in growth indicators (percent inhibition in the concentration intervals between the test culture and the dimethyl sulfoxide solvent control culture and linear approximation of the concentrations effecting a 90% reduction).

5.6.7 Utilization of nitrogen sources by mycobacterial cells

Inoculum was prepared by allowing the organism to grow the organism up to the stationary phase in minimal medium without nitrate/nitrite and then palleting the cells aseptically in a centrifuge tube rotating at 10000 rpm for 10 minutes. The cell pallet was then suspended to equal volume of the minimal medium without any nitrogen

source. The cells were washed thrice with minimal media, without any nitrogen source and sonicated for 2 minutes. 1% of this suspension was used as inoculum size for each experiment yielding approximately 105 cells per ml. 20 different sets of minimal medium were prepared with 20 different amino acids and inoculated with nitrogen free cells. 250 µl of the culture containing ~105 cells/ml was added to each well of 96 well plates, thus exactly maintaining the head space to culture volume ratio at 0.5. Air supply of the culture in micro plate was blocked by applying micro plate sealer (Nunc Inc.). Then, the plates were incubated in a CO2 incubator at 37°C. XRMA assay was done as described in the section. Cells with asparagine were taken as reference for calculation of this data.

5.6.8 Inhibitory activity of amino acids on the biosynthetic activity of purified *Mycobacterium yuberculosis* Glutamine Synthetase

A modified protocol was followed to carry out *M. tuberculosis* glutamine synthetase biosynthetic assay, as described earlier. The reaction was started by adding 7.6 mM of ATP in 200 µl of reaction mixture containing 20 mM imidazole buffer pH 7.0, 100 mM L-glutamic acid, 50 mM $MgCl_2$, 50 mM NH_4Cl, and 62.5 µg/ml of enzyme in a test tube. In this reaction, ammonium chloride, L-glutamic acid, and ATP were used as substrate and Mg^{2+} ion as a co-factor to yield inorganic phosphate, glutamine, and ammonia. 10 mM of each amino acid were used in the assay to determine their inhibitory activity against the enzyme. In the modified protocol, to stop the reaction, 12 % w/v L-ascorbic acid in 1 N HCL and 2% w/v ammonium molybdate in ddH_2O were mixed in a 2:1 proportion, and 600 µl of that was added to 200 µl of reaction mixture and mixed well to develop a blue color immediately. It was incubated for 7 minutes to get the fully developed color. After that, 600 µl of 1% sodium citrate tribasic dihydrate in 1% acetic acid in ddH_2O was added to the reaction mixture to restrict the further development of color due to hydrolysis of ATP. Incubation of the reaction mixture with 22.5 mM EDTA served as the blank. A Cary 50 Bio Spectrophotometer was used to monitor the color at 655 nm after 30 minutes of incubation.

5.6.9 Time dependence inhibition by L-Alanine, L-Glycine and L-Serine

All the enzyme assay components except substrate are equilibrated at 25°C in a pre-incubation tube. Sufficient enzyme for 6-10, assays is added to give a solution of *at least* 50 times the concentration necessary for a standard assay of enzyme activity. 10 mM L-Glycine/L-Alanine/L-Serine, 7.6 mM ATP, 50 mM $MgCl_2$ and 62.5 µg/ml protein were incubated in 50 mM Hepes buffer (pH 6.8). Once the solution has been mixed, 4 µl of pre-incubation mixture is removed at different time interval and is added into 196 µl the enzyme assay mixture containing the substrate at saturating concentration and then the assay is carried out at 37°C. L-Glycine, L-Alanine and L-Serine were taken for time dependent experiments. The enzyme in the pre incubation tube is periodically (seconds to hours, depending on the observed inactivation rate) removed in identical aliquots from the pre-incubation tube, diluted as above, and assayed. All inactivation experiments are monitored relative to a control sample which is done exactly as the earlier experiment except without inactivator added (an equal volume of buffer is added). The enzyme activity in this sample is set to 100% at each time point. This control takes into account the normal loss of enzyme activity under the conditions of the experiment and not as a result of the presence of the inactivator.

5.7 Discussion

In conclusion, we developed and validated a robust assay protocol based on the reduction of XTT that allows rapid screening of inhibitors against mycobacterial cultures (Table - 4). In earlier reported protocols, the dyes took at least 12 hours to produce a minimum signal about the viability of mycobacterial bacilli which makes it unacceptable particularly when bacilli from anaerobic cultures are used (52, 53, 54). It becomes even more difficult to apply these protocols on *M. smegmatis* because most of the cells multiply during incubation as well. Generally, reduction of XTT in mycobacterial culture is a very slow process (56, 57). Here, application of menadione

has increased the XTT reduction to such an extent that the assay incubation takes only 20 minutes for *M. smegmatis* and 40 minutes for *M. tuberculosis/M. bovis* BCG (Figure 3-7). However, a similar method has been used for antimicrobial susceptibility testing of fungus (62, 62). Initially the applicability of this assay protocol was checked on different mycobacterial cells using both fast growing non-pathogenic *M. smegmatis* and slow growing non-pathogenic *M. bovis* BCG or attenuated *M. tuberculosis*. The mechanism of superoxide production in liquid culture due to the addition of menadione is a poorly understood process. It was earlier reported that menadione was metabolized to a semiquinone by various flavoenzymes, such as NADPH cytochrome P-450 reductase, NADH cytochrome *b*5 reductase, and NADH-ubiquinone reductase (63). This semiquinone was further converted to the parent quinone in the presence of oxygen, thereby generating reactive superoxides (63). It was also reported that the conversion of menadione to the semiquinone could occur by non-enzymatic reactions with various thiols present in the cells (64). On the other hand, although XTT does not require the use of solvent like isopropanol for the solubilization of its reduced form, some safety concerns still remains as it belongs to the tetrazolium class of dyes in general (65). Initial dose response effect of menadione clearly indicated that the reduction of XTT followed a linear relationship till 80 µM of menadione was added in the assay mix (Figure 3 & 4). The linearity in XTT reduction was maintained for a longer period of time if lower concentration of menadione was added. At 80 µM of menadione, XTT reduction reached the plateau within 30 minutes of incubation with *M. smegmatis* cell suspension. In order to reach the same level of reduction, it requires almost 70 minutes when 60 µM of menadione was added under identical condition. Considering the molar extinction coefficient value of reduced XTT, it could be concluded that early termination of XTT reduction was taking place under the condition mentioned. Probably the cellular components participating in XTT reduction with the help of menadione could become exhausted and as a result the plateau was obtained. This was further corroborated from the results obtained from increased cell concentrations (Figure 4 & 5). Apart from the linearity in XTT reduction, its extent was also varied with the mycobacterium species used. In case of *M. bovis* BCG and *M. tuberculosis,* the extent of XTT reduced was almost 50% less compared to *M.*

smegmatis indicating deficiency of the crucial component/s in the earlier bacilli type participating in reaction with menadione. These also proportionately affected the S/N ratios determined in all the three bacilli using this protocol (Table 1-3). Interestingly, the S/N ratio obtained using *M. smegmatis* cells was ~9.0 which was significantly higher compared to > 5.0 in *M. bovis* BCG and > 6.5 for *M. tuberculosis*. We are currently involved in elucidating the underlying reason and its implication because of this difference in the extent of XTT reduction. Interestingly, the hypoxia induced dormant culture of all three mycobacterium species did not show any significant change in the extent of XTT reduction compared to their aerobic stages (Figure 6 & 7). This menadione mediated enhanced reduction of XTT could be extended to other dyes like resazurin, NBT and WST-1 etc. For all three species of mycobacterium, the Z' values determined varied around ~ 0.9 which clearly indicated the robustness of the protocols (Table 1-3). The determined MIC values using this protocol were closer to the values obtained from REMA and CFU based assays than NR assay. Altogether, we propose a robust assay by using XTT for primary or secondary screening of diverse compound libraries against both aerobic and hypoxic mycobacterium cultures.

By applying XRMA, the utilization of amino acids by *M. tuberculosis* was explored in detail. Interestingly L-Glutamine did not support the growth of *M. tuberculosis*, which is the product of biosynthetic assay which is catalyzed by GS. It is believed that the enzyme's release into the growth medium and the presence there of all its substrates and reaction products indicate that the extracellular enzyme catalyzes the synthesis of glutamine, a major cell wall component of only pathogenic mycobacteria (66). How the poly (L-glutamate/ glutamine) heteropolymer is synthesized and attached to the cell wall is not clear. The enzyme's involvement in nitrogen metabolism and ammonia production may contribute to the capacity of *M. tuberculosis* to inhibit phagosome acidification in infected monocytes and phagosome-lysosome fusion (67, 68, 69). Feedback inhibition of glutamine synthetase by various amino acids and nucleotides has been reported in many bacteria, e.g. *Escherichia coli* (70), *Bacillus licheniformis* (71), *Klebsiella aerogenes* (72), *Rhodopseudomonas capsulata* (73), *Nitrosomonas europaea* (74), *Chlorobium vibrioforme* (75) and *Methylcocccus capsulatus* (76). The purified enzyme from *M. tuberculosis was* similarly inhibited. Thus at 10 mM final

concentration of alanine, serine and glycine inhibited the biosynthetic activity by 54.4%, 51.1% and 78.8*%,* respectively. The time dependent inhibition was observed against these three amino acids. No time dependent inhibition was found, which indicates that the inhibition is uncompetitive in nature.

5.8 References

1. Reitzer L: Nitrogen assimilation and global regulation in Escherichia coli**.** *Annu Rev Microbiol* 2003, 57:155-176.

2. Fisher SH: Regulation of nitrogen metabolism in Bacillus subtilis: vive la difference! *Mol Microbiol* 1999, 32:223-232.

3. Parish T, Stoker NG: glnE is an essential gene in Mycobacterium tuberculosis**.** *J Bacteriol* 2000, 182:5715-5720.

4. Fink D, Falke D, Wohlleben W, Engels A: Nitrogen metabolism in Streptomyces coelicolor A3(2): modification of glutamine synthetase I by an adenylyltransferase**.** *Microbiology* 1999, 145(Pt 9):2313-2322.

5. Schulz AA, Collett HJ, Reid SJ: Nitrogen and carbon regulation of glutamine synthetase and glutamate synthase in Corynebacterium glutamicum ATCC 13032**.** *FEMS Microbiol Lett* 2001, 205:361-367.

6. Britton KL, Baker PJ, Rice DW, Stillman TJ: Structural relationship between the hexameric and tetrameric family of glutamate dehydrogenases**.** *Eur J Biochem* 1992, 209:851-859.

7. Duncan PA, White BA, Mackie RI: Purification and properties of NADPdependent glutamate dehydrogenase from Ruminococcusm flavefaciens FD-1**.** *Appl Environ Microbiol* 1992, 58:4032-4037.

8. Antonopoulos DA, Aminov RI, Duncan PA, White BA, Mackie RI: Characterization of the gene encoding glutamate dehydrogenase (gdhA) from the ruminal bacterium Ruminococcus flavefaciens FD-1**.** *Arch Microbiol* 2003, 179:184-190.

9. Schwacha A, Bender RA: The product of the Klebsiella aerogenes nac (nitrogen assimilation control) gene is sufficient for activation of the hut operons and repression of the gdh operon**.** *J Bacteriol* 1993, 175:2116-2124.

10. Hanssler E, Muller T, Palumbo K, Patek M, Brocker M, Kramer R, Burkovski A: A game with many players: control of gdh transcription in Corynebacterium glutamicum**.** *J Biotechnol* 2009.

11. Camarena L, Poggio S, Garcia N, Osorio A: Transcriptional repression of gdhA in Escherichia coli is mediated by the Nac protein**.** *FEMS Microbiol Lett* 1998, 167:51-56.

12. Miller SM, Magasanik B: Role of NAD-linked glutamate dehydrogenase in nitrogen metabolism in Saccharomyces cerevisiae**.** *J Bacteriol* 1990, 172:4927-4935.

13. Consalvi V, Chiaraluce R, Politi L, Vaccaro R, De RM, Scandurra R: Extremely thermostable glutamate dehydrogenase from the hyperthermophilic archaebacterium Pyrococcus furiosus**.** *Eur J Biochem* 1991, 202:1189-1196.

14. Rice DW, Hornby DP, Engel PC: Crystallization of an NAD+-dependent glutamate dehydrogenase from Clostridium symbiosum**.** *J Mol Biol* 1985, 181:147-149.

15. Chavez S, Candau P: An NAD-specific glutamate dehydrogenase from cyanobacteria. Identification and properties**.** *FEBS Lett* 1991, 285:35-38.

16. Stuart Shapiro: Reglation of Secondary Metabolism in Actinomycetes**.** CRC Press inc; 1989:35-38. Ref Type: Generic

17. Veronese FM, Nyc JF, Degani Y, Brown DM, Smith EL: Nicotinamide adenine dinucleotide-specific glutamate dehydrogenase of Neurospora. I. Purification and molecular properties**.** *J Biol Chem* 1974, 249:7922-7928.

18. Minambres B, Olivera ER, Jensen RA, Luengo JM: A new class of glutamate dehydrogenases (GDH). Biochemical and genetic characterization of the first member, the AMP-requiring NAD-specific GDH of Streptomyces clavuligerus**.** *J Biol Chem* 2000, 275:39529-39542.

19. Kawakami R, Sakuraba H, Ohshima T: Gene cloning and characterization of the very large NAD-dependent l-glutamate dehydrogenase from the psychrophile Janthinobacterium lividum, isolated from cold soil**.** *J Bacteriol* 2007, 189:5626-5633.

20. Lu CD, Abdelal AT: The gdhB gene of Pseudomonas aeruginosa encodes an arginine-inducible NAD(+)-dependent glutamate dehydrogenase which is subject to allosteric regulation**.** *J Bacteriol* 2001, 183:490-499.

21. Harth G, Horwitz MA: Inhibition of Mycobacterium tuberculosis glutamine synthetase as a novel antibiotic strategy against tuberculosis: demonstration of efficacy in vivo**.** *Infect Immun* 2003, 71:456-464.

22. Odell LR, Nilsson MT, Gising J, Lagerlund O, Muthas D, Nordqvist A, Karlen A, Larhed M: Functionalized 3-amino-imidazo[1,2-a]pyridines: a novel class of drug-like Mycobacterium tuberculosis glutamine synthetase inhibitors**.** *Bioorg Med Chem Lett* 2009, 19:4790-4793.

23. Harth G, Clemens DL, Horwitz MA: Glutamine synthetase of Mycobacterium tuberculosis: extracellular release and characterization of its enzymatic activity**.** *Proc Natl Acad Sci USA* 1994, 91:9342-9346.

24. Tullius MV, Harth G, Horwitz MA: High extracellular levels of Mycobacterium tuberculosis glutamine synthetase and superoxide dismutase in actively growing cultures are due to high expression and extracellular stability rather than to a protein-specific export mechanism**.** *Infect Immun* 2001, 69:6348-6363.

25. Harth G, Zamecnik PC, Tang JY, Tabatadze D, Horwitz MA: Treatment of Mycobacterium tuberculosis with antisense oligonucleotides to glutamine synthetase mRNA inhibits glutamine synthetase activity, formation of the poly-L glutamate/glutamine cell wall structure, and bacterial replication**.** *Proc Natl Acad Sci USA* 2000, 97:418-423.

26. Amon J, Titgemeyer F, Burkovski A: A Genomic View on Nitrogen Metabolism and Nitrogen Control in Mycobacteria**.** *J Mol Microbiol Biotechnol* 2008.

27. Harth G, Maslesa-Galic S, Tullius MV, Horwitz MA: All four Mycobacterium tuberculosis glnA genes encode glutamine synthetase activities but only GlnA1 is abundantly expressed and essential for bacterial homeostasis**.** *Mol Microbiol* 2005, 58:1157-1172.

28. Sarada KV, Rao NA, Venkitasubramanian TA: Isolation and characterisation of glutamate dehydrogenase from Mycobacterium smegmatis CDC 46**.** *Biochim Biophys Acta* 1980, 615:299-308.

29. O'Hare HM, Duran R, Cervenansky C, Bellinzoni M, Wehenkel AM, Pritsch O, Obal G, Baumgartner J, Vialaret J, Johnsson K, Alzari PM: Regulation of glutamate metabolism by protein kinases in mycobacteria**.** *Mol Microbiol* 2008.

30. Ahmad S, Bhatnagar RK, Venkitasubramanian TA: Changes in the enzyme activities involved in nitrogen assimilation in Mycobacterium smegmatis under various growth conditions**.** *Ann Inst Pasteur Microbiol* 1986, 137B:231-237.

31. Camardella L, Di FR, Antignani A, Ciardiello MA, di PG, Coleman JK, Buchan L, Guespin J, Russell NJ: The Antarctic Psychrobacter sp. TAD1 has two cold-active glutamate dehydrogenases with different cofactor specificities. Characterisation of the NAD+ dependent enzyme**.** *Comp Biochem Physiol A Mol Integr Physiol* 2002, 131:559-567.

32. Belanger AE, Hatfull GF: Exponential-phase glycogen recycling is essential for growth of Mycobacterium smegmatis**.** *J Bacteriol* 1999, 181:6670-6678.

33. Villarino A, Duran R, Wehenkel A, Fernandez P, England P, Brodin P, Cole ST, Zimny-Ardnt U, Jungblut PR, Cervenansky C, Alzari PM: Proteomic identification of M. tuberculosis protein kinase substrates: PknB recruits GarA, a FHA domain-containing protein, through activation loop-mediated interactions**.** *J Mol Biol* 2005, 350:953-963.

34. England P, Wehenkel A, Martins S, Hoos S, Andre-Leroux G, Villarino A, Alzari PM: The FHA-containing protein GarA acts as a phosphorylation dependent molecular switch in mycobacterial signaling**.** *FEBS Lett* 2009, 583:301-307.35. Niebisch A, Kabus A, Schultz C, Weil B, Bott M: Corynebacterial protein kinase G controls 2-oxoglutarate dehydrogenase activity via the phosphorylation status of the OdhI protein**.** *J Biol Chem* 2006, 281:12300-12307.

36. Harth, G., and M. A. Horwitz. 1999. An inhibitor of exported *Mycobacterium tuberculosis* glutamine synthetase selectively blocks the growth of pathogenic mycobacteria in axenic culture and in human monocytes: extracellular proteins as potential novel drug targets. J. Exp. Med. 189:1425-1436.

37. Wayne LG, and Hayes LG. An in vitro model for sequential study of shiftdown of *Mycobacterium tuberculosis* through two stages of non-replicating persistence. *Infect Immun* 1996; **64:** 2062-69.

38. Manning, J.M., S. Moore, W.B. Rowe, and A. Meister. 1969. Identification of L-methionine-*S*-sulfoximine as the diastereomer of L-methionine-*S, R*-sulfoximine that inhibits glutamine synthetase. *Biochemistry* 8: 2681-2685

39. Harth G, Clemens DL, Horwitz MA. Glutamine synthetase of *Mycobacterium tuberculosis*: extracellular release and characterization of its enzymatic activity. Proc Natl Acad Sci U S A. 1994;91:9342–9346.

40. Khan A, Sarkar D. Identification of a respiratory-type nitrate reductase and its role for survival of *Mycobacterium smegmatis* in Wayne model. *Microbial pathogenesis* 2006; **41:** 90-95.

41. Raynaud C, Etienne G, Peyron P, Laneelle M A, Daffe M. Extracellular enzyme activities potentially involved in the pathogenicity of Mycobacterium tuberculosis. Microbiology. 1998;**144**:577–587.

42. K. Weldingh, I. Rosenkrands, S. Jacobsen, P. B. Rasmussen, M. J. Elhay, and P. Andersen Two-Dimensional Electrophoresis for Analysis of Mycobacterium tuberculosis Culture Filtrate and Purification and Characterization of Six Novel Proteins Infect. Immun., August 1, 1998; 66(8): 3492 - 3500.

43. Wietzerbin, J., Lederer, F., Petit, J.F. (1975) Structural study of the poly-L-Glutamic acid of the cell wall of *Mycobacterium tuberculosis* var hominis, strain Brevannes. *Biochem Biophys Res Commun* **62**: 246–252.

44. Merrick, M. J., and R. A. Edwards. 1995. Nitrogen control in bacteria. Microbiol. Rev. **59:**604-622.

45. Clemens, D.L., and M.A. Horwitz. 1995. Characterization of the *Mycobacterium tuberculosis* phagosome and evidence that phagosomal maturation is inhibited. *J. Exp. Med.* 181: 257-270

46. Harth, G., P. C. Zamecnik, J. Y. Tang, D. Tabatadze, and M. A. Horwitz. 2000. Treatment of *Mycobacterium tuberculosis* with antisense oligonucleotides to glutamine synthetase mRNA inhibits glutamine synthetase activity, formation of the poly-L-glutamate/glutamine cell wall structure, and bacterial replication. Proc. Natl. Acad. Sci. USA **97:**418-423.

47. T. Parish and N. G. Stoker glnE Is an Essential Gene in Mycobacterium tuberculosis J. Bacteriol., October 15, 2000; 182(20): 5715 - 5720.

48. Tullius MV, Harth G, Horwitz MA. Glutamine synthetase *glnA1* is essential for growth of *Mycobacterium tuberculosis* in human THP-1 macrophages and guinea pigs. Infect Immun. 2003;71:3927–3936.

49. Harth, G., and M. A. Horwitz. 2003. Inhibition of *Mycobacterium tuberculosis* glutamine synthetase as a novel antibiotic strategy against tuberculosis: demonstration of efficacy in vivo. Infect. Immun. **71:**456-464.

50. Harth, G., and M. A. Horwitz. 1997. Expression and efficient export of enzymatically active *Mycobacterium tuberculosis* glutamine synthetase in *Mycobacterium smegmatis* and evidence that the information for export is contained within the protein. J. Biol. Chem. **272:**22728-22735.

51. Tullius, M. V., G. Harth, and M. A. Horwitz. 2001. High extracellular levels of *Mycobacterium tuberculosis* glutamine synthetase and superoxide dismutase in actively growing cultures are due to high expression and extracellular stability rather than to a protein-specific export mechanism. Infect. Immun. **69:**6348-6363.

52. N. K. Taneja, J. S. Tyagi. Resazurin reduction assays for screening of anti-tubercular compounds against dormant and actively growing *Mycobacterium tuberculosis, Mycobacterium bovis BCG and Mycobacterium smegmatis*. Journal of Antimicrobial Chemotherapy doi:10.1093/jac/dkm207

53. Collins L, Franzblau SG. Microplate Alamar Blue assay versus BACTEC 460 system for high-throughput screening of compounds against *Mycobacterium tuberculosis* and *Mycobacterium avium* Antimicrob Agents Chemother 1997; 41: 1004–9.

54. J. C. Palomino, A. Martin and F. Portaels. Rapid drug resistance detection in *Mycobacterium tuberculosis*: a review of colorimetric methods. Clin Microbiol Infect 2007; 13: 754–762

55. Wayne LG, Hayes LG. An in vitro model for sequential study of shiftdown of *Mycobacterium tuberculosis th*rough two stages of non-replicating persistence. Infect Immun 1996 :64: 2062-9

56. Anandi Martin, Fran¸coise Portaels , Juan Carlos Palomino Colorimetric redox-indicator methods for the rapid detection of multidrug resistance in *Mycobacterium*

tuberculosis: a systematic review and meta-analysis Journal of Antimicrobial Chemotherapy (2007) 59, 175–183

57. A. De Logu, P. Uda, M.L. Pellerano, M.C. Pusceddu, B. Saddi, M.L. Schivo Comparison of Two Rapid Colorimetric Methods for Determining Resistance of Mycobacterium tuberculosis to Rifampin, Isoniazid, and Streptomycin in Liquid Medium Eur J Clin Microbiol Infect Dis (2001) 20 :33–39

58. *K*isaburo Umemoto, Electrochemical Studies of the reduction mechanism of Tetrazolium salt and Formazan, Bull.Chem.Soc.Jpn., 62,3783-3789 (1989).

59. Mark W. Sutherland *and* Barbara A. Learmonth. The Tetrazolium Dyes MTS and XTT Provide New Quantitative Assays for Superoxide and Superoxide Dismutase Free Radical Research 1997, Vol. 27, No. 3, Pages 283-289

60. Zhang JH, Chung TDY, Oldenburg KR: A simple statistical parameter for use in evaluation and validation of high throughput screening assays *J Biomol Screen* 1999; 4:67-73.

61. Meletiadis et al. Colorimetric Assay for Antifungal Susceptibility Testing of *Aspergillus* Species J Clin Microbiol 2001 39 3402-3408

62. Michael M. Tunney, Gordon Ramage,Tyler R. Field, Thomas F. Moriarty, Douglas G. Storey, Rapid Colorimetric Assay for Antimicrobial Susceptibility Testing of *Pseudomonas aeruginosa* ANTIMICROBIAL AGENTS AND CHEMOTHERAPY, May 2004, p. 1879–1881, vol.48, No.5

63. Castro FAV, Mariani D, Panek AD, Eleutherio ECA, Pereira MD (2008). Cytotoxicity Mechanism of Two Naphthoquinones (Menadione and Plumbagin) in *Saccharomyces cerevisiae*. PLoS ONE 3(12): e3999. doi:10.1371/journal.pone.0003999

64. Peter Schopfer, Eiri Heyno, Friedel Drepper, and Anja Krieger-Liszkay , Naphthoquinone-Dependent Generation of Superoxide Radicals by Quinone Reductase Isolated from the Plasma Membrane of Soybean

65. Dominic A. Scudiere, Robert H. Shoemaker, Kenneth D. Paul!, Anne Monks, Siobhan Tierney, Thomas H. Nofziger, Michael J. Currens, Donna Seniff, and Michael R. Boyd Evaluation of a Soluble Tetrazolium/Formazan Assay for Cell Growth and

Drug Sensitivity in Culture Using Human and Other Tumor Cell Lines CANCER RESEARCH 48. 4827-4833. September 1, 1988

66. Hirschfield, G. R., McNeil, M. & Brennan, P. J. Peptidoglycan- associated polypeptides of Mycobacterium tuberculosis (1990) J. Bacteriol. 172, 1005-1013.

67. Crowle, A. J., Dahl, R., Ross, E. & May, M. H. Evidence that vesicles containing living, virulent Mycobacterium tuberculosis or Mycobacterium avium in cultured human macrophages are not acidic. (1991) Infect.Immun. 59, 1823-1831.

68. Armstrong, J. A. & D'Arcy Hart, P. Response of cultured macrophages to Mycobacterium tuberculosis, with observations on fusion of lysosomes with phagosomes. (1971) J. Exp. Med. 134, 713-740

69. Gordon, A. H., D'Arcy Hart, P. & Young, M. R. Ammonia inhibits phagosome lysosome fusion in macrophages. (1980) Nature (London) 286, 79-80.

70. Kingdon HS, Stadtman ER. Regulation of glutamine synthetase. X. Effect of growth conditions on the susceptibility of Escherichia coli glutamine synthetase to feedback inhibition. J Bacteriol. 1967 Oct;94(4):949-57

71. Hubbard JS, Stadtman ER. Regulation of glutamine synthetase. VI. Interactions of inhibitors for Bacillus licheniformis glutamine synthetase. J Bacteriol. 1967 Oct;94(4):1016-24

72. Bender RA, Magasanik B. Autogenous regulation of the synthesis of glutamine synthetase in Klebsiella aerogenes. J Bacteriol. 1977 Oct;132 (1):106-12.

73. Johansson BC, Gest H. Inorganic nitrogen assimilation by the photosynthetic bacterium Rhodopseudomonas capsulate J Bacteriol. 1976 Nov;128 (2):683-8.

74. Bhandari B, Nicholas DJ. Some properties of glutamine synthetase from the nitrifying bacterium Nitrosomonas europaea. Aust J Biol Sci. 1981;34(5-6):527-39

75. Sunil Khanna, D.J.D. Nicholas, Adenylylation of glutamine synthetase in *Chlorobium vibrioforme* f. *Thiosulfatophilum* FEMS Microbiology Letters Volume 18, Issue 3, pages 173–175, May 1983

76. J. Colin Murrell and Howard Dalton. Purification and Properties of Glutamine Synthetase from *Methylococcus capsulatus* (Bath). Journal of General Microbiology 129 (1983), 1187-1196

APPENDIX 1

Reprints of Publications from thesis

Development of a Simple Assay Protocol for High-Throughput Screening of *Mycobacterium tuberculosis* Glutamine Synthetase for the Identification of Novel Inhibitors

UPASANA SINGH, VINITA PANCHANADIKAR, and DHIMAN SARKAR

Mycobacterium tuberculosis glutamine synthetase (GS) is an essential enzyme involved in the pathogenicity of the organism. The screening of a compound library using a robust high-throughput screening (HTS) assay is currently thought to be the most efficient way of getting lead molecules, which are potent inhibitors for this enzyme. The authors have purified the enzyme to a >90% level from the recombinant *Escherichia coli* strain YMC21E, and it was used for partial characterization as well as standardization experiments. The results indicated that the K_m of the enzyme for L-glutamine and hydroxylamine were 63 mM and 8.3 mM, respectively. The K_m for ADP, arsenate, and Mn^{2+} were 2 µM, 5 µM, and 25 µM, respectively. When the components were adjusted according to their K_m values, the activity remained constant for at least 3 h at both 25° C and 37° C. The Z′ factor determined in microplate format indicated robustness of the assay. When the signal/noise ratios were determined for different assay volumes, it was observed that the 200-µl volume was found to be optimum. The DMSO tolerance of the enzyme was checked up to 10%, with minimal inhibition. The IC_{50} value determined for L-methionine S-sulfoximine on the enzyme activity was 3 mM. Approximately 18,000 small molecules could be screened per day using this protocol by a Beckman Coulter HTS setup. (*Journal of Biomolecular Screening* 20005:000-000)

Key words: glutamine synthetase, high-throughput screening, *Mycobacterium tuberculosis*, Beckman Coulter

INTRODUCTION

Mycobacterium tuberculosis is the causative agent of tuberculosis (TB), a widespread disease that is responsible for 2 to 3 million deaths annually.[1,2] About one-third of the world's population is infected with the bacterium with no signs of disease, and 10% of these infected individuals carry the latent form of the organism, which has the chance to get reactivated, causing these individuals to develop the disease during their lifetime. Furthermore, HIV infection has increased the risk of reactivation of *Mycobacteria*.[3] Currently, TB chemotherapy includes a long-term regimen of drug treatment for 6 to 9 months. Moreover, the antibiotics are not effective to the latent form of infection. Most alarmingly, most of the currently isolated pathogenic strains are resistant to the available drugs.[4] Thus, there is an urgent need for the discovery of new molecules with a novel mode of action. High-throughput screening (HTS) of libraries of chemically diverse compounds is thought to be one of the most efficient means of identifying novel molecules that inhibit a novel target. Few targets have been suggested in recent literature; an inhibitor could lead to the development of a novel drug against TB.[5,6] Likewise, glutamine synthetase (GS) has been suggested as one potentially important determinant of *M. tuberculosis* pathogenesis.[7-10] Inhibition of extracellular enzyme activity in *M. tuberculosis* culture, in infected THP-1 cell as well as in in vivo condition of guinea pig model by the substrate analogues, showed the potential of GS as a drug target against TB.[11,12] The 3-dimensional structure of the enzyme has also been extensively studied.[13] Conventionally, GS activity is monitored by biosynthetic as well as transfer assays.[7,14,15] The present study evaluates the kinetic properties of *M. tuberculosis* GS in transfer assay as well as converts it to a robust high-throughput assay for screening of a large, chemically diverse library.

Combichem Bioresource Center, National Chemical Laboratory, Pune, India.

Received Dec 1, 2004, and in revised form Apr 13, 2005. Accepted for publication Apr 24, 2005.

Journal of Biomolecular Screening X(X); 2005
DOI: 10.1177/1087057105278013

MATERIALS AND METHODS

Materials

All the chemicals were obtained from Sigma. Unosphere 6 column matrix was purchased from BioRad. Beckman Coulter platform integrated with Biomek 2000, ORCA Robot, Thermo Forma CO_2 incubator, Shaker, and BMG Polar Star were used to conduct

screening of in-house compounds obtained from natural product fractions using SEP BOX from Sepiatek, Germany.

Purification of GS. The enzyme GS was purified to homogeneity by following a modified method published earlier.[11-13] *Escherichia coli* YMC21E culture was grown in LB medium until 1.2 OD at 600 nm. The fully-grown culture was centrifuged at 2000*g* for 10 min, and the pellet thus obtained was resuspended in 2 ml of buffer (containing 10 mM imidazole pH 7.0, 10 mM $MnCl_2$, 5 mM PMSF, and 5 mM 2-mercaptoethanol) per gram of wet cell pellet. Then the cell suspension was subjected to lysis using a French press until the OD at 600 nm dropped to 90% of the initial value. It was then centrifuged at 10,860*g* for 30 min. The supernatant was treated with 10% streptomycin sulfate by 10% volume of the supernatant and kept for 15 min and then centrifuged at 10,860*g* for 20 min. The supernatant was treated with 1 M acetic acid to a pH 5.15 and kept for 15 min. Again, the same was centrifuged at 10,860*g* for 20 min. The supernatant thus obtained was treated with 100% saturated ammonium sulfate 30% by volume. The pH was adjusted to 4.4 by adding 1 M acetic acid and kept for 15 min. It was at 10,860*g* for 20 min. The pellet was resuspended in 5 ml buffer containing 50 mM Hepes buffer pH 7.2, 10 mM $MnCl_2$, and 0.1 M NaCl centrifuged and dialyzed extensively against the same buffer. The dialyzed was centrifuged as mentioned earlier. The supernatant was subjected to ion exchange chromatography by using a Unosphere 6 column. The protein was loaded in the column equilibrated with a buffer consisting of 10 mM imidazole, 10 mM $MnCl_2$, and 100 mM NaCl. *M. tuberculosis* GS was eluted from the column after applying an isocratic condition with 1.0 M NaCl in the loading buffer. The protein was incubated for 1 min at 80° C. The whole preparation was centrifuged at 10,860*g* for 20 min to remove the precipitate. The supernatant obtained at this stage contains more than 90% pure *M. tuberculosis* GS. The characterization and standardization experiments were carried out using this enzyme preparation. When the preparation was run through a Sepharose HR 6 column, it eluted at 640 kd, indicating dodecamer composition of the protein. The N-terminal sequence of the eluted protein confirmed that it was a glnA1 gene product of *M. tuberculosis* (data not shown). The protein concentration was measured by the Lowry method.[16]

Enzyme assays. A modified procedure was followed to carry out *M. tuberculosis* GS transfer assay as described earlier.[14,15] The reaction was started by adding 400 µM ADP in 2 ml of reaction mixture containing 20 mM imidazole buffer pH 7.0, 60 mM hydroxylamine-HCl pH 7.0, 3 mM $MnCl_2$, 30 mM glutamine, and 20 mM arsenate with sufficient volume of enzyme. In this reaction, hydroxylamine and L-glutamine were used as substrates in the presence of ADP and arsenate and metal ion as cofactors to yield γ-glutamylhydroxamate and ammonia. During enzymatic reaction, an unstable intermediate called γ-glutamyl arsenate is formed. It was proposed that arsenate binds the same site as phosphate in the biosynthetic reaction and attacks glutamine through its oxygen to form the intermediate. Subsequently, hydroxylamine binds the ammonium site and attacks the intermediate already bound on the enzyme surface to release γ-glutamylhydroxamate and ammonia.[14,17] The stop reagent, 0.5 ml, containing $FeCl_3$ (5%), TCA (24%), and HCl (0.6 N), was added to stop the reaction as well as to form the purplish complex between γ-glutamylhydroxamate and $FeCl_3$ in acidic condition.[18] This reaction is being carried out to detect the enzyme activity in crude cell lysate because of its very specific color development, which nullifies the potential of assay artifacts. Incubation of the reaction mixture without ADP served as a blank. The color was monitored at 540 nm in a Cary 50 Bio spectrophotometer.

K_m values were determined using varied concentrations of L-glutamine (5-500 mM), hydroxylamine (0.8-200 mM), ADP (0.5-20 µM), $MnCl_2$ (2-320 µM), and Na_3AsO_4 (1-50 µm), keeping other components at a constant level. A Hanes-Wolf plot was drawn from the data point to find out the K_m values of the respective components.

The final assay mix contained 20 mM imidazole buffer pH 7.0, 300 mM L-glutamine, 20 µM ADP, 60 mM hydroxylamine pH 7.0, 50 µM Na_3AsO_4, and 250 µM $MnCl_2$.

The reaction was started by adding ADP in the reaction mixture and was monitored at 540 nm after addition of stopping reagent. In the classical assay, water was added instead of ADP in the blank. To use the HTS platform more conveniently in the microplate format, EDTA was added in a whole-reaction mix, which serves as a blank. The microplate format assays were carried out using 200 µl reaction mix, and the plates were incubated for 3 h at 25° C followed by addition of 50 µl stopping reagent to develop color. After adding the stopping reagent, the reading was taken using a 520-nm filter in BMG polar star. To calculate the activity, the reading in the blank well (plus EDTA) was subtracted from the control well unless otherwise mentioned. The Z′ factor was determined by following a published procedure.[19] L-methionine S-sulfoximine, a known inhibitor of the enzyme, was used to further validate the assay.[7,10,12] The dose-response curve was plotted by using a varied concentration of the inhibitor ranging from 0.25 to 20 mM in the same assay mix.

Adoption of the protocol to the Beckman Coulter HTS system was done using SAMI software. The program includes the following steps: 1) transfer a set of 3 assay plates containing 5 µl of compound solution of 1.25 mg/ml concentrations from Carousal to Biomek 2000, 2) add 175 µl of reaction mix to all wells, 3) start the reaction by adding 20 µl of ADP, 4) move plates to shaker for 30 s, 5) move the plates to the carousal again for a 3-h incubation at room temperature, 6) move the plates to Biomek 2000 for addition of 50 µl of stopping reagent, 7) move the plates to the BMG Polar Star for reading, and 8) return the plates to Carousal. The program takes 3 h, 33 min, to complete a screening of 12 plates and 5 h, 52 min, for 60 plates.

RESULTS

The purification profile of *M. tuberculosis* GS in *E. coli* strain YMC21E was evidenced from the SDS-PAGE analysis (Fig. 1). This preparation was used for the determination of K_m of all the

Table 1. K_m of Different Substrates and Cofactors of *Mycobacterium tuberculosis* Glutamine Synthetase Transferase Activity

Substrate Used	*K_m Determined*	*K_m Reported*
L-glutamine	60 mM	2.4 mM
ADP	2 µM	?
Mn^{2+}	25 µM	?
Arsenate	5 µM	?
Hydroxylamine	8.3 mM	?

The reaction was carried out with sufficient amount of *Mycobacterium tuberculosis* glutamine synthetase in a reaction mixture having all other components as mentioned in the Materials and Methods section, with varied concentrations of 1) glutamine, 2) hydroxylamine, 3) ADP, 4) arsenate, and 5) Mn^{2+}. In the inset are shown the representative Hanes-Wolf plots drawn using the data obtained from the above-mentioned protocol with varied hydroxylamine (plot I) and L-glutamine (plot II).

substrates and cofactors required in the transfer assay. Hanes-Wolf plots were drawn to find out the K_m values of all the constituents of assay mixture (Table 1). All the components were added at the saturating level with respect to their K_m values to get linearity in activity for a longer period of incubation as well as insensitizing the protocol for competitive inhibitors to be picked up during screening. During this standardization stage, we found that divalent cations (Mg^{++}, Co^{++}, Ca^{++}, and Zn^{++}) were not supporting the enzymatic reaction as reported earlier.[7]

Validation

Linearity of the assay, effect of DMSO, and the inhibition of enzyme activity were monitored to validate the HTS format in a 96-well plate. The activity was monitored for 3 h at 37° C and 25° C, respectively, to check the linearity of assay (Fig. 2). The results indicated that the enzyme activity was found to be linear at least for 3 h at both the temperatures. When the incubation was extended to 5 h at 25° C, the linearity was still maintained (data not shown). Similar results were obtained when experiments were carried out without shaking (data not shown).

To assess the robustness of the assay protocol in microplate format, the Z′ factor as well as signal/noise (S/N) ratio were determined with varying assay volumes and enzyme concentrations (Table 2). It was observed that both the Z′ values as well as the S/N ratio improves with an increase in assay volumes.[19] As 0.5 µg/ml protein in 200 µl was showing the best result, the same was used to carry out subsequent assays. It was noted that the color developed in the final assay mix was stable up to 150 min (data not shown).

The effect of DMSO was checked to decide the volume of compound solution to be used for screening. The results showed that the enzyme activity was not changed significantly even at 10% DMSO concentration (Fig. 3). Mixing of reagents for 30 s on a shaker is required to obtain uniformity in readings (data not shown).

The dose-response effect of L-methionine S-sulfoximine was checked to determine the IC_{50} value in the standardized protocol

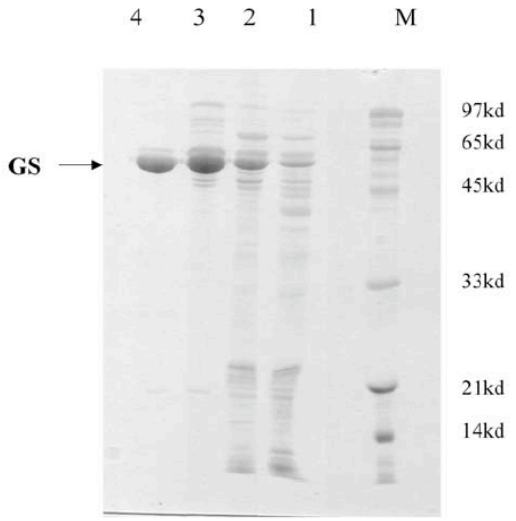

FIG. 1. SDS-PAGE of *Mycobacterium tuberculosis* glutamine synthetase (GS) at different stages of purification. Equivalent amount of proteins were loaded in lanes as follows: 1) crude extract, 2) AS cut, 3) ion exchange chromatography, 4) after heating at 80° C and 5) 6 L marker pro-

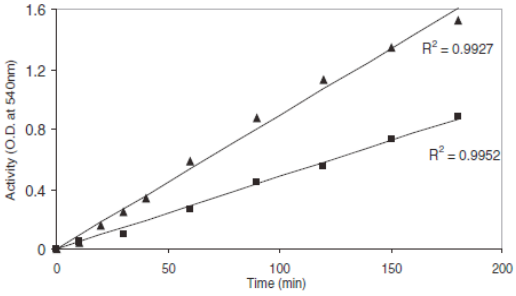

FIG. 2. Time curve of *Mycobacterium tuberculosis* glutamine synthetase (GS) activity 1) at 37° C and 2) at 25° C. The reaction was carried out with 0.5 µg/ml of *M. tuberculosis* GS in a reaction mixture containing 300 mM L-glutamine, 60 mM hydroxylamine pH 7.0, 20 µM ADP, 50 µM sodium arsenate, and 250 µM $MnCl_2$ at pH 7.1 at temperatures of 37° C (▲) and 25° C (■). The experiment was carried out in a final volume of 200 µl in a 96-well microplate as described in the Materials and Methods section. For each, a blank without ADP was carried out simultaneously. The result is the average of 3 identical experiments.

(Fig. 4). The IC_{50} value obtained was 3 mM using a modified protocol. The plate assay also showed an almost similar result as the tube assay, indicative of true adoption of the assay in plate format. When the assay protocol was run on the Beckman Coultier HTS system, it was found that the system would take 3 h, 33 min, for 12 plates. The utilization time for 60 plates using the same program

Table 2. Determination of Signal/Noise Ratio and Z′ Factor from 96-Well Plate Format Assays Done at Different Volumes

	Assay Volume					
	Z′ Factor			*Signal/Noise Ratio*		
Protein Concentration (µg/ml)	*100 µl*	*150 µl*	*200 µl*	*100 µl*	*150 µl*	*200 µl*
0.25	0.71 ± 0.034	0.91 ± 0.019	0.91 ± 0.012	3.2 ± 0.098	5.23 ± 0.088	6.68 ± 0.066
0.50	0.86 ± 0.023	0.93 ± 0.014	0.92 ± 0.011	6.26 ± 0.066	10.19 ± 0.076	12.17 ± 0.092

The reaction was carried out with the indicated amount of protein in a reaction mixture containing 20 mM imidazole pH 7.0, 300 mM L-glutamine, 60 mM hydroxylamine pH 7.0, 20 µM ADP, 50 µM sodium arsenate, and 250 µM $MnCl_2$ at 25° C in a 96-well plate for 3 h. The rest are described in the Materials and Methods section. The result is an average of 3 identical experiments.

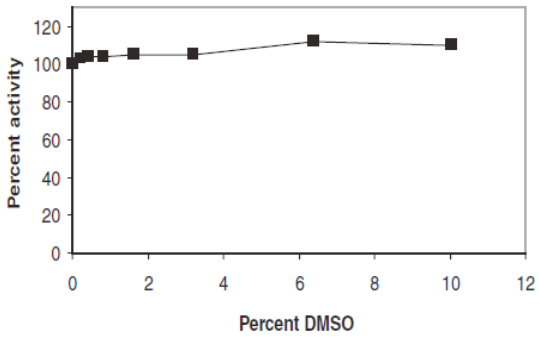

FIG. 3. Effect of DMSO on *Mycobacterium tuberculosis* glutamine synthetase. The DMSO concentrations were varied, as indicated in the reaction mixture that contained otherwise all the components mentioned in Figure 2, and incubated at 25° C for 3 h. The result is the average of 3 identical experiments.

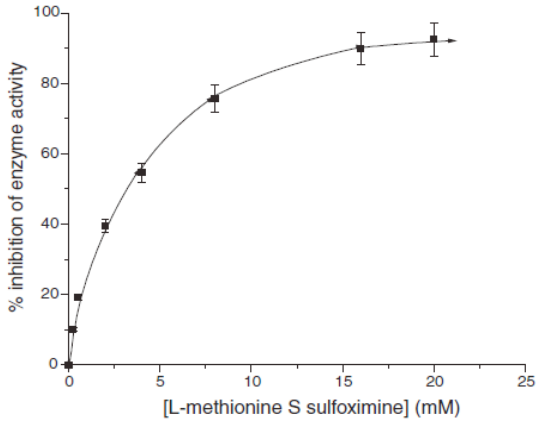

FIG. 4. Dose-response curve for L-methionine S-sulfoximine. L-methionine S-sulfoximine concentrations were varied, as indicated (0.25-20 mM) in the reaction mixture that contained otherwise all the components described in Figure 2, and incubated at 25° C for 3 h. The result is an average of 3 identical experiments.

would take 5 h, 52 min, as indicated by SAMI software (data not shown).

DISCUSSION

A colorimetric assay for HTS is advantageous if the development of color takes place instantaneously and remains stable for a substantial period of time. Among the transfer and biosynthetic reactions of GS, the former was selected for further study for the development of assay format to HTS due to the fast and stable color formation of the assay mixture, which brings flexibility and convenience in screening programs. In addition to GS's playing a major role in *M. tuberculosis* pathogenicity, this enzyme is also found to be associated with certain human brain disorders.[20,21] Considering the possibility of GS's becoming a target in the future and developing new molecules against those diseases, we attempted to provide a screening solution. A simple assay in a 96-well format for HTS of *M. tuberculosis* GS was developed by modifying a classical assay used earlier to check the enzyme activity in crude cell extract.[14] The developed assay is robust and meets all the stringent HTS criteria. The HTS criteria considered here are 1) linearity of enzyme activity for more than 3 h, 3) DMSO tolerance, 3) reproducible IC_{50} value for the standard inhibitor, and 4) robustness of the assay protocol (Figs. 2-4, Table 2). The results indicated that the Z′ factor alone is not sufficient for considering the robustness of the assay protocol; the S/N value is also very important. Therefore, along with the quality of the enzyme, optimum concentrations of the reagents and assay volume play important roles in obtaining a better S/N value. The high acidity of the stopping solution in this assay reduces the interference of colored compounds, except for a few, such as tannins.[22]

The present assay was developed using purified recombinant GS, and the composition of the assay mix was optimized based on its K_m values (Fig. 1, Table 1). The K_m value for L-glutamine of the *E. coli* enzymes was also determined and found that it is giving almost the same value as mentioned earlier[14] (data not shown). This proves the authenticity of our K_m data as well. An S/N ratio of ~10 was obtained using these optimized assay conditions (Table 2). A limited attempt was made earlier to determine the better inhibitor against this enzyme from structural analogues of L-glutamine.[18] Because of the allosteric nature of *M. tuberculosis* GS, apart from the picking up of competitive inhibitors, there are possibilities to pick up compounds with uncompetitive, noncompetitive, and

allosteric inhibitors of the enzyme using this high-throughput assay and diverse chemical library. We have successfully screened ~617 natural product fractions, 20 synthetic compounds, and 7 standard antibiotics including rifampicin. The results did not show any plate or distribution effect (data not shown). Further screening is presently under way in our laboratory.

ACKNOWLEDGMENTS

We are thankful to the director of the National Chemical Laboratory, Pune, Indiam for providing financial assistance through an in-house project. We are also thankful to Dr. D. Eisengberg, University of California, Los Angeles, for providing the *E. coli* clone YMC21E of *M. tuberculosis* GS as a gift.

REFERENCES

1. Kochi A: The global tuberculosis situation and the new control strategy of the World Health Organization. *Tubercle* 1991;72:1-6.
2. Dye C, Scheele S, Dolin P, Pathania V, Raviglione MC: Consensus statement: global burden of tuberculosis estimated incidence, prevalence and mortality by country. WHO Global Surveillance and Monitoring Project. *JAMA* 1999;282:677-686.
3. Barnes P, Blotch AD, Davidson BT, Snyder Jr DE: Tuberculosis in patients with immunodeficiency virus syndrome. *N Engl J Med* 1991;324:1644-1650.
4. Rattan A, Kalia A, Ahmed N: Multidrug-resistant *Mycobacterium tuberculosis*: molecular perspectives. *Emerg Infect Dis* 1998;4(2):195-209.
5. Wayne LG, Sohaskey CD: Nonreplicating persistence of *Mycobacterium tuberculosis*. *Annu Rev Microbial* 2001;55:139-163.
6. Khasnobis S, Escuyer VE, Chatterjee D: Emerging therapeutic targets in tuberculosis: post-genomic era. *Expert Opin Ther Targets* 2002;6(1):21-40.
7. Hearth G, Clemens DL, Horwitz MA: Glutamine synthetase of *Mycobacterium tuberculosis*: extracellular release and characterization of its enzymatic activity. *Proc Natl Acad Sci U S A* 1994;91:9342-9346.
8. Raynaud C, Etienne G, Payron P, Lanelle MA, Daffe M: Extracellular enzyme activities potentially involved the pathogenicity of *Mycobacterium tuberculosis*. *Microbiology* 1998;144:577-587.
9. Hearth G, Zamecnik PC, Tang JY, Tabatadze D, Horwitz MA: Treatment of *Mycobacterium tuberculosis* with antisense oligonucleotides to glutamine synthetase mRNA inhibits glutamine synthetase activity, formation of the poly-L-glutamate/glutamine cell wall structure, and bacterial replication. *Proc Natl Acad Sci U S A* 2000;97:418-423.
10. Harth G, Horwitz MA: An inhibitor of exported *Mycobacterium tuberculosis* glutamine synthetase selectively blocks the growth of pathogenic mycobacteria in axenic culture and in human monocytes: extracellular proteins as potential as potential novel drug targets. *J Exp Med* 1999;189(9):1425-1435.
11. Tullius MV, Harth G, Horwitz MA: Glutamine synthetase GlnA1 is essential for growth of *Mycobacterium tuberculosis* in human THP-1 macrophages and guinea pigs. *Infect Immun* 2003;71(7):3927-3936.
12. Hearth G, Horwitz MA: Inhibition of *Mycobacterium tuberculosis* glutamine synthetase as a novel antibiotic strategy against tuberculosis: demonstration of efficacy in vivo. *Infect Immun* 2003;71(1):456-464.
13. Gill HS, Pflucgel GMU, Eisenberg D: Multicopy crystallographic refinement of a relaxed glutamine synthetase from *Mycobacterium tuberculosis* highlights flexible loops in the enzymatic mechanism and its regulation. *Biochemistry* 2002;41:9863-9872.
14. Wollfolk CA, Shapiro B, Stadtman ER: Regulation of glutamine synthetase: I. Purification and properties of glutamine synthetase from *Escherichia coli*. *Arch Biochem Biophys* 1966;116:177-192.
15. Shapiro BM, Stadtman ER: Glutamine synthetase (*Escherichia coli*). *Methods Enzymol* 1970;17a:910-922.
16. Lowry OH, Rosebrough NJ, Farr AL, Randall RJ: Protein measurement with Folin phenol reagent. *J Biol Chem* 1951;193:265-275.
17. Eisenberg D, Gill SH, Pfluegl GMU, Rotstein SH: Structure-function relationships of glutamine synthetase. *Biochemica et Biophysica Acta* 2000;1477:122-145.
18. Lipmann F, Tuttle CL: A specific micro method for the determination of acyl phosphatase. *J Biol Chem* 1945;159:21.
19. Zhang JH, Chung TDY, Oldenburg KR: A simple statistical parameter for use in evaluation and validation of high throughput screening assays. *J Biomol Screen* 1999;4:67-73.
20. Gunnersen D, Haley B: Detection of glutamine synthetase in the cerebrospinal fluid of diseased patients: a potential diagnostic biochemical marker. *Proc Natl Acad Sci U S A* 1992;89:11949-11953.
21. Tumani H, Shen GQ, Peter JB, Bruck W: Glutamine synthetase in cerebrospinal fluid, serum and brain: a diagnostic marker for Alzheimer disease. *Arch Neurol* 1999;56:1241-1246.
22. Carter JM: *A Guide to Assay Development*. Westborough, MA: D & MD; 2003.

Address reprint requests to:@RR = *Dhiman Sarkar, Ph.D.*
Combi Chem-Bio Resource Center
National Chemical Laboratory
Dr. Homi Bhabha Rd.
Pune 411008, India

E-mail: dsarkar@dalton.ncl.res.in

Journal of Biomolecular Screening
http://jbx.sagepub.com

Development of a Simple High-Throughput Screening Protocol Based on Biosynthetic Activity of Mycobacterium tuberculosis Glutamine Synthetase for the Identification of Novel Inhibitors

Upasana Singh and Dhiman Sarkar

J Biomol Screen 2006; 11; 1035 originally published online Sep 14, 2006;
DOI: 10.1177/1087057106292798

The online version of this article can be found at:
http://jbx.sagepub.com/cgi/content/abstract/11/8/1035

Published by:
SAGE
http://www.sagepublications.com

On behalf of:
SBS
Society for Biomolecular Sciences

Development of a Simple High-Throughput Screening Protocol Based on Biosynthetic Activity of *Mycobacterium tuberculosis* Glutamine Synthetase for the Identification of Novel Inhibitors

UPASANA SINGH and DHIMAN SARKAR

A high-throughput screening protocol has been developed for *Mycobacterium tuberculosis* glutamine synthetase by quantitative estimation of inorganic phosphate. The K_m values determined at pH 6.8 are 22 mM for L-glutamic acid, 0.75 mM for NH_4Cl, 3.25 mM for $MgCl_2$, and 2.5 mM for adenosine triphosphate. The K_m value for glutamine is affected significantly by the increase in pH of assay buffer. At the saturating level of the substrate, the enzyme activity at pH 6.8 and 25° C is found to be linear up to 3 h. The reduction of enzyme activity is negligible even in presence of 10% DMSO. The Z′ factor and signal-to-noise ratio are found to be 0.75 and 6.18, respectively, when the enzyme is used at 62.5 μg/ml concentration. The IC_{50} values obtained at pH 6.8 for both L-methionine S-sulfoximine and DL-phosphothriacin are 500 μM and 30 μM, respectively, which is lowest compared to the values obtained at other pH levels. The Beckman Coulter high-throughput screening platform was found to take 5 h 9 min to complete the screening of 60 plates. For each assay plate, a replica plate is used to normalize the data. Screening of 1164 natural product fractions/extracts and synthetic molecules from an in-house library was able to identify 12 samples as confirmed hits. Altogether, the validation data from screening of a small set of an in-house library coupled with Z′ and signal-to-noise values indicate that the protocol is robust for high-throughput screening of a diverse chemical library. (*Journal of Biomolecular Screening* 2006:1035-1042)

Key words: glutamine synthetase, biosynthetic activity, high-throughput screening, *Mycobacterium tuberculosis*, Beckman Coulter

INTRODUCTION

THE WORLD HEALTH ORGANIZATION has estimated that *Mycobacterium tuberculosis* is the single infectious agent that causes about 2 to 3 million deaths annually.[1] Every 10 s, 1 person dies of tuberculosis.[2] One third of the world's population is latently infected by the pathogen without any symptoms of the diseases but has the possibility for the infection to be reactivated any time in their life.[3] In some parts of the world, the proportion of the multidrug-resistant strains has been increasing alarmingly.[4] HIV-infected patients are particularly susceptible to *M. tuberculosis*.[5] In the past 40 years, no new drug has been discovered for combating tuberculosis.[6] There is an urgent medical need to discover and develop novel therapeutic agents against *M. tuberculosis*.

Inhibitors of some of the targets that have been suggested in the recent literature might lead to the development of novel drugs against the pathogen.[7-13] Glutamine synthetase is one such target for the disease.[14-19] Extracellular glutamine synthetase is an essential enzyme for the survival of *M. tuberculosis*.[15-19] This enzyme is secreted by all pathogenic mycobacteria. It is suggested that this extracellular enzyme functions in the regulation of ammonia in the phagosomal compartment as well as synthesis of the cell wall component.[17] Inhibition of extracellular enzyme activity in *M. tuberculosis* culture, in infected THP-1 cells as well as in the in vivo condition of the guinea pig model by the substrate analogs, showed the potential of glutamine synthetase as a drug target against tuberculosis.[19] The 3-dimensional structure of the enzyme has also been extensively studied.[20-22] Conventionally, glutamine synthetase activity is monitored through biosynthetic as well as transfer assays.[23,24] A high-throughput assay has already been developed based on transfer activity.[23] The components involved in biosynthetic activity are different from the components

Combi Chem-Bio Resource Center, National Chemical Laboratory, Pune, India.

Received Mar 2, 2006, and in revised form Jul 9, 2006. Accepted for publication Jul 11, 2006.

Journal of Biomolecular Screening 11(8); 2006
DOI:10.1177/1087057106292798

of transfer activity of the enzyme.[23,24] The enzyme participates in biosynthetic activity only under in vivo conditions in which L-glutamic acid, ammonia and adenosine triphosphate (ATP) participate as substrates to generate L-glutamine, adenosine diphosphate (ADP), and Pi.[23,24] So, even though L-methionine S-sulfoximine and DL-phosphothriacin inhibit the activities of the enzyme, finding true inhibitors for in vivo efficacy could become very difficult if they are picked up by screening using the transfer assay.[23] Development of a high-throughput screening (HTS) assay protocol based on biosynthetic activity of the enzyme for identifying novel chemical structure against *M. tuberculosis* has immense importance in the current situation.

The present study evaluates the kinetic properties of *M. tuberculosis* glutamine synthetase in biosynthetic activity as well as converts it to a robust high-throughput assay protocol for screening of a chemically diverse synthetic and natural product library.

MATERIALS AND METHODS

Materials

All the chemicals were obtained from Sigma. A Beckman Coulter platform integrated with Biomek 2000, ORCA Robot, Thermo Forma CO_2 incubator, Shaker and BMG POLARStar was used to conduct screening of an in-house library obtained from natural product fractions using SEP BOX from Sepiatek, Germany, and synthetic compounds from an in-house depository. A Cary 50 Bio Spectrophotometer was used to carry out the initial standardization of biosynthetic experiments.

Purification of the enzyme

The enzyme was purified from recombinant *Escherichia coli* strain YMC21E by using a modified method.[23] The enzyme preparation was used for further standardization and characterization of the enzyme for biosynthetic activity of the enzyme as well as development of the HTS screening protocol.

Transfer assay

The monitoring of γ-glutamylhydroxamate production due to the conversion of L-glutamine and hydroxylamine by glutamine synthetase is called a transfer assay. The transfer assay was carried out to check the enzyme activity in crude extract using 20 mM imidazole buffer pH 7.0, 300 mM L-glutamine, 60 mM hydroxylamine, 20 µM ADP, 50 µM $NaAsO_4$, and 250 µm $MnCl_2$. The stop reagent, containing $FeCl_3$ (5%), TCA (24%), and HCL (0.6 N), was added to stop the reaction as well as to form the purplish complex between γ-glutamylhydroxamate and $FeCl_3$ in the acidic condition.[23]

Biosynthetic assay

A modified protocol was followed to carry out *M. tuberculosis* glutamine synthetase biosynthetic assay, as described earlier.[24] The reaction was started by adding 7.6 mM of ATP in 200 µl of reaction mixture containing 20 mM imidazole buffer pH 7.0, 100 mM L-glutamic acid, 50 mM $MgCl_2$, 50 mM NH_4Cl, and sufficient amount of enzyme in a test tube. In this reaction, ammonium chloride, L-glutamic acid, and ATP were used as substrate and Mg^{2+} ion as a cofactor to yield inorganic phosphate, glutamine, and ammonia. In the modified protocol, to stop the reaction, 12% w/v L-ascorbic acid in 1 N HCL and 2% w/v ammonium molybdate in ddH_2O were mixed in a 2:1 proportion, and 600 µl of that was added to 200 µl of reaction mixture and mixed well to develop a blue color immediately.[25] It was incubated for 7 min to get the fully developed color. After that, 600 µl of 1% sodium citrate tribasic dihydrate in 1% acetic acid in ddH_2O was added to the reaction mixture to restrict the further development of color due to hydrolysis of ATP.[25] Incubation of the reaction mixture with 22.5 mM EDTA served as the blank. A Cary 50 Bio Spectrophotometer was used to monitor the color at 655 nm after a 30-min incubation.

At pH 6.8, K_m values for substrates were determined in 50 mM HEPES buffer in the presence of 62.5 µg/ml of enzyme using increasing concentrations of L-glutamic acid (4.0 to 256 mM) and ammonium chloride (0.25 to 16.0 mM), respectively, keeping magnesium chloride (25 mM) and ATP (7.6 mM) at the saturating level. Similarly, the K_m values of L-glutamic acid and ammonium chloride were determined in Tris-acetate buffer pH 6.5 using increasing concentrations from 16 to 256 mM and 0.03125 to 4.0 mM, respectively, keeping magnesium chloride (70 mM) and ATP (4 mM) at the saturating level. We observed that Tris-acetate buffer does not have any significant effect on enzyme activity. At pH 7.5, when the concentrations of L-glutamic acid and ammonium chloride were varied from 2 to 256 mM and 0.5 to 32 mM, respectively, the concentrations of magnesium chloride (25 mM) and ATP (15 mM) were kept at the saturating level in 50 mM HEPES buffer. For the determination of K_m values at pH 8.0, varying concentrations of L-glutamic acid and ammonium chloride were used from 25 to 1000 mM and 0.25 to 16 mM at the saturating level of magnesium chloride (25 mM) and ATP (10 mM) in HEPES buffer. A Hanes-Wolf plot was drawn to find the K_m values of the respective components separately at all 4 different pH levels, as mentioned above. Considering the physiological relevance and determined K_m values, it was decided that a pH level of 6.8 would be used for further development of screening protocol.

The final assay mix contained 50 mM HEPES buffer pH 6.8, 220 mM L-glutamic acid (pH adjusted to 6.8), 7.5 mM NH_4Cl, 32.5 mM $MgCl_2$, and 62.5 µg/ml enzyme. The reaction was started by adding 7.6 mM ATP (pH adjusted ~ 6.8) in the reaction mixture and incubated for 2 h at 25° C. Adding stop reagent terminated the reaction, and citrate was added within 10 min. The whole mixture was kept at room temperature for another 30 min prior to reading the color using a 620-nm filter.

HTS protocol

The assay plates were made by adding 5 µl of samples in DMSO at 10 mg/ml concentration to the respective wells

according to the following plate map. Five microliters of DMSO was added to the control and blank wells. Five microliters of 420 mM EDTA was added in the blank wells. The same volume of water was added to the other wells, and then 80 µl of the reaction mix was added to all the wells. The plate was kept on the shaker for 2 min for proper mixing. Then, 10 µl of 76 mM working solution of ATP was added to all wells to start the reaction. After incubation, 75 µl stop reagent was added and allowed to develop the color for approximately 7 min. The reading was taken after 30 min of the addition of 75 µl sodium citrate in the reaction mix using 620-nm filters in the BMG POLARStar. The Z′ factor was determined by following a published procedure.[26] L-methionine S-sulfoximine and DL-phosphothriacin are 2 known inhibitors that were used to further validate the assay. Using a varied concentration of the inhibitor ranging from 0.125 mM to 5 mM, dose-response curves were plotted at the different pH levels mentioned earlier. A total of 1070 natural products and 94 synthetic compounds including 7 standard antibiotics including rifampicin were screened as single-point data using 0.5 mg/ml concentrations in the final assay mix.

Adoption of the protocol to the Beckman Coulter HTS system was done using SAMI software. The program includes the following steps: 1) transfer of a set of 3 assay plates containing 5 µl of compound solutions of 10 mg/ml concentration DMSO/EDTA/water from the carousel to Biomek 2000, 2) addition of 80 µl of reaction mix to all wells, 3) starting the reaction by adding 10 µl of ATP, 4) moving the plates to the shaker for 30 s, 5) moving the plates to the carousal again for a 2-h incubation at room temperature, 6) moving the plates to Biomek 2000 for an addition of 75 µl of stop reagent, 7) moving the plates to the BMG POLARStar for reading, and 8) returning the plates to the carousel.

Replica plate

The library consists of plant extracts and fractions, many of which are colored and interfere with the readings obtained in the assay plate. It becomes very difficult to identify the real inhibitors from the screening data. To get the readings in assay plates corrected for the color interference, the same screening is carried out with an identical plate map and other conditions except the addition of inhibitors. The inhibitors in the replica plate are added after the reaction is terminated. For presenting the data, the plate reader needs to have a template assigned with blank, control and sample for the respective wells mentioned in the plate map. After reading the plate, the values for each well are shown after deducting the average value obtained from blank wells. The reading from the replica plate is used to normalize the reading, obtained in the corresponding assay plate. The following formula is used to estimate the inhibition by the sample:

$$\text{Percent inhibition} = 100 - \frac{[(S)_A - \{(C)_R - (S)_R\}]}{(C)_A} \times 100, \quad (1)$$

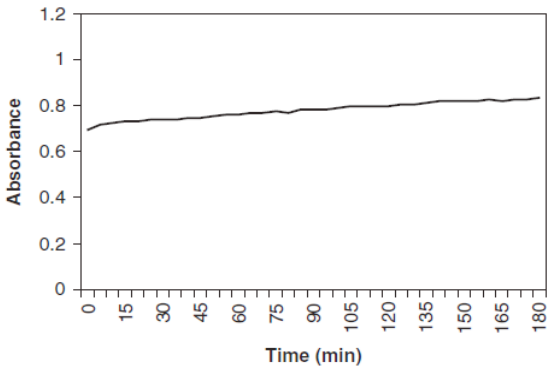

FIG. 1. Kinetics of color development in the assay mix. Stability profile of the color developed in the final reaction mix. The reaction was carried out with 62.5 µg/ml of *Mycobacterium tuberculosis* glutamine synthetase in a reaction mixture containing 220 mM glutamic acid, 7.5 mM ammonium chloride, 7.6 mM adenosine triphosphate, and 25 mM magnesium chloride at pH 6.8, as described in "Materials and Methods." The development of color was monitored at 655 nm up to 45 min at the interval of 2 min by using a Cary 50 Bio Spectrophotometer.

where $(S)_A$ is the sample reading in the assay plate, $(S)_R$ is the sample reading in the replica plate, $(C)_R$ is the reading of the control in the replica plate, and $(C)_A$ is the reading of the control in the assay plate.

RESULTS

Rapid development and stability of color are considered the most valuable aspects in accepting any absorbance-based assay principle for developing a high-throughput assay protocol. The colorimetric estimation of phosphate typically involves the interaction of phosphate, molybdate, and reducing agents or dyes to produce a colored complex.[25] The reduction of the phosphomolybdate complex in a strong acid solution results in a formation of molybdenum blue. Numerous assays for quantitating phosphate, based on this reaction, have been developed with varying sensitivities and applications, mainly by altering the nature of the reducing agent.[27] Similarly, in the glutamine synthetase biosynthetic assay, ferrous sulfate was used conventionally as a reducing agent for Pi detection.[24] The crux of the assay system was a continuous increase in color due to the hydrolysis of ATP.[25] The major objective during the development of the screening protocol was to control the rate of ATP hydrolysis as well as to increase the sensitivity range with respect to Pi concentration. In this protocol, the reducing agent was changed from $FeSO_4$ to ascorbic acid for rapid development of color in a highly acidic condition. Once the color was developed, sodium citrate was used to control the hydrolysis of ATP. In this process, the increase in color was confined to a negligible extent of 3% to 4% up to 50 min after the addition of sodium citrate in the reaction mix (**Fig. 1**).

Table 1. Mean ± SD K_m Values Obtained for the Respective Substrates and Cofactors at Different pH Levels

	Estimated K_m (mM)			
Assay pH	*L-Glutamic Acid*	*Ammonium Chloride*	*Magnesium Chloride*	*Adenosine Triphosphate*
6.5	29 ± 1.41	0.21 ± 0.034	7.5 ± 0.047	0.026 ± 0.026
6.8	22 ± 1.4	0.75 ± 0.017	3.25 ± 0.35	2.5 ± 0.106
7.5	36 ± 2	0.75 ± 0.017	6 ± 0.70	2.6 ± 0.26
8.0	165 ± 2.1	1 ± 0.028	2.5 ± 0.033	4.5 ± 0.036

As described in the "Materials and Methods" section. The ±standard deviation and K_m values are obtained from 3 identical experiments.

Recently, it was clearly shown that the K_m values for all the components of *M. tuberculosis* glutamine synthetase participating in the transfer assay are higher than for other bacterial enzymes.[23] The enzyme obtained from other bacterial sources characteristically depends on Mg^{2+} for its biosynthetic activity and mainly on Mn^{2+} for the transfer activity.[24] An earlier report on the enzyme activity purified from extracellular medium of *M. tuberculosis* culture indicated that the optimum pH levels for biosynthetic and transfer activities are 7.5 and 7.0, respectively.[15] To get a broader picture of the pattern of substrates and cofactor use by this recombinant *M. tuberculosis* glutamine synthetase, the K_m values were determined at 4 different pH levels ranging from 8.0 to 6.5 (**Table 1**).

The enzyme was purified from recombinant *E. coli* strain YMC21E by following an earlier published method.[23] More than 90% pure enzyme was used for the determination of K_m of all the substrates and cofactor required in the biosynthetic assay (**Fig. 2**). Hanes-Wolf plots were drawn to find the K_m values of all the constituents of assay mixture. The results indicated that the affinity for both L-glutamic acid and ATP is highest at pH 6.8. The K_m for other constituents remained within a narrow range with respect to pH, ranging from 6.8 to 8.0. As the pH dropped further to 6.5, the most significant change observed was the dramatic decrease in K_m values of ATP (**Table 1**). Otherwise, the K_m values for L-glutamic acid and $MgCl_2$ started increasing again when the pH was changed from 6.8 to 6.5. Biosynthetic activity of *M. tuberculosis* glutamine synthetase is not supported by any other metal ions except Mg^{2+} (data not shown).

Validation

Linearity of the assay, effect of DMSO, and the inhibition of enzyme activity were monitored to validate the HTS format in a 96-well plate. The activity was monitored for 3 h at 37° C and 25° C, respectively, to check the linearity of the assay (**Fig. 3A**). The results indicated that the enzyme activity was found to be linear at least for 3 h at 25° C and for only 60 min at 37° C.

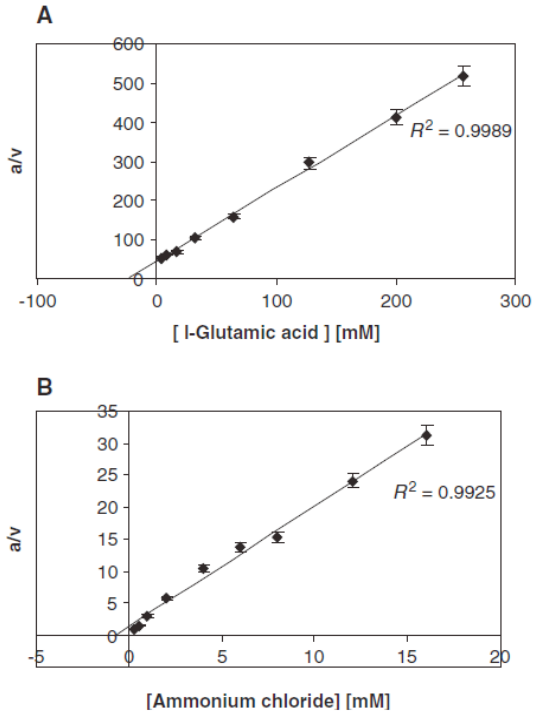

FIG. 2. K_m values determined for different substrates and cofactors of *Mycobacterium tuberculosis* glutamine synthetase in biosynthetic activity at different pH levels. All the experiments were carried out using 62.5 µg/ml of *M. tuberculosis* glutamine synthetase as mentioned in the "Materials and Methods" section. (**A**) Hanes-Wolf plots of initial velocity pattern were drawn for the biosynthetic reaction with varied L-glutamic acid from 4 mM to 256 mM at pH 6.8, keeping ammonium chloride (8 mM), adenosine triphosphate (ATP; 7.6 mM), and magnesium chloride (25 mM) at the saturating level. (**B**) Varying concentrations of ammonium chloride from 0.25 mM to 16 mM were used at the saturating level of L-glutamic acid (220 mM), ATP (7.6 mM), and magnesium chloride (25 mM).

To assess the robustness of the assay protocol in microplate format, the Z′ factors as well as signal-to-noise (S/N) ratios were determined with varying enzyme concentrations (**Table 2**). The results clearly indicated that the enzyme activity was linearly increasing with respect to enzyme concentration in the assay mix. As 62.5 µg/ml protein in 100 µl volume showed the best results with respect to Z′ factor and S/N ratio, the same was used to carry out the screening protocol.

The effect of DMSO was checked to decide the volume of compound solution to be used for screening. The results showed that the enzyme activity was not changed significantly even at 10% DMSO concentration (**Fig. 3B**). Mixing of reagents for 30 s on a shaker was required to obtain uniformity in readings (data not shown).

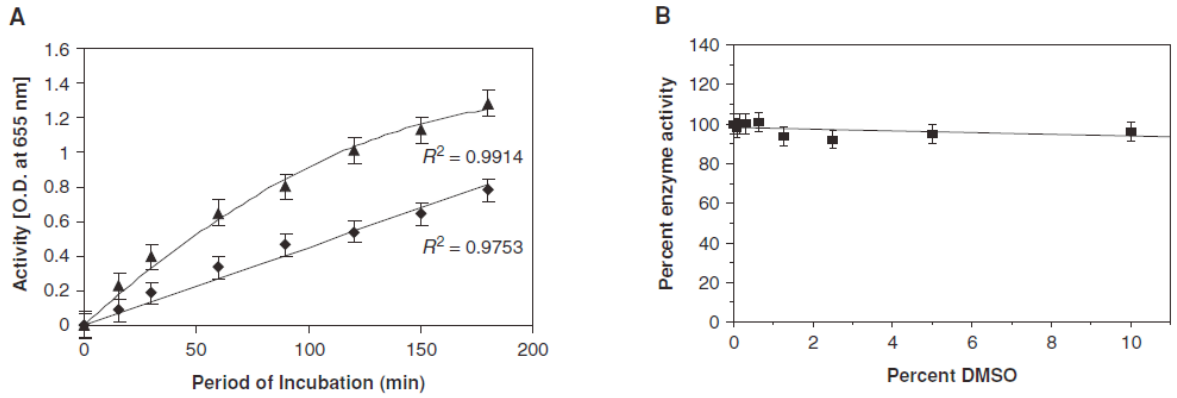

FIG. 3. Time curve of *Mycobacterium tuberculosis* glutamine synthetase activity and effect of DMSO on *M. tuberculosis* glutamine synthetase. The reaction was carried out at pH 6.8 with 100 µl of reaction mix containing 62.5 µg/ml of the enzyme and all other components at saturating level. (**A**) The line obtained at 37° C (▲) is following a nonlinear equation, whereas at 25° C (■), it is linear up to 2 h. (**B**) The DMSO tolerance was checked up to 10% in identical experimental conditions as mentioned above. The results for each data point in both the experiments were obtained from 8 identical wells. The plots are representative of 3 such identical experiments.

Table 2. Determination of the Signal-to-Noise (S/N) Ratio and Z′ Factor for Different Enzyme Concentrations Used in High-Throughput Format

Protein Concentration (µg/ml)	*Z′ Factor*	*S/N Ratio*
10.4	0.43 ± 0.066	2.26 ± 0.017
20.8	0.27 ± 0.074	3.37 ± 0.013
41.66	0.58 ± 0.120	4.30 ± 0.016
62.5	0.75 ± 0.031	6.18 ± 0.019

The reaction was carried out with a different amount of the enzyme in reaction mixture containing 50 mM HEPES buffer pH 6.8, 220 mM L-glutamic acid (pH adjusted to 6.8), 7.5 mM ammonium chloride, 25 mM magnesium chloride, and 7.6 mM adenosine triphosphate (pH adjusted to 6.8) at 25° C in a 96-well plate for 2 h as mentioned in **Figure 3**. The results are the average of 3 identical experiments and ±standard deviation.

The dose-response effect of L-methionine S-sulfoximine and phosphothriacin was checked to find IC_{50} values at pH 6.5, 6.8, 7.5, and 8.0 (**Fig. 4A, B**). The IC_{50} values obtained for both L-methionine S-sulfoximine and DL-phosphothriacin were found to be 500 µM and 30 µM, respectively, at pH 6.8. When the assay was carried out at pH 7.5 and 8.0, respectively, using all the components of the assay mix with respect to their K_m values, the IC_{50} values increased with pH (**Table 3**). This indicated that the affinities of the standard inhibitors are higher at pH 6.8 and that the increased sensitivity could be helpful in identifying even weak inhibitors from random screening. Both the plate and tube assay have shown an almost similar result, which is indicative of true adoption of the assay in plate format.

A chemically diverse library consisted of extract/fractions from medicinal plants as well as synthetic compounds. These samples were often poorly soluble in aqueous phase or interfered with the absorbance or fluorescence of the analyte in the reaction mixture. To avoid this type of color interference, another plate with an identical plate map was used in which the compound was added at the end of the reaction before taking the readout. This calculation makes it very easy to pick up the actives from the natural product/synthetic library with better estimation of the inhibition profile (equation 1). When the assay protocol was run on the Beckman Coulter HTS system, it was found that the system would take 2 h 47 min for 12 plates. The utilization time for 30 assay and replica plates, each using the same program, was 5 h 9 min, as indicated by SAMI software (data not shown).

The inhibition profile obtained from the assay plates after screening 1164 samples was corrected by using the data from replica plates and using a formula (equation 1). The inhibition data for all compounds are shown as a scatter plot with regard to the respective compounds (**Fig. 5A**). The major reason for selecting 500 µg/ml concentrations of the samples for screening is the varied composition of the active ingredient in the crude extracts and fractions obtained from medicinal plants. Even after use of a 500 µg/ml concentration, most of the compounds belong in the range in which negligible affect is observed. The result clearly justified the use of such high concentrations of samples in screening the assay. The histogram of the same data confirmed the earlier observation as well as the robustness of the screening protocol (**Fig. 5B**). Of 1164 samples screened, only 29 showed greater than 40% inhibition. The confirmation experiment was carried out using a fresh stock solution of the hits obtained from the primary screen, and 12 samples of the 29 hits were identified as confirmed hits.

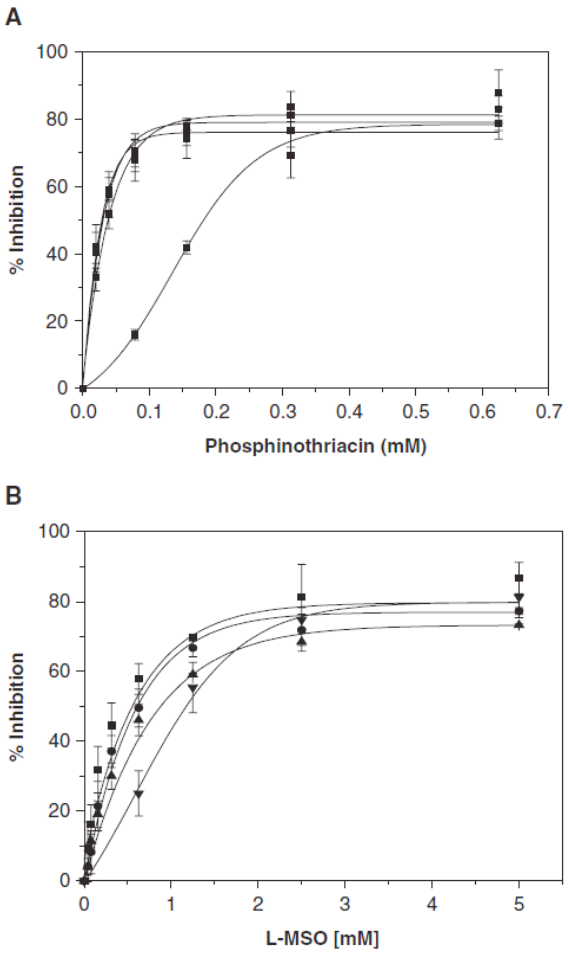

FIG. 4. Dose-response effect of inhibitors on biosynthetic activity of *M. tuberculosis* glutamine synthetase. Varied concentrations of (**A**) L-methionine S-sulfoximine and (**B**) phosphinothricin ranging from 0.25 to 5.0 mM were incubated with 62.5 µg/ml of the enzyme at 25° C for 15 min. Then, the reaction was carried out using all the components at saturating level with respect to pH as mentioned in the "Materials and Methods" section.

Table 3. Means ± Standard Deviations of IC_{50} Values Obtained for Inhibitors at Respective pH Levels

	IC_{50} Values	
Assay pH	*L-Methionine S-Sulfoximine (mM)*	*Phosphinothricin (µM)*
6.5	1.25 ± 0.11	200 ± 3.1
6.8	0.5 ± 0.04	30 ± 3.5
7.5	0.6 ± 0.05	50 ± 3.8
8.0	0.8 ± 0.08	60 ± 4.2

The results are representative of 3 identical experiments, and the ±standard deviation values are as described in **Figure 3**.

DISCUSSION

The major challenge in the biosynthetic assay was to substantially protect the rapid increase in color due to ATP hydrolysis under the reaction conditions used. It was clearly shown in this study that addition of citrate in the assay mix blocked a further increase in color development (**Fig. 1**). Many coupled assays previously designed to carry out screening of chemical libraries are ineffective because of mainly the inability to stop this continuous increase in color.[28] In earlier studies, it was reported that the activity of this enzyme from other bacterial sources was seen to be optimum at pH 7.5.[24] We have clearly shown that for the *M. tuberculosis* enzyme, the affinities for the substrates are highest at the pH range of 6.8 to 6.5 (**Table 1**). The optimum enzyme activity at pH 6.8 supports its physiological relevance for the extracellular function of the enzyme. So the screening of a chemical library on biosynthetic activity at pH 6.8 has a better prospect to get a mycobacterial glutamine synthetase inhibitor than at any other higher pH. The results also indicated that the assay protocol is robust for HTS (**Table 2**).

The HTS criteria considered here were 1) linearity of enzyme activity for more than 2 h (**Fig. 3A**), 2) DMSO tolerance (**Fig. 3**), and 3) reproducibility of the IC_{50} value for the standard inhibitor (**Fig. 4A, B**). The assay protocol was needed to successfully overcome 1 more validation step using a library consisting mainly of extracts and fractions from medicinal plants along with synthetic compounds. It was observed that many samples from natural products and synthetic libraries consist of colored molecules with poor solubility in aqueous solution. These samples caused interference in the readout during screening and increased the number of false positives and false negatives. To overcome this bottleneck, replica plates were used to obtain more accurate estimates about the interference in the readout caused by the extracts or fractions. After correction in the reading, 29 samples were picked from a set of 1164 for further confirmation studies. Without this correction, it was not possible to identify any extract/fraction as a true inhibitor of the enzyme. Two main reasons were considered in deciding the cutoff of 40% inhibition: 1) very low quantity of the active ingredient may be present in the crude extracts of the plants used and 2) the enzyme is allosteric in nature. The scattered plot and histogram of screening data clearly indicated that the protocol was robust in screening any chemical library (**Fig. 5A, B**). Finally, 12 samples were identified as confirmed hits. Currently, the chromatographic separations are being carried out and guided by its inhibition of *M. tuberculosis* glutamine synthetase to identify the inhibitors.

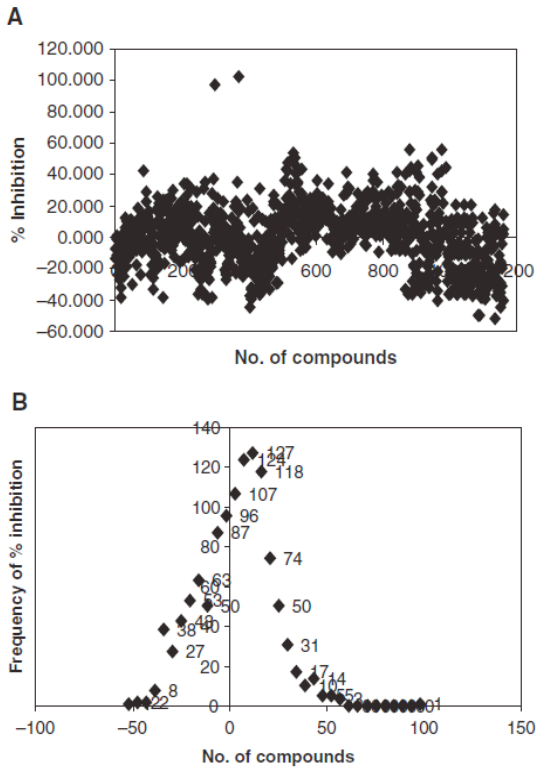

FIG. 5. Analysis of the data obtained from screening of a diverse chemical library on *M. tuberculosis* glutamine synthetase. Samples consisting of extracts and fractions of plants including synthetic compounds were screened at 500 µg/ml concentration using a high-throughput protocol for biosynthetic assay of the enzyme as described in the "Materials and Methods" section. (**A**) Scattered plot of percentage inhibition data obtained from screening of the library. (**B**) The histogram of the analyzed screening data mentioned above.

ACKNOWLEDGMENTS

We are thankful to the director of the National Chemical Laboratory, Pune, India, for providing financial assistance through an in-house project. We are also thankful to Dr. D. Eisengberg, University of California, Los Angeles, for providing the *E. coli* clone YMC21E of *M. tuberculosis* glutamine synthetase as a gift. Miss Upasana Singh is a junior research fellow of Lady Tata Memorial Trust, Mumbai, India.

REFERENCES

1. Kochi A: The global tuberculosis situation and the new control strategy of the World Health Organization. *Tubercle* 1991;72:1-6.
2. Frothingham R, Stout JE, Hamilton CD: Current issues in global tuberculosis control. *Int J Infect Dis* 2005;9:297-311.
3. Gupta R, Marcos AE, Mario CR: Tuberculosis as a major global health problem in the 21st century: a WHO perspective. *Semin Respir Crit Care Med* 2004;25:245-253.
4. Morris RP, Nguyen L, Gatfield J, Visconti K, Nguyen K, Schnappinger D, et al: Ancestral antibiotic resistance in *Mycobacterium tuberculosis*. *Proc Natl Acad Sci U S A* 2005;34:12200-12205.
5. Barnes P, Blotch AD, Davidson BT, Snyder JDE: Tuberculosis in patients with immunodeficiency virus syndrome. *N Engl J Med* 1991;324:1644-1650.
6. Warner DF, Mizrahi V: Mycobacterial genetics in target validation. *Drug Discov Today* 2004;1(2):93-98.
7. Khasnobis S, Escuyer VE, Chatterjee D: Emerging therapeutic targets in tuberculosis: post genomic era. *Expert Opin Ther Targets* 2002;6(1):21-40.
8. Kim P, Zhang YM, Shenoy G, Nguyen QA, Boshoff HJ, Manjunatha UH, et al: Structure-activity relationships at the 5-position of thiolactomycin: an intact (5*R*)-isoprene unit is required for activity against the condensing enzymes from *Mycobacterium tuberculosis* and *Escherichia coli*. *J Med Chem* 2006;49:159-171.
9. Ravindranadh VS, Boshoff H, Qiao C, Bennett EM, Barry CE, Aldrich CC: Rationally designed nucleoside antibiotics that inhibit siderophore biosynthesis of *Mycobacterium tuberculosis*. *J Med Chem* 2006;49:31-34.
10. Harth G, Gali SM, Tullius MV, Horwitz MA: All four *Mycobacterium tuberculosis gln* A genes encode glutamine synthetase activities but only GlnA1 is abundantly expressed and essential for bacterial homeostasis. *Mol Microbiol* 2005;58:1157-1172.
11. Anishetty S, Mrudula P, Gautam P: Potential drug targets in *Mycobacterium tuberculosis* through metabolic pathway. *Comput Biol Chem* 2005;29:368-378.
12. Srivastava SK, Dube D, Tewari N, Dwivedi N, Tripathi RP, Ramachandran R: *Mycobacterium tuberculosis* NAD^+-dependent DNA ligase is selectively inhibited by glycosylamine compared with human DNA ligase I. *Nucleic Acids Res* 2005;33:7090-7101.
13. Wayne LG, Sohaskey CD: Nonreplicating persistence of *Mycobacterium tuberculosis*. *Ann Rev Microbiol* 2001;55:139-163.
14. Raynaud C, Etienne G, Payron P, Lanelle MA, Daffe M: Extracellular enzyme activities potentially involved the pathogenicity of *Mycobacterium tuberculosis*. *Microbiology* 1998;144:577-587.
15. Harth G, Clemens DL, Horwitz MA: Glutamine synthetase of *Mycobacterium tuberculosis*: extracellular release and characterization of its enzymatic activity. *Proc Natl Acad Sci U S A* 1994;91:9342-9346.
16. Harth G, Horwitz MA: An inhibitor of exported *Mycobacterium tuberculosis* glutamine synthetase selectively blocks the growth of pathogenic mycobacteria in axenic culture and in human monocytes: extracellular proteins as potential novel drug targets. *J Exp Med* 1999;189:1425-1435.
17. Harth G, Zamecnik PC, Tang JY, Tabatadze D, Horwitz MA: Treatment of *Mycobacterium tuberculosis* with antisense oligonucleotide to glutamine synthetase mRNA inhibits glutamine synthetase activity, formation of the poly-L-glutamate/glutamine cell wall structure, and bacterial replication. *Proc Natl Acad Sci U S A* 2000;97:418-423.
18. Harth G, Horwitz MA: Inhibition of *Mycobacterium tuberculosis* glutamine synthetase as a novel antibiotic strategy against tuberculosis: demonstration of efficacy in vivo. *Infect Immun* 2003;71(1):456-464.
19. Tullius MV, Harth G, Horwitz MA: Glutamine synthetase GlnA1 is essential for growth of *Mycobacterium tuberculosis* in human THP-1 macrophages and guinea pigs. *Infect Immun* 2003;71:3927-3936.
20. Gill HS, Pflucgel GMU, Eisenberg D: Multicopy crystallographic refinement of a relaxed glutamine synthetase from *Mycobacterium tuberculosis* highlights flexible loops in the enzymatic mechanism and its regulation. *Biochemistry* 2002;41:9863-9872.

21. Eisenberg D, Gill SH, Pfluegl GMU, Rotstein SH: Structure-function relationships of glutamine synthetase. *Biochim Biophys Acta* 2000;1477:122-145.
22. Mehta R, Pearson TJ, Mahajan S, Nath A, Hickey MJ, Sherman DR, et al: Adenylylation and catalytic properties of *Mycobacterium tuberculosis* glutamine synthetase expressed in *Escherichia coli* versus mycobacteria. *J Biol Chem* 2004;279:22477-22482.
23. Singh U, Sarkar D: Development of a simple assay protocol for high-throughput screening of *Mycobacterium tuberculosis* glutamine synthetase for the identification of novel inhibitors. *J Biomol Screen* 2005;10:725-729.
24. Wollfolk CA, Shapiro B, Stadtman ER: Regulation of glutamine synthetase. I. Purification and properties of glutamine synthetase from *Escherichia coli*. *Arch Biochem Biophys* 1966;116:177-192.
25. Gawronski JD, Benson DR: Microtiter assay for glutamine synthetase biosynthetic activity using inorganic phosphate detection. *Anal Biochem* 2004;327:114-118.
26. Zhang JH, Chung TDY, Oldenburg KR: A simple statistical parameter for use in evaluation and validation of high throughput screening assays. *J Biomol Screen* 1999;4:67-73.
27. Romo G, Nieto SS, Ruiz MG: A modified colorimetric method for the determination of orthophosphate in the presence of high ATP concentration. *Anal Biochem* 1992;200:235-238.
28. Black MJ, Jones EM: Inorganic phosphate determination in the presence of labile organic phosphate: assay for carbamyl phosphate phosphatase activity. *Anal Biochem* 1983;135:233-238.

Address reprint requests to:
Dhiman Sarkar, Ph.D.
Combi Chem-Bio Resource Center
National Chemical Laboratory
Dr. Homi Bhabha Rd.
Pune 411008, India

E-mail: d.sarkar@ncl.res.in